

ISSN (p) 1857-1727

ISSN (e) 2345-1688

Volume 10

No. 2, 2015

# CHEMISTRY

## JOURNAL OF MOLDOVA

General, Industrial and Ecological Chemistry

**Editor-in-chief: Gheorghe DUCA**

NCAA national scientific journals ranking: Category B

Academy of Sciences of Moldova  
Institute of Chemistry  
Moldova State University

© Chemistry Journal of Moldova  
Institute of Chemistry A.S.M. (publisher)

# CHEMISTRY JOURNAL OF MOLDOVA

## General, Industrial and Ecological Chemistry

is included/abstracted/indexed in:

CAS (Chemical Abstracts Service/SciFinder)  
VINITI (Russian Scientific and Technical Information Institute)  
DOAJ (Directory Open Access Journals)  
SHERPA/ROMEO  
OAJI (Open Academic Journals Index)  
HINARI, Research in Health Programme, WHO  
EVISA (European Virtual Institute for Speciation Analysis)  
EIFL-OA Moldova (On-line Journals of Moldova)  
BASE (Bielefeld Academic Search Engine)  
Cite Factor (Directory Indexing of International Research Journals)  
PubsHub Journals & Congresses  
Academic Keys  
Scholar Steer  
Electronic Journals Library Database  
Electronic Catalog of Academy of Sciences of Belarus  
V. I. Vernadsky National Library of Ukraine  
ZDB (Berlin State Library)  
Library of Academy of Economic Studies of Moldova  
Library of Moldova State University  
Digital library of Manchester University (UK)  
Digital library of Cambridge University (UK)  
Digital library of Sheffield University (UK)  
Digital library of Ghent University (Belgium)  
Digital library of Wroclaw University (Poland)  
Digital library of University of Texas at Austin (USA)  
Digital library of Indiana University (USA)  
Digital library of Simon Fraser University (Canada)  
Digital library of University of Saskatchewan (Canada)  
Digital library of S.B.M.S. College (India)  
Digital library of Kanazawa University (Japan)

### Indexing under process for:

Thomson ISI  
SCOPUS  
ROAD (Directory of Open Access Scholarly Resources)

### Editorial production and secretariat:

Dr. Larisa Postolachi  
Lilia Anghel  
Dr. Elena Gorincioi

---

### Editorial office address:

Institute of Chemistry of Academy of Sciences of Moldova, 3, Academiei Str., Chisinau, MD-2028, Republic of Moldova  
Tel: + 373 22 725490; Fax: +373 22 739954; e-mail: chemjm@asm.md, chemjm@gmail.com, chemjm\_correspondence@yahoo.com  
Web: www.cjm.asm.md

# CHEMISTRY JOURNAL OF MOLDOVA

## General, Industrial and Ecological Chemistry

**Editor-in chief:** Academician Gheorghe DUCA, Academy of Sciences of Moldova  
**Editors:** Corr. member Tudor LUPASCU, Academy of Sciences of Moldova  
Dr. Viorica GLADCHI, Moldova State University

### Local Editorial Board:

**Dr. Hab. A. ARICU**  
Academy of Sciences of Moldova

**Dr. Hab. I. BULHAC**  
Academy of Sciences of Moldova

**Dr. G. DRAGALINA**  
Moldova State University

**Corr. member I. GERU**  
Academy of Sciences of Moldova

**Dr. Hab. M. GONTA**  
Moldova State University

**Acad. A. GULEA**  
Moldova State University

**Dr. V. KULCITKI**  
Academy of Sciences of Moldova

**Dr. Hab. F. MACAEV**  
Academy of Sciences of Moldova

**Dr. R. NASTAS**, scientific secretary  
of the editorial board,  
Academy of Sciences of Moldova

**Dr. Hab. I. POVAR**  
Academy of Sciences of Moldova

**Dr. Hab. V. RUSU**  
Academy of Sciences of Moldova

**Dr. Hab. R. STURZA**  
Technical University of Moldova

**Dr. Hab. V. SARAGOV**  
A. Russo State University of Balti

**Dr. Hab. N. UNGUR**  
Academy of Sciences of Moldova

**Acad. P. VLAD**  
Academy of Sciences of Moldova

### International Editorial Board:

**Acad. S. ALDOSHIN**  
Russian Academy of Sciences

**Acad. S. ANDRONATI**  
National Academy of Sciences of Ukraine

**Prof. V. ARION**  
University of Vienna, Austria

**Prof. M. BAHADIR**  
Technical University of Braunschweig, Germany

**Acad. I. BERSUKER**  
University of Texas at Austin, USA

**Prof. J. de BOER**  
Vrije University Amsterdam, The Netherlands

**Prof. L. CHIBOTARU**  
Katholieke Universiteit Leuven, Belgium

**Prof. F. FRIMMEL**  
University of Karlsruhe, Germany

**Prof. A. GARABADZHIU**  
St-Petersburg State Institute of Technology,  
Russia

**Acad. V. GONCHEARUK**  
National Academy of Sciences of Ukraine

**Acad. F. LAKHVICH**  
National Academy of Sciences of Belarus

**Acad. J. LIPKOWSKI**  
Polish Academy of Sciences

**Acad. V. LUNIN**  
Lomonosov Moscow State University, Russia

**Prof. I. SANDU**  
A.I. Cuza University, Iasi, Romania

**Acad. B. SIMIONESCU**  
Romanian Academy, Iasi, Romania

**Infobase Index (IBI Factor for the year 2015 is 3.2)**  
**Universal Impact Factor (for the year 2014 is 0.135)**

## ISSUE CONTENTS LIST WITH GRAPHICAL ABSTRACTS

## NEWS AND EVENTS

7

THE 6<sup>TH</sup> INTERNATIONAL CONFERENCE

## “ECOLOGICAL &amp; ENVIRONMENTAL CHEMISTRY” 2017

March 2-3, 2017, Chisinau, Republic of Moldova

Main scope of the conference is development of the international cooperation in the fields of ecological chemistry, environmental protection and promotion of the healthy life style by seeking harmony between ecology and chemical processes of pollution, purification, and methods of prevention of anthropogenic impact on the environment and human health, as well as issues related to environmental education, training and environmental safety.

## REVIEW PAPER

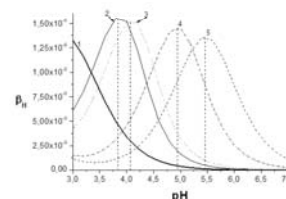
## ANALYTICAL CHEMISTRY

8

## BUFFER CAPACITY IN HETEROGENEOUS MULTICOMPONENT SYSTEMS. REVIEW

Oxana Spinu, Igor Povar

The quantitative basis of the theory of buffer properties for two-phase acid-base buffer systems and for multicomponent heterogeneous systems has been derived. The analytical equations with respect to all components for diverse multicomponent systems were deduced. It has been established, that the buffer capacities of components are mutually proportional.



## FULL PAPER

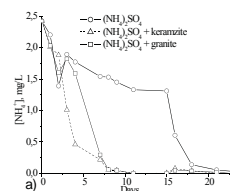
## ECOLOGICAL CHEMISTRY

26

## STUDY OF STABLE NITROGEN FORMS IN NATURAL SURFACE WATERS IN THE PRESENCE OF MINERAL SUBSTRATES

Petru Spataru, Igor Povar, Elena Mosanu, Ana Trancalan

The influence of substrates on the oxidation of reduced toxic forms of nitrogen in river water was investigated by laboratory modelling. Granite and expanded clay accelerate the oxidation of ammonium and nitrite ions from 2 to 4 times. The presence of calcium carbonate in water hinders the oxidation of nitrogen in the polluted water.



## FULL PAPER

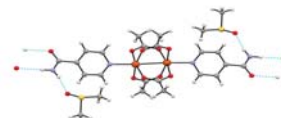
## INORGANIC AND COORDINATION CHEMISTRY

33

NEW SOLVATOMORPH OF TETRAKIS(μ<sub>2</sub>-ACETATO-O,O')-BIS(ISONICOTINAMIDE-N)-DI-COPPER(II): SYNTHESIS, IR, TGA AND X-RAY STUDY

Diana Chisca, Eduard Coropceanu, Oleg Petuhov, Lilia Croitor

Dinuclear tetracarboxylato-bridged copper(II) solvato-morph  $[\text{Cu}_2(\text{OAc})_4(\text{ina})_2] \cdot 2\text{dmsO}$  was prepared and studied by IR spectroscopy, TGA analysis and single crystal X-ray method. Cu(II) ions are bridged by four *syn,syn-η':η':μ* carboxylates, showing a paddle-wheel cage-type with a square-pyramidal geometry.



## FULL PAPER

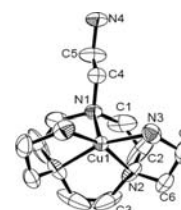
## INORGANIC AND COORDINATION CHEMISTRY

40

## SYNTHESIS, CRYSTAL STRUCTURE, AND PROPERTIES OF COPPER(II) COMPLEXES WITH 1,4,7-TRIS(2-AMINOETHYL)-1,4,7-TRIAZACYCLONONANE

Masahiro Mikuriya, Mayu Hamagawa, Natsuki Tomioka, Daisuke Yoshioka, Naoko Uehara, Rika Fujimori, Hiroki Yamamoto, Yoshinari Ando, Shoichi Hori, Taro Kuriyama, Ryoji Mitsuhashi, Makoto Handa

Three kinds of copper(II) complexes with 1,4,7-tris(2-aminoethyl)-1,4,7-triazacyclononane (taetacn),  $[\text{Cu}(\text{taetacn})](\text{ClO}_4)_2$  (**1**),  $[\text{Cu}(\text{Htaetacn})](\text{ClO}_4)_3$  (**2**), and  $[\text{Cu}(\text{Htaetacn})](\text{BF}_4)_3$  (**3**) were synthesized and characterized by elemental analyses, IR and UV-Vis spectroscopies. The spectral features are in harmony with an octahedral geometry for **1** and a square-pyramidal coordination for **2** and **3**.



## FULL PAPER

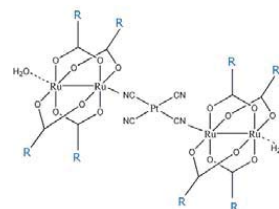
## INORGANIC AND COORDINATION CHEMISTRY

48

**MIXED-METAL COMPLEXES OF RUTHENIUM(II,III) CARBOXYLATE AND TETRACYANIDOPLATINATE(II)**

Masahiro Mikuriya, Kenta Ono, Shun Kawauchi, Daisuke Yoshioka, Ryoji Mitsuhashi, Makoto Handa

Mixed-metal complexes constructed from dinuclearruthenium(II,III) carboxylates and tetracyanidoplatinate(II),  $[\{\text{Ru}_2(\text{O}_2\text{CCH}_3)_4\}_2\text{Pt}(\text{CN})_4]\cdot 2\text{H}_2\text{O}$  (**1**) and  $[\{\text{Ru}_2\{\text{O}_2\text{CC}(\text{CH}_3)_3\}_4\}_2\text{Pt}(\text{CN})_4]\cdot 2\text{H}_2\text{O}$  (**2**), were synthesized and characterized by elemental analysis and IR and UV-vis spectroscopies.



## FULL PAPER

## NATURAL PRODUCT CHEMISTRY AND SYNTHESIS

54

**GC-MS ANALYSIS OF THE FATTY ACID METHYL ESTER IN JAPANESE QUAIL FAT**

Ion Dragalin, Olga Morarescu, Maria Sedcenco, Radu Marin Rosca

The accumulated as production waste fat from Faraon quail breeds has been investigated for the first time by using GC-MS technique, preventively converting it *via* methanolysis to fatty acid methyl esters. The test results, regarding the content of unsaturated fatty acids having a favorable to human body *cis*-configuration (77.8%), confirm their nutritional value and the possibility of using this fat in cosmetic, pharmaceutical and food industries.

## FULL PAPER

## NATURAL PRODUCT CHEMISTRY AND SYNTHESIS

58

**SYNTHESIS OF NEW NITROGEN-CONTAINING DRIMANE AND HOMODRIMANE SESQUITERPENOIDS FROM SCLAREOLIDE**

Lidia Lungu

The synthesis of new nitrogen-containing drimane and homodrimane sesquiterpenoids in cycle B is reported. A comparative study of the microwave (MW) assisted synthesis of drimenone versus classical conditions has been done. The drimanic and homodrimanic oximes were prepared on the base of ketones derived from commercially available sclareolide. The drimanic amine was obtained by reduction of corresponding oxime with  $\text{LiAlH}_4$ . The structure of novel compounds was confirmed using IR,  $^1\text{H}$  and  $^{13}\text{C}$  NMR analyses.

## FULL PAPER

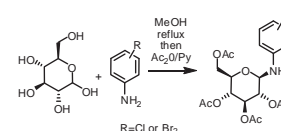
## ORGANIC CHEMISTRY

62

**NEW N-GLUCOSYLATED SUBSTITUTED ANILINES**

Vsevolod Pogrebnoi

The reaction of (+)-*D*-glucose with 4-chloroaniline or 3,5-dibromoaniline leads almost exclusively to the  $\beta$ -configuration of glucosylated anilines. The acetylating of 2-(3,5-dibromophenylamino)-6-(hydroxymethyl)tetrahydro-2*H*-pyran-3,4,5-triol is less selective than in case of the 2-(4-chlorophenylamino)-6-(hydroxymethyl)tetrahydro-2*H*-pyran-3,4,5-triol.



## FULL PAPER

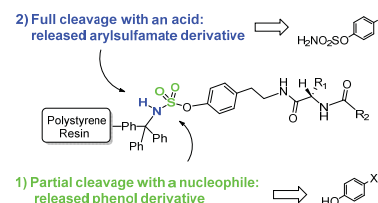
## ORGANIC CHEMISTRY

68

**A SEQUENTIAL DUAL CLEAVAGE OF THE ARYLSULFAMATE LINKER TO PROVIDE BOTH SULFAMATE AND PHENOL DERIVATIVES**

Diane Fournier, Liviu Ciobanu, Donald Poirier

Tyramine sulfamate was linked to the trityl chloride resin and this polymeric support used to introduce two levels of molecular diversity by formation of peptide bonds. A dual cleavage strategy next generated in a sequential way (without resin split) two types of compounds (phenol and arylsulfamate derivatives), which are therapeutically attractive types of compounds.



## FULL PAPER

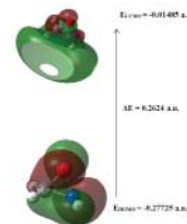
## PHYSICAL CHEMISTRY AND CHEMICAL PHYSICS

77

**OXAZIRIDINE (C-CH<sub>3</sub>NO), C-CH<sub>2</sub>NO RADICALS AND CL, NH<sub>2</sub> AND METHYL DERIVATIVES OF OXAZIRIDINE; STRUCTURES AND QUANTUM CHEMICAL PARAMETERS**

Mohammad Taghi Taghizadeh, Morteza Vatanparast, Saeed Nasirianfar

Oxaziridine [c-CH<sub>3</sub>NO (X<sup>1</sup>A)], c-CH<sub>2</sub>NO (X<sup>2</sup>A) radicals and Cl, NH<sub>2</sub> and methyl derivatives of oxaziridine structures have been optimized via DFTB3LYP level of theory using 6-311++G (d, p) basis set. Population analysis had been carried out. Vertical ionization energy (VIE) and adiabatic ionization energy (AIE), Fukui indices and some quantum chemical parameters were calculated. N-O bond was determined as weakest bond in oxaziridine triangle. The effect of electron withdrawing and electron donating groups on stability of weakest bond were assessed.



## SHORT COMMUNICATION

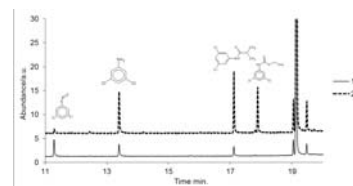
## FOOD CHEMISTRY

89

**THE SURFACE PHOTOCHEMISTRY OF PROCYMIDONE IN PRESENCE OF AMMONIUM FERRIC CITRATE**

Ivan Osipov

Procyimdone was chosen as the model compound and its phototransformation was followed under sunlight irradiation. The main photodegradation products on silica is 3,5-dichloroaniline and 3,5-dichlorophenylisocyanate. The use of ammonium ferric citrate enhances the degradation of the procyimdone.



## SHORT COMMUNICATION

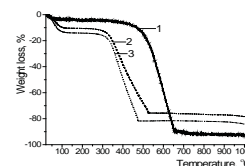
## INDUSTRIAL CHEMISTRY

92

**MODIFICATION OF CARBONACEOUS ADSORBENTS WITH MANGANESE COMPOUNDS**

Irina Ginsari, Larisa Postolachi, Vasile Rusu, Oleg Petuhov, Tatiana Goreacioc, Tudor Lupascu, Raisa Nastas

Four series of samples containing manganese supported carbonaceous adsorbents were prepared. Obtained results reveal the importance of surface chemistry of carbonaceous adsorbents on the manganese loading.



## SHORT COMMUNICATION

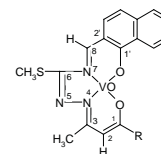
## INORGANIC AND COORDINATION CHEMISTRY

95

**COORDINATION COMPOUNDS OF OXOVANADIUM(IV) BASED ON S-METHYLISOTHIOSEMICARBAZIDE AS DYES FOR THERMOPLASTIC PLASTIC**

Maria Cocu, Stefan Manole

We have investigated the properties as dyes of coordination compounds synthesized by us previously (8-(1',2'-naphthyl)-1-R-3-methyl-6-thiomethyl-4,5,7-triazanona-1,3,5,7-tetraenato-1,1'-diolato(-)-O<sup>1</sup>, O<sup>1'</sup>, N<sup>4</sup>, N<sup>7</sup>-vanadil, where R=CH<sub>3</sub> (1), C<sub>6</sub>H<sub>5</sub> (2)), which can be used for colouring thermoplastic masses. The compounds have a high photostability (7 points), thermostability (>250°) and an intensity of colour that give a low consumption (0.006-0.010g).



## SUPPLEMENTARY MATERIAL

## PHYSICAL CHEMISTRY AND CHEMICAL PHYSICS

99

**OXAZIRIDINE (C-CH<sub>3</sub>NO), C-CH<sub>2</sub>NO RADICALS AND CL, NH<sub>2</sub> AND METHYL DERIVATIVES OF OXAZIRIDINE; STRUCTURES AND QUANTUM CHEMICAL PARAMETERS****(Supplementary material)**

Mohammad Taghi Taghizadeh, Morteza Vatanparast, Saeed Nasirianfar

Supplementary material contains Tables S1 to S9 and Figures S1 to S4.

109

**INSTRUCTIONS FOR AUTHORS**

# **The 6<sup>th</sup> International Conference ECOLOGICAL & ENVIRONMENTAL CHEMISTRY 2017**

**March 2-3, 2017, Chisinau, Republic of Moldova**

The 6<sup>th</sup> International Conference **ECOLOGICAL & ENVIRONMENTAL CHEMISTRY 2017** (EEC-2017) will be held on 2-3 March, 2017 in Chisinau, Republic of Moldova.

**Main Scope:** Development of the international cooperation in the fields of ecological chemistry, environmental protection and promotion of the healthy life style by seeking harmony between ecology and chemical processes of pollution, purification, and methods of prevention of anthropogenic impact on the environment and human health, as well as issues related to environmental education, training and environmental safety.

The 6<sup>th</sup> International Conference **ECOLOGICAL & ENVIRONMENTAL CHEMISTRY 2017** will serve as the main arena for discussion, experience and ideas exchange of the recent achievements in the field related to the investigation of mechanisms and chemical processes that take place in natural waters, atmosphere and soils under the influence of anthropogenic pollutants, the pollutants impact on the human health and habitat, as well as with the methods of chemical risk assessment, environment pollution prevention and mitigation.

## **Topics proposed for discussion:**

- A. **Ecological Chemistry**
  - a. Physico-chemical and chemico-biological processes which determine composition, structure and chemical properties of the environment
  - b. Water, air and waste treatment methods and technologies
  - c. Chemical risk assessment of human health and environment
- B. **Environmental Chemistry**
  - a. Chemistry of water
  - b. Chemistry of air
  - c. Chemistry of soil
- C. **Green Chemistry**
  - a. Preventing and reducing the negative impact of chemistry on the environment
  - b. Design of ecological friendly technologies and chemical products that minimize the use and generation of hazardous substances
- D. **Ecological Chemistry in Research and Education**
  - a. Ecological chemistry research and innovation activities
  - b. Ecological chemistry in education

**Conference Chairman**

**Academician Gheorghe DUCA**

*President of the Academy of Sciences of Moldova*

*1, Stefan cel Mare Blvd. MD 2001, Chisinau, Republic of Moldova*

*Tel: +373-22-271478; +373-22-271478; Fax: +373-22-276014*

*e-mail: [ecochem2017@mrda.md](mailto:ecochem2017@mrda.md)*

web page: [www.asm.md](http://www.asm.md); [www.ecochem2017.mrda.md](http://www.ecochem2017.mrda.md) (in process)



# BUFFER CAPACITY IN HETEROGENEOUS MULTICOMPONENT SYSTEMS. REVIEW

Oxana Spinu\*, Igor Povar

*Institute of Chemistry of Academy of Sciences of Moldova, 3, Academiei str., Chisinau MD-2028, Republic of Moldova*

*\*e-mail: oxana\_spinu@yahoo.com; phone (+373 22) 73 97 36*

**Abstract.** The quantitative basis of the theory of buffer properties for two-phase acid-base buffer systems and for multicomponent heterogeneous systems has been derived. The analytical equations for buffer action with respect to all components for diverse multicomponent systems were deduced. It was found a remarkable relation of proportionality between  $\beta_i$  quantities. It is shown, that the buffer properties in relation to the solid phase components are amplified with an increase of solubility due to protolytic or complex formation equilibria in saturated solutions. It has been established, that the buffer capacities of components are mutually proportional, whereas for heterogeneous systems these relationships depend on the stoichiometric composition of solid phases. The deduced equations can be applied to the assessment of buffer action of the systems "Natural mineral – soil solution", containing soluble and insoluble chemical species. A number of the important conclusions concerning the investigated buffer systems has been made. The obtained results can be used in various areas of chemical and biochemical researches, especially in soil science, ecological sciences, analytical chemistry, pharmacology, pharmaceuticals, medical industry and synthetic organic chemistry

**Keywords:** buffer action, complex formation, thermodynamic stability, extraction multicomponent system, heterogeneous equilibria.

*Received: April 2015/ Revised final: September 2015/ Accepted: September 2015*

## Introduction

Buffer capacity is an important concept in many areas of science: analytical and electroanalytical chemistry [1], geochemistry [2], biochemistry [3], medicine and pharmaceutical industry [4], water treatment [5], agriculture [6], environment [7], etc. The capacity of buffer systems to oppose (resist) to the variation of their composition (usually to  $pH$  changes) by influence of external fluxes of chemical compounds of natural or anthropogenic character, that shift chemical equilibria, is called buffer property, and its efficiency – buffer action. Despite of an abundance of the information on buffer systems, the quantitative theory of buffer action has been developed only for mono-phase systems [8,9]. The buffer action of mono-phase buffers is usually based on protolytic equilibria between water, a weak acid or base or ampholytic compound and their conjugate pairs [10,11]. The widespread use of buffers as well as the variety of chemical processes and phenomena associated with a certain acidity of solutions explains the constant interest in designing and studying new buffer systems.

Unlike the classical mono-phase buffer systems in which the buffer components are dissolved in a unique phase, in two-phase (heterogeneous) buffers they are distributed between two phases: in aqueous phase and solid (gaseous or liquid) phase. The aqueous (buffer) phase contains all the charged particles and a restricted quantity of electro-neutral species. The solid phase contains in significant quantities only electro-neutral particles and serves as their reservoir by means of which the equilibrium is adjusted and one of parameters of buffer system is maintained constantly [9-18]. The buffer action of two-phase systems is based on the shift of complex equilibria, both homogeneous and heterogeneous in the aqueous phase and between phases, respectively [19-21]. By increasing the acidity of solution the role of simultaneous proceeding protolytic reactions with participation of salt anions increases; with an increase of alkalinity the contribution of complex formation reactions occurring with participation of salt cations amplifies. Authors [15] have proved that the buffer capacity is a special case of the sensitivity analysis, as a more general theoretical approach, which studies the answer of system to various external perturbations (as for example, the variation of the certain component concentration). We believe that it is more correct to consider, as a potential reservoir of buffer heterogeneous systems, the complex chemical heterogeneous equilibria with participation of solid phases [16]. Unfortunately, so far there are a small number of studies dedicated to the systematic investigations and the development of theoretical aspects of the buffer action for two-phase systems [8,9,14-21]. Besides, in the majority of these studies only the  $pH$  – buffer properties of heterogeneous systems were investigated. The concept of "buffer action" helps to find out which reactions control the composition of natural waters, including soil solutions [22-32]. The parameters of buffer action are integrated functions of all the soil chemical components by virtue of their capacity, by means of chemical reactions and sorption-desorption processes, to extinguish or strengthen the effect of entered pollutants [33].

The aim of the present paper has been to develop the quantitative aspects of the buffer action of various components of heterogeneous systems and to establish their interrelation. In this paper, the quantitative aspects of the theory for two-phase buffers with partition equilibria of acid-base pairs between two liquids (aqueous and organic) are



considered in detail. It is proved that the heterogeneous multicomponent systems possess buffer action with respect to all components “*i*” of acid-base mixtures. Analytical equations for the buffer capacities of two-phase systems with respect to all the components of heterogeneous systems have been deduced. Moreover, it has been shown that the quantities in these systems are reciprocally proportional. In contrast to classical mono-phase buffers, in two-phase buffer systems the maximum buffer capacity  $\beta_H$  occurs when  $pH_{max}$  is equal to  $pK_d + \log(1 + P(HA))$ , where  $K_d$  and  $P(HA)$  are respectively the dissociation constant and the repartition constant of the acid between two phases.

## Theoretical part

### Buffer action of the systems “Mineral – saturated solution”

The buffer action of soil is one of its fundamental physicochemical characteristics. The soil buffer action composes of the buffer action of a set of mineral and organic components and presented by solid, liquid and gaseous compounds. The buffer capacity of soils in relation to chemical compounds is defined by the content of chemical elements in the soil solution (the parameter of intensity) and on the content of mobile compounds of these elements in solid phases (the parameter of capacity). The buffer capacity of soils can be discovered by the fact that the increase of amounts of toxic metals (*TM*) is not accompanied by an increase of their content in plants; the different buffer action of the soils in relation to one element is manifested in unequal toxic concentrations for plants [33]. The same soil can possess different buffer action in relation to different metals.

The complexity of the soil solution composition containing mineral phases and a large set of involved chemical compounds determine the possibility of simultaneous chemical reactions along with the capacity of solid phases of minerals to maintain relatively constant the aqueous solution composition [19-21,29-32,34-40]. Under real conditions the buffer action of natural heterogeneous aqueous systems is expressed so as the consumption of any element from solution causes the partial dissolution of solid phases and as a result the composition of the solution is restored.

Currently, extensive information on negative (harmful) transformations of soils, as a result of progressing acid and alkaline loads (in the form of mineral fertilizers, chemicals for protection of plants and industrial emissions dropping out with atmospheric precipitation) has been gathered. Thus, the quantitative assessment of the acid - base buffer action, revealing the degree of influence of the systematic use of fertilizers and technogenic pollution by substances of the acid and alkaline nature is an actual problem of the agrology. Besides, the buffer action of soils contains important information on the processes of soil formation (their orientation and intensity) which is used for the soil diagnostics and classification [33].

As a criterion for quantitative assessment of the intensity of buffer action of the studied multicomponent heterogeneous systems, one can use the value of the buffer capacity  $\beta_i^S$  (the superscript index “*S*” specifies the presence of solid phases), which can be defined as a partial derivative:

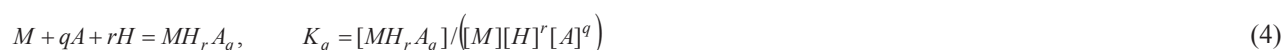
$$\beta_i^S = \left( \frac{\partial C_i^0}{\partial \ln[i]} \right)_{C_j^0 (j \neq i)}$$

where  $C_i^0$  and  $[i]$  denote the initial (analytical) concentration in mixture and equilibrium concentration of the component “*i*” of solid phase, correspondingly, the subscript index shows that the initial concentrations of other components of the mixture are maintained constant.

We will examine the process of formation of the sparingly soluble salt of arbitrary stoichiometric composition  $M_m A_{n(S)}$  (*M* - metal ion, *A* - anion of salt):



The following set of possible simultaneous reactions in the saturated solution is taken into account:



For the sake of simplicity, the charges of species are omitted. Near to the reaction equations, the corresponding equilibrium constants are specified. The mass balance (*MB*) conditions in this system can be formulated by the following equations:

$$C_M^0 = \Delta C_M + C_M^r = \Delta C_M + \sum_{i=1} \sum_{j=0} i[M_i(OH)_j] + \sum_{q=1} \sum_{r=0} [MH_r A_q] \quad (6)$$

$$C_A^0 = \Delta C_A + C_A^r = \Delta C_A + \sum_{l=0} [H_l A] + \sum_{q=1} \sum_{r=0} q[MH_r A_q] \quad (7)$$

$$C_H^0 = [H] - [OH] + \sum_{l=1} l[H_l A] - \sum_{i=1} \sum_{j=1} j[M_i(OH)_j] + \sum_{q=1} \sum_{r=1} r[MH_r A_q] \quad (8)$$

The quantity  $C_i^r$  represents the residual concentration in solution of the ion “ $i$ ”, e.g. the total concentration of all the species, containing a given ion, while  $\Delta C_i$  is its molar quantity in the solid phase in 1 L of solution [14-17,41-42]. In the Eq.(8)  $C_H^0$  denotes the excess of  $H^+$  ions in relation to hydroxyl ions in two-phase mixtures ( $C_H^0 = -C_{OH}^0$ ). The square brackets designate the equilibrium concentrations of species in solution.

From the stoichiometric composition of the solid phase, the following ratio is obtained:

$$\frac{\Delta C_M}{m} = \frac{\Delta C_A}{n} \text{ or } \Delta C_A = \frac{n}{m} \Delta C_M \quad (9)$$

On the basis of the written equations it is possible to deduce the formulas for calculating the buffer capacity in relation to any component of the mixture. After a series of transformation, one can finally get:

$$\beta_M^S = - \frac{\left( \sum_{i=1} \sum_{j=0} ij[M_i(OH)_j] + \frac{m}{n} \sum_{l=1} l[H_l A] - \sum_{q=1} \sum_{r=1} r[MH_r A_q] + \frac{m}{n} \sum_{q=1} \sum_{r=1} rq[MH_r A_q] \right)^2}{[H] + [OH] + \sum_{l=1} l^2[H_l A] + \sum_{i=1} \sum_{j=0} j^2[M_i(OH)_j] + \sum_{q=1} \sum_{r=1} r^2[MH_r A_q]} +$$

$$+ \frac{m^2}{n^2} \sum_{l=0} [H_l A] + \sum_{q=1} \left( \frac{m^2 q^2}{n^2} - 2 \frac{mq}{n} + 1 \right) \sum_{q=1} \sum_{r=0} [MH_r A_q] + \sum_{i=1} \sum_{j=0} i^2 [M_i(OH)_j] \quad (10)$$

or

$$\beta_M^S = \varphi_3 - \frac{\varphi_1^2}{\varphi_2}, \quad (11)$$

where  $\varphi_1$ ,  $\varphi_2$  and  $\varphi_3$  denote the following concentration functions:

$$\varphi_1 = \sum_{i=1} \sum_{j=0} ij[M_i(OH)_j] + \frac{m}{n} \sum_{l=1} l[H_l A] - \sum_{q=1} \sum_{r=1} r[MH_r A_q] + \frac{m}{n} \sum_{q=1} \sum_{r=1} rq[MH_r A_q]$$

$$\varphi_2 = [H] + [OH] + \sum_{l=1} l^2[H_l A] + \sum_{i=1} \sum_{j=0} j^2[M_i(OH)_j] + \sum_{q=1} \sum_{r=1} r^2[MH_r A_q] \quad (12)$$

$$\varphi_3 = \frac{m^2}{n^2} \sum_{l=0} [H_l A] + \sum_{q=1} \left( \frac{m^2 q^2}{n^2} - 2 \frac{mq}{n} + 1 \right) \sum_{q=1} \sum_{r=0} [MH_r A_q] + \sum_{i=1} \sum_{j=0} i^2 [M_i(OH)_j]$$

Similarly, it is possible to prove that, for the buffer capacity towards proton, the following expression is valid:

$$\left( \frac{\partial C_H^0}{\partial \ln[H]} \right)_{C_M^0, C_A^0} \equiv \beta_H^S = \varphi_2 - \frac{\varphi_1^2}{\varphi_3} \quad (13)$$

For the buffer capacity towards the anion of the solid phase one can deduce:

$$\beta_A^S = \frac{n^2}{m^2} \varphi_3 - \frac{n^2}{m^2} \frac{\varphi_1^2}{\varphi_2} = \frac{n^2}{m^2} \left( \varphi_3 - \frac{\varphi_1^2}{\varphi_2} \right) = \frac{n^2}{m^2} \beta_M^S \quad (14)$$

On the basis of obtained Eq.(11), Eq.(13) and Eq.(14) the following remarkable conclusion follows: the buffer capacities towards different components are reciprocally proportional, while the buffer capacities in relation to the ions of the solid phase are interconnected through its stoichiometric coefficients:

$$\frac{\beta_A^S}{n^2} = \frac{\beta_M^S}{m^2} \quad (15)$$

It is worthy to mention that the obtained relations are only valid in the presence of the mineral (solid phase)  $M_m A_{n(S)}$ . The thermodynamic stability area of the latter is determined by the value of the Gibbs energy of the overall process (1)-(5) [14,43,44]:

$$\Delta G_{S,tot} = -mRT \ln \frac{C_M^r}{C_M^0} - nRT \ln \frac{C_A^r}{C_A^0} \quad (16)$$

The solid-phase is stable if  $\Delta G_{S,tot} > 0$ . The condition  $\Delta G_{S,tot} = 0$  corresponds to the beginning of its dissolution and (or) sedimentation.

The analysis of the derived equations shows that the buffer capacities grow with the increase of the precipitate solubility, e.g. by rising the residual concentration of the component of minerals.

### Buffer properties for liquid two-phase acid-base buffer systems

The concept of buffering is closely related to the problem of controlling the chemical composition of multicomponent systems. For analytical chemists it is essential to preserve as a constant not only the pH value (e.g., the proton concentration), but the concentrations of other components in the system. In the examined extraction systems, the organic phase serves as the buffer reservoir [31,45-47]. At present, for these systems there is no rigorous theoretical base allowing a priori estimation of their buffer effectiveness as well as a systematic search for new heterogeneous mixtures with high buffer action. Janjić et al. [45] have investigated the buffer action with respect to the hydrogen ion (proton) for the multicomponent two-phase systems containing both separate organic acids and bases, and their mixtures. These authors made an attempt to deduce an equation for an assessment of buffer capacity of such systems. However, the obtained expressions are bulky and in some cases neglect a number of side equilibria, occurring in the organic phase.

For two-phase buffers with polyprotic acids, the following process of formation in aqueous solution of the polyprotic acid of stoichiometric composition  $H_n A$  takes place:



The following set of concomitantly reactions proceeding in two-phase systems "Aqueous solution (aq) – organic solvent (o)" proceeds:



Here and below, for sake of convenience, the charges of species are omitted, the subscript (aq) is also neglected in the case of equilibria taking place only in aqueous solution. Near to equations the associated equilibrium constants are specified:  $K_n$  is the protonation constant of polyprotic acid  $H_n A$  and  $P(H_k A)$  is the constant of distribution of the molecular acid  $H_k A$  between two non-mixing liquids. For simplicity, it has been assumed that the system obeys ideal behavior of the studied systems where the ionic strength is zero. Consequently, the ion activities are equal to their concentrations, while the activity of pure species is equal to unity (or included in the equilibrium constants) [24,25,48,49]. The conditions of mass balance in the given heterogeneous system can be formulated as follows:

$$C_A^0 = \tilde{a} = \sum_{n=0} [H_n A]_{aq} + [H_k A]_o = [A] \left( 1 + \sum_{n=1} K_n [H]^n \right) + P(H_k A) K_k [H]^k [A] \quad (20)$$

$$C_H^0 = [H] - [OH] + \sum_{n=1} n[H_n A] + k[H_k A]_o = [H] - K_w [H]^{-1} + [A] \sum_{n=1} n K_n [H]^n + k P(H_k A) K_k [H]^k [A] \quad (21)$$

The  $C_A^0$  value in the Eq.(20) represents the analytical concentration of the anion  $A^{n-1}$  of acid in considered heterogeneous system. In the Eq.(21)  $C_H^0$  denotes the excess of  $H^+$  ions towards to hydroxyl - ions in the two-phase mixture ( $C_H^0 = -C_{OH}^0$ ) [12]. When deducing Eq.(20) and Eq.(21) it was assumed that the volume of water phase  $V_{aq}$  is equal to the volume of organic phase  $V_o$ :

$$V_{aq} = V_o \quad (22)$$

We present here only final results, omitting the intermediate deduction of the equations through the equilibrium constants Eqs.(17) - (19) as it has been done in the Eqs.(20) and (21):

$$\beta_A = \left( \frac{\partial C_A^0}{\partial \ln[A]} \right)_{C_H^0} = \sum_{n=0} [H_n A]_{aq} + [H_k A]_o + \left( \frac{\partial \ln[H]}{\partial \ln[A]} \right)_{C_H^0} \left( \sum_{n=1} n[H_n A] + k[H_k A]_o \right) \equiv \tilde{a} + \tilde{n} \left( \frac{\partial \ln[H]}{\partial \ln[A]} \right)_{C_H^0} \quad (23)$$

where through  $\tilde{n}$  is designated the sum that the third member of the Eq.(23) contains. Considering that  $C_H^0 = const$ :

$$\left( \frac{\partial C_H^0}{\partial \ln[A]} \right)_{C_H^0} = 0 = \tilde{n} + \left( [H] + [OH] + \sum_{n=1} n^2[H_n A] + k^2[H_k A]_o \right) \left( \frac{\partial \ln[H]}{\partial \ln[A]} \right)_{C_H^0} \equiv \tilde{n} + \tilde{h} \left( \frac{\partial \ln[H]}{\partial \ln[A]} \right)_{C_H^0} \quad (24)$$

Whence

$$\left( \frac{\partial \ln[H]}{\partial \ln[A]} \right)_{C_H^0} = -\frac{\tilde{n}}{\tilde{h}} \quad (25)$$

Substituting the obtained expression for the partial derivative Eq.(24) in the Eq.(23), it is finally received:

$$\beta_A = \tilde{a} - \frac{\tilde{n}^2}{\tilde{h}} = C_A^0 - \frac{\left( \sum_{n=1} n[H_n A] + k[H_k A]_o \right)^2}{[H] + [OH] + \sum_{n=1} n^2[H_n A] + k^2[H_k A]_o} \quad (26)$$

In the case of monoprotic acid  $HA$ ,  $n = 1$ , within the range of  $pH$  values, where the concentrations of  $[H^+]$  and  $[OH^-]$  can be neglected, the Eq.(26) becomes significantly simpler,  $\beta_A \cong [A]$ , e.g. the buffer capacity is equal to the equilibrium concentration of the anion of acid.

In a similar way, for the buffer capacity in relation to proton, it is possible to obtain the following expression:

$$\beta_H \equiv \left( \frac{\partial C_H^0}{\partial \ln[H]} \right)_{C_A^0} = [H] + [OH] + \sum_{n=1} n^2[H]^n + k^2[H_k A]_o^k - \frac{\left( \sum_{n=1} n[H_n A] + k[H_k A]_o \right)^2}{C_A^0} \equiv \tilde{h} - \tilde{n}^2 / \tilde{a} \quad (27)$$

It is important to notice, that for monoprotic acid the Eq.(27) simplifies significantly:

$$\beta_H \equiv \left( \frac{\partial C_H^0}{\partial \ln[H]} \right)_{C_A^0} = [H] + [OH] + [HA] + [HA]_o - \frac{([HA] + [HA]_o)^2}{C_A^0} \quad (28)$$

The maximum buffer capacity for a given  $C_A^0$  occurs when  $(\partial \beta_H / \partial \ln[H])_{C_A^0} = 0$ , i.e. when:

$$pH_{max} = pK_d + \log(1 + P(HA)) \quad (29)$$

where  $K_d = 1 / K_l$  is the dissociation constant of weak acid  $HA$ . It is well-known that for the mono-phase buffer system  $pH_{max} = pK_d$ . Consequently, in comparison with classical aqueous buffers, the  $pH_{max}$  value in the case of two-phase systems is shifted by  $\log(1 + P(HA))$ , which depends mainly on the nature of organic solvent. From the Eqs.(26) and (27) a remarkable identity follows:

$$\beta_A \tilde{h} = \beta_H \tilde{a} \quad (30)$$

Therefore, the investigated heterogeneous system shows buffer properties with respect to both ions of the polyprotic acid, and the values of buffer capacity  $\beta_A$  and  $\beta_H$  are reciprocally proportional. For monoprotic acids, since  $h = [H] + [OH] + [HA] + [HA]_o$  and  $\tilde{a} = C_A^0$ , the identity Eq.(30) becomes:

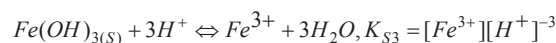
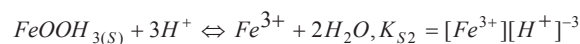
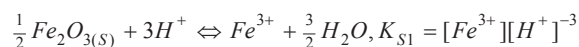
$$\beta_A = ([H] + [OH] + [HA] + [HA]_o) = \beta_H ([A] + [HA] + [HA]_o).$$

Similarly, it is possible to obtain the expressions for calculating the buffer capacities in the case of the polyprotic base  $BH_m$  as well.

## Results and discussion

### Buffer action of heterogeneous system “Mineral - saturated solutions”

The buffer action of heterogeneous system “Mineral - saturated solutions” depends on the chemical composition of the water solutions, as well as on the composition and properties of the mineral phases. We will examine a concrete real system “Iron (III) minerals - saturated solution”, although the approach developed here can be applied for any other. As iron occurs in many minerals and materials, it is mostly present in all superficial waters. The average concentration of iron in river waters is 0.7 mg/L [50]. With an increase of the acidity of waters (up to a critical threshold of water biota survival; for example, for mollusks this threshold is  $pH$  6.0 and for perches it is  $pH$  4.5), the content of iron (III) increases rapidly because of the interaction of iron (III) hydroxide of natural materials with acid:



We find the following important relation of proportionality between the buffer capacities of heterogeneous systems, “ $Fe(OH)_{3(s)}$  - saturated aqueous solution”:

$$\beta_H^S = 3^2 \beta_{Fe}^S \quad (31)$$

In the case of formation of poorly soluble oxy-hydroxides of the stoichiometric composition  $M(OH)_{n(S)}$ ,  $MOOH_{(S)}$  or  $1/2M_2O_{n(S)}$ , the relation (31) can be generalized [14,16,51]:

$$\frac{\beta_H^S}{n^2} = \frac{\beta_M^S}{1^2} \quad (32)$$

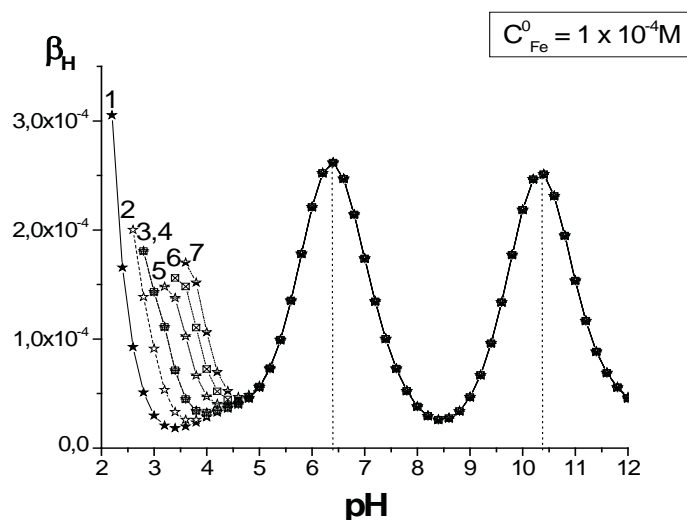
Besides the process of dissolution of the mineral of iron, a set of possible equilibria in the system “Mineral phase – soil solution” (see Table 1) is considered [52]. For the calculations the following composition heterogeneous mixture was used (mol L<sup>-1</sup>):  $C_{Fe}^0 = 1 \cdot 10^{-6} \div 1 \cdot 10^{-4}$ ,  $C_F^0 = 5 \cdot 10^{-6}$ ,  $C_{Org}^0 = C_{PO_4}^0 = C_{SO_4}^0 = 1 \cdot 10^{-4}$ ,  $C_{CO_3}^0 = 1 \cdot 10^{-3}$ .

Table 1

The equilibrium constants of the analyzed reactions.	
The equations of reactions	logK
$Fe^{3+} + H_2O = FeOH^{2+} + H^+$	-2.187
$Fe^{3+} + 2H_2O = Fe(OH)_2^+ + 2H^+$	-4.59
$Fe^{3+} + 3H_2O = Fe(OH)_3^0 + 3H^+$	-12.56
$Fe^{3+} + 4H_2O = Fe(OH)_4^- + 4H^+$	-21.59
$1/2 \alpha - Fe_2O_{3(s)} hematite + 3H^+ = Fe^{3+} + 3/2 H_2O$	-0.85
$1/2 \gamma - Fe_2O_{3(s)} maghemite + 3H^+ = Fe^{3+} + 3/2 H_2O$	+1.75
$1/2 \varepsilon - Fe_2O_{3(s)} + 3H^+ = Fe^{3+} + 3/2 H_2O$	+2.35
$\alpha - FeOOH_{(S)} goethite + 3H^+ = Fe^{3+} + 3H_2O$	+0.40
$\gamma - FeOOH_{(S)} lepidocrocite + 3H^+ = Fe^{3+} + 3H_2O$	+3.70

Equations of reactions	logK
$2\text{-line} - \text{Fe}(\text{OH})_{3(\text{S})} + 3\text{H}^+ = \text{Fe}^{3+} + 3\text{H}_2\text{O}$	+3.00
$6\text{-line} - \text{Fe}(\text{OH})_{3(\text{S})} + 3\text{H}^+ = \text{Fe}^{3+} + 3\text{H}_2\text{O}$	+3.40
$\text{Fe}^{3+} + \text{F}^- = \text{FeF}^{2+}$	6.04
$\text{Fe}^{3+} + 2\text{F}^- = \text{FeF}_2^+$	10.47
$\text{Fe}^{3+} + \text{SO}_4^{2-} = \text{Fe}(\text{SO}_4)^+$	4.05
$\text{Fe}^{3+} + 2\text{SO}_4^{2-} = \text{Fe}(\text{SO}_4)_2^-$	5.38
$\text{Fe}^{3+} + \text{H}^+ + 2\text{SO}_4^{2-} = \text{FeH}(\text{SO}_4)_2$	8.10
$\text{Fe}^{3+} + \text{Org}^{3-} = \text{FeOrg}$	8.00
$\text{Org}^{3-} + \text{H}^+ = \text{HOrg}^{2-}$	4.30
$2\text{Fe}^{3+} + 2\text{H}_2\text{O} = \text{Fe}_2(\text{OH})_2^{4+} + 2\text{H}^+$	-2.85
$3\text{Fe}^{3+} + 4\text{H}_2\text{O} = \text{Fe}_3(\text{OH})_4^{5+} + 4\text{H}^+$	-6.29
$\text{Fe}^{3+} + \text{H}^+ + \text{PO}_4^{3-} = \text{FeHPO}_4^+$	19.87
$\text{Fe}^{3+} + 2\text{H}^+ + \text{PO}_4^{3-} = \text{FeH}_2\text{PO}_4^{2+}$	21.70
$\text{Fe}^{3+} + 3\text{H}^+ + \text{PO}_4^{3-} = \text{FeH}_3\text{PO}_4^{3+}$	26.61
$\text{CO}_3^{2-} + \text{H}^+ = \text{HCO}_3^-$	10.329
$\text{CO}_3^{2-} + 2\text{H}^+ = \text{H}_2\text{CO}_3$	16.681
$\text{H}^+ + \text{PO}_4^{3-} = \text{HPO}_4^{2+}$	12.38
$2\text{H}^+ + \text{PO}_4^{3-} = \text{H}_2\text{PO}_4^+$	19.57
$3\text{H}^+ + \text{PO}_4^{3-} = \text{H}_3\text{PO}_4$	21.72
$\text{H}^+ + \text{F}^- = \text{HF}$	3.17

Figure 1 shows the calculation results of the buffer capacity  $\beta_{\text{Fe}}^S$  as a function of  $pH$  for the various iron (III) minerals. The analysis of the derived equations for the heterogeneous system showed that the increase in the total concentration  $C_{\text{Fe}}^0$  for the  $pH$  values above 4.5, as well as the nature of the mineral have an insignificant effect on the area of the buffer action of studied system due to the very low solubility of iron oxy - hydroxides minerals. The appearance of maxima on the curves  $\beta_H^S(pH)$  and  $\beta_{\text{Fe}}^S(pH)$  (Figures 1-3) is due to the dissociation process of carbonic acid with formation of  $\text{HCO}_3^-$  ions ( $pH = 6.36$ ) and  $\text{CO}_3^{2-}$  ( $pH = 10.34$ ).



**Figure 1. The curves of dependence of the buffer capacity  $\beta_H$  on  $pH$  for the system “Iron (III) mineral - saturated aqueous solution”. The used concentrations (mol L<sup>-1</sup>):**

$$C_{\text{Fe}}^0 = 1 \cdot 10^{-4}, \quad C_{\text{F}}^0 = 5 \cdot 10^{-6},$$

$$C_{\text{Org}}^0 = C_{\text{PO}_4}^0 = C_{\text{SO}_4}^0 = 1 \cdot 10^{-4},$$

$$C_{\text{CO}_3}^0 = 1 \cdot 10^{-3}$$

- 1 -  $\alpha\text{-Fe}_2\text{O}_3$  (hematite),
- 2 -  $\gamma\text{-Fe}_2\text{O}_3$  (maghemite),
- 3 -  $\varepsilon\text{-Fe}_2\text{O}_3$ ,
- 4 -  $\alpha\text{-FeOOH}$  (goethite),
- 5 -  $\gamma\text{-FeOOH}$  (lepidocrocite),
- 6 -  $\text{Fe}(\text{OH})_3$  (2-line ferrihydrite),
- 7 -  $\text{Fe}(\text{OH})_3$  (6-line ferrihydrite).

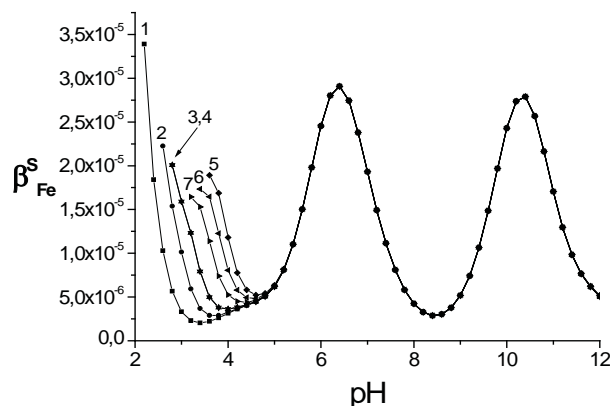


**Figure 2. The curves of dependence of the buffer capacity  $\beta_{Fe}^S$  on  $pH$  for the system “Iron (III) mineral - saturated aqueous solution”. The used concentrations (mol L<sup>-1</sup>):  $C_{Fe}^0 = 1 \cdot 10^{-4}$ ,  $C_F^0 = 5 \cdot 10^{-6}$ ,  $C_{Org}^0 = C_{PO_4}^0 = C_{SO_4}^0 = 1 \cdot 10^{-4}$ ,  $C_{CO_3}^0 = 1 \cdot 10^{-3}$ .  
1 -  $\alpha$ -Fe<sub>2</sub>O<sub>3</sub> (hematite), 2 -  $\gamma$ -Fe<sub>2</sub>O<sub>3</sub> (maghemite), 3 -  $\epsilon$ -Fe<sub>2</sub>O<sub>3</sub>, 4 -  $\alpha$ -FeOOH (goethite), 5 -  $\gamma$ -FeOOH (lepidocrocite), 6 - Fe(OH)<sub>3</sub> (2-line ferrihydrite), 7 - Fe(OH)<sub>3</sub> (6-line ferrihydrite).**

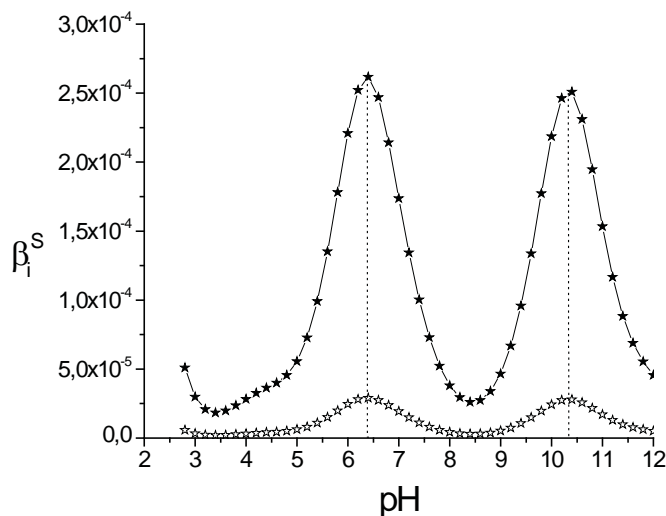
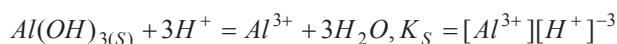


**Figure 3. Buffer capacities  $\beta_H^S$  (1) and  $\beta_{Fe}^S$  (2) versus  $pH$  for the system “Hematite - saturated aqueous solution”.**

**The used concentrations (mol L<sup>-1</sup>):  $C_{Fe}^0 = 1 \cdot 10^{-5}$ ,  $C_F^0 = 5 \cdot 10^{-6}$ ,  $C_{Org}^0 = C_{PO_4}^0 = C_{SO_4}^0 = 1 \cdot 10^{-4}$ ,  $C_{CO_3}^0 = 1 \cdot 10^{-3}$ .**

The iron (III) ions and its complexes have a significant contribution only in very acidic solutions up to  $pH$  4.5. The analysis of the data presented in Figures 2 and 3 allows us to conclude that the studied heterogeneous system has a buffer capacity in relation to ions of hydrogen and iron (III). We will note down that these relations are valid only in the presence of solid phases.

Another example of real natural system that we examined is “Gibbsite – saturated aqueous solution”. By increasing the acidity in aqueous solutions the content of aluminium grows quickly due to the interaction of the gibbsite with an acid:



An important interrelation between the buffer capacities of the heterogeneous system “Gibbsite  $Al(OH)_{3(s)}$  - saturated aqueous solution” system can be identified [53,54]:

$$\beta_H^S = 9\beta_{Al}^S \quad (33)$$



Besides the process of gibbsite dissolution, a set of possible equilibria in the system “*Mineral phase – natural water*”, listed in Table 2 has been taken into account [52]. The following composition of the heterogeneous system has been used for the calculations:  $C_{Al}^0 = 1 \cdot 10^{-4} \text{ mol L}^{-1}$ ,  $C_F^0 = 5 \cdot 10^{-6} \text{ mol L}^{-1}$ ,  $C_{Org}^0 = 1 \cdot 10^{-4} \text{ mol L}^{-1}$ ,  $C_{PO_4}^0 = 1 \cdot 10^{-4} \text{ mol L}^{-1}$ ,  $C_{SO_4}^0 = 1 \cdot 10^{-4} \text{ mol L}^{-1}$  and  $C_{CO_3}^0 = 1 \cdot 10^{-3} \text{ mol L}^{-1}$ . One can state that the influence of  $H^+$  in the studied  $pH$  interval may be neglected, and the  $OH^-$  ions exercise influence on  $\beta_H^S$  only at  $pH > 8.5$ . The aluminium ions and their hydroxocomplexes make a significant contribution in acid solutions up to  $pH$  5.5 and at  $pH > 8$  because of the predominance of the stable anionic hydroxocomplex  $Al(OH)_4^-$ . The results of the calculations of the buffer capacities  $\beta_H^S$  as a function of  $pH$  for different compositions of the heterogeneous mixture are shown in Figures 4–5. Obviously, an increase of the total concentration  $C_{Al}^0$  (Figure 4) augments the area of the buffer action because of the extension of the  $pH$  interval of the thermodynamic stability of the solid phase. At concentrations of fluoride  $C_F^0 = 5 \cdot 10^{-4} \text{ mol L}^{-1}$ , the  $\beta_H^S$  value increases sharply in the range of  $pH$  values of the gibbsite dissolution – formation with a simultaneous narrowing of the total  $pH$  range of the buffer action (Figure 5).

Table 2

Equilibrium constants and values of enthalpies ( $\Delta H$ ).

Equations of reactions	$\log K$	$\Delta H \text{ (cal mol}^{-1}\text{)}$
$Al^{3+} + H_2O = AlOH^{2+} + H^+$	-4.99	11900
$Al^{3+} + 2H_2O = Al(OH)_2^+ + 2H^+$	-10.00	22000
$Al^{3+} + 4H_2O = Al(OH)_4^- + 4H^+$	-23.00	44060
$Al(OH)_3(s) + 3H^+ = Al^{3+} + 3H_2O$	9.35	-22800
$Al^{3+} + F^- = AlF^{2+}$	7.02	1100
$Al^{3+} + 2F^- = AlF_2^+$	12.76	2000
$Al^{3+} + 3F^- = AlF_3$	17.03	2500
$Al^{3+} + 4F^- = AlF_4^-$	19.73	2200
$Al^{3+} + 5F^- = AlF_5^{2-}$	20.92	1800
$Al^{3+} + SO_4^{2-} = AlSO_4^+$	3.01	2150
$Al^{3+} + 2SO_4^{2-} = Al(SO_4)_2^-$	4.90	2840
$Al^{3+} + Org^{3-} = AlOrg$	8.39	—
$Al^{3+} + H^+ + Org^{3-} = AlHOrg^+$	13.09	—
$Org^{3-} + H^+ = HOrg^{2-}$	6.83	—
$Org^{3-} + 2H^+ = H_2Org^-$	12.73	—
$Org^{3-} + 3H^+ = H_3Org$	14.49	—
$H^+ + F^- = HF$	3.17	3460
$H_2O = H^+ + OH^-$	-14.00	13340
$2Al^{3+} + 2H_2O = Al_2(OH)_2^{4+} + 2H^+$	-6.3	—
$3Al^{3+} + 4H_2O = Al_3(OH)_4^{5+} + 4H^+$	-12.1	—
$Al^{3+} + H_2PO_4^- = AlH_2PO_4^{2+}$	3.1	—
$PO_4^{3-} + H^+ = HPO_4^{2-}$	12.0	—
$PO_4^{3-} + 2H^+ = H_2PO_4^-$	19.21	—
$PO_4^{3-} + 3H^+ = H_3PO_4$	21.36	—

Note: 1 cal = 4.184 J, Org - organic ligand, the „—” specifies the absence of experimental data.

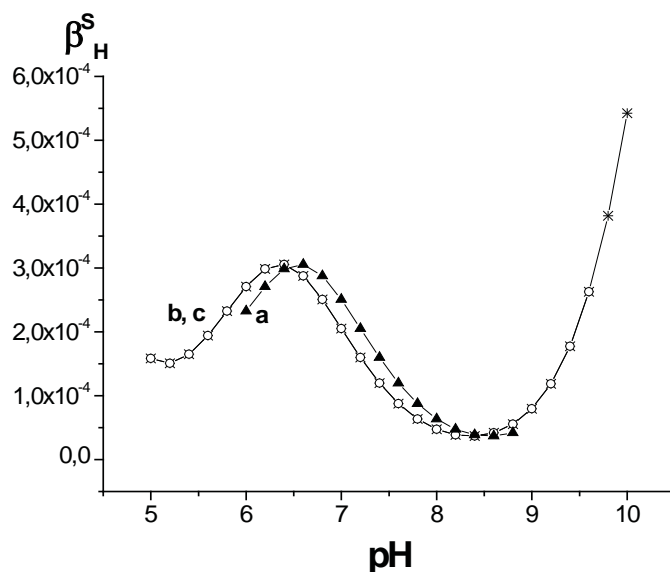


Figure 4. Buffer capacity  $\beta_H^S$  versus  $pH$  for the “Gibbsite - saturated aqueous solution” system.

Concentrations ( $\text{mol L}^{-1}$ ):

$C_{Al}^0$  : a -  $1 \cdot 10^{-3}$ , b -  $1 \cdot 10^{-4}$ , c -  $1 \cdot 10^{-5}$ ,  $C_F^0 = 5 \cdot 10^{-6}$ ,  $C_{Org}^0 = C_{PO_4}^0 = C_{SO_4}^0 = 1 \cdot 10^{-4}$ ,  $C_{CO_3}^0 = 1 \cdot 10^{-3}$ .

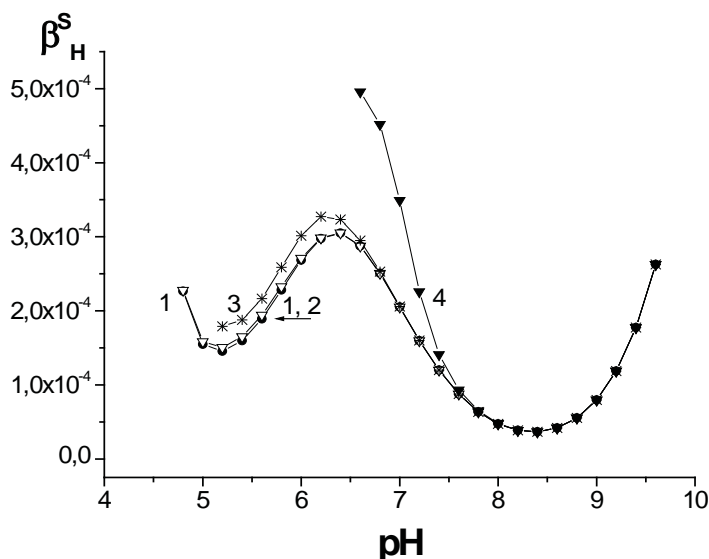


Figure 5. Buffer capacity  $\beta_H^S$  versus  $pH$  for the “Gibbsite - saturated aqueous solution” system.

Concentrations ( $\text{mol L}^{-1}$ ):

$C_F^0$  : 1 -  $5 \cdot 10^{-7}$ , 2 -  $5 \cdot 10^{-6}$ , 3 -  $5 \cdot 10^{-5}$ , 4 -  $5 \cdot 10^{-4}$ ,  $C_{Al}^0 = C_{Org}^0 = C_{PO_4}^0 = C_{SO_4}^0 = 1 \cdot 10^{-4}$ ,  $C_{CO_3}^0 = 1 \cdot 10^{-3}$ .

The dependences of  $\beta_H^S(pH)$  for different concentrations of carbonate ion are presented in Figure 6. By taking into account the contribution of equilibria including carbonate ion in the total buffer capacity  $\beta_H^S$ , the  $\beta_{CO_3}^H$  value was calculated separately. A comparison of the calculated curves shows that equilibria with  $CO_3^{2-}$  participation have a substantial contribution to  $\beta_H^S$  at a  $C_{CO_3}^0 > 1 \cdot 10^{-4} \text{ mol L}^{-1}$  (Figures 7a and 7b). The analysis of the obtained data

presented in Figures 4–7, taking into account Eq.(33) allows us to conclude that the investigated heterogeneous system has a considerable buffer capacity towards to aluminium as well.

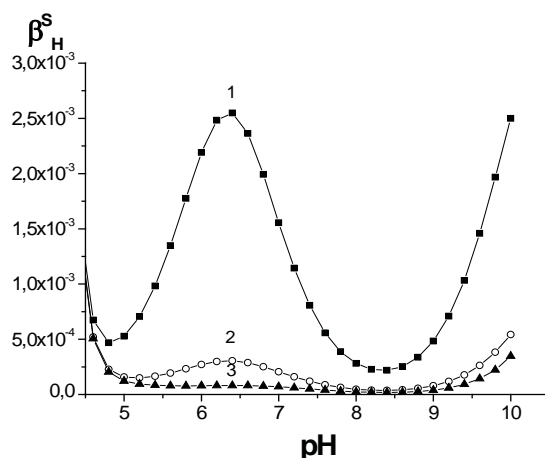


Figure 6. Buffer capacity  $\beta_H^S$  versus  $pH$  for the “Gibbsite - saturated aqueous solution” system.

Concentrations (mol L<sup>-1</sup>):

$C_{CO_3}^0$  : 1 –  $1 \cdot 10^{-2}$ , 2 –  $1 \cdot 10^{-3}$ , 3 –  $1 \cdot 10^{-4}$ ,  $C_{Al}^0 = C_{PO_4}^0 = C_{SO_4}^0 = 1 \cdot 10^{-4}$ ,  $C_F^0 = 5 \cdot 10^{-6}$ .

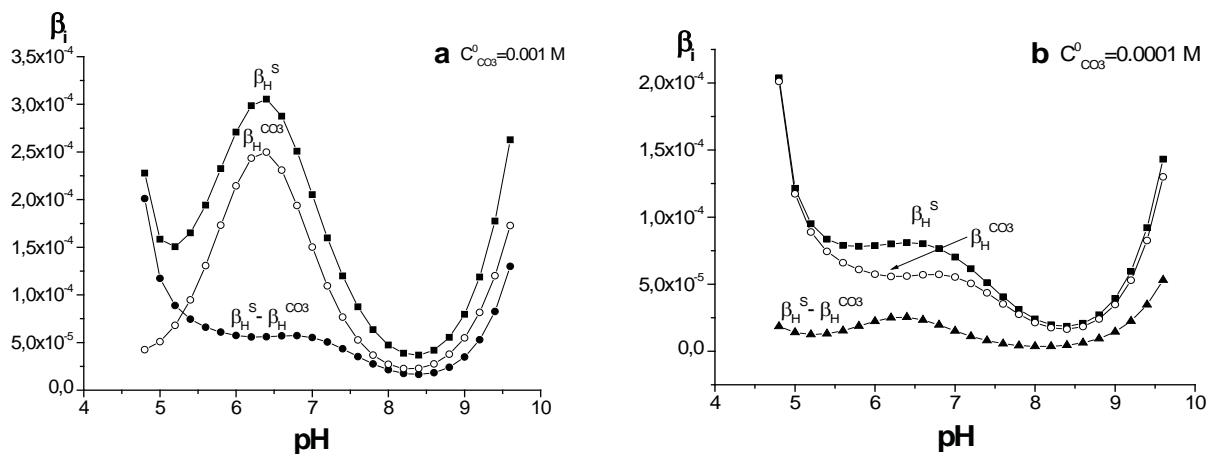


Figure 7. Total buffer capacity  $\beta_H^S$  versus  $pH$ , carbonate buffer capacity  $\beta_{CO_3}^H$  vs.  $pH$  and their difference

$\beta_H^S - \beta_{CO_3}^H$  for the “Gibbsite - saturated aqueous solution” system.

Concentrations (mol L<sup>-1</sup>):  $C_{CO_3}^0$  : a –  $1 \cdot 10^{-3}$ , b –  $1 \cdot 10^{-4}$ ,  $C_{Al}^0 = C_{PO_4}^0 = C_{SO_4}^0 = 1 \cdot 10^{-4}$ ,  $C_F^0 = 5 \cdot 10^{-6}$ .

The influence of temperature on the value of the buffer capacity was also studied [55]. The results of the calculations are presented in Figure 8. The equilibrium constants for different temperatures have been estimated by the Van't Hoff equation.

$$\log K_2 = \log K_1 + (1/T_1 - 1/T_2) \Delta H / 2.303R$$

The necessary values of enthalpies ( $\Delta H$ ) are listed in Table 2.  $T_1$  was set to 298 K = 25 °C. It was assumed that the temperature insignificantly influences the  $\Delta H$  values inside the investigated temperature range. An analysis of the curves in Figure 8 shows that the buffer capacity increases with a temperature decrease, whereas the  $pH$  interval of 5.5 – 7.0 of the maximum values of the buffer capacity displaces slightly.

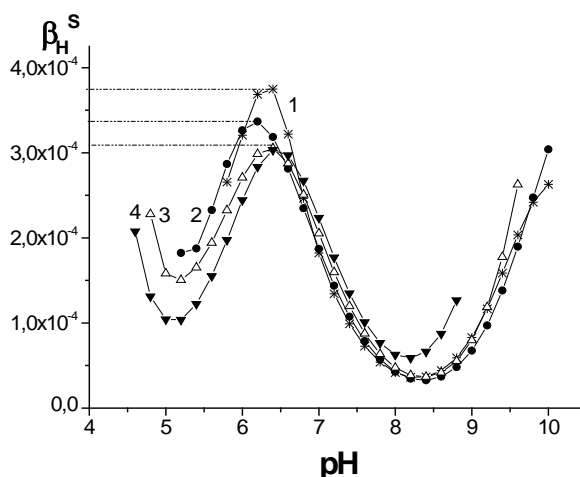


**Figure 8. Buffer capacity  $\beta_H^S$  versus  $pH$  for the “Gibbsite - saturated aqueous solution” system at different temperatures ( $t$ , °C): (1)  $-5$ , (2)  $+10$ , (3)  $+25$  and (4)  $+40$ . Concentrations ( $\text{mol L}^{-1}$ ):  $C_{\text{CO}_3}^0 = 1 \cdot 10^{-3}$ ,  $C_{\text{Al}}^0 = C_{\text{PO}_4}^0 = C_{\text{Org}}^0 = C_{\text{SO}_4}^0 = 1 \cdot 10^{-4}$ ,  $C_{\text{F}}^0 = 5 \cdot 10^{-6}$ .**

### **Buffer properties for liquid two-phase acid-base buffer systems**

#### *Buffer with mono- and diprotic acids*

The theoretically calculated and experimentally measured dependences of the buffer capacity on  $pH$  in the case of two-phase system 1-octanol – water for monoprotic  $n$ -hexanoic acid and diprotic 1,2-benzenedicarboxylic acid are shown in Figure 9 and Figure 10, respectively. Experimental data [45,56] were obtained at 25 °C and constant ionic strength. For both systems, the experimental data correlate well with the theoretical curves, calculated by Eqs.(27 – 28) that confirms their correctness. The values in Figures 9 and 10 testify the validity of Eq.(29). (The necessary equilibrium constants were taken from [45,56].)

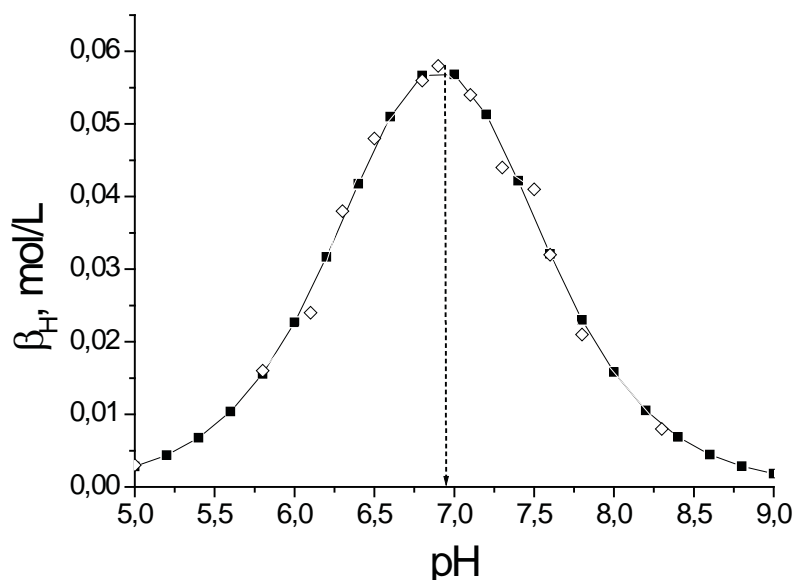


**Figure 9. Buffer capacity versus  $pH$  for two-phase system containing  $n$ -hexanoic acid  $HA$  and 1-octanol: (■) the calculated values; (◇) experimental data [56]; 1-octanol : water = 1:1;  $C_A^0 = 0.1 \text{ mol L}^{-1}$ ,  $I = 0$ ,  $t = 25 \text{ °C}$ .**

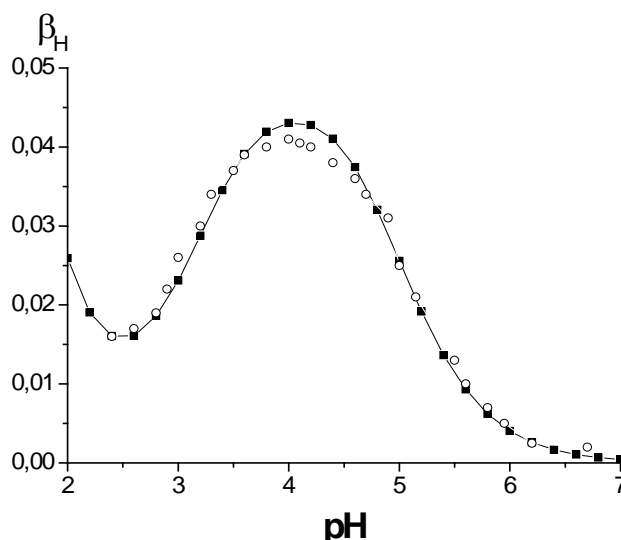


**Figure 10.** Dependence of buffer capacity on  $pH$  for two-phase system containing 1,2-benzenedicarboxylic acid and 1-octanol: (■) calculated values; (○) experimental data [45]; 1-octanol : water=1:1;  $C_A^0 = 0.0488 \text{ mol L}^{-1}$ ,  $I = 1 \text{ (NaCl)}$ ,  $t = 25 \text{ }^\circ\text{C}$ .

*Two-phase buffers with monoprotic acids in which dimerization occurs*

Mono-component systems: propanoic acid – water – benzene (I) and decanoic acid – water – benzene (II): The numerical values of the equilibrium constants used for calculating the theoretical buffer curves as well as the experimental data were taken from [56]. The theoretical and experimental data are presented in Figure 11 (a,b). It can be seen that the theoretical curves are in good agreement with experimental values.

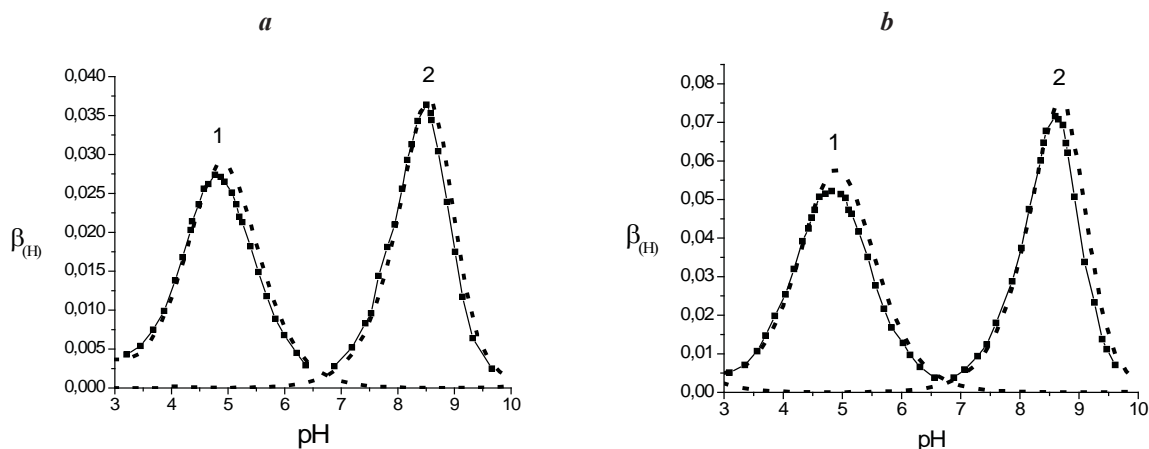


**Figure 11.** Buffer capacity  $\beta_H$  versus  $pH$  for mono-component two-phase systems with propanoic (a) and decanoic (b) acids,  $C_A^0 = 0.05 \text{ mol L}^{-1}$  (a) and  $C_A^0 = 0.1 \text{ mol L}^{-1}$  (b) and  $\alpha = 1$ ; (■) – experimental values, dotted lines – experimental curves,  $I = 0.1$ ,  $t = 25 \text{ }^\circ\text{C}$ .

On Figure 12 the functional dependence  $\beta_H = f(pH)$  for (2,4-dichlorophenoxy)acetic acid for aqueous solution and two-phase mixture by means of different organic solvents is graphically illustrated. One can see that high  $\beta_H$  values within a large  $pH$  range ( $3.75 \div 5.75$ ) can be assured by using different organic solvents [57]. The necessary equilibrium data were taken from [58].

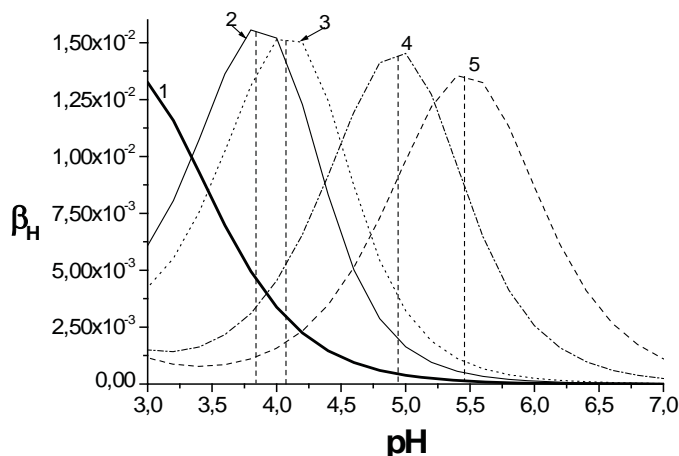


**Figure 12. Buffer capacity  $\beta_H$  versus  $pH$  for mono-component two-phase systems with (2,4-dichlorophenoxy) acetic acid,  $C_A^0 = 0.05 \text{ mol L}^{-1}$ ,  $\alpha = 1$ ,  $t = 25^\circ\text{C}$  for different organic solvents: 1 – no solvent; 2 – ethylbenzene; 3 – 1-octanol; 4 – chlorbenzene; 5 – nitrobenzene.**

*pH and pA buffer properties of two-component system in which mixed dimer occurs*

The authors [56] found that the rule of additivity for calculating the total buffer capacity as a sum of separate contributions for this system is not valid. As a result, there are some substantial deviations of the theoretical curves from experimental data within the interval of  $pH$  from 4 to 7. The experimental data for this system, along with the calculated theoretical curve are presented in Figure 13. As one can see, the experimental values  $\beta_H = f(pH)$  are in good agreement with those calculated, contrasting to the results received by authors [56]. Thus, the experiment confirms the validity of our developed theoretical approach.

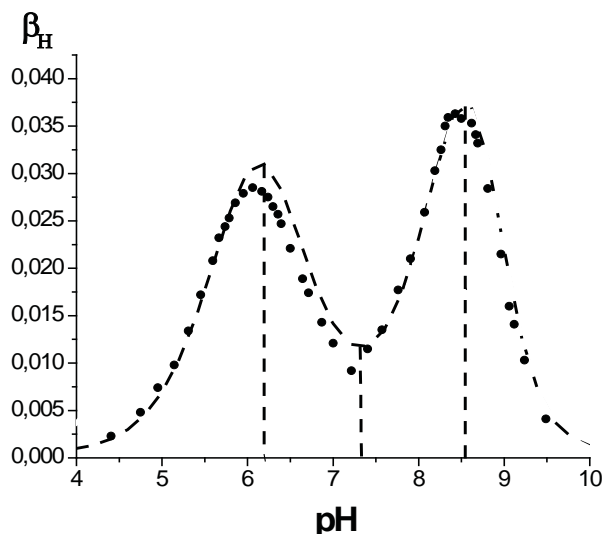


**Figure 13. Experimental data [56] (•) and calculated values (---) for  $\beta_H(pH)$  as a sum of the contributions of separate acids for the two-component two-phase buffer system containing hexanoic and decanoic acids.  $V(C_6H_6) \div V(H_2O) = 1 \div 1$ ,  $C_A^0 = C_B^0 = 0.05 \text{ mol L}^{-1}$ ,  $I = 0.1$ ,  $t = 25^\circ\text{C}$ .**

In Figure 14 the curves of dependences  $\beta_H = f(pH)$ ,  $\beta_A = f(pH)$  and  $\beta_B = f(pH)$  are presented. From here it is possible to conclude, that the buffer capacity of two-phase mixtures containing an acid capable to form homogeneous and mixed dimers in the organic solvent, is much higher with respect to anions, than to proton, i.e.  $\beta_A(\beta_B) > \beta_H$ . At the same time, the maximum value of both functions is registered in the conditions of predominance of the un-bonded anion in aqueous phase.

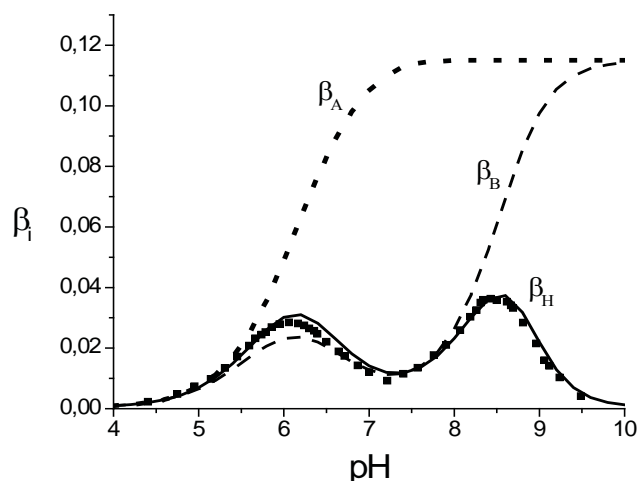


**Figure 14.** Curves  $\beta_H = f(pH)$ ,  $\beta_A = f(pH)$  and  $\beta_B = f(pH)$  for the two-component two-phase buffer system, containing hexanoic and decanoic acids.  $V(C_6H_6) \div V(H_2O) = 1 \div 1$ ,  $C_A^0 = C_B^0 = 0.05 \text{ mol L}^{-1}$ ,  $I = 0.1$ ,  $t = 25^\circ\text{C}$ .

On Figure15 the functional dependence  $\beta_A = f(pA)$  for (2.4-dichlorophenoxy)acetic acid for aqueous solution and water-1-octanol mixture is depicted. One can notice that the presence of organic solvent amplifies significantly (approximately by 70 times) the  $\beta_A$  value at  $pA = 5.4$ . Therefore, two-phase mixtures can be successfully used for designing new buffers with respect to any component for investigated systems. The developed approach can be expanded to other, more complicated systems, containing metal-ligand complexes.

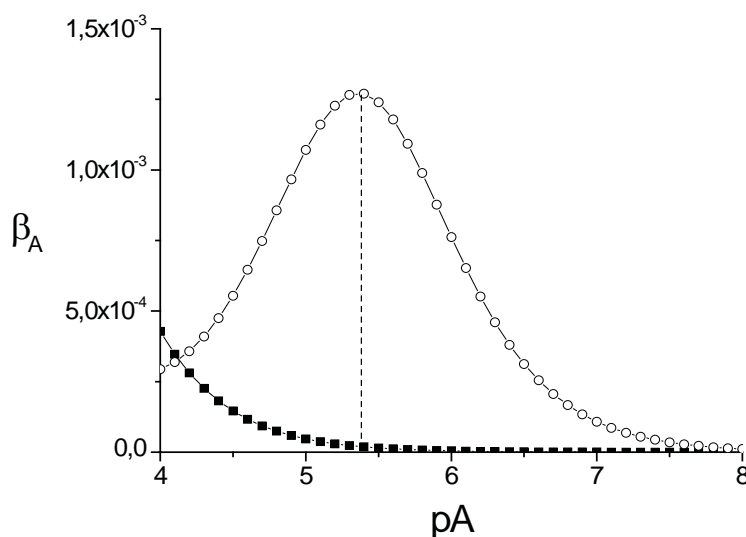


**Figure 15.** Buffer capacity  $\beta_A$  versus  $pA$  for the mono-component system with (2.4-dichlorophenoxy) acetic acid in water (curve 1) and water-1-octanol mixture (curve 2),  $C_H^0 = 0.005 \text{ mol L}^{-1}$ ,  $\alpha = 1$ ;  $t = 25^\circ\text{C}$ .

## Conclusions

The analyzed heterogeneous systems manifest buffer actions towards protons, cations or anions of weak bases or acids. The deduced analytical expressions for buffer capacities in respect to all ions of distributed species between two immiscible liquids are reported. For all investigated systems a relation of proportionality between buffer capacities is found. On the basis of the analysis of found identities it can be concluded that it is sufficient to measure only the  $\beta_H$  value, while the quantity  $\beta_A$  can be calculated from a set of expressions identities derived in this work. This conclusion is especially valuable since for the  $\beta_H$  measurement it is necessary to determine potentiometrically the  $pH$  values while for the  $\beta_A$  determination it is required to measure the  $pA = -\log[A]$  values. It is known, that the  $pH$ -metric method is



much more precisely and does not require special ion-selective electrodes as for  $pA$  measurement, which have been developed so far only for a few number of anions. The experimental evidence completely confirms the validity of the derived equations. The relation of proportionality between the buffer capacities in respect to all ions of the species distributed between phases has been also found for the heterogeneous systems of the type “Solid phase-saturated aqueous solution”, which serves as a proof of the generality of this phenomenon. It is demonstrated that the  $pH_{max}$  value of the maximal buffer capacity shifts for two-phase system in comparison with classical aqueous buffer mixtures by  $\log(I + P(HA))$  which depends mainly on the nature of organic solvent. Also, it has been explained the nature of synergic effect of the total buffer action of heterogeneous mixtures. Generally, the mixture of acids and bases shows a cumulative effect, but in the case of interaction of distributed species in the organic phase, it manifests a synergic effect, e.g. the buffer action amplifies. It is finally worth noting that heterogeneous buffer systems can be created on the basis of well-known species and do not require any special installations. The deduced relations may be used for search and design of new ion-molecular two-phase buffers with required properties. Owing to the described properties, the considered heterogeneous systems can find widespread use in various areas of chemical and biochemical researches, especially in analytical chemistry, pharmacology, pharmaceuticals, medical industry and synthetic organic chemistry.

## References

- Roy, R.N.; Roy, L.N.; Stegner, J.M.; Sechler, S.A.; Jenkins, A.L.; Krishchenko, R.; Henson, I.B. Buffer standards for the physiological pH of N, N - bis (2- hydroxyethyl) - 2-aminoethanesulfonic acid (BES) from (278.15 to 328.15) K. *Electroanalytical Chemistry*, 2011, 663, pp. 8-13.
- Dolejs, D.; Wagner, T. Thermodynamic modeling of non-ideal mineral–fluid equilibria in the system Si–Al–Fe–Mg–Ca–Na–K–H–O–Cl at elevated temperatures and pressures: Implications for hydrothermal mass transfer in granitic rocks. *Geochimica and Cosmochimica Acta*, 2008, 72, pp. 526-553.
- Roy, L.N.; Roy, R.N.; Wollen, J.T.; Harmon, M.A.; Stegner, J.M.; Shah, A.A.; Henson, I.B. Buffer standards for the biological pH of the amino acid n - [2 - hydroxyethyl] piperazine-n' - [3 - propanesulfonic acid], HEPPS, from (278.15 to 328.15) K. *Journal of Chemical and Engineering Data*, 2011, 56, pp. 4126-4132.
- Kay, J.W.; Steven, R.J.; McGuigan, J.A. S.; Elder, H.Y. Automatic determination of ligand purity and apparent dissociation constant ( $K_{app}$ ) in  $Ca^{2+}/Mg^{2+}$  buffer solutions and the  $K_{app}$  for  $Ca^{2+}/Mg^{2+}$  anion binding in physiological solutions from  $Ca^{2+}/Mg^{2+}$  - macroelectrode measurements. *Computers in Biology and Medicine*, 2008, 38, pp. 101-110.
- Totsche, O.; Fyson, A.; Kalin, M.; Steinberg, C.E.W. Titration Curves: A useful instrument for assessing the buffer systems of acidic mining waters. *Environmental Science and Pollution Research*, 2006, 13, pp. 215-224.
- Dougherty, D.P.; Neta, C.E.; McFeeters, R.F.; Lubkin, S.R.; Breidt, F.J. Semi-mechanistic partial buffer approach to modelling pH, the buffer properties, and the distribution of ionic species in complex solutions. *Journal of Agricultural and Food Chemistry*, 2006, 54, pp. 6021-6029.
- Upadhyay, N.; Majestic, B.J.; Herckes, P. Solubility and speciation of atmospheric iron in buffer systems simulating cloud conditions. *Atmospheric Environment*, 2011, 45, pp. 1858-1866.
- Perrin, D.D.; Dempsey B. Buffers for pH and metal ion control. Chapman and Hall: London, 1974, 175 p.
- Komari, N.P. Chemical metrology. Ionic heterogeneous equilibria. Vishcha Shkola: Kharkov, 1984, 208 p. (in Russian).
- Povar, I. On homogeneous ion buffer systems. *Russian Journal of Inorganic Chemistry*, 2000, 45(10), pp. 1628-1631.
- Povar, I.; Spinu, O. On the theory of homogeneous metal-ligand buffers. Abstracts of communications of The International Conference dedicated to the 55th anniversary from the foundation of the Institute of Chemistry of the Academy of Sciences of Moldova. Chisinau, Moldova, May 28-30, 2014, p. 174.
- Charykov, A.K.; Osipov N.N. Carbonic acids and carboxylate complexes in chemical analysis. Khimia: Leningrad, 1991, pp. 204–207 (in Russian).
- Pfendt, L.B. Two-phase liquid and solid-liquid pH buffers based on solubility equilibria: Theoretical considerations. *Analyst*, 1995, 120, pp. 2129-2144.
- Povar, I.; Rusu, V. Buffer capacity of heterogeneous chemical equilibria in natural waters. *Canadian Journal of Chemistry*, 2012, 90, pp. 395-402.
- Fishtik, I.; Povar, I. Buffer Capacity in Multiple Chemical Reaction Systems Involving Solid Phases. *Canadian Journal of Chemistry*, 2006, 84, pp. 1036-1044.
- Povar, I. Buffering properties of heterogeneous water-salt systems in relation to the components of a low-solubility precipitate. *Russian Journal of Inorganic Chemistry*, 2000, 45, pp. 1632 – 1636.
- Povar, I. Method for graphic representation of heterogeneous chemical equilibria in systems sparingly soluble compound-complexing agent-aqueous solution. *Russian Journal of Inorganic Chemistry*, 1997, 42, pp. 607-612.
- Povar, I.; Luca, C. Considerations regarding the ionic-molecular buffer solutions. *Revue de Chimie*, 2003, 54, pp. 312-316 (in Romanian).

19. Povar, I.; Spinu, O. Quantitative theory of the buffer action of soil minerals. Collection of scientific papers of the Conference with International Participation "Chernozems of Moldova – development, protecting and restoring their fertility", dedicated to the 60th anniversary of the founding of the IPAPS "N.Dimo". Chisinau, Republic of Moldova, September 12-13, 2013, pp. 272-277.
20. Povar, I. Buffer properties of the system such as slightly soluble salt - saturated solution in respect to precipitate components. Abstracts of the XXII-th Session of Scientific Communications. Olanesti, Romania, 23-25 October, 1996, V. 2, pp. 685- 690 (in Romanian).
21. Spinu, O.; Povar, I. Relationships between buffer capacities of chemical components in heterogeneous natural systems. Book of Abstracts International Conference on Physical Chemistry (ROMPHYSICHEM 15). Bucharest, Romania, September 11-13, 2013, p. 153.
22. Van Breemen, N.; Wielemaker, W.G. Buffer intensities and equilibrium pH of minerals and soils: 1. The Contribution of minerals and aqueous carbonate to pH buffering. *Soil Science Society of America Journal*, 1974, 38, pp. 55-60.
23. Stumm, W.; Morgan, J.J. *Aquatic Chemistry*. 3rd Edition. Wiley: New York, 1995, 1040 p.
24. Filep, D.; Radly, M. The forms of acidity and acid-base buffer action of soils. *Pedology*, 1989, 12, pp. 48-59 (in Russian).
25. Lozovik, P.A.; Potapova, I. Yu.; Bantsevich, T.V. Buffer capacity of surface waters as a geochemical factor of their resistance to acidification. *Geochemistry International*, 2007, 45, pp. 938-944.
26. Langmuir, D. *Aqueous Environmental Geochemistry*. Prentice Hall: New Jersey, 1997, 600 p.
27. Poznyak, S.P.; Gamkalo, M.Z. Acid-base buffer action of Ukrainian Carpathians. *Pedology*, 2001, 6, pp. 660-669.
28. Sokolova, T.A.; Motuzova, G.V.; Malinina, M.S.; Obukhovskaya, T.D. Chemical basis of soil buffer action. MGU: Moscow, 1991, 106 p. (in Russian).
29. Povar, I.; Spinu, O. Buffer properties of soil minerals. Part.1 Theoretical Aspects. *Chemistry Journal of Moldova*, 2013, 8(2), pp. 67-72.
30. Povar, I.; Spinu, O. Buffer capacity of aquatic ecosystems as a geochemical factor of their resistance to pollution. Collected papers of the International Scientific Conference "Actual Problems of Search and Environmental Geochemistry". Kiev, Ukraine, July 1 - 2, 2014, pp. 94-96.
31. Povar, I.; Spinu, O. Thermodynamics of complex chemical equilibria in heterogeneous multicomponent systems. Printing House of the Academy of Sciences of Moldova: Chisinau, 2014, 452 p. (in Romanian).
32. Spinu, O.; Povar, I. Buffer properties of the system "calcium carbonate – soil solution". Collection of scientific papers of the Conference with International Participation "Chernozems of Moldova – development, protecting and restoring their fertility", dedicated to the 60th anniversary of the founding of the IPAPS "N.Dimo". Chisinau, Republic of Moldova, September 12-13, 2013, pp. 318-322.
33. Zaytseva T.F. The buffer action of soils and the questions of their diagnostic. *Bulletin of Academy of Sciences of the USSR, Series of Biological Sciences*, 1987, 14, pp. 69-80 (in Russian).
34. Samohvalova, V.; Spinu, O.; Povar, I. Buffering soil regarding the content of heavy metals. Collected articles of IX Congress of Soil Science and Agrochemistry. Nikolayev, Ukraine, June 30 - July 4, 2014, pp. 149-151.
35. Povar, I. Ion Buffer Capacity Approach as a tool for the Assessment of Long-Term Effects in Natural Attenuation/ Intrinsic Chemical Remediation of Metals in Contaminated Groundwaters, Soils and Sediments. Proceeding of the International Conference "Trans boundary River Basin Management and International Cooperation for Healthy Dniester". Odessa, Ukraine, 30 September - 1 October, 2009, pp. 215-219.
36. Spinu, O.; Povar, I. Use of the buffer capacity theory for evaluating the resistance of aquatic heterogeneous ecosystems to changes of metal contaminant levels. Book of Abstracts of International Symposium „The Environment and Industry” – SIMI. Bucharest, Romania, October 28-30, 2013, pp. 141-142.
37. Spinu, O.; Povar, I. Application of the buffer theory for natural remediation of ionic pollutants in aquatic ecosystems. Book of Abstracts of WASTE net 2015 Scientific Conference "Sustainable Solutions to Wastewater Management: Maximizing the Impact of Territorial Co-Operation". Kavalla, Greece, 19th - 21st June, 2015, p. 34.
38. Povar, I.; Spinu, O. The use of the buffer capacity theory for thermodynamic assessment of the natural control of heavy metal contents in polluted ecosystems. Book of abstracts of XIX International Conference on Chemical Thermodynamics RCCT-2013. Moscow, Russia, June 24-28, 2013, p. 53.
39. Povar, I. Methodology of Chemical Buffer Capacity Theory as an Instrument for Evaluating the Attenuation and Natural Remediation of Ionic Pollutants in Contaminated Aquatic Ecosystems. Proceeding of the International Symposium „The Environment and Industry” – SIMI. Bucharest, Romania, 28-30 October, 2009, pp. 315- 320.
40. Povar, I.; Rusu, V.; Spinu, O. Buffer capacity approach as a tool for assessing the fate of ionic pollutants in aquatic ecosystems. Abstracts of the V-th International Conference "Ecological Chemistry". Chisinau, Moldova, 2-3 March, 2012, p. 57.
41. Garcia-Gil, J.C.; Ceppi, S.B.; Velasco, M.I.; Polo, A.; Senesi, N. Long-term effects of amendment with municipal solid waste compost on the elemental and acidic functional group composition and pH-buffer capacity of soil humic acids. *Geoderma*, 2004, 121, pp. 135-142.

42. Descourvières, C.; Niels, H.; Bradley, M.; Patterson, C. O.; Henning P. Geochemical controls on sediment reactivity and buffering processes in a heterogeneous aquifer. *Applied Geochemistry*, 2010, 25, pp. 261-275.
43. Povar, I. Thermodynamic calculation of the minimum solubility pH of slightly soluble oxides and hydroxides in polynuclear hydrolysis of metal ion. *Ukrainian Chemical Journal*, 1994, 60, pp. 371-378 (in Russian).
44. Povar I.; Rusu V. Aluminium heterogeneous speciation in natural waters. *Canadian Journal of Chemistry*, 2012, 90, pp. 326-332.
45. Janjić, T.J.; Milosavljević, E.B.; Nanayakkara, W.; Srdanovic, M. K. Two-phase buffer systems with diprotic acids. *Analytica Chimica Acta*, 1983, 152, pp. 229-237.
46. Povar, I.; Spinu, O. The influence of mixed dimerization on buffering actions in two-phase liquid systems. Abstracts of communications of The International Conference dedicated to the 55th anniversary from the foundation of the Institute of Chemistry of the Academy of Sciences of Moldova. Chisinau, Moldova, May 28-30, 2014, p. 172.
47. Povar, I.; Spinu, O. How to amplify the buffer capacity by mixing organic solvents with an aqueous solution. Abstracts of communications of The International Conference dedicated to the 55th anniversary from the foundation of the Institute of Chemistry of the Academy of Sciences of Moldova. Chisinau, Moldova, May 28-30, 2014, p. 173.
48. Mukerjee, P.; Ostrow, J.D. Effects of added dimethylsulfoxide on  $pK_a$  values of uncharged organic acids and pH values of aqueous buffers. *Tetrahedron Letters*, 1998, 39, pp. 423-426.
49. Barbosa, J.; Barron, D.; Buti, S.; Marques, I. Assignment of  $pH_s$  values of reference buffer solutions for standardization of potentiometric sensors in THF–water. *Polyhedron*, 1999, 18, pp. 3361-3367.
50. Friberg, L.; Nordberg, G.F.; Vouk, V.B. Handbook on the toxicology of metals. Vol. II. Elsevier: Amsterdam, 1986, pp. 276-297.
51. Povar, I. Buffer properties of heterogeneous systems containing sparingly soluble acids and metal hydroxides. *Russian Journal of Inorganic Chemistry*, 1996, 41, pp. 1167-1172.
52. Allison Geoscience Consultants. MINTEQA2/PRODEFA2, A Geochemical Assessment Model for Environmental Systems: User Manual Supplement for Version 4.0. Inc. Flowery Branch: Georgia, 1998.
53. Povar, I.; Spinu, O. Buffer capacity for heterogeneous aqueous systems. Abstracts of the V-th International Conference “Ecological Chemistry”. Chisinau, Moldova, March 2-3, 2012, p. 56.
54. Povar, I. Thermodynamics of the Complex Chemical Equilibria in Heterogeneous Systems “Solid Phase - Multicomponent Aqueous Solution”. D.Sc. Thesis, Kishinev, Moldova, 1998 (in Russian and Romanian).
55. Povar I. Relationship between the temperature coefficients of the equilibrium concentration of the components and the buffer properties of a system. *Russian Journal of Inorganic Chemistry*, 1995, 40, pp. 668- 671.
56. Janjić, T.J.; Milosavljević, E.B. Two-phase buffer systems in which acid dimerization occurs in the organic phase. *Analitica and Chimica Acta*, 1980, 120, pp. 101-109.
57. Povar, I.; Spinu, O. Acid-Base Buffer Properties of Heterogeneous Multicomponent Extraction Systems. *Solvent Extraction and Ion Exchange*, 2015, 33(2), pp. 196-209.
58. Kalemkiewicz, J.; Szlachta, J. Studies on the Physical Chemistry of (2,4-Dichlorophenoxy) acetic Acid in Two-phase Systems Organic Solvent-Water. *Journal of Solution Chemistry*, 2007, 36, pp. 211-220.

## STUDY OF STABLE NITROGEN FORMS IN NATURAL SURFACE WATERS IN THE PRESENCE OF MINERAL SUBSTRATES

Petru Spataru<sup>a\*</sup>, Igor Povar<sup>a</sup>, Elena Mosanu<sup>b</sup>, Ana Trancalan<sup>a</sup>

<sup>a</sup>*Institute of Chemistry of Academy of Sciences of Moldova, 3, Academiei str., Chisinau MD-2028, Republic of Moldova*

<sup>b</sup>*Institute of Ecology and Geography of Academy of Sciences of Moldova, 1, Academiei str., Chisinau MD-2028, Republic of Moldova*

\*e-mail: spatarupetru@yahoo.com

**Abstract.** The influence of substrates on the oxidation of reduced toxic forms of nitrogen in river water was investigated by laboratory modelling. Granite and expanded clay accelerate the oxidation of ammonium and nitrite ions from 2 to 4 times. The presence of calcium carbonate in water hinders the oxidation of nitrogen in the polluted water.

**Keywords:** granite, expanded clay, calcium carbonate, ammonium, nitrite.

*Received: May 2014/ Revised final: September 2015/ Accepted: November 2015*

### Introduction

Experimental data regarding mineral forms of nitrogen, hydrochemistry research and water quality of large and small rivers in the Republic of Moldova have been published in a number of reviews [1,2]. A key reason for the research of mineral nitrogen is the toxicity of the different forms of its mineral and especially reduced forms. A bibliographic review shows that for a wide range of bacteria, in contrast to the situation in animal [3] and plant cells [4,5], ammonium is not toxic, even up to 1 mol/L of synthetic solutions [6]. This happens because the most bacteria prefer ammonium as a nitrogen source; some species even produce ammonium ion, for example *N<sub>2</sub>-fixing Rhizobia Cyanobacteria* and *Proteolytic Clostridia* produce ammonium through the fermentation of aminoacids. Resistance to ammonium is a common property in terms of bacteria [6]. However, nitrites are highly toxic to humans, flora and fauna, being an important concern regarding water quality. Nitrites are also involved in the pathology of gastric cancer [7,8] and are a possible cause of migraines [9]; they also compromise the binding capacity of oxygen in the blood and may result in respiratory deficiencies of aquatic animals and humans [10,11]. Understanding the toxicity of reduced forms of nitrogen requires the identification of methods of enhancing the oxidation of the nitrification process. Changing forms of nitrogen in surface water objects have been extensively studied. Pollution sources related to human activities have an obvious impact on the processes of nitrification and denitrification (oxidation of ammonia, nitrite and nitrate reduction etc.). Hu X.M. et al. reported the removal rates of  $\text{NH}_4^+\text{-N}$  during the nitrification-denitrification process and the total nitrogen (TN) reached 94% and 82%, respectively. From the mass balance, it followed that 87% of  $\text{NH}_4^+\text{-N}$  was removed by shortcut nitrification [12]. In a series of previous publications the process of the oxidation of reduced forms of nitrogen in surface water using pebbles, polymer film and aeration was investigated [13]. These papers reported changes of nitrogen forms in surface waters. The gravel and polymeric film in addition with aeration have the effect of decreasing the concentration of ammonium ions in water. Pebbles and polymeric film speed the oxidation of ammonium, while aeration diminishes its quantity in another way. This research is a continuation of the aforementioned studies.

### Materials and methods

In 2012, a number of water samples were taken from the Nistru River in May and its tributaries (rivulet near the Racovatul de Sud village in January, rivulet near the Cunicea village in May) and from the Prut River in June, as well as from the Isnovat rivulet in October. The tests of natural water were performed according to ISO methods published in specialized literature [14-19]. Laboratory trials were initiated in glass vessels and respected the minimum recommended water-sample model volume (3L). The same volume and conditions for the whole series of samples from laboratory simulation experience are essential [20]. A solution of  $(\text{NH}_4)_2\text{SO}_4$  or  $\text{NH}_4\text{Cl}$  was added to each sample to obtain the ammonium ion concentrations between 1.75 and 2.5 mg/L.

The substrate constituted a fourth part of the total volume of each water samples. It was used 1.0 - 2.5 mm of the substrate granulometric fraction. In the samples 2 grams of chemically pure fine powder of  $\text{CaCO}_3$  were added. The purity of all used substances corresponded to the ISO requirements [14-18]. Model water samples were kept in natural lighting and away from direct sunlight. Laboratory simulations were performed under the static conditions. The stirring was done after each test series. The tests were completed at the same day time.

Contents of ammonium and nitrite ions were determined by standard methods (Nessler and Griess reagents), using the HACH Spectrophotometer DR/2500 and UV-VIS. The contents of ammonium and nitrites in natural water were taken into account in all laboratory simulations.



## Results and discussion

The study has been carried out both in small and large rivers, in sections with different pollution levels. The process of oxidation of reduced nitrogen in water from the rivulet near the Racovatul de Sud village, collected in January with granite and clay porous substrates, has been experimentally proved.

The presence of granite and clay foam accelerates the oxidation of ammonium ions to the level below its maximum allowable concentration (MAC) during 7-8 days, and under the limit of quantification by 11 days (Figure 1a). Ammonium ions oxidation in the presence of granite has an insignificant delay compared with that in the presence of expanded clay samples, but the formation of nitrite ions and its decreasing concentrations in the same samples delay by 3-4 days, exceeding MAC of about 1 mg/L (Figure 1b). The nitrite concentration in reference sample under the same conditions reaches maximum with a delay of 31 days, after which it decreases and subsequently begins again to raise. After 59 days, within the realized simulation in the reference samples (without substrates) the significant final reduction of  $\text{NO}_2^-$  does not achieve. Multiple laboratory simulations of water from different rivers in winter conditions, similar to reference samples, were carried out to ensure that braking reduced nitrogen oxidation in winter samples was not an incidentally event. In the same way the impact of granite and keramzite was tested. This blocking effect is evident for both of cases of ammonium oxidation and more obvious of the oxidation stage of nitrites to nitrates. We should mention after 20-30 days there have not been registered any significant changes, even the results presented below were obtained in 59 days.

Spring samples from the Nistru River and the rivulet near the Cunicea village have been investigated by means of a similar model, using both water samples in the presence and absence of  $\text{CaCO}_3$ . The changes described in Figure 2a show that in the presence of  $\text{CaCO}_3$  the braking of the ammonium ions oxidation takes place. The decreasing nitrite amount due to its slow formation is similar in the water samples taken from the Nistru River, section Varancau.

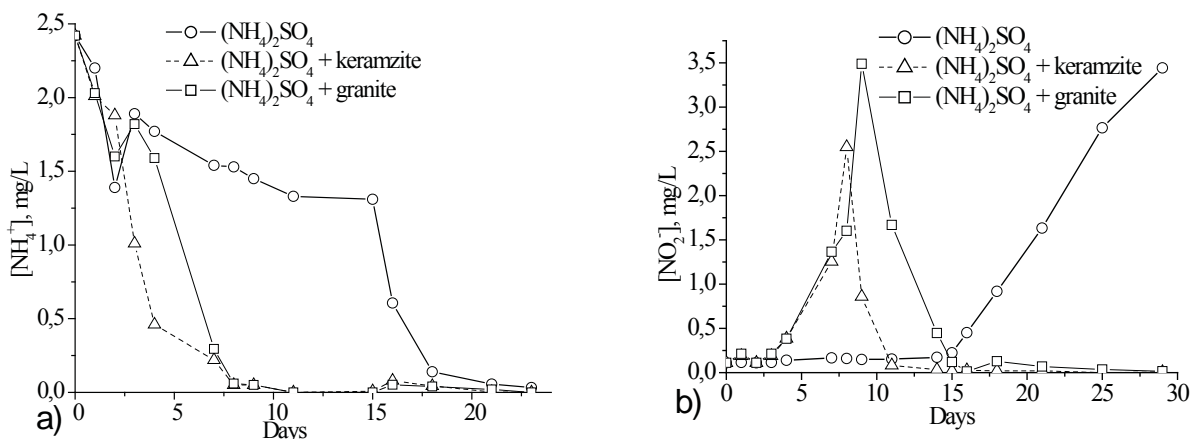


**Figure 1. Dynamics of ammonium ion (a) and nitrite ion (b) concentrations in water samples collected from the rivulet near the Racovatul de Sud village in January 2012.**

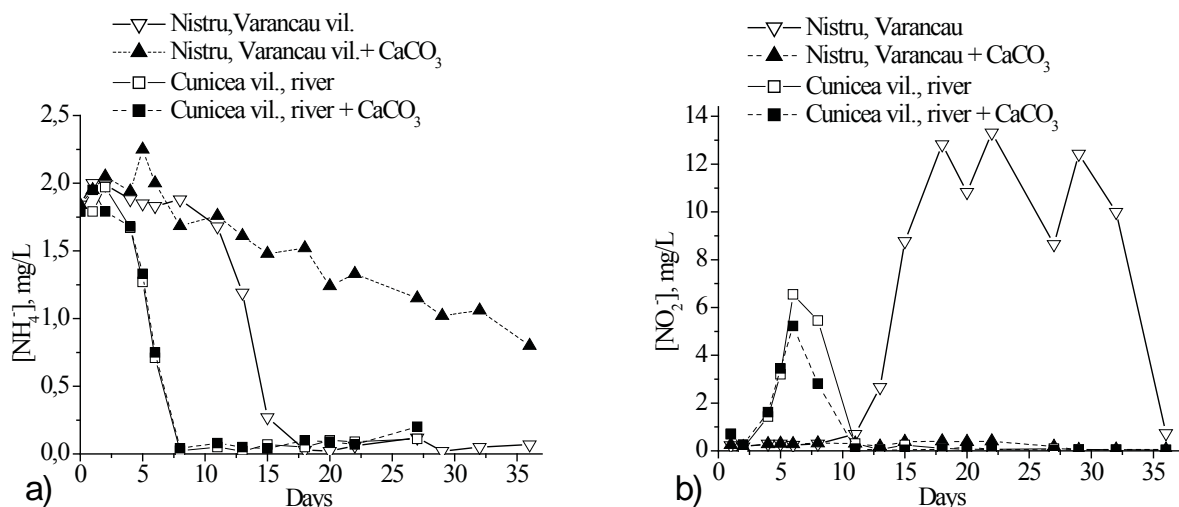


**Figure 2. Dynamics of ammonium ion (a) and nitrite ion (b) concentrations in water samples taken from the Nistru River, section Varancau and the rivulet near the Cunicea village in May 2012.**

The Nistru River, downstream of the Soroca city (section Varancau) is obviously polluted by sewage. Thus, the difference of cationic detergents amounts between the samples of Nistru River, in Varancau and the Cunicea village is easily explained. In the sample without the substrate, nitrification is significant, obtaining high concentrations (12-14 mg/L) of nitrites [21,22]. Formation of considerable quantities of nitrites shows that from day 11 to day 30 the rate of oxidation of ammonium ions and the  $\text{NO}_3^- \rightarrow \text{NO}_2^-$  reduction exceeds the nitrite ions oxidation  $\text{NO}_2^- \rightarrow \text{NO}_3^-$  [23].

In the sample with  $\text{CaCO}_3$ , the ammonium ions oxidation is stopped. At the same time the level of 0.4 mg/L of nitrite ions concentration, as for nitrate ions concentration, remains invariable in the analyzed sample within the studied period of time. Thus, the ratio of the maximum concentrations of nitrites in model samples with and without  $\text{CaCO}_3$  (Nistru River, section Varancau) is larger by almost two orders of magnitude. In the same figure, the dynamics of the concentrations of  $\text{NH}_4^+$  and  $\text{NO}_2^-$  ions for river near the Cunicea village, whose waters do not contain synthetic surfactants, is also depicted. The oxidation of ammonium ions in the rivulet water of the Cunicea village is similar in both samples (with and without  $\text{CaCO}_3$ ). The difference between the indices of nitrite ions in these samples reveals that calcium ions bind some water-soluble organic substances, and therefore has a small slowing effect on the rate of  $\text{NO}_2^-$  oxidation to nitrates, or causes nitrate ions reduction.

Water samples of the Nistru River at the Bursuc village (Figure 3), which is downstream of the Varancau village, are less polluted that can be explained by the sedimentation processes of suspended particles. A part of the organic matter is precipitated by cationic surfactants, which therefore remain in smaller quantities in water. The braking effect is evident in the Nistru River (section Bursuc) samples in presence  $\text{CaCO}_3$ , but less than the last-mentioned ones. The water sample collected in summer from the Sculeni section of the Prut River was less polluted, and those sampled downstream of the Ungheni city after wastewater treatment plants (WWTP) was more polluted, giving to the braking effect a perceptibly different value. In the last of samples mentioned above, by the addition of  $\text{CaCO}_3$ , the impediment of the nitrification process was practically complete.

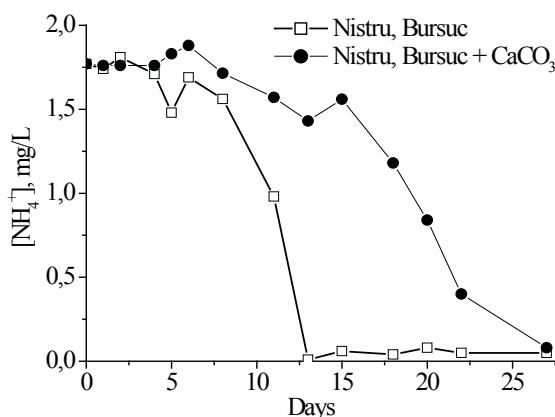


**Figure 3. Dynamics of ammonium ion concentrations in water sample collected from the Nistru River (section Bursuc) in May 2012.**

In the samples from the Ungheni section (Prut River), as in the Nistru River, section Varancau, the ratio between the maximum nitrite ion concentrations with and without calcium carbonate is about two orders. In polluted samples of the Nistru and Prut Rivers with added  $\text{CaCO}_3$ , the formation of nitrite ions is mostly likely due to the reduction of nitrate ions than to the oxidation of ammonium ions to form  $\text{NO}_2^-$ . The toxic properties of some pollutants (mostly probably cationic organic substances) are amplified in the presence of calcium carbonate within laboratory simulations. For the samples taken from the Nistru and Prut rivers, downstream cities, where massive amounts of effluents from sewage treatment plants reach their waters, the abovementioned phenomenon is revealed. Wastewaters accumulated in the treatment plants are mostly of domestic origin. So, the large amounts of pollutants in wastewaters constitute synthetic detergents. Previous research [24] proved that anionic and non-ionic surface-active substances at the MAC level decreased by a smaller amount the speed of the nitrification process. It is known that the process of the nitrogen oxidation is delayed in the presence of cationic surfactants and amines. This process has been also studied in the case of the mixture of cationic and anionic detergents [24]. For such mixture, the toxicity of cationic surfactants decreases [21,22]. On the contrary, the toxicity of cationic surfactants amplifies with the water hardness increasing [25]. The phenomenon of the nitrification braking in the presence of  $\text{CaCO}_3$  is characteristic for the water sections collected downstream WWTP of cities. In the presence of mixtures of cationic and anionic surfactants, a preferential binding of anionic surfactants to calcium carbonate particles has been found [26,27]. Consequently, it can be assumed that the decomposition of the associates formed from anionic and cationic surfactants contribute to braking of the

nitrogen oxidation. This decomposition was performed by treatment with fine powder of  $\text{CaCO}_3$ . In waters there are remained soluble surface-active cationic substances which manifest bactericidal effect. The enzymes concentration, which accelerates the nitrogen oxidation, decreases. Thus, the influence of  $\text{CaCO}_3$  on the investigated processes can be understood. Additionally, it is expected to suppose the formation of associates of  $\text{CaCO}_3$  with anionic organic species,  $\text{NH}_4^+$  and  $\text{NH}_2\text{OH}$ , which could also lead to braking of the  $\text{NH}_4^+ \rightarrow \text{NO}_2^-$  process [21,23]. This is one of two possible causes that might decrease the nitrite ions concentration. The second cause could be shrinking the soluble organic matter due to its sedimentation on the solid particles of  $\text{CaCO}_3$ , decreasing the speed of the  $\text{NO}_3^- \rightarrow \text{NO}_2^-$  process.

The same phenomenon was registered for the samples taken in the Prut River close to Sculeni village. Within the areas of the Prut River at the Ungheni city and the Sculeni village, the presence of  $\text{CaCO}_3$  has a smaller influence on the ammonium ion oxidation process (Figure 4a). In the rivulet flowing through the Cunicea village, where detergents are absent, the samples with and without  $\text{CaCO}_3$  show the same nitrification path for both the dynamics of ammonium oxidation and variation of nitrite ion concentrations. Obviously, it has to be taken into account that nitrite ions could appear due to reduction of nitrate ions, especially for polluted waters containing more organic substances, which are able to act as reducing agents. That is why in the samples taken from the Nistru River, section Varancau (Figure 2), from the Prut River, section Sculeni and the Prut River after WWTP (Figure 4) the nitrite ions are found to be in higher concentrations that they could be formed from the ammonium oxidation.

The impact of granite, keramzite, calcium carbonate and their mixture on the water samples collected from the Isnovat River in October was investigated. These studies demonstrate that granite, keramzite and their mixture have a stimulatory influence on nitrification dynamics (Figures 5 and 6). These cases are similar to those of winter samples.

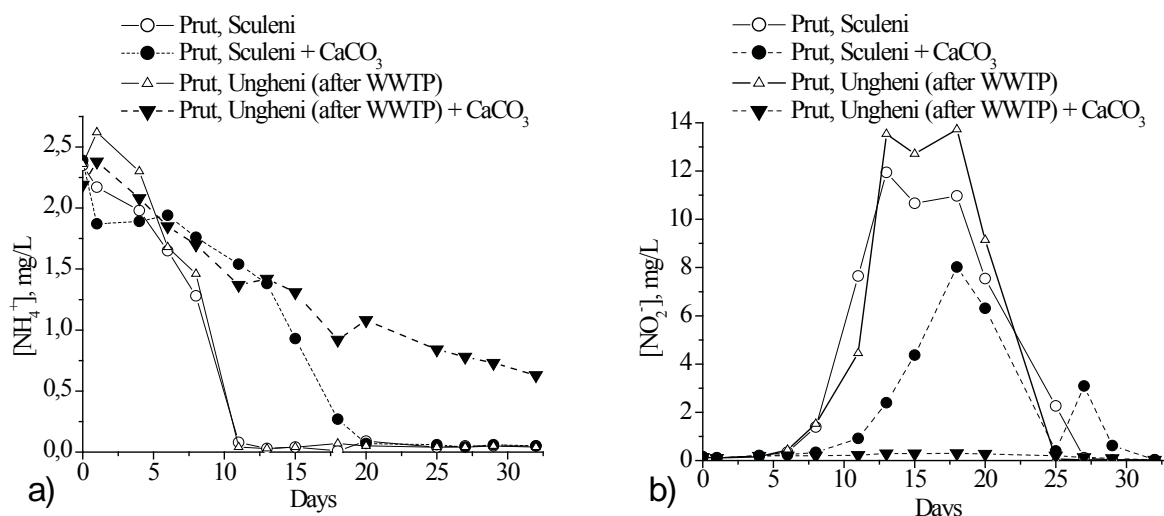


Figure 4. Dynamics of ammonium ion (a) and nitrite ion (b) concentrations in water samples collected from the Prut River, Sculeni section and after WWTP in June 2012.

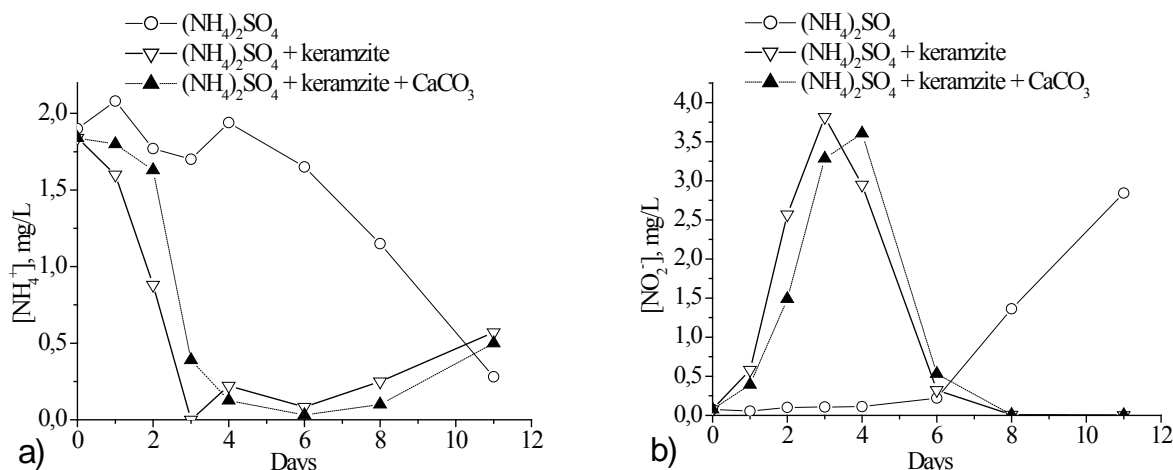
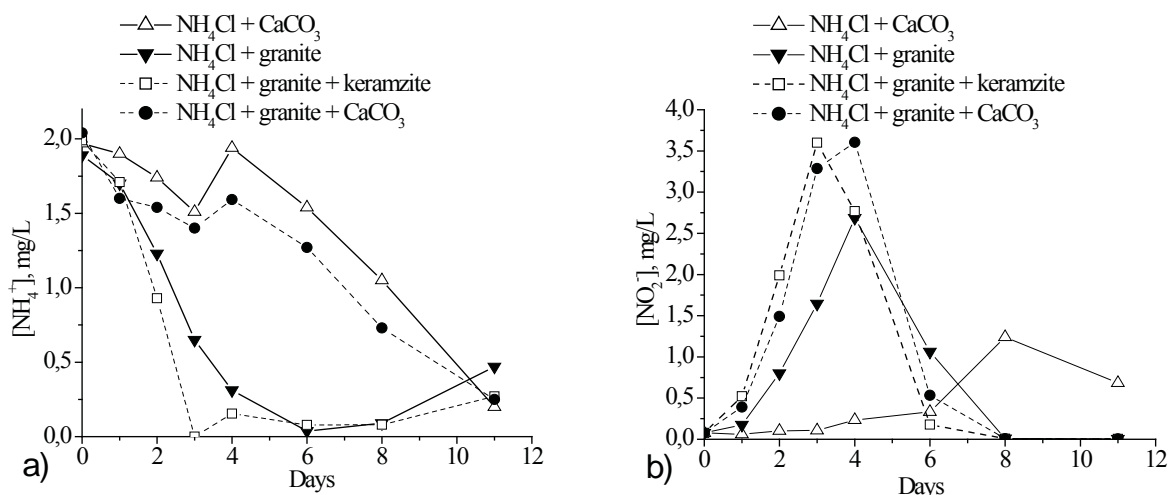


Figure 5. Dynamics of ammonium ion (a) and nitrite ion (b) concentrations in the presence of keramzite and  $\text{CaCO}_3$  in the water samples taken from the Isnovat River in October 2012.



The dependence of ammonium ion concentrations on the time demonstrates the stimulation of the ammonium ions oxidation in the presence of granite, compared to the reference sample (e.g. the sample of natural water to which was initially added 2 mg/L of ammonium ions).

It should be noted that the rates of ammonium ions oxidation of reference samples and those with calcium carbonate are very close (Figures 5 and 6). In the last samples taken from the Isnovat River the decreasing the ammonium ion amounts has an insignificant delay, dissimilar for samples of the Nistru River (spring) and the Prut River (summer). The difference is only in the dynamics trend of nitrite ion concentrations and their values. When in the reference sample the nitric index just starts to increase, in the sample with  $\text{CaCO}_3$ , it reaches the maximum value. Accordingly, in the last case, the maximum value (on the eighth day) is 1.3 mg/L, while for the reference sample it is reached after 11 days of the model initiation with a maximum value of 3.01 mg/L. A significant delay occurs in the case of granite and calcium carbonate mixture. In these samples, the nitrite ions concentration achieves the highest peak. Conversely, the nitrite ions concentration in the sample with granite and  $\text{CaCO}_3$  separately, are among the lowest ones. Unlike the water sample containing expanded clays with calcium carbonate, the ammonium ions oxidation occurs analogously as with the keramzite sample.



**Figure 6. Dynamics of ammonium ion (a) and nitrite ion (b) concentrations in models with granite and  $\text{CaCO}_3$  only, mixtures of granite and keramzite or granite and  $\text{CaCO}_3$  in the Isnovat River waters collected in October 2012.**

The obtained results (see all figures) show increasing or decreasing the blocking phenomena (stimulating oxidation of nitrogen reduced forms in river waters) in polluted samples in the presence of suspended particles of calcium carbonate, keramzite and granite substrates. The stimulate effect of nitrogen oxidation has been explained by authors [25,28,29] through the adsorption of cationic surfactants on the surfaces of granite and expanded clay. Additionally, the phenomenon of adsorption of ammonium ions onto the surface of calcium carbonate itself or in combination with other low cost adsorbents from polluted waters was revealed in a series of published works [30-32]. Unfortunately, all above mentioned papers do not contain a rigorous explanation about the mechanism of observed phenomena. This question will constitute an objective of our next communication.

Finally, it is interesting to mention the assumption of authors [27] that even the  $\text{CaCO}_3$  nanoparticles are almost insoluble in water, once dispersed in water the  $\text{Ca-OH}$  group can be formed on the particle surface, which may become either positively ( $\text{Ca-OH}_2^+$ ) or negatively ( $\text{Ca-O}^-$ ) charged by combining or releasing a proton, depending on the pH of medium. For example, being dispersed in pure water, the pH of the dispersion is 9.93, indicating that the  $\text{CaCO}_3$  nanoparticles are positively charged in neutral water.

## Conclusions

Granite and keramzite substrates, separately and in their mixtures, show a similar effect in assisting the oxidation of nitrogen reduced forms in natural surface waters, accelerating the oxidation of ammonium and nitrite ions from 2 to 4 times.

Calcium carbonate in its mixtures with granite or expanded clays (compared to samples containing separate substrates) in the river waters slows in a different way the oxidation of ammonium nitrogen, while it causes no braking

nitrification in non-polluted water. The impact of expanded clay, granite substrates and  $\text{CaCO}_3$  is comparable for samples collected in different seasons.

Organic pollutants, especially the cationic surfactants, coming from the urban activities, in the presence of calcium carbonate produce a clear impact on the braking process of oxidation of nitrogen reduced forms in natural waters.

## References

1. Gladchi, V.; Goreaceva, N.; Duca, G.; Bunduchi, E.; Borodaev, R.; Mardari, I.; Romanciuc, L. Chemical composition and redox state of medial Nistru waters. *Environment*, 2008, 3(39), pp. 20-28 (in Romanian).
2. Zubcov, E.; Bagrin, N.; Ungureanu, L.; Bilețchi, L.; Borodin, N.; Bogonin, Z. The dynamic of hydrochemical indexes and quality of the Prut river. *The Bulletin of Academy of Science of Moldova, Life Science*, 2011, 313(1), pp. 103-110 (in Romanian).
3. Martinelle, K.; Häggström, L. Mechanisms of ammonia and ammonium ion toxicity in animal cells: Transport across cell membranes. *Journal of Biotechnology*, 1993, 30, pp. 339-350.
4. Britto, D.T.; Siddiqi, M.Y.; Glass, A.D.M.; Kronzucker, H.J. Futile transmembrane  $\text{NH}_4^+$  cycling: A cellular hypothesis to explain ammonium toxicity in plants. *Proceedings of the National Academy of Sciences USA*, 2001, 98, pp. 4255-4258.
5. Britto, D.T.; Konzucker, H.J.  $\text{NH}_4^+$  toxicity in higher plants: a critical review. *Journal of Plant Physiology*, 2002, 159, pp. 567-584.
6. Müller, T.; Walter, B.; Wirtz, A.; Burkovski, A. Ammonium Toxicity in Bacteria. *Current Microbiology*, 2006, 52, pp. 400-406.
7. Brunning-Fann, C.S.; Kaneene, J.B. The effects of nitrate, nitrite, and N-nitroso compounds on human health. *Veterinary and Human Toxicology*, 1993, 35(6), pp. 521-538.
8. Weng, Y.M.; Hotchkiss, J.H.; Babish, J.G. N-nitrosamine and mutagenicity formation in Chinese salted fish after digestion. *Food Additives and Contaminants*, 1992, 9(1), pp. 29-37.
9. Bradberry, S.M.; Gazzard, B.; Vale, J.A. Methemoglobinemia caused by the accidental contamination of drinking water with sodium nitrite. *Clinical Toxicology*, 1994, 32(2), pp. 173-178.
10. Blackall, L.L., A Summary of Recent Microbial Discoveries in Biological Nutrient Removal from Wastewater. *Australasian Biotechnology*, 2000, 10(3), pp. 29-32.
11. Van Leeuwen, F.X.R. Safe drinking water: The toxicologist's approach. *Food and Chemical Toxicology*. 2000, 38(1), pp. 51-58.
12. Hu, X.M.; Chen, Y.W.; Liao, Y.G.; Yan, W.F.; Zhu, S.M.; Shen, S. B. High  $\text{NH}_4^+$ -N concentration wastewater treatment by shortcut nitrification-denitrification using a system of A/O inner loop fluidized bed biofilm reactors. *Water Science and Technology*, 2013 67(5), pp. 1083-1091.
13. Sandu, M.; Spataru, P.; Arapu, T.; Lupascu, T. Biochemical oxidation – a pathway for ammonia removal from aquatic systems. *Methods and Techniques for Cleaning-up Contaminated Sites*, Annable, M.D.; Teodorescu, M.; Hlavinek, P.; Diels L. Eds. Springer: Sinaia, Romania, 2006, pp. 137-143.
14. ISO 7150-1:2001. Water quality - Determination of ammonium -Spectrometric method.
15. ISO 7890-3:1988. Water quality - Determination of nitrate - Part 3: Spectrometric method using sulfosalicylic acid.
16. ISO 8466-1:1990. Water quality - Calibration and evaluation of analytical methods and estimation of performance characteristics - Part 1: Statistical evaluation of the linear calibration function.
17. SR ISO 7890-3:2000 Water quality - The determination of the content of nitrates. The part 3: The spectrometric method with sulfosalicylic acid.
18. SM SR EN 26777:2006 Water quality - determination of the content of nitrites. The method of the spectrometry of molecular absorption.
19. Lozan, R.; Sandu, M.; Ropot, V. The method of determination of nitrites. RU Patent, 1990, No. 1638619 (in Russian).
20. Matveeva, N. P.; Klimenko, O.A.; Trunov, N. M. Simulation of self-purification of natural treatment of organic pollutants in the laboratory. *Gidrometeoizdat: Leningrad*, 1988, pp. 26-31 (in Russian).
21. Sandu, M.; Spataru, P.; Negru, M.; Mosanu, E.; Dragutan, D.; Goreacioc, T. The dynamic of nitrification process in the presence of cationic surfactants. *International symposium "The Environment and Industry"*, Bucharest, 2007, vol. 1, pp. 277-281 (in Romanian).
22. Sandu, M.; Spataru, P.; Mosanu, E.; Tarata, A. Nitrification capacity water tributaries of the Prut River and the factors that influence. *XXX-th Romanian Chemistry Conference, Romanian Academy, Calimanesti-Caciulata, Valcea*, 2008, p. 384 (in Romanian).
23. Philip, S.; Laanbroek H. J.; Verstraete, W. Origin, causes and effects of increased nitrite concentrations in aquatic environments. *Reviews in Environmental Science and Biotechnology*, 2002, 1, pp. 115-141.

24. Spataru, P. Transformations of organic substances in surface waters of Republic of Moldova. Ph.D. in Chemistry, State University of Moldova, Chisinau, 2011 (in Romanian).
25. Lewis, M. A. The effects of mixtures and other environmental modifying factors on the toxicities of surfactants to freshwater and marine life. *Water Research*, 1992, 26(8), pp. 1013–1023.
26. Cui, Z.G.; Cui, Y.Z.; Cui, C.F.; Chen, Z.; Binks, B. P. Aqueous foams stabilized by in situ surface activation of  $\text{CaCO}_3$  Nanoparticles via Adsorption of Anionic Surfactant. *Langmuir*, 2010, 26(15), pp. 12567–12574.
27. Cui, Z.G.; Cui, C.F.; Zhu, Y.; Binks, B. P. Multiple phase inversion of emulsions stabilized by in situ surface activation of  $\text{CaCO}_3$  nanoparticles via adsorption of Fatty acids. *Langmuir*, 2012, 28(1), pp. 314–320.
28. Atkin, R.; Craig, V.S.J.; Biggs, S. Adsorption kinetics and structural arrangements of cationic surfactants on silica surfaces. *Langmuir*, 2000, 16, pp. 9374–9380.
29. Sayari, A.; Hamoudi, S.; Yong, Y. Applications of pore-expanded mesoporous silica. 1. Removal of heavy metal cations and organic pollutants from wastewater. *Chemistry of Materials*, 2005, 17(1), pp. 212–216.
30. Morse, J.W. The surface chemistry of calcium carbonate minerals in natural waters: An overview. *Marine Chemistry*, 1986, 20(1), pp. 91–112.
31. Srinivasan, R.; Hoffman, W.D.; Wolfe III, J.E.; Prcin, L.J. Evaluation of removal of orthophosphate and ammonia from rainfall runoff using aboveground permeable reactive barrier composed of limestone and zeolite. *Journal of Environmental Science and Health, Part A: Hazardous Substances and Environmental Engineering*, 2008, 43(12), pp. 1441–1450.
32. Warren, L.A.; Maurice, P.A. Microbially mediated calcium carbonate precipitation: implications for interpreting calcite precipitation and for solid-phase capture of inorganic contaminants. *Geomicrobiology Journal*, 2001, 18(1), pp. 93–115.

# NEW SOLVATOMORPH OF TETRAKIS( $\mu_2$ -ACETATO-O,O')-BIS(ISONICOTINAMIDE-N)-DI-COPPER(II): SYNTHESIS, IR, TGA AND X-RAY STUDY

Diana Chisca<sup>a,b</sup>, Eduard Coropceanu<sup>b</sup>, Oleg Petuhov<sup>b</sup>, Lilia Croitor<sup>a\*</sup>

<sup>a</sup>Institute of Applied Physics of Academy of Sciences of Moldova, 5, Academiei str., Chisinau MD-2028, Republic of Moldova

<sup>b</sup>Institute of Chemistry of Academy of Sciences of Moldova, 3, Academiei str., Chisinau MD-2028, Republic of Moldova

\*e-mail: croitor.lilia@gmail.com; phone: (+ 373 22) 73 81 54; fax: (+ 373 22) 72 58 87

**Abstract.** Dinuclear tetracarboxylato-bridged copper(II) complex,  $[\text{Cu}_2(\text{OAc})_4(\text{ina})_2] \cdot 2\text{dmsO}$  (**1**), where  $\text{OAc}^- = \text{CH}_3\text{COO}^-$ ,  $\text{ina}$ =isonicotinamide and  $\text{dmsO}$ =dimethylsulfoxide, has been prepared and crystal structure has been determined by single X-ray diffraction. The compound consists of dinuclear units, in which two Cu(II) ions are bridged by four *syn,syn*- $\eta^1:\eta^1:\mu$ -acetato bridges, showing a paddle-wheel cage-type with a square-pyramidal geometry. In the crystal structure, intermolecular N-H $\cdots$ O hydrogen bonds link the molecules into a 1D linear chain.

**Keywords:** copper, isonicotinamide, X-ray, paddle-wheel structure.

Received: August 2015/ Revised final: September 2015/ Accepted: October 2015

## Introduction

The design and preparation of metal-organic frameworks have attracted intense interest in the field of supramolecular chemistry and crystal engineering owing to their potential applications as well as their structural variations that are currently of interest in the field of materials [1-7]. A successful strategy in building such networks is to employ appropriate bridging ligands that can bind metal ions in different modes and provide a possible way to achieve diverse dimensionalities. Copper(II) metal-organic frameworks are of considerable interest because of their structural and photoluminescent biological function, catalytic and magnetic properties [8-11]. Isonicotinamide and its related compounds are reported to represent a group of small molecules as a drug candidate to prevent and/or reverse diabetes by protecting  $\beta$ -cells from damage and death [12].

The retrieval of Cambridge Structural Database (CSD) revealed that the combination of Cu(II) with isonicotinamide resulted in structural diversity, including mono- [13-15], binuclear [14, 16-18], 1D [7, 16, 19-21] and 2D polymeric arrays [7, 22, 23]. In all studies isonicotinamide coordinates to the copper(II) ion in a monodentate form through the pyridine N atom or in a bidentate one [16] thus providing possibilities for polymeric coordination networks. Pyridine-2,5-dicarboxylic acid combines the advantages of both organic multicarboxylic acids and heteroaromatic compounds and displays versatile coordination modes through its one N atom and four carboxylate O atoms, which in alliance with Cu(II) leads to the formation of coordination homometallic [23-27] and/or heterometallic [26, 28-30] polymers. With that in mind, in this contribution, we intended to extend the dimensionality of a new coordination compound obtained by the combination of isonicotinamide with pyridine-2,5-dicarboxylate ligands. However, in the synthetic conditions we were unable to obtain any new coordination compounds with simultaneous presence of pyridine-2,5-dicarboxylic acid and isonicotinamide ligand in one molecule, and a new solvatomorph of tetrakis( $\mu_2$ -acetato-O,O')-bis(isonicotinamide-N)-di-copper(II) was obtained instead. So, we report herein the synthesis and X-ray characterization of a binuclear mixed-ligand Cu(II) complex,  $[\text{Cu}_2(\text{OAc})_4(\text{ina})_2] \cdot 2\text{dmsO}$  (**1**), where  $\text{OAc}^- = \text{CH}_3\text{COO}^-$ ,  $\text{ina}$  = isonicotinamide and  $\text{dmsO}$  = dimethylsulfoxide.

## Experimental section

### Materials and methods

All reagents and solvents were obtained from commercial sources and were used without further purification. Elemental analysis was performed on an Elementar Analysen systeme GmbH Vario El III elemental analyzer. The IR spectra were obtained in vaseline oil on a FT IR Spectrum-100 Perkin Elmer spectrometer in the range of 400 - 4000  $\text{cm}^{-1}$ . The thermogravimetric analysis (TGA) was carried out with a Derivatograph Q-1500 thermal analyzer in an air flow at a heating rate of 10  $^\circ\text{C}/\text{min}$  in the temperature range of 25 - 1000  $^\circ\text{C}$ .

### Synthesis of $[\text{Cu}_2(\text{OAc})_4(\text{ina})_2] \cdot 2\text{dmsO}$ (**1**).

$\text{Cu}(\text{OAc})_2 \cdot \text{H}_2\text{O}$  (20 mg, 0.1 mmol), isonicotinamide (12.2 mg, 0.1 mmol) and pyridine-2,5-dicarboxylic acid (8.3 mg, 0.05 mmol) were dissolved in 8 mL mixture of methanol and dimethylsulfoxide (5:3). The reaction mixture was stirred in the ultrasonic bath at 60  $^\circ\text{C}$  for ~ 30 min, filtered off and then slowly cooled to 5  $^\circ\text{C}$  temperature giving green crystals. Yield: ~ 48 %. Anal. calc. for  $\text{C}_{24}\text{H}_{36}\text{N}_4\text{O}_{12}\text{S}_2\text{Cu}_2$  (%): C=37.71; H=4.71; N=7.33. Found: C=37.65; H=4.62; N=7.47. IR ( $\text{cm}^{-1}$ ): 3300(m), 3163(w), 2953(v.w), 2924(m), 2921(w), 2854(m), 2794(v.w), 1678(m), 1616(m), 1614(s), 1557(m), 1408(s), 1347(m), 1230(m), 1069(m), 1050(v.w), 1025(w), 722(m), 682(w).

**X-ray structure determination**

Diffraction measurement for **1** was carried out at room temperature on a Xcalibur “Oxford Diffraction” diffractometer equipped with CCD area detector and a graphite monochromator utilizing MoK $\alpha$  radiation. Final unit cell dimensions were obtained and refined on an entire data set. All calculations to solve the structure and to refine the proposed model were carried out with the programs SHELXS97 and SHELXL97 [31]. The structure was solved by direct methods and refined by full-matrix least-squares methods on  $F^2$  by using the SHELXL97 program package. All non-hydrogen atoms were refined anisotropically. Hydrogen atoms attached to carbon atoms were placed in geometrically idealized positions and refined by using a riding model. The X-ray data and the details of the refinement for **1** are summarized in Table 1. Selected geometric parameters for **1** are given in Tables 2 and 3. The figures were produced using the Mercury program [32]. CCDC-1408326 contains the supplementary crystallographic data for this paper. These data can be obtained free of charge from The Cambridge Crystallographic Data Centre via [www.ccdc.cam.ac.uk/data\\_request/cif](http://www.ccdc.cam.ac.uk/data_request/cif).

Table 1

**Crystal and structure refinement data for compound 1.**

Parameters	Value
Empirical formula	C <sub>24</sub> H <sub>36</sub> N <sub>4</sub> O <sub>12</sub> S <sub>2</sub> Cu <sub>2</sub>
Formula weight	763.77
Crystal system	Triclinic
Space group	<i>P</i> -1
<i>Z</i>	1
<i>a</i> (Å)	7.3195(12)
<i>b</i> (Å)	8.0763(12)
<i>c</i> (Å)	13.833(2)
$\alpha$ (°)	93.024(13)
$\beta$ (°)	97.026(13)
$\gamma$ (°)	96.063(13)
<i>V</i> (Å <sup>3</sup> )	805.3(2)
<i>D<sub>c</sub></i> (g/cm <sup>-3</sup> )	1.575
$\mu$ (mm <sup>-1</sup> )	1.514
<i>F</i> (000)	394
Crystal size (mm)	0.12 x 0.12 x 0.05
Reflections collected/unique	4284 / 2837 [R(int) = 0.0418]
Reflections with [ <i>I</i> > 2σ( <i>I</i> )]	1977
Data/ restraints/ parameters	2837 / 0 / 211
GOF on $F^2$	0.987
<i>R<sub>p</sub></i> , <i>wR<sub>2</sub></i> [ <i>I</i> > 2σ( <i>I</i> )]	0.0592, 0.0943
<i>R<sub>p</sub></i> , <i>wR<sub>2</sub></i> (all data)	0.0943, 0.1101

Table 2

**Selected bond lengths (Å) and angles (°) in coordination metal environment in 1.**

Bond	<i>d</i> , Å	Bond	<i>d</i> , Å
Cu(1)-O(1)	1.971(3)	Cu(1)-O(4) <sup><i>i</i></sup>	1.977(3)
Cu(1)-O(3)	1.980(3)	Cu(1)-N(1)	2.175(4)
Cu(1)-O(2) <sup><i>i</i></sup>	1.970(3)		
Angle	$\omega$ , deg	Angle	$\omega$ , deg
O(2) <sup><i>i</i></sup> -Cu(1)-O(1)	168.66(14)	O(4) <sup><i>i</i></sup> -Cu(1)-O(3)	168.50(14)
O(2) <sup><i>i</i></sup> -Cu(1)-O(4) <sup><i>i</i></sup>	88.76(14)	O(2) <sup><i>i</i></sup> -Cu(1)-N(1)	97.10(14)
O(1)-Cu(1)-O(4) <sup><i>i</i></sup>	88.96(15)	O(1)-Cu(1)-N(1)	94.21(14)
O(2) <sup><i>i</i></sup> -Cu(1)-O(3)	89.77(15)	O(4) <sup><i>i</i></sup> -Cu(1)-N(1)	98.12(15)
O(1)-Cu(1)-O(3)	90.25(15)	O(3)-Cu(1)-N(1)	93.39(15)

Symmetry transformations used to generate equivalent atoms: <sup>*i*</sup> -*x*+2, -*y*+1, -*z*+1

Table 3

**Hydrogen bond distances (Å) and angles (°) for 1.**

<i>D-H</i> ⋯ <i>A</i>	<i>d</i> ( <i>D-H</i> )	<i>d</i> ( <i>H</i> ⋯ <i>A</i> )	<i>d</i> ( <i>D</i> ⋯ <i>A</i> )	<(DHA)	Symmetry transformation for acceptor
N(2)-H(1N1)⋯O(6)	0.88(4)	2.05(5)	2.913(6)	169(4)	<i>x</i> , <i>y</i> -1, <i>z</i>
N(2)-H(2N1)⋯O(5)	0.87(5)	2.08(5)	2.937(6)	171(5)	- <i>x</i> , - <i>y</i> , - <i>z</i>



## Results and discussion

### Crystal structure analysis

The interaction in the system  $\text{Cu}(\text{OAc})_2$  – isonicotinamide (*ina*) – pyridine-2,5-dicarboxylic acid (2,5-pdc) resulted in the acid-free dinuclear compound of the composition  $[\text{Cu}_2(\text{OAc})_4(\text{ina})_2] \cdot 2\text{dmsO}$  (**1**). Complex **1** represents chromophore being intensively green colored. Upon exposure to air, the adduct is stable in solid state and is soluble in water and common organic solvents such as methanol and *N,N*-dimethylformamide.

The complex structure **1** reproduces features for two reported binuclear  $\text{Cu}(\text{II})$  complexes, solvent-free [17] and acetonitrile solvate [14] tetrakis( $\mu_2$ -acetato- $\text{O},\text{O}'$ )-bis(isonicotinamide- $\text{N}$ )-di-copper(II). As it is evidenced from comparison of the unit cell dimensions and crystal systems, compounds **1** and the last one (*P*-1;  $a=7.200(1)$ ,  $b=8.103(1)$ ,  $c=13.449(1)$  Å;  $\alpha=90.41(0)$ ,  $\beta=96.33(0)$ ,  $\gamma=96.12(0)^\circ$ ;  $V=775.172$  Å<sup>3</sup>) [14] are isomorphous with consequential increase of the unit cell volume in **1** (Table 1). Compound **1** (Figure 1a) consists of centrosymmetric paddle-wheel dinuclear units with the two copper(II) atoms held together through four *syn,syn*- $\eta^1:\eta^1:\mu$ -acetate bridges (Cu–O distances vary from 1.970(3) to 1.980(3) Å) acting as equatorial ligands for each Cu(II) center. Each copper atom has a square-pyramidal geometry where the ‘peripheral’ coordination site on the metal ion is occupied by an isonicotinamide ligand coordinated through the pyridine nitrogen atom at a distance of 2.175(4) Å. The copper atoms are displaced by 0.196 Å from the basal planes toward the apical positions. The two amide functionalities of coordinated *ina* molecules are oriented in a linear fashion but pointing in opposite directions. Each amide moiety forms two symmetry related N–H  $\cdots$  O hydrogen bonds, with an adjacent metal complex, resulting in infinite linear chains (Figure 1b). The remaining N–H proton on each amide functionality forms a N–H  $\cdots$  O hydrogen bond ( $d(\text{N} \cdots \text{O})$  2.91 Å) to the included dimethylsulfoxide (Figure 1b,c). The Cu  $\cdots$  Cu separation within the paddle-wheel dinuclear core is 2.626 Å, and the Cu  $\cdots$  Cu distance between adjacent metal-complexes within each hydrogen-bonded chain is 17.0 Å. The shortest through-space inter-chain distance between Cu(II) ions is 6.325 Å.

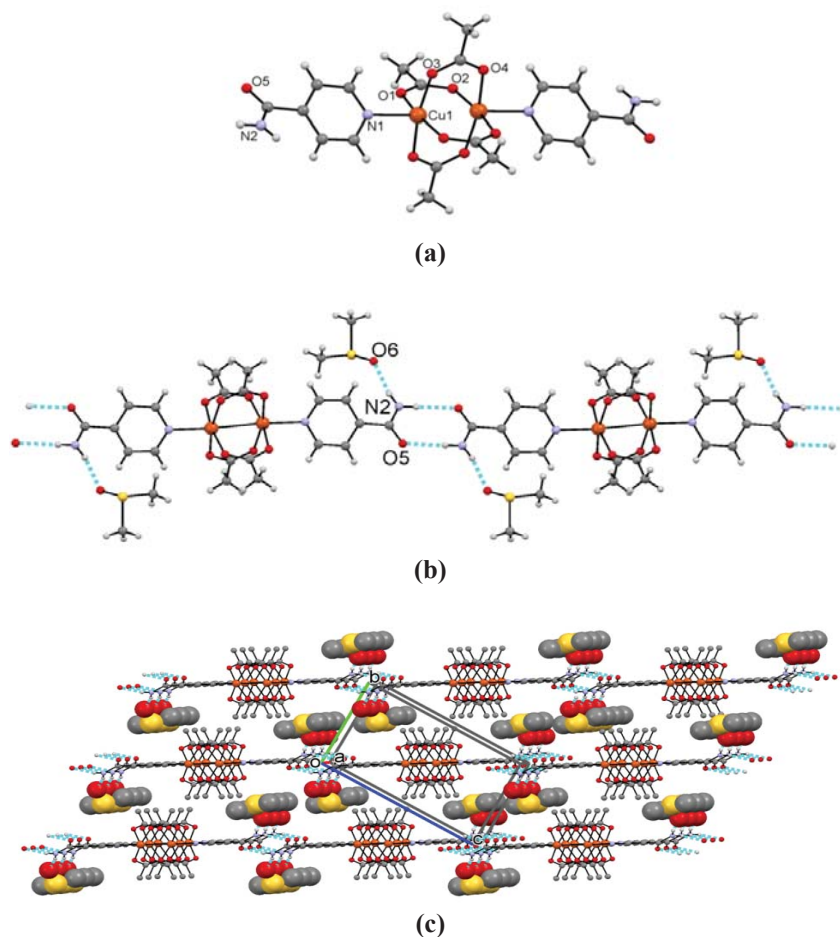


**Figure 1.** View of the: dinuclear Cu(II) molecule (a); infinite chain of dinuclear Cu(II)-complexes held together by self-complementary amide  $\cdots$  amide hydrogen-bond interactions (b) and crystal packing in **1** with *dmsO* molecules shown in the space-filling mode, C-bound H-atoms are omitted for clarity (c).

The structural parameters of compound **1** compare well with some paddle-wheel copper(II) binuclear and polymeric related complexes, as shown in Table 4. The above findings together with the reported complexes reveal that monodentate 4-phenylpyridine affords longer Cu...Cu separations, while hexadentate 2,4,6-tri(4-pyridyl)-1,3,5-triazine ligand provides shorter Cu...Cu separations with lower deviation of Cu(II) from O<sub>4</sub> - plane (Table 4).

Table 4

Structural data for some relevant paddle-wheel copper(II) complexes.

Compound <sup>a</sup>	Space group	Cu...Cu, Å	Deviation of Cu(II) from O <sub>4</sub> -plane, Å	Reference
[Cu <sub>2</sub> (OAc) <sub>4</sub> (ina) <sub>2</sub> ]·2dmsol ( <b>1</b> )	<i>P</i> -1	2.626	0.196	Present work
[Cu <sub>2</sub> (OAc) <sub>4</sub> (ina) <sub>2</sub> ]	<i>P</i> 2 <sub>1</sub> / <i>c</i>	2.648	0.212	[17]
[Cu <sub>2</sub> (OAc) <sub>4</sub> (ina) <sub>2</sub> ]·CH <sub>3</sub> CN	<i>P</i> -1	2.611	0.191	[14]
[Cu <sub>2</sub> (OMba) <sub>4</sub> (ina) <sub>2</sub> ]	<i>P</i> 2 <sub>1</sub> / <i>c</i>	2.637	0.203	[18]
[Cu <sub>2</sub> (OAc) <sub>4</sub> (4-ppy) <sub>2</sub> ]	<i>I</i> 4 <sub>1</sub> / <i>a</i>	2.654	0.211	[33]
[Cu <sub>2</sub> (OAc) <sub>4</sub> (ppca) <sub>2</sub> ]	<i>C</i> 2/ <i>c</i>	2.644	0.209	[34]
[Cu <sub>2</sub> (OAc) <sub>4</sub> (4-acpy) <sub>2</sub> ]	<i>P</i> 2 <sub>1</sub> / <i>c</i>	2.631	0.203	[35]
[Cu <sub>2</sub> (OAc) <sub>4</sub> (dpva) <sub>2</sub> ]	<i>P</i> 2 <sub>1</sub> / <i>c</i>	2.648	0.210	[36]
[Cu <sub>2</sub> (OAc) <sub>4</sub> (CF <sub>3</sub> -py) <sub>2</sub> ]	<i>C</i> ccm	2.623	0.202	[37]
{[Cu <sub>2</sub> (OAc) <sub>4</sub> (tpt) <sub>2</sub> ]·2CH <sub>3</sub> OH} <sub>n</sub>	<i>P</i> 2 <sub>1</sub> / <i>n</i>	2.605	0.186	[38]

<sup>a</sup>Abbreviation: HMba=4-Methylbenzoic acid;

4-ppy=4-phenylpyridine;

ppca=N-phenyl-4-pyridinecarboxamide;

4-acpy=4-acetylpyridine;

dpva=N,N-dimethyl-4-(pyridin-4-yl)diazenyl) aniline;

CF<sub>3</sub>-py=4-trifluoromethylpyridine;

tpt= 2,4,6-tri(4-pyridyl)-1,3,5-triazine.

Notably, our survey of the Cambridge Structural Database (ConQuest Version 1.17) reveals 6 discrete compounds built up from Cu(II) atom, isonicotinamide molecule and acetate anion, 2 of them being mononuclear compounds, namely L-(diacetato)-diaqua-bis(4-carbamoyl-pyridine)-copper [38] and (acetato-O,O')-(acetato-O)-(acetic acid-O)-bis(isonicotinamide-N)-copper(II) acetic acid solvate [12], and 4 being binuclear compounds, tetrakis(μ<sub>2</sub>-acetato-O,O')-bis(isonicotinamide-N)-di-copper(II) acetonitrile solvate [12], bis-(μ<sub>2</sub>-acetato-O,O')-bis(acetato-O)-bis(isonicotinamide-N)-copper(II) methanol solvate [12], bis(μ<sub>2</sub>-acetato-O,O')-bis(acetato-O,O')-tetrakis(isonicotinamide-N)-di-copper(II) [39] and tetrakis(μ<sub>2</sub>-acetato-O,O')-bis(isonicotinamide-N)-di-copper(II) [17]. In all these compounds *ina* coordinates in monodentate mode through the pyridine N atom, while acetate ligands show diverse coordination modes: monodentate deprotonated [38], bidentate bridging modes [12,17] and combination of monodentate deprotonated-bidentate bridging modes [12], bidentate chelating-bridging modes [39] and monodentate protonated-monodentate deprotonated-bidentate chelating modes [12] within one compound.

### Infrared spectroscopy study

The IR spectrum confirms the presence of the organic ligands used in the synthesis (through the typical vibrations of pyridine rings, amide, and carboxylic groups) [40]. The spectrum exhibits very strong and broad bands due to stretching vibrations of coordinated carboxylate groups at 1408 cm<sup>-1</sup> ν<sub>s</sub>(COO) and 1614 cm<sup>-1</sup> ν<sub>as</sub>(COO) of acetate anions. The absorption bands at 3300, 3163 and 1619 cm<sup>-1</sup> can be attributed to ν(NH) and δ(NH<sub>2</sub>), respectively and the oscillations at 1557 and 1025 cm<sup>-1</sup> show the presence of aromatic rings. The vibrations at 2953, 2924 and 2854 cm<sup>-1</sup> are attributed to ν(CH), at 1347 cm<sup>-1</sup> to δ(CH) and the vibrations at 1678 and 1230 cm<sup>-1</sup> correspond to ν(C=O) and ν(C-N), respectively. The presence of dimethylsulfoxide in the complex is documented by the oscillations at 2794 cm<sup>-1</sup> ν<sub>as</sub>(CH<sub>3</sub>), 2921 cm<sup>-1</sup> ν<sub>s</sub>(CH<sub>3</sub>), 1069 and 1050 cm<sup>-1</sup> ν(-S=O), 722 cm<sup>-1</sup> ν(-C-S-C-) and 682 cm<sup>-1</sup> ν(-C-S-).

### Thermogravimetric analysis

The decomposition of **1** was investigated by combined TG-DTA. It was found that **1** has three separate weight loss steps (Figure 2). The first weight loss step is observed in the range of 165-188 °C corresponding to the loss of the two solvated *dmsol* molecules (found, 20.9%; calcd., 20.5 %). In the range of 195-239 °C takes place the second weight loss that can be attributed to two *ina* molecules (found, 31.5%; calcd., 31.7%). Both processes are endothermic. Beginning with 340 °C, a strong exothermic process was observed, with maximum at 430 °C, caused by oxidative degradation of the remaining compound. The final residue corresponds to CuO with no changes to 1000 °C.



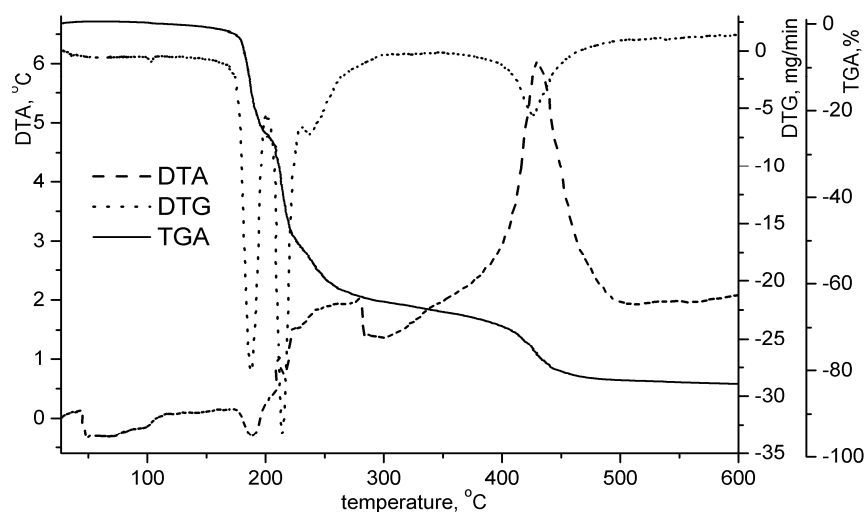


Figure 2. TG-DTA pattern of compound 1.

## Conclusions

A new dinuclear tetracarboxylato-bridged copper(II) solvatomorph  $[\text{Cu}_2(\text{OAc})_4(\text{ina})_2] \cdot 2\text{dmsO}$  (**1**) ( $\text{OAc}^- = \text{CH}_3\text{COO}^-$ ,  $\text{ina}$ =isonicotinamide and  $\text{dmsO}$ =dimethylsulfoxide) was prepared and studied by IR spectroscopy, TGA analysis and single crystal X-ray method. Four carboxylate ligands bridge two copper ions in a *syn, syn*- $\eta^1:\eta^1:\mu$  mode showing a paddle-wheel unit. Isonicotinamide ligands coordinate to copper(II) in a monodentate form through the nitrogen atom of pyridine. The Cu(II) cation is pentacoordinated in a  $\text{NO}_4$ -environment in the shape of distorted square-pyramid. The amide moiety of isonicotinamide ligands forms  $\text{N}-\text{H} \cdots \text{O}$  hydrogen bonds resulting in infinite linear chains.

## Acknowledgments

The authors acknowledge the financial support from the Grant for Young Scientists (Project 15.819.02.03F).

## References

- Seo, J.; Bonneau, C.; Matsuda, R.; Takata, M.; Kitagawa, S. Soft secondary building unit: dynamic bond rearrangement on multinuclear core of porous coordination polymers in gas media. *Journal of the American Chemical Society*, 2011, 133, pp. 9005-9013.
- Rosi, N.L.; Kim, J.; Eddaoudi, M.; Chen, B.L.; O'Keeffe, M.; Yaghi, O.M. Rod packings and metal-organic frameworks constructed from rod-shaped secondary building units. *Journal of the American Chemical Society*, 2005, 127, pp. 1504-1518.
- Ye, B.H.; Tong, M.L.; Chen, X.M. Metal-organic molecular architectures with 2,2'-bipyridyl-like and carboxylate ligands. *Coordination Chemistry Reviews*, 2005, 249, pp. 545-565.
- Robin, A.Y.; Fromm, K.M. Coordination polymer networks with O- and N-donors: What they are, why and how they are made. *Coordination Chemistry Reviews*, 2006, 250, pp. 2127-2157.
- Moulton, B.; Zaworotko, M.J. From molecules to crystal engineering: supramolecular isomerism and polymorphism in network solids. *Chemical Reviews*, 2001, 101, pp. 1629-1658.
- Janiak, C. Engineering coordination polymers towards applications. *Dalton Transactions*, 2003, 14, pp. 2781-2804.
- Dakovic, M.; Jaglicic, Z.; Kozlevcar, B.; Popovic, Z. Association of copper(II) isonicotinamide moieties via different anionic bridging ligands: Two paths of ferromagnetic interaction in the azide coordination compound. *Polyhedron*, 2010, 29, pp. 1910-1917.
- Adhikary, C.; Koner, S. Structural and magnetic studies on copper(II) azido complexes. *Coordination Chemistry Reviews*, 2010, 254, pp. 2933-2958.
- Meng, Z.-S.; Yun, L.; Zhang, W.-X.; Hong, C.-G.; Herchel, R.; Ou, Y.-C.; Leng, J.-D.; Peng, M.-X.; Lin, Z.-J.; Tong, M.-L. Reactivity of 4-amino-3,5-bis(pyridin-2-yl)-1,2,4-triazole, structures and magnetic properties of polynuclear and polymeric Mn(II), Cu(II) and Cd(II) complexes. *Dalton Transactions*, 2009, pp. 10284-10295.
- Li, X.; Cheng, D.-Y.; Lin, J.-L.; Li, Z.-F.; Zheng, Y.-Q. Di-, tetra-, and hexanuclearhydroxy-bridged copper(II) cluster compounds: syntheses, structures, and properties. *Crystal Growth and Design*, 2008, 8, pp. 2853-2861.
- Ford, P.C.; Cariati, E.; Bourassa, J. Photoluminescence properties of multinuclear copper(I) compounds. *Chemical Reviews*, 1999, 99, pp. 3625-3648.

12. Fukaya, M.; Tamura, Y.; Chiba, Y.; Tanioka, T.; Mao, J.; Inoue, Y.; Yamada, M.; Waeber, C.; Ido-Kitamura, Y.; Kitamura, T.; Kaneki, M. Protective effects of a nicotinamide derivative, isonicotinamide, against streptozotocin-induced  $\beta$ -cell damage and diabetes in mice. *Biochemical and Biophysical Research Communications*, 2013, 442, pp. 92-98.
13. Perec, M.; Baggio, R.F.; Pena, O.; Sartoris, R.P.; Calvo, R. Synthesis and structures of four new compounds of the copper(II)-carboxylate-pyridinecarboxamide system. *Inorganica Chimica Acta*, 2011, 373, pp. 117-123.
14. Aakeroy, C.B.; Beatty, A.M.; Desper, J.; O'Shea, M.; Valdes-Martinez, J. Directed assembly of dinuclear and mononuclear copper(II)-carboxylates into infinite 1-D motifs using isonicotinamide as a high-yielding supramolecular reagent. *Dalton Transactions*, 2003, pp. 3956-3962.
15. Dakovic, M.; Popovic, Z. Uncommon isonicotinamide supramolecular synthons in copper(II) complexes directed by nitrate and perchlorate anions. *Acta Crystallographica Section C*, 2009, 65, pp. m361-m366.
16. Moncol, J.; Mudra, M.; Lonnecke, P.; Hewitt, M.; Valko, M.; Morris, H.; Svorec, J.; Melnik, M.; Mazur, M.; Koman, M. Crystal structures and spectroscopic behavior of monomeric, dimeric and polymeric copper(II) chloroacetate adducts with isonicotinamide, *N*-methylnicotinamide and *N,N*-diethylnicotinamide. *Inorganica Chimica Acta*, 2007, 360, pp. 3213-3225.
17. Zhang, J.-P.; Lin, Y.-Y.; Huang, X.-C.; Chen, X.-M. Copper(I) 1,2,4-triazolates and related complexes: studies of the solvothermal ligand reactions, network topologies, and photoluminescence properties. *Journal of the American Chemical Society*, 2005, 127, pp. 5495-5506.
18. Necefoglu, H.; Cimen, E.; Tercan, B.; Dal, H.; Hokelek, T. Tetra-kis( $\mu$ -4-methyl-benzoato- $k^2O:O'$ )bis-[(isonicotinamide- $kN$ )copper(II)]. *Acta Crystallographica Section E*, 2010, 66, pp. m334-m335.
19. Ucar, I.; Bulut, A.; Buyukgungor, O. *catena*-Poly[[[diaquabis(pyridine-4-carboxamide- $kN$ )copper(II)]- $\mu_2$ -squarato- $kO^1:O^3$ ] dihydrate]. *Acta Crystallographica Section C*, 2005, 61, pp. m218-m220.
20. Gor, K.; Kurkcuglu, G.S.; Yesilel, O.Z.; Buyukgungor, O. One-dimensional bimetallic cyano complexes with nicotinamide and isonicotinamide ligands. *Journal of Molecular Structure*, 2014, 1060, pp. 166-175.
21. Nazir, S.; Rashid, M.A.; Arif, M.; Romerosa, A.; Whitwood, A.C. Metal backbone polymers  $[M(isn-\kappa N_{py})_4(\mu-SiF_6-\kappa F, F')]$  ( $M=Cu, Co, Ni$ ; isn=isonicotinamide) containing an unusual hexafluoridosilicato bridge. *Inorganica Chimica Acta*, 2015, 427, pp. 198-202.
22. Pasan, J.; Sanchiz, J.; Lloret, F.; Julve, M.; Ruiz-Perez, C. Copper(II)-phenylmalonate complexes with the bifunctional ligands nicotinamide and isonicotinamide. *Polyhedron*, 2011, 30, pp. 2451-2458.
23. Llano-Tome, F.; Bazan, B.; Urtiaga, M.-K.; Barandika, G.; Lezama, L.; Arriortua, M.-I.  $Cu^{II}$ -PDC-bpe frameworks (PDC = 2,5-pyridinedicarboxylate, bpe = 1,2-di(4-pyridyl)ethylene): mapping of herringbone-type structures. *CrystEngComm*, 2014, 16, pp. 8726-8735.
24. Shankar, K.; Das, B.; Baruah, J.B. Organic cations controlling the nuclearity of copper(II) 2,5-pyridinedicarboxylates. *RSC Advances*, 2013, 3, pp. 26220-26229.
25. Saha, R.; Biswas, S.; Mostafa, G. pH-Triggered construction of NLO active CMOFs: change in supramolecular assembly, water clusters, helical architectures and their properties. *CrystEngComm*, 2011, 13, pp. 1018-1028.
26. Niu, C.-Y.; Meng, L.; Feng, C.-L.; Dang, Y.-L.; Kou, C.-H. A one-dimensional copper(II) coordination polymer constructed by pyridyl-2,5-dicarboxylate: Helical structure and magnetic property. *Journal of Molecular Structure*, 2011, 997, pp. 60-63.
27. Mohapatra, C.; Chandrasekhar, V. Two-dimensional homometallic- to a three dimensional heterometallic coordination polymer: a metalloligand approach. *Crystal Growth and Design*, 2014, 14, pp. 406-409.
28. Du, G.; Kan, X.; Li, H. Synthesis, crystal structure, and magnetic properties of two 3d-4f heterometallic coordination polymers. *Polyhedron*, 2011, 30, pp. 3197-3201.
29. Hu, X.-L.; Sun, C.-Y.; Qin, C.; Wang, X.-L.; Wang, H.-N.; Zhou, E.-L.; Li, W.-E.; Su, Z.-M. Iodine-templated assembly of unprecedented 3d-4f metal-organic frameworks as photocatalysts for hydrogen generation. *Chemical Communications*, 2013, 49, pp. 3564-3566.
30. Xia, Z.-Q.; Wei, Q.; Chen, S.-P.; Feng, X.-M.; Xie, G.; Qiao, C.-F.; Zhang, G.-C.; Gao, S.-L. Copper(II)-lanthanide(III) coordination polymers constructed from pyridine-2,5-dicarboxylic acid: Preparation, crystal structure and photoluminescence. *Journal of Solid State Chemistry*, 2013, 197, pp. 489-498.
31. Sheldrick, G.M. A short history of *SHELX*. *Acta Crystallographica Section A*, 2008, 64, pp. 112-122.
32. Macrae, C.F.; Edgington, P.R.; McCabe, P.; Pidcock, E.; Shields, G.P.; Taylor, R.; Towler, M.; van de Streek, J. Mercury: visualization and analysis of crystal structures. *Journal of Applied Crystallography*, 2006, 39, pp. 453-457.
33. Tong, M.-L.; Li, W.; Chen, X.-M.; Zheng, S.-L.; Ng, S.W. Tetra- $\mu$ -acetato- $k^2O:O'$ -bis[(4-phenylpyridine- $kN$ )copper(II)]. *Acta Crystallographica Section C*, 2002, 58, pp. m232-m234.
34. Ge, C.-H.; Zhang, X.-D.; Guan, W.; Guo, F.; Liu, Q.-T. Roles of anions in pyridinecarboxamide-copper(II) supramolecular networks. *Chinese Journal of Chemistry*, 2006, 23, pp. 1001-1006.
35. Youngme, S.; Cheansirisomboon, A.; Danvirutai, C.; Pakawatchai, C.; Chaichit, N.; Engkagul, C.; van Albada, G.A.; Costa, J.S.; Reedijk, J. Three new polynuclear tetracarboxylato-bridged copper(II) complexes: Syntheses, X-ray structure and magnetic properties. *Polyhedron*, 2008, 27, pp. 1875-1882.

36. Xu, L.-Y.; Chen, H.-X.; Sun, X.-J.; Gu, P.-Y.; Ge, J.-F.; Li, N.-J.; Xu, Q.-F.; Lu, J.-M. Synthesis, structures and optical properties of coordination compounds bearing *N,N*-dimethyl-4-(pyridin-4-yl diazenyl) aniline. *Polyhedron*, 2012, 35, pp. 7-14.
37. Fontanet, M.; Popescu, A.-R.; Fontrodona, X.; Rodriguez, M.; Romero, I.; Teixidor, F.; Vinas, C.; Aliaga-Alcalde, N.; Ruiz, E. Design of dinuclear copper species with carboranylcarboxylate ligands: study of their steric and electronic effects. *Chemistry - A European Journal*, 2011, 17, pp. 13217-13229.
38. Tsintsadze, G.V.; Kiguradze, R.A.; Shnulin, A.N. Crystal and molecular structure of bis-(aceto)-bis-(amidoisonicotinato)-diaquo-copper(II). *Russian Journal of Structural Chemistry*, 1985, 26, pp. 406-413.
39. Perec, M.; Baggio, R. Di- $\mu$ -acetato-bis-[(acetato-*k*<sup>2</sup>*O,O'*)bis(iso-nicotinamide-*kN*)copper(II)]. *Acta Crystallographica Section E*, 2010, 66, pp. m275-m276.
40. Nakamoto, K. Infrared and Raman spectra of inorganic and coordination compounds. Wiley: New York, 1986, 432 p.

# SYNTHESIS, CRYSTAL STRUCTURE, AND PROPERTIES OF COPPER(II) COMPLEXES WITH 1,4,7-TRIS(2-AMINOETHYL)-1,4,7-TRIAZACYCLONONANE

Masahiro Mikuriya<sup>a\*</sup>, Mayu Hamagawa<sup>a</sup>, Natsuki Tomioka<sup>a</sup>, Daisuke Yoshioka<sup>a</sup>, Naoko Uehara<sup>a</sup>, Rika Fujimori<sup>a</sup>, Hiroki Yamamoto<sup>a</sup>, Yoshinari Ando<sup>a</sup>, Shoichi Hori<sup>a</sup>, Taro Kuriyama<sup>a</sup>, Ryoji Mitsuhashi<sup>a</sup>, Makoto Handa<sup>b</sup>

<sup>a</sup>Department of Applied Chemistry for Environment and Research Center for Coordination Molecule-based Devices, School of Science and Technology, Kwansei Gakuin University, 2-1 Gakuen, Sanda 669-1337, Japan

<sup>b</sup>Department of Chemistry, Interdisciplinary Graduate School of Science and Engineering, Shimane University, 1060 Nishikawatsu, Matsue 690-8504, Japan

\*e-mail: junpei@kwansei.ac.jp; phone: (+81 79) 565 8365; fax: (+81 79) 565 9729

**Abstract.** Three kinds of copper(II) complexes with 1,4,7-tris(2-aminoethyl)-1,4,7-triazacyclononane (taetacn), [Cu(taetacn)](ClO<sub>4</sub>)<sub>2</sub> (**1**), [Cu(Htaetacn)](ClO<sub>4</sub>)<sub>3</sub> (**2**), and [Cu(Htaetacn)](BF<sub>4</sub>)<sub>3</sub> (**3**) were synthesized and characterized by elemental analyses, IR and UV-Vis spectroscopies. The spectral features are in harmony with an octahedral geometry for **1** and a square-pyramidal coordination for **2** and **3**. The crystal structure of **2** was determined by the single-crystal X-ray diffraction method at 293 K. It crystallizes in the orthorhombic space group *Pnma* with *a* = 20.605(3) Å, *b* = 12.7944(18) Å, *c* = 9.8972(14) Å, *V* = 2609.2(6) Å<sup>3</sup>, *D<sub>x</sub>* = 1.582 g/cm<sup>3</sup>, and *Z* = 4. The *R*1 [*I* > 2σ(*I*)] and *wR*2 (all data) values are 0.0723 and 0.2389, respectively, for all 3253 independent reflections. The compound consists of square-pyramidal copper(II) cation with protonated Htaetacn and tetrahedral ClO<sub>4</sub><sup>−</sup> anions. The temperature dependence of magnetic susceptibilities obeyed the Curie-Weiss law with *Θ* = −2.4, −5.2 and −7.2 K for **1**, **2**, and **3**, respectively. Cyclic voltammetry of **2** in DMF showed two quasi-reversible reduction waves (*E*<sub>pc</sub> = −0.98, *E*<sub>pc</sub> = −0.92; *E*<sub>pc</sub> = −1.30, *E*<sub>pc</sub> = −1.22 V versus Fc/Fc<sup>+</sup>).

**Keywords:** copper(II) complex, magnetic properties, macrocyclic ligand, 1,4,7-triazacyclononane.

Received: October 2015/ Revised final: October 2015/ Accepted: October 2015

## Introduction

There have been a considerable interest in coordination chemistry of macrocyclic ligands in the past five decades [1,2]. Small macrocyclic ligand, 1,4,7-triazacyclononane (tacn), is one of the most studied compounds among macrocyclic ligands [3–6] because of the too small size to incorporate metal ion in the triaza-ring, generating mononuclear metal complexes with a sandwich structure [7] and a piano-stool structure [8]. Previously, we reported on metal complexes with cyclam-based octadentate ligand having four 2-aminoethyl groups as pendant arms, 1,4,8,11-tetrakis(2-aminoethyl)-1,4,8,11-tetraazacyclodecane (taec) [9–16]. The taec ligand forms unique dinuclear metal complexes, where the two metal ions are bound by the four pendant groups outside the cyclam ring. Substitution of the 2-aminoethyl pendant groups by other groups such as salicylideneaminoethyl groups also afforded similar dinuclear metal complexes [17–20]. Concerning these cyclam-based ligands with four pendant groups, the corresponding tacn-based hexadentate ligands with three pendant groups are of interest [21–23]. Especially, 1,4,7-tris(2-aminoethyl)-1,4,7-triazacyclononane (taetacn), as shown in Figure 1, is interesting for us due to the comparison with the taec ligand. However, there are still only few reports on metal complexes with taetacn [21,22]. Therefore, we have been engaged in synthesis of metal complexes with taetacn and found out that a mononuclear nickel(II) complex with octahedral geometry is formed by reactions of taetacn and nickel(II) salt [24].

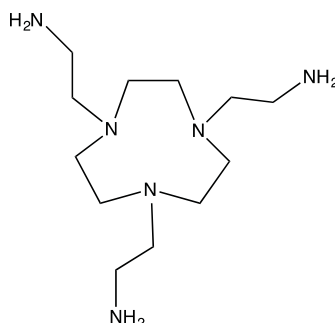


**Figure 1.** The hexadentate macrocyclic ligand taetacn.

In this study, we synthesized new metal complexes with taetacn from reactions of copper(II) salts and taetacn and characterized the isolated complexes. Herein we report on the synthesis, variable temperature magnetic moments, and electronic spectra of  $[\text{Cu}(\text{taetacn})](\text{ClO}_4)_2 \cdot \text{H}_2\text{O}$  (**1**) and  $[\text{Cu}(\text{Htaetacn})](\text{ClO}_4)_3 \cdot \text{H}_2\text{O}$  (**2**), where taetacn denotes 1,4,7-tris(2-aminoethyl)-1,4,7-triazacyclononane. We also report on the crystal structure and electrochemical properties of  $[\text{Cu}(\text{Htaetacn})](\text{ClO}_4)_3 \cdot \text{H}_2\text{O}$  (**2**).

## Experimental

**Synthesis.** The ligand taetacn was synthesized by a reaction of tacn with *N*-(*p*-tosylsulfonyl)aziridine according to the method described in the literature [24]. Other reagents and solvents were obtained from commercial sources and were used without further purification.

### $[\text{Cu}(\text{taetacn})](\text{ClO}_4)_2 \cdot \text{H}_2\text{O}$ (**1**)

Copper(II) perchlorate hexahydrate (31.5 mg, 0.086 mmol) dissolved in methanol (1 cm<sup>3</sup>) was added to a methanol solution of taetacn (22.4 mg, 0.087 mmol) in methanol (1 cm<sup>3</sup>). The resulting solution was kept at ambient temperature overnight to give blue crystals. The crystals were filtered, washed with small amount of methanol, and dried *in vacuo*. Yield: 19.7 mg (43%). Anal. Found: C, 26.80; H, 6.33; N, 15.78%. Calcd for  $\text{C}_{12}\text{H}_{32}\text{Cl}_2\text{CuN}_6\text{O}_9$ : C, 26.75; H, 5.99; N, 15.60%. IR (KBr):  $\nu(\text{OH})$  3569;  $\nu(\text{NH})$  3328, 3279;  $\nu(\text{CH})$  2954, 2876;  $\delta(\text{NH})$  1595;  $\nu(\text{ClO})$  1088, 625 cm<sup>-1</sup>. Diffuse reflectance spectrum:  $\lambda_{\text{max}}$  292, 694 nm.

### $[\text{Cu}(\text{Htaetacn})](\text{ClO}_4)_3 \cdot \text{H}_2\text{O} \cdot \text{CH}_3\text{OH}$ (**2**)

Copper(II) perchlorate hexahydrate (27.2 mg, 0.073 mmol) dissolved in methanol (1 cm<sup>3</sup>) was added to a magnetically stirred solution of taetacn (9.5 mg, 0.037 mmol) in methanol (1 cm<sup>3</sup>). The resulting solution was kept at ambient temperature overnight to give purple crystals. The crystals were filtered, washed with small amount of methanol, and dried *in vacuo*. Yield: 7.9 mg (32%). Anal. Found: C, 23.16; H, 5.12; N, 12.84%. Calcd for  $\text{C}_{13}\text{H}_{37}\text{Cl}_3\text{CuN}_6\text{O}_{14}$ : C, 23.26; H, 5.55; N, 12.52%. IR (KBr):  $\nu(\text{OH})$  3546;  $\nu(\text{NH})$  3323, 3280;  $\nu(\text{NH}_3^+)$  3178;  $\nu(\text{CH})$  2944, 2884;  $\delta(\text{NH})$  1596;  $\nu(\text{ClO})$  1099, 624 cm<sup>-1</sup>. Diffuse reflectance spectrum:  $\lambda_{\text{max}}$  287, 572, 638sh, 845 nm.

Complex **2** was also prepared by reaction of taetacn and copper(II) perchlorate hexahydrate in the 1:3 mole ratio instead of the 1:2 ratio. Yield: 10.5 mg (15%). Anal. Found: C, 22.60; H, 4.81; N, 12.97%. Calcd for  $[\text{Cu}(\text{Htaetacn})](\text{ClO}_4)_3 \cdot \text{H}_2\text{O}$  ( $\text{C}_{12}\text{H}_{33}\text{Cl}_3\text{CuN}_6\text{O}_{13}$ ): C, 22.54; H, 5.20; N, 13.15%. IR (KBr):  $\nu(\text{OH})$  3585;  $\nu(\text{NH})$  3322, 3280;  $\nu(\text{NH}_3^+)$  3180;  $\nu(\text{CH})$  2988, 2943, 2883;  $\delta(\text{NH})$  1596;  $\nu(\text{ClO})$  1102, 625 cm<sup>-1</sup>. Diffuse reflectance spectrum:  $\lambda_{\text{max}}$  290, 574, 640sh, 828 nm.

### $[\text{Cu}(\text{Htaetacn})](\text{BF}_4)_3 \cdot \text{H}_2\text{O} \cdot \text{CH}_3\text{OH}$ (**3**)

Copper(II) tetrafluoroborate hexahydrate (31.5 mg, 0.091 mmol) dissolved in methanol (1 cm<sup>3</sup>) was added to a methanol solution of taetacn (22.4 mg, 0.087 mmol) in methanol (1 cm<sup>3</sup>). The resulting solution was kept at ambient temperature overnight to give a deep blue precipitate. The precipitate was filtered, washed with small amount of methanol, and dried *in vacuo*. Yield: 40.0 mg (73%). Anal. Found: C, 24.47; H, 5.61; N, 13.24%. Calcd for  $\text{C}_{13}\text{H}_{37}\text{B}_3\text{CuF}_{12}\text{N}_6\text{O}_2$ : C, 24.65; H, 5.89; N, 13.27%. IR (KBr):  $\nu(\text{NH})$  3323, 3279;  $\nu(\text{NH}_3^+)$  3181;  $\nu(\text{CH})$  2955, 2884;  $\delta(\text{NH})$  1604;  $\nu(\text{BF})$  1053, 624. Diffuse reflectance spectrum:  $\lambda_{\text{max}}$  288, 578, 640sh, 840 nm.

Complex **3** was also prepared by reaction of taetacn and copper(II) tetrafluoroborate hexahydrate in the 1:2 and 1:3 mole ratio instead of the 1:1 ratio. Yield: 19.3 mg (36%); 22.5 mg, (42%). Anal. Found: C, 23.48; H, 5.60; N, 13.30%. Calcd for  $[\text{Cu}(\text{Htaetacn})](\text{BF}_4)_3 \cdot 2\text{H}_2\text{O}$  ( $\text{C}_{12}\text{H}_{35}\text{B}_3\text{CuF}_{12}\text{N}_6\text{O}_2$ ): C, 23.27; H, 5.70; N, 13.57%. IR (KBr):  $\nu(\text{NH})$  3341, 3285;  $\nu(\text{NH}_3^+)$  3182;  $\nu(\text{CH})$  2954, 2884;  $\delta(\text{NH})$  1603;  $\nu(\text{BF})$  1082, 625 cm<sup>-1</sup>. Diffuse reflectance spectrum:  $\lambda_{\text{max}}$  282, 577, 640sh, 840 nm.

**Measurements.** Elemental analyses for carbon, hydrogen, and nitrogen were done using a Thermo-Finnigan FLASH EA1112 series CHNO-S analyzer. Infrared spectra were measured with a JASCO MFT-2000 FT-IR Spectrometer in the 4000–600 cm<sup>-1</sup> region. Electronic spectra were measured with a Shimadzu UV-vis-NIR Recording Spectrophotometer (Model UV-3100). Cyclic voltammetric measurements were performed using a BAS ALS-Model 1200B Electrochemical analyzer. A three-electrode cell consisting of a glassy carbon electrode, a platinum-wire counter electrode and a non-aqueous Ag/Ag<sup>+</sup> electrode was used. Ferrocene (Fc) was used as the internal standard (for Fc/Fc<sup>+</sup>,  $E_{1/2} = 0.054$  V vs. Ag/Ag<sup>+</sup>). Magnetic susceptibilities were measured with a Quantum Design MPMS-XL7 SQUID susceptometer operating at a magnetic field of 0.5 T over a range of 4.5–300 K. The susceptibilities were corrected for the diamagnetism of the constituent atoms using Pascal's constants [25]. The effective magnetic moments were calculated from the equation  $\mu_{\text{eff}} = 2.828\sqrt{\chi_{\text{M}} T}$ , where  $\chi_{\text{M}}$  is the molar magnetic susceptibility per mole of copper(II) unit.

**X-Ray crystallography.** X-Ray diffraction data for **2** were collected on a Bruker SMART APEX CCD diffractometer (Mo K $\alpha$  radiation) at 293 K and indexed using the SMART software. Crystal data and details concerning data collection are given in Table 1. The cell parameters were refined by full-matrix least-squares on  $F^2$ . Integrated intensity information for each reflections was obtained and corrected using the SAINT+ program package including the reduction program SAINT and the empirical absorption correction program SADABS. The structure was solved using the SHELXTL program. The structure was solved by direct methods, and the residual non-hydrogen atoms were located by D-Fourier synthesis. All of non-hydrogen atoms were refined by full-matrix least-squares on  $F^2$ . The hydrogen atoms



except for those of water molecules were inserted at their ideal positions and fixed there. All of the calculations were carried out on a Windows 7 Core i5 computer utilizing the SHELXTL software package [26] and SHELXL-2014/7 [27]. CCDC 1417656 for **2** contains supplementary crystallographic data for this paper. The data can be obtained free of charge at [www.ccdc.cam.ac.uk/conts/retrieving.html](http://www.ccdc.cam.ac.uk/conts/retrieving.html) [or from the Cambridge Crystallographic Data Centre, 12 Union Road, Cambridge CB12 1EZ, UK; fax: (internet.) +44 1223 336033; e-mail: [deposit@ccdc.cam.ac.uk](mailto:deposit@ccdc.cam.ac.uk)].

Table 1

## Crystal and experimental data.

Parameter	Value
Chemical formula	C <sub>12</sub> H <sub>31</sub> Cl <sub>3</sub> CuN <sub>6</sub> O <sub>12</sub>
Formula weight	621.32
Temperature, (K)	293
Crystal system	Orthorhombic
Space group	<i>Pnma</i>
<i>Z</i>	4
<i>a</i> , (Å)	20.605(3)
<i>b</i> , (Å)	12.7944(18)
<i>c</i> , (Å)	9.8972(14)
<i>V</i> , (Å <sup>3</sup> )	2609.2(6)
<i>D<sub>x</sub></i> , (g/cm <sup>3</sup> )	1.582
Radiation: Mo Ka, λ, (Å)	0.71073
μ (Mo Ka), (mm <sup>-1</sup> )	1.208
<i>F</i> (000)	1284
Crystal size, (mm <sup>3</sup> )	0.60 x 0.30 x 0.30
No. of reflections collected	15491
No. of independent reflections	3253
θ range for data collection, (°)	1.977 - 28.528
Data/Restraints/Parameters	3253/0/167
Goodness-of-fit on <i>F</i> <sup>2</sup>	0.955
<i>R</i> indices [ <i>I</i> > 2σ( <i>I</i> )]	<i>R</i> 1 = 0.0723, <i>wR</i> 2 = 0.2199
<i>R</i> indices (all data)	<i>R</i> 1 = 0.0990, <i>wR</i> 2 = 0.2389
(Δ/σ) <sub>max</sub>	0.023
(Δρ) <sub>max</sub> , (eÅ <sup>-3</sup> )	0.826
(Δρ) <sub>min</sub> , (eÅ <sup>-3</sup> )	-0.411
Measurement	Bruker Smart APEX CCD diffractometer
Program system	SHELXTL
Structure determination	Direct methods (SHELXS-97)
Refinement	full matrix least-squares (SHELXL-2014/7)
CCDC deposition number	1417656

## Results and discussion

The taetacn ligand was reacted with copper(II) perchlorate in a molar ratio of 1:1, 1:2, and 1:3 in methanol. Only the 1:1 ratio case afforded a 1:1 complex, [Cu(taetacn)](ClO<sub>4</sub>)<sub>2</sub> (**1**), whereas a protonated complex, [Cu(Htaetacn)](ClO<sub>4</sub>)<sub>3</sub> (**2**), was isolated for the 1:2 and 1:3 cases. Single crystals suitable for the X-ray structure analysis were obtained from the methanol solution of **2**, and the crystal structure was determined by the X-ray diffraction method. The formulation of mononuclear species of **1** and **2** was confirmed by the elemental analysis, infrared and electronic absorption spectroscopies, and magnetic susceptibility measurements (4.5–300 K).

In the infrared spectra of the perchlorate complexes, **1** and **2**, two N-H stretching vibration bands of the 2-aminoethyl pendant groups were observed at 3328–2323 cm<sup>-1</sup> and 3280–3279 cm<sup>-1</sup>. These two bands can be assigned to the antisymmetric ν<sub>as</sub>(NH<sub>2</sub>) and symmetric ν<sub>s</sub>(NH<sub>2</sub>) vibrations, respectively. In the case of **2**, another N-H stretching band due to NH<sub>3</sub><sup>+</sup> was observed at 3178–3180 cm<sup>-1</sup>, in accordance with the presence of the protonated 2-aminoethyl pendant group. Stretching band of the perchlorate ion appeared as a strong broad band at around 1088–1102 cm<sup>-1</sup>. Small splitting of the band suggests no coordination of the perchlorate ions to the copper center [28]. The infrared spectrum of the tetrafluoroborate complex **3** shows a similar spectral feature to that of the perchlorate **2** with ν<sub>as</sub>(NH<sub>2</sub>) at 3323–3341 cm<sup>-1</sup>, ν<sub>s</sub>(NH<sub>2</sub>) at 3279–3285 cm<sup>-1</sup>, ν(NH<sub>3</sub><sup>+</sup>) at 3181–3182 cm<sup>-1</sup> and ν(BF<sub>4</sub><sup>-</sup>) at 1053–1082 cm<sup>-1</sup>.

The diffuse reflectance spectra of **1** and **2** are shown in Figure 2. In the spectra of **1**, one absorption band appeared at around 694 nm in the visible region. This band may be attributed to d-d transition (<sup>2</sup>E<sub>g</sub> → <sup>2</sup>T<sub>2g</sub>) of an octahedral

copper(II) ion. On the other hand, three bands appeared in the visible region of the spectra of **2**. The band at 572 nm may be assigned to spin-allowed  $^2B_1 \rightarrow ^2E$  transition, a shoulder at 638 nm to a spin-allowed  $^2B_1 \rightarrow ^2B_2$  transition, and a band at around 845 nm to spin-allowed  $^2B_1 \rightarrow ^2A_1$  transition [29]. The spectral feature is in harmony with a square-pyramidal copper(II) ion. The electronic spectra of **1** and **2** in  $H_2O$  become a little similar to each other, although keeping the difference between **1** and **2** in the solid state to some extent in the visible region [**1**: 275 nm ( $\epsilon = 4600 \text{ mol}^{-1}\text{dm}^3\text{cm}^{-1}$ ), 606 nm ( $\epsilon = 130 \text{ mol}^{-1}\text{dm}^3\text{cm}^{-1}$ ); **2**: 275 nm ( $\epsilon = 4300 \text{ mol}^{-1}\text{dm}^3\text{cm}^{-1}$ ), 578 nm ( $\epsilon = 160 \text{ mol}^{-1}\text{dm}^3\text{cm}^{-1}$ ), and 802 nm ( $78 \text{ mol}^{-1}\text{dm}^3\text{cm}^{-1}$ )]. The diffuse reflectance spectrum of **3** is similar to that of **2**, suggesting the similar square-pyramidal geometry of the copper(II) ion in **3**.

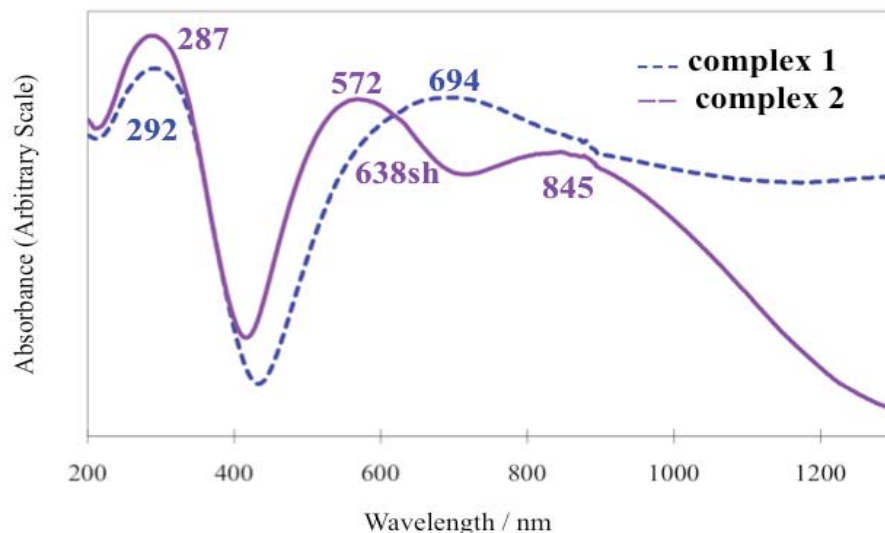


Figure 2. Diffuse reflectance spectra of **1** and **2**.

In the crystal, the asymmetric unit consists of one half of  $[Cu(Htaetacn)]^{3+}$  cation, and one and a half of  $ClO_4^-$  ions. The complex cation structure drawn by ORTEP program is shown in Figure 3. The molecule has a crystallographic mirror plane intersecting the Cu1, N1, C4, C5, and N4 atoms. In the cation, the copper(II) atom is coordinated by three amino nitrogen atoms of tacn moiety and two amino nitrogen atoms of the pendant groups in a distorted square pyramid.

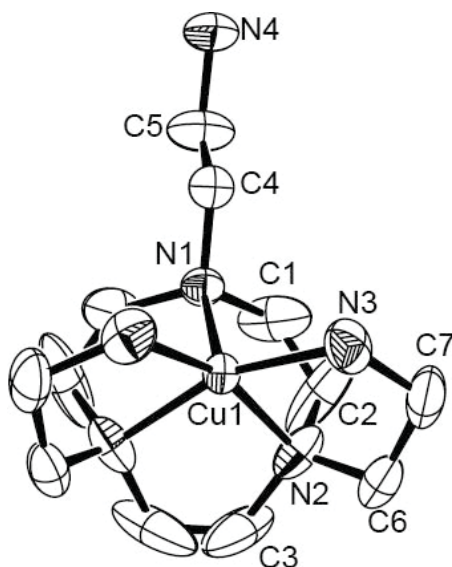


Figure 3. ORTEP drawing of the structure of the copper complex showing the 50% probability level thermal ellipsoids.

Selected bond lengths (Å) and angles (°): Cu1-N1 2.242(5), Cu1-N2 2.015(4), Cu1-N3 2.012(4); N1-Cu1-N2 83.52(17), N1-Cu1-N3 112.73(17), N2-Cu1-N3 85.4(2), N2-Cu1-N2<sup>i</sup> 84.9(3), N2-Cu1-N3<sup>i</sup> 160.0(2), N3-Cu1-N3<sup>i</sup> 98.1(3). Symmetry code: (i)  $x, 1/2 - y, z$ .



It is to be noted that one pendant arm is protonated and does not take part in coordination to the metal atom. This is in contrast with the case for  $[\text{Ni}(\text{taetacn})](\text{ClO}_4)_2 \cdot \text{H}_2\text{O}$ , where the metal atom takes an octahedral geometry with three pendant amino groups [24]. The axial Cu1-N1 distance (2.242(5) Å) is considerably longer than those with the basal Cu-N distances (2.012(4) and 2.015(4) Å). The  $\tau$  value is 0.0, showing the square-pyramidal geometry around the copper atom [30]. In the crystal, the protonated amino nitrogen atom N4 is surrounded by four perchlorate-oxygen atoms by hydrogen bonds  $[\text{N4} \cdots \text{O3} (x, y, 1+z) 2.965 \text{ Å}, \text{N4} \cdots \text{O7} (x, y, 1+z) 3.065 \text{ Å}]$  (Figure 4).

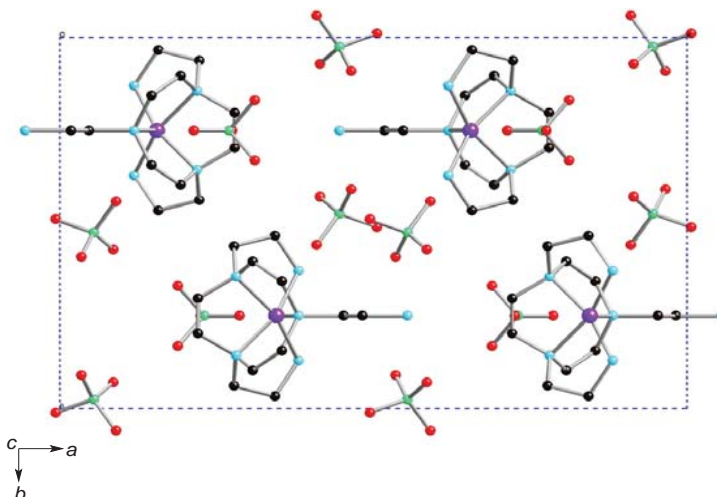


Figure 4. Packing diagram of **2** viewed along the *c* axis. Hydrogen atoms are omitted for clarity.

The magnetic moment of **1** is  $1.96 \mu_{\text{B}}$  at 300 K. This value is larger than the spin-only value of copper(II) ( $1.73 \mu_{\text{B}}$ ,  $S = 1/2$ ), being typical for the octahedral copper(II) complexes due to spin-orbital coupling with the excited *T* state [18]. The moment decreases slightly with the lowering of temperature, reaching a value of  $1.86 \mu_{\text{B}}$  at 4.5 K. In Figure 5, magnetic susceptibilities and inverses of magnetic susceptibilities of **1** were plotted versus temperature. As can be seen in Figure 5, the magnetic data obey the Curie-Weiss law,  $\chi = C/(T - \theta)$ , with a small Weiss constant ( $\theta = -2.4 \text{ K}$ ,  $C = 0.481 \text{ cm}^3\text{Kmol}^{-1}$ ). This result shows that magnetic interaction between copper(II) ions is weak. The magnetic moments of **2** and **3** are 2.02 and  $2.04 \mu_{\text{B}}$ , respectively, at 300 K and decrease to 1.78 and  $1.81 \mu_{\text{B}}$ , respectively, at 4.5 K, with the lowering of temperature. The magnetic data obey the Curie-Weiss law (**2**:  $\theta = -5.2 \text{ K}$ ,  $C = 0.527 \text{ cm}^3\text{Kmol}^{-1}$ ; **3**:  $\theta = -7.2 \text{ K}$ ,  $C = 0.515 \text{ cm}^3\text{Kmol}^{-1}$ ), similarly to **1**.

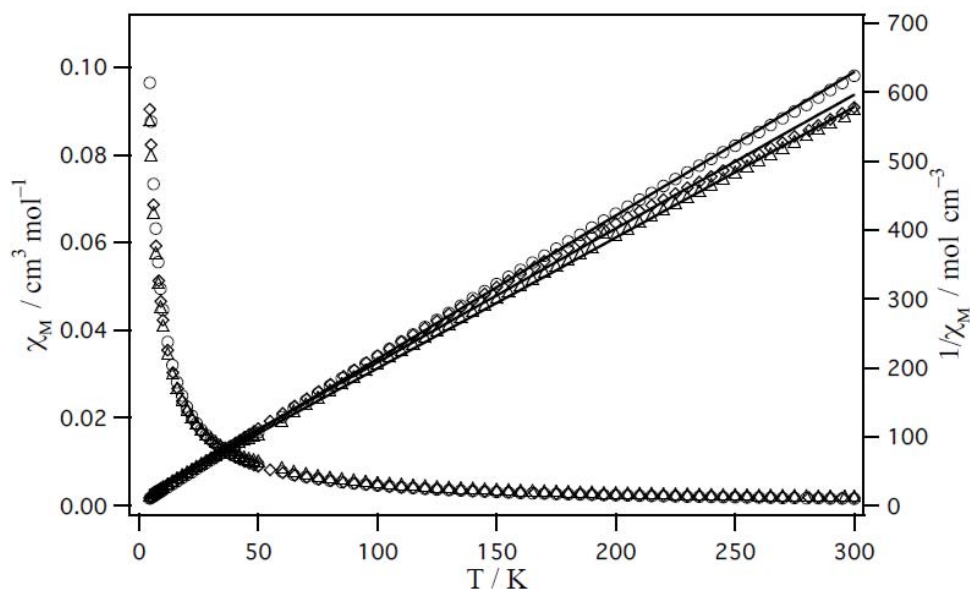
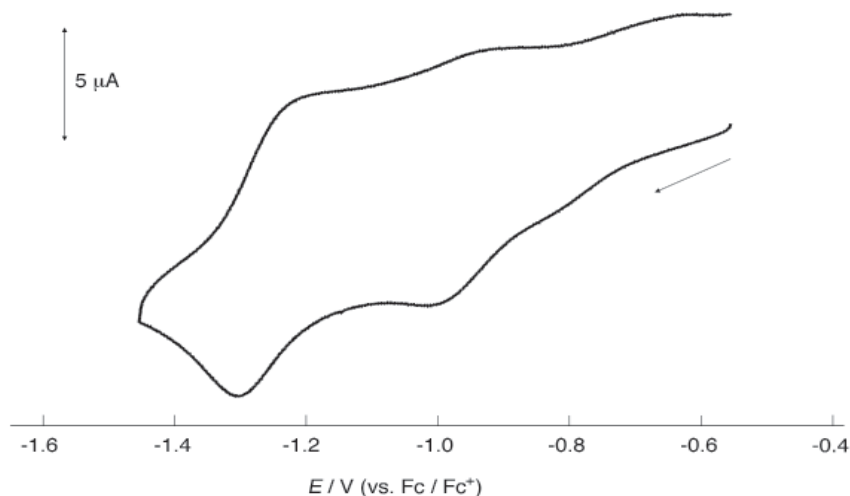


Figure 5. Temperature dependence of magnetic susceptibilities and inverse magnetic susceptibilities for **1** (circles), **2** (triangles) and **3** (diamonds).

The cyclic voltammogram of **2** was measured in DMF containing tetrabutylammonium perchlorate (0.1 M), (Figure 6). In the  $-0.6$  to  $-1.5$  V versus Fc/Fc<sup>+</sup> region, two reduction waves are observed. Both the reduction waves have the characteristic of an electrochemically quasi-reversible couples ( $E_{pc} = -0.98$ ,  $E_{pa} = -0.92$ ,  $E_{1/2} = 0.95$  V versus Fc/Fc<sup>+</sup>;  $E_{pc} = -1.30$ ,  $E_{pa} = -1.22$ ,  $E_{1/2} = -1.26$  V versus Fc/Fc<sup>+</sup>). The former may be assigned to the Cu(II)/Cu(I) couple for the square-pyramidal copper(II) and the latter may be due to the Cu(II)/Cu(I) couple for the octahedral copper(II) center, suggesting the existence of the two species in solution as found in solution spectra. This is in contrast with the case for the nickel(II) complex with taetacn, which shows only one species in solution [24].



**Figure 6.** Cyclic voltammogram of **2** in DMF: [complex] = 0.001 M, [TBAP] = 0.2 M (TBAP = tetrabutylammonium perchlorate), scan rate = 100 mV S<sup>-1</sup>.

## Conclusions

By using taetacn ligand, synthesis of mononuclear copper(II) complexes, [Cu(taetacn)](ClO<sub>4</sub>)<sub>2</sub>·H<sub>2</sub>O, [Cu(Htaetacn)](ClO<sub>4</sub>)<sub>3</sub>·H<sub>2</sub>O, and [Cu(Htaetacn)](BF<sub>4</sub>)<sub>3</sub>·H<sub>2</sub>O, was accomplished in this study. The analytical data, infrared spectra, UV-vis-NIR spectra, and temperature dependence of magnetic susceptibilities are consistent with mononuclear structures with octahedral and square-pyramidal geometries for these systems.

## Acknowledgements

The present work was partially supported by Grant-in-Aid for Scientific Research No. 26410080 from the Ministry of Education, Culture, Sports, Science and Technology (MEXT, Japan) and the MEXT-Supported Program for the Strategic Research Foundation at Private Universities, 2010–2014.

## References

1. Wainwright, K.P. Synthetic and structural aspects of the chemistry of saturated polyaza macrocyclic ligands bearing pendant coordinating groups attached to nitrogen. *Coordination Chemistry Reviews*, 1997, 166, pp. 35–90.
2. Gale, P.A.; Steed, J.W. Eds. *Supramolecular chemistry: from molecules to nanomaterials*. John Wiley & Sons: West Sussex, 2012, Vol. 4, pp. 1851–1876.
3. Belousoff, M.J.; Duriska, M.B.; Graham, B.; Batten, S.R.; Moubaraki, B.; Murray, K.S.; Spiccia, L. Synthesis, X-ray crystal structures, magnetism, and phosphate ester cleavage properties of copper(II) complexes of N-substituted derivatives of 1,4,7-triazacyclononane. *Inorganic Chemistry*, 2006, 45, pp. 3746–3755.
4. Romakh, V.B.; Therrien, B.; Suss-Fink, G.; Shul'pin, G.B. Dinuclear manganese complexes containing chiral 1,4,7-triazacyclononane-derived ligands and their catalytic potential for the oxidation of olefins, alkanes, and alcohols. *Inorganic Chemistry*, 2007, 46, pp. 1315–1331.
5. Barta, C.A.; Bayly, S.R.; Read, P.W.; Patrick, B.O.; Thompson, R.C.; Orvig, C. Molecular architectures for trimetallic d/f/d complexes: structural and magnetic properties of a LnNi<sub>2</sub> core. *Inorganic Chemistry*, 2008, 47, pp. 2280–2293.
6. Yang, C.-T.; Sreerama, S.G.; Hsieh, W.-Y.; Liu, S. Synthesis and characterization of a novel macrocyclic chelator with 3-hydroxy-4-pyrone chelating arms and its complexes with medically important metals. *Inorganic Chemistry*, 2008, 47, pp. 2719–2727.

7. Zoumpa, L.J.; Margulis, T.N. Trigonal distortion in a nickel(II) complex. Structure of  $[\text{Ni}(\text{[9]eneN}_3)_2](\text{NO}_3)_2 \cdot \text{H}_2\text{O}$ . *Inorganica Chimica Acta*, 1978, 28, pp. L157–L159.
8. Chaudhuri, P.; Wieghart, K.; Tsai, Y.-H.; Kruger, C. Reaction of  $\text{LM}(\text{CO})_3$  complexes ( $\text{M} = \text{Cr}, \text{Mo}, \text{W}$ ;  $\text{L} = 1,4,7\text{-triazacyclononane}$ ) with bromine, iodine, and nitric acid. Syntheses of air-stable hydridocarbonyl and hydridonitrosyl complexes. Crystal structure of  $[\text{LMo}(\text{CO})_3\text{Br}](\text{ClO}_4) \cdot \text{H}_2\text{O}$ . *Inorganic Chemistry*, 1984, 23, pp. 427–432.
9. Kida, S.; Murase, I.; Harada, C.; Daizeng, L.; Mikuriya, M. Synthesis and properties of copper(II) triperchlorates with  $N,N',N'',N'''$ -tetrakis(2-aminoethyl)-1,4,8,11-tetraazacyclotetradecane and an anion. *Bulletin of the Chemical Society of Japan*, 1986, 59, pp. 2595–2597.
10. Mikuriya, M.; Kida, S.; Murase, I. Crystal and molecular structure of a novel mixed-spin binuclear nickel(II) complex with  $N,N',N'',N'''$ -tetrakis(2-aminoethyl)-1,4,8,11-tetraazacyclotetradecane. *Journal of the Chemical Society, Dalton Transaction*, 1987, pp. 1261–1262.
11. Mikuriya, M.; Kida, S.; Murase, I. Preparation and crystal structures of binuclear copper(II) complexes of  $N,N',N'',N'''$ -tetrakis(2-aminoethyl)-1,4,8,11-tetraazacyclotetradecane containing azide, cyanate, or thiocyanate ion. *Bulletin of the Chemical Society of Japan*, 1987, 60, pp. 1355–1359.
12. Mikuriya, M.; Kida, S.; Murase, I. Crystal and molecular structures of  $[\text{Cu}_2(\text{taec})\text{X}](\text{ClO}_4)_3 \cdot n\text{H}_2\text{O}$  ( $\text{taec} = N,N',N'',N'''$ -tetrakis(2-aminoethyl)-1,4,8,11-tetraazacyclotetradecane;  $\text{X} = \text{I}, \text{F}, \text{NO}_2$ , and  $\text{CH}_3\text{COO}$ ;  $n = 0, 1$ , or  $2$ ). Effect of incorporation of an anion X on the structure of the complex cation. *Bulletin of the Chemical Society of Japan*, 1987, 60, pp. 1681–1689.
13. Mikuriya, M.; Kida, S.; Kohzuma, T.; Murase, I. X-ray crystal structure and electrochemical property of a novel monohydroxo-bridged binuclear cobalt(II) complex with  $N,N',N'',N'''$ -tetrakis(2-aminoethyl)-1,4,8,11-tetraazacyclotetradecane. *Bulletin of the Chemical Society of Japan*, 1988, 61, pp. 2666–2668.
14. Mikuriya, M.; Murase, I.; Asato, E.; Kida, S. A novel  $\mu$ -carbonato-bridged binuclear nickel(II) complex with  $N,N',N'',N'''$ -tetrakis(2-aminoethyl)-1,4,8,11-tetraazacyclotetradecane. *Chemistry Letters*, 1989, pp. 497–500.
15. Murase, I.; Mikuriya, M.; Sonoda, H.; Fukuda, Y.; Kida, S. Synthesis and X-ray structural characterization of novel binuclear complexes of copper(II), nickel(II), and cobalt(II) with an octadentate ligand,  $N,N',N'',N'''$ -tetrakis(2-aminoethyl)-1,4,8,11-tetraazacyclotetradecane. *Journal of the Chemical Society, Dalton Transaction*, 1986, pp. 953–959.
16. Mikuriya, M.; Kida, S.; Murase, I. Preparation and crystal structures of binuclear copper(II) complexes of  $N,N',N'',N'''$ -tetrakis(2-aminoethyl)-1,4,8,11-tetraazacyclotetradecane containing azide, cyanate, or thiocyanate ion. *Bulletin of the Chemical Society of Japan*, 1987, 60, pp. 1355–1359.
17. Wada, S.; Mikuriya, M. Synthesis and structural characterization of dinuclear manganese(III) complexes with cyclam-based macrocyclic ligands having Schiff-base pendant arms as chelating agents. *Bulletin of the Chemical Society of Japan*, 2008, 81, pp. 348–357.
18. Wada, S.; Saka, K.; Yoshioka, D.; Mikuriya, M. Synthesis, crystal structures, and magnetic properties of dinuclear and hexanuclear copper(II) complexes with cyclam-based macrocyclic ligands having four Schiff-base pendant arms. *Bulletin of the Chemical Society of Japan*, 2010, 83, pp. 364–374.
19. Mikuriya, M.; Kuriyama, T.; Omote, M. Synthesis and properties of dinuclear oxido vanadium(IV) complexes with cyclam-based macrocyclic ligands having four Schiff-base pendant arms. *Advancing Coordination, Bioinorganic and Applied Inorganic Chemistry*. Eds. Menik, M.; Segl'a, P.; Tatarko, M. Slovak University of Technology Press: Bratislava, 2015, pp. 118–125.
20. Wada, S.; Kotera, T.; Mikuriya, M. Synthesis and structural characterization of a dinuclear palladium(II) complexes with  $N,N',N'',N'''$ -tetrakis(2-*p*-toluenesulfonamidoethyl)cyclam. *Bulletin of the Chemical Society of Japan*, 2008, 81, pp. 1454–1460.
21. Hammershoi, B.A.; Sargeson, A.M. Macrocyclic hexamine cage complexes of cobalt(III): synthesis, characterization, and properties. *Inorganic Chemistry*, 1983, 22, pp. 3554–3561.
22. Taylor, S.G.; Snow, M.R.; Hambley, T.W. The structures and energy minimization analysis of the macrocyclic cage complex  $[\text{Co}(\text{nosartacn})]^{3+}$  and its precursor  $[\text{Co}(\text{taetacn})]^{3+}$ . *Australian Journal of Chemistry*, 1983, 36, pp. 2359–2368.
23. Wieghardt, K.; Schoffmann, E.; Nuber, N.; Weiss, J. Syntheses, properties, and electrochemistry of transition-metal complexes of the macrocycle 1,4,7-tris(2-pyridylmethyl)-1,4,7-triazacyclononane (L). Crystal structures of  $[\text{NiL}](\text{ClO}_4)_2$ ,  $[\text{MnL}](\text{ClO}_4)_2$ , and  $[\text{PdL}](\text{PF}_6)_2$  containing a distorted-square-base-pyramidal  $\text{Pd}^{\text{II}}\text{N}_5$  core. *Inorganic Chemistry*, 1986, 25, pp. 4877–4883.
24. Mikuriya, M.; Hamagawa, M.; Tomioka, N.; Fujimori, R.; Yoshioka, D.; Hori, S.; Kuriyama, T.; Sakiyama, H.; Handa, M.; Mitsuhashi, R. Nickel(II) complex with 1,4,7-tris(2-aminoethyl)-1,4,7-triazacyclononane. *Chemical Papers*, 2016, 70, pp. 69–74.
25. Kahn, O. *Molecular Magnetism*; VCH Publishers: New York, 1993, 380 p.

26. Sheldrick, G.M. SHELXS-97 and SHELXL-97. Program for crystal structure resolution and analysis. Göttingen, Germany: University of Göttingen, 1997.
27. Sheldrick, G.M. Crystal structure refinement with SHELXL. *Acta Crystallographica Section C*, 2015, 71, pp. 3–8.
28. Nakamoto, K. *Infrared and Raman Spectra of Inorganic and Coordination Compounds, Part B: Applications in Coordination, Organometallic, and Bioinorganic Chemistry*. Sixth Ed. John Wiley & Sons, Inc: Hoboken, 2009 pp. 110-117.
29. Murakami, Y.; Sakata, K. Chapter 2 Electronic Spectra. In Ueno, K. Ed. *Kireto Kagaku* (Vol. 1). Nankodo: Tokyo, 1976, pp. 228-377 (in Japanese).
30. Addison, A.W.; Rao, T.N.; Reedijk, J.; van Rijn, J.; Verschoor, G.C. Synthesis, structure, and spectroscopic properties of copper(II) compounds containing nitrogen-sulphur donor ligands; the crystal and molecular structure of aqua[1,7-bis(*N*-methylbenzimidazol-2'-yl)-2,6-dithiaheptane]copper(II) perchlorate. *Journal of the Chemical Society. Dalton Transaction*, 1984, pp. 1349–1356.

# MIXED-METAL COMPLEXES OF RUTHENIUM(II,III) CARBOXYLATE AND TETRACYANIDOPLATINATE(II)

Masahiro Mikuriya<sup>a\*</sup>, Kenta Ono<sup>a</sup>, Shun Kawauchi<sup>a</sup>, Daisuke Yoshioka<sup>a</sup>,  
Ryoji Mitsuhashi<sup>a</sup>, Makoto Handa<sup>b</sup>

<sup>a</sup>Department of Applied Chemistry for Environment and Research Center for Coordination Molecule-based Devices, School of Science and Technology, Kwansei Gakuin University, 2-1 Gakuen, Sanda 669-1337, Japan

<sup>b</sup>Department of Chemistry, Interdisciplinary Graduate School of Science and Engineering, Shimane University, 1060 Nishikawatsu, Matsue 690-8504, Japan

\*e-mail: junpei@kwansei.ac.jp; phone: (+81 79) 565 8365; fax: (+81 79) 565 9729

**Abstract.** Mixed-metal complexes constructed from dinuclear ruthenium(II,III) carboxylates and tetracyanidoplatinate(II),  $[\{Ru_2(O_2CCH_3)_4\}_2Pt(CN)_4] \cdot 2H_2O$  (**1**) and  $[\{Ru_2\{O_2CC(CH_3)_3\}_2Pt(CN)_4\} \cdot 2H_2O$  (**2**), were synthesized and characterized by elemental analysis and IR and UV-vis spectroscopies. These data are in accordance with the formulation of the  $PtRu_4$  complexes with two lantern-type dinuclear  $Ru_2$  and  $Pt(CN)_4$  units. A broad band at near-IR and a distinctive band at visible region (1088 and 443 nm for **1** and 1090 and 446 nm for **2**), which can be ascribed to a  $\delta(Ru_2) \rightarrow \delta^*(Ru_2)$  and a  $\pi(RuO, Ru_2) \rightarrow \pi^*(Ru_2)$  transitions, respectively, were observed in the diffused reflectance spectra. Temperature-dependence of magnetic susceptibilities (4.5–300 K) showed that antiferromagnetic interaction between the two 3/2 spins of the  $Ru_2$  units through tetracyanidoplatinate(II) is weak ( $zJ = -0.1 \text{ cm}^{-1}$ ) with zero-field-splitting values of 45 and  $65 \text{ cm}^{-1}$  for **1** and **2**, respectively.

**Keywords:** dinuclear ruthenium(II,III) carboxylate, magnetic property, mixed-metal complex, tetracyanidoplatinate(II).

Received: October 2015/ Revised final: October 2015/ Accepted: October 2015

## Introduction

Dinuclear metal carboxylates with a lantern-type (or paddlewheel-type) dinuclear core are interesting compounds and have attracted much attention over the past five decades because of the unique dinuclear core [1-5]. It is known that most of these compounds have metal-metal bonds between the two metal atoms, giving diamagnetic property for these systems. In this context, dinuclear ruthenium carboxylates are unique compounds, showing paramagnetic properties irrespective of the lantern-type (or paddlewheel-type) dinuclear core with metal-metal bonding. Especially, interesting features are that mixed-valent ruthenium(II,III) carboxylates  $[Ru_2(O_2CR)_4]^+$  have three unpaired electrons on the  $\pi^*2\delta^*$  orbitals in the metal-metal bonds and show various functional properties such as liquid crystalline properties as well as magnetic properties [3-42]. These ruthenium carboxylates are useful as building block for constructing magnetic materials. We reported on some metal-assembled complexes such as one-dimensional chain compounds prepared by application of bidentate linking ligands to dinuclear ruthenium carboxylates. Most of these compounds are antiferromagnetic between the dinuclear ruthenium units through the linking ligands and the strength of the magnetic interaction depends on the linking ligands [17-32]. Dinuclear ruthenium carboxylates form polymeric mixed-metal complexes by reaction with octacyanidometalate  $[M(CN)_8]^{4-}$  ( $M = W$ ), hexacyanidometalate ion  $[M(CN)_6]^{3-}$  ( $M = Fe, Co$ , and so on) and some of them show an antiferromagnetic interaction between the dinuclear ruthenium units through the diamagnetic cyanidometalate ion and a ferrimagnetic interaction among the hetero metal ions [33-42].

Recently, our continuing study on these systems led us to obtain mixed-metal complexes with dicyanidoargentate(I) and tetracyanidonickelate(II) ions [41,42]. In these mixed-metal systems, it was difficult to obtain single crystals to elucidate the polymeric structures. In this study, we extended these systems to mixed-metal complexes with tetracyanidoplatinate(II) ion  $[Pt(CN)_4]^{2-}$  in the hope of obtaining new mixed-metal systems of ruthenium(II,III) carboxylates. The isolated complexes were characterized based on elemental analysis, infrared and UV-vis spectra, and temperature dependence of magnetic susceptibilities (4.5–300 K).

## Experimental

**Synthesis:** Unless otherwise specified, commercial chemicals were used as supplied. Tetrafluoroborate salts of dinuclear ruthenium(II,III) acetate and pivalate,  $[Ru_2\{O_2CCH_3\}_4(H_2O)_2]BF_4$  and  $[Ru_2(O_2CC(CH_3)_3)_4(H_2O)_2]BF_4$ , were synthesized according to the literature methods [6,7].

### $[\{Ru_2(O_2CCH_3)_4\}_2Pt(CN)_4] \cdot 2H_2O$ (**1**)

Potassium tetracyanidoplatinate(II) (30 mg, 0.080 mmol) was dissolved in 5 mL of  $H_2O$ . To an aqueous solution (5 mL) of  $[Ru_2\{O_2CCH_3\}_4(H_2O)_2]BF_4$  (50 mg, 0.089 mmol) was added this solution, stirred overnight. The resulting precipitate was filtered, washed with small amount of water, and dried *in vacuo*. Yield: 34 mg (35%). Anal. Found: C, 20.12; H,



2.34; N, 4.73%. Calcd. for  $C_{20}H_{28}N_4O_{18}PtRu_4$ : C, 19.82; H, 2.33; N, 4.62%. IR (KBr):  $\nu(\text{CH})$  2934;  $\nu(\text{CN})$  2150, 2138;  $\nu_{\text{as}}(\text{CO}_2^-)$  1443;  $\nu_{\text{s}}(\text{CO}_2^-)$  1401  $\text{cm}^{-1}$ . Diffuse reflectance spectrum:  $\lambda_{\text{max}}$  250, 290sh, 443, 1088 nm.

**$[\{\text{Ru}_2\{\text{O}_2\text{CC}(\text{CH}_3)_3\}_4\}_2\text{Pt}(\text{CN})_4]\cdot 2\text{H}_2\text{O}$  (**2**)**

Potassium tetracyanidoplatinate(II) (14 mg, 0.037 mmol) was dissolved in 5 mL of  $\text{H}_2\text{O}$ . To an aqueous solution (5 mL) of  $[\text{Ru}_2\{\text{O}_2\text{CC}(\text{CH}_3)_3\}_4(\text{H}_2\text{O})_2]\text{BF}_4$  (28 mg, 0.038 mmol) was added this solution, stirred overnight. The resulting precipitate was filtered, washed with small amount of water, and dried *in vacuo*. Yield: 24 mg (42%). Anal. Found: C, 34.35; H, 4.75; N, 3.73%. Calcd. for  $C_{44}H_{80}N_4O_{17}PtRu_4$ : C, 34.39; H, 5.25; N, 3.65%. IR (KBr):  $\nu(\text{CH})$  2967, 2936, 2910, 2876;  $\nu(\text{CN})$  2137;  $\nu_{\text{as}}(\text{CO}_2^-)$  1488;  $\nu_{\text{s}}(\text{CO}_2^-)$  1421  $\text{cm}^{-1}$ . Diffuse reflectance spectrum:  $\lambda_{\text{max}}$  262, 304, 446, 1090 nm.

**Measurements:** Elemental analyses for carbon, hydrogen, and nitrogen were conducted using a ThermoFinnigan FLASH EA1112 series CHNO-S analyzer. Infrared spectra were measured with a JASCO MFT-2000 FT-IR Spectrometer in the 4000—600  $\text{cm}^{-1}$  region. Electronic spectra were measured with a Shimadzu UV-vis-NIR Recording Spectrophotometer (Model UV-3100). Magnetic susceptibilities were measured with a Quantum Design MPMS-XL7 SQUID susceptometer operating at a magnetic field of 0.5 T over a range of 4.5—300 K. The susceptibilities were corrected for the diamagnetism of the constituent atoms using Pascal's constants. The effective magnetic moments were calculated from the equation  $\mu_{\text{eff}} = 2.828\sqrt{\chi_{\text{M}}T}$ , where  $\chi_{\text{M}}$  is the molar magnetic susceptibility per mole of dinuclear ruthenium(II,III) unit.

## Results and discussion

Reaction of the mixed-valent dinuclear ruthenium(II,III) acetate and ruthenium(II,III) pivalate with tetracyanidoplatinate(II) ion gave orange and brown precipitates, respectively. Formulation of the mixed-metal systems of two dinuclear ruthenium(II,III) carboxylate units with one tetracyanidoplatinate(II) unit,  $[\{\text{Ru}_2(\text{O}_2\text{CCH}_3)_4\}_2\text{Pt}(\text{CN})_4]\cdot 2\text{H}_2\text{O}$  (**1**) and  $[\{\text{Ru}_2\{\text{O}_2\text{CC}(\text{CH}_3)_3\}_4\}_2\text{Pt}(\text{CN})_4]\cdot 2\text{H}_2\text{O}$  (**2**), was confirmed by the elemental analyses, infrared and electronic spectra, and temperature dependence of magnetic susceptibility data (4.5—300 K).

The infrared spectra of the present complexes are shown in Figure 1. In the infrared spectra, C-H stretching vibrations were observed at 2934  $\text{cm}^{-1}$  for **1** and at 2967, 2936, 2910, and 2876  $\text{cm}^{-1}$  for **2**, respectively, in agreement with the presence of the methyl or *t*-butyl groups. Distinctive sharp bands were observed at 2150 and 2138  $\text{cm}^{-1}$  in **1** and 2137  $\text{cm}^{-1}$  in **2**. These bands may be assigned to  $\nu(\text{CN})$  stretching band of tetracyanidoplatinate(II) ion. These bands appeared at a little higher energy region compared with that of  $\text{K}_2[\text{Pt}(\text{CN})_4]$  ( $\nu(\text{CN})$ : 2134 and 2121  $\text{cm}^{-1}$ ), suggesting the bridging of the tetracyanidoplatinate(II) to the dinuclear ruthenium carboxylate units [43–45]. Two strong bands were observed at 1443 and 1401  $\text{cm}^{-1}$  assignable to asymmetrical and symmetrical stretching vibrations of the *syn-syn* acetate bridges, respectively, for **1**, where as two strong bands observed at 1488 and 1421  $\text{cm}^{-1}$  assignable to asymmetrical and symmetrical stretching vibrations of the *syn-syn* pivalate bridges, respectively, for **2**.

Diffused reflectance spectra of **1** and **2** are shown in Figure 2. A weak broad absorption band, which is typical for ruthenium(II,III) carboxylate and can be attributed to a  $\delta(\text{Ru}_2) \rightarrow \delta^*(\text{Ru}_2)$  transition, was observed at around 1088 nm in solid of **1** [8]. A distinctive band at 443 nm in **1** may be due to  $\pi(\text{RuO}, \text{Ru}_2) \rightarrow \pi^*(\text{Ru}_2)$  transition [11,12]. From these spectral feature, we can consider that the lantern-type dinuclear structure of the mixed-valent dinuclear ruthenium(II,III) carboxylate is maintained in the present mixed-metal complexes, because the spectra contain the characteristic bands of dinuclear ruthenium(II,III) carboxylate. The spectra contain another feature due to the presence of tetracyanidoplatinate(II) moiety. The bands at 250 and 290 nm in **1** can be assigned to the  $^1A_{1g} \rightarrow ^1E_u$  and  $^1A_{1g} \rightarrow ^1B_{1u}$  transitions, respectively, of the tetracyanidoplatinate(II) moiety [46]. Similar spectral feature was observed for **2**: 1090 ( $\delta(\text{Ru}_2) \rightarrow \delta^*(\text{Ru}_2)$ ), 446 ( $\pi(\text{RuO}, \text{Ru}_2) \rightarrow \pi^*(\text{Ru}_2)$ ), 304 ( $^1A_{1g}(\text{Pt}) \rightarrow ^1B_{1u}(\text{Pt})$ ), 262 ( $^1A_{1g}(\text{Pt}) \rightarrow ^1E_u(\text{Pt})$ ) nm.

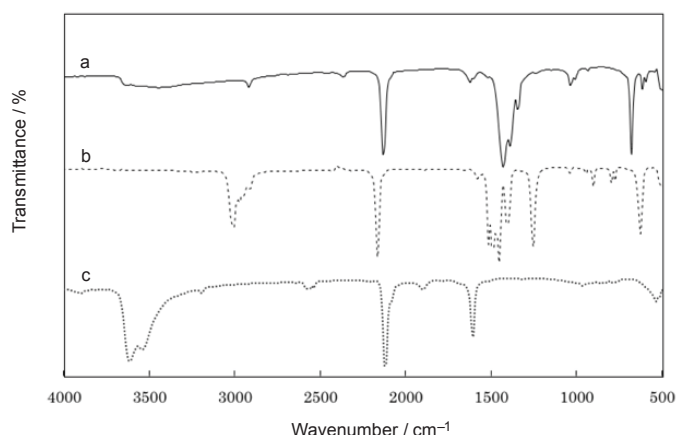


**Figure 1. Infrared spectra: 1 (a), 2 (b), and  $\text{K}_2\text{Pt}(\text{CN})_4$  (c).**

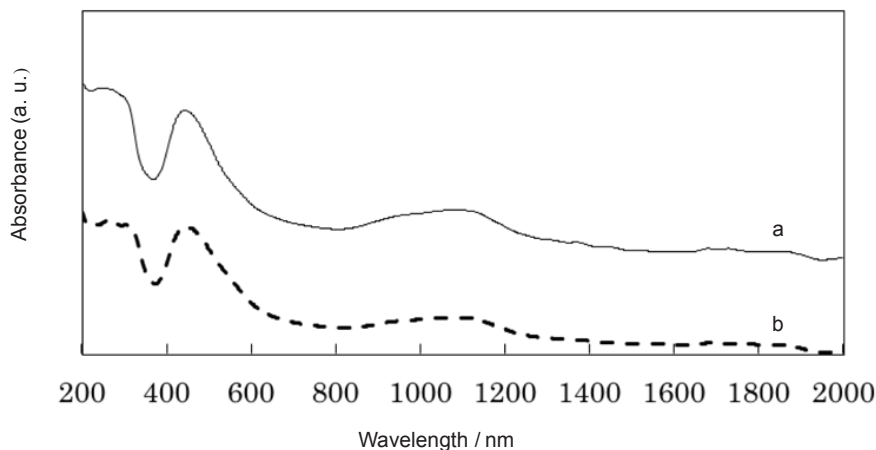


Figure 2. Diffused reflectance spectra of **1** (a) and **2** (b).

Temperature dependence of effective magnetic moments is shown in Figure 3. The magnetic moments per dinuclear ruthenium(II,III) unit of **1** and **2** are 4.30 and 4.41  $\mu_B$ , respectively, at 300 K. These values are a little higher than the spin-only value of  $S = 3/2$  ( $3.87 \mu_B$ ). The magnetic moments gradually decrease with lowering of temperature and reach the minimum values, 3.20 and 3.28  $\mu_B$ , respectively, at 4.5 K. These magnetic behaviors are typical for dinuclear ruthenium(II,III) carboxylates having a large zero-field-splitting (ZFS) with a weak antiferromagnetic interaction [3-5]. The magnetic data were analyzed by a molecular field approximation [47] considering the ZFS effect to estimate the magnitude of the antiferromagnetic interaction [9, 10], using the following equations:

$$\chi' = \chi / \{1 - (2zJ / Ng^2\mu_B^2)c\} \quad (1)$$

$$\chi = (\chi_{||} + 2\chi_{\perp}) / 3 \quad (2)$$

$$\chi_{||} = (Ng^2\mu_B^2 / kT)[1 + 9\exp(-2D / kT)] / 4\{1 + \exp(-2D / kT)\} \quad (3)$$

$$\chi_{\perp} = (Ng^2\mu_B^2 / kT)[4 + (3kT / D)\{1 - \exp(-2D / kT)\}] / 4\{1 + \exp(-2D / kT)\} \quad (4)$$

where  $zJ$  - is the exchange integral multiplied by the number of interacting neighbors,

$\chi$  - is the magnetic susceptibility of the individual dinuclear unit,

$D$  - is the ZFS parameter.

The  $g$  value was treated isotropic. Best fitting curve was obtained with the parameters:  $zJ = -0.10 \text{ cm}^{-1}$ ,  $g = 2.10$ ,  $D = 45 \text{ cm}^{-1}$  for **1**. The similar parameter values  $zJ = -0.10 \text{ cm}^{-1}$ ,  $g = 2.10$ ,  $D = 60 \text{ cm}^{-1}$  were obtained for **2**. These results show that a weak antiferromagnetic interaction is operating between the two dinuclear ruthenium 3/2 spins through the diamagnetic tetracyanidoplatinate(II) bridge, being consistent with a long separation of the  $\text{Ru}_2$  units through the  $\text{Pt}(\text{CN})_4$  bridge for the present complexes.

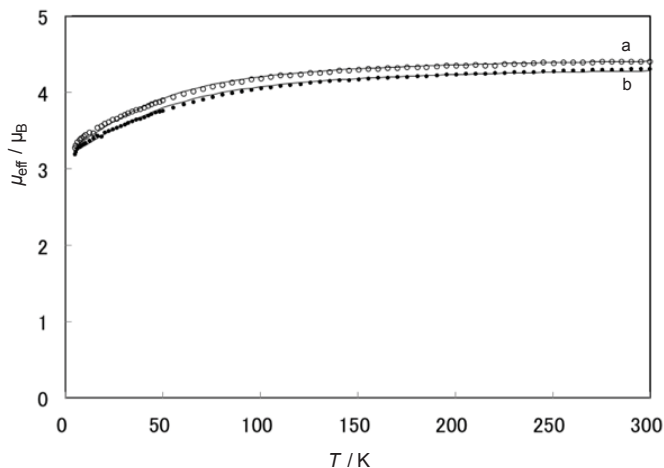
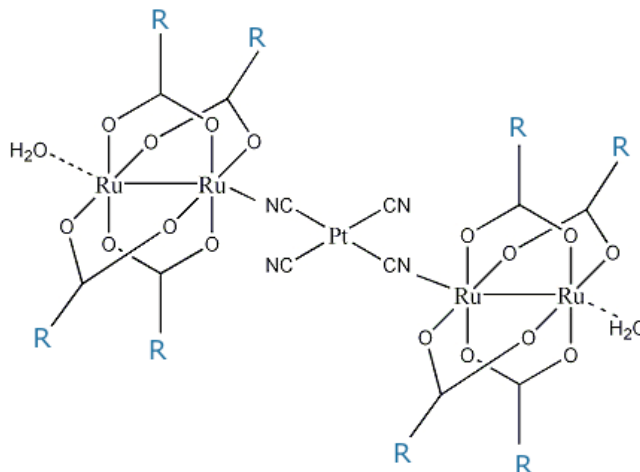


Figure 3. Temperature dependence of the magnetic moments of **1** (a) and **2** (b).





**Figure 4. Proposed structure for the present complexes.**

From the above results, we can assume a pentanuclear structure with a linear arrangement of two dinuclear ruthenium units and one tetracyanidoplatinate(II) ion shown in Figure 4 for **1** and **2**.

### Conclusions

By using tetracyanidoplatinate(II), the preparation of the mixed-metal complexes of dinuclear ruthenium(II,III) carboxylate,  $[\{\text{Ru}_2(\text{O}_2\text{CCH}_3)_4\}_2\text{Pt}(\text{CN})_4] \cdot 2\text{H}_2\text{O}$  (**1**) and  $[\{\text{Ru}_2\{\text{O}_2\text{CC}(\text{CH}_3)_3\}_2\}_2\text{Pt}(\text{CN})_4] \cdot 2\text{H}_2\text{O}$  (**2**), was achieved. The elemental analysis, infrared spectra, UV-vis-NIR spectra, and temperature dependence of magnetic susceptibilities are consistent with pentanuclear structures composed of two dinuclear ruthenium units bridged by one tetracyanidoplatinate(II) ion. In accordance with the structural feature, a weak antiferromagnetic interaction through the tetracyanidoplatinate(II) ion was observed for the present complexes.

### Acknowledgements

The present work was partially supported by Grant-in-Aid for Scientific Research No. 26410080 from the Ministry of Education, Culture, Sports, Science and Technology (MEXT, Japan) and the MEXT-Supported Program for the Strategic Research Foundation at Private Universities, 2010–2014.

### References

1. Cotton, F. A.; Murillo, C. A.; Walton, R. A. Multiple Bonds between Metal Atoms. 3rd ed. Springer Science and Business Media: New York, 2005, 706 p.
2. Mikuriya, M. Copper(II) acetate as a motif for metal-assembled complexes. Bulletin of the Japanese Society of Coordination Chemistry, 2008, 52, pp. 17-28 (in Japanese).
3. Mikuriya, M.; Yoshioka, D.; Handa, M. Magnetic interactions in one-, two-, and three-dimensional assemblies of dinuclear ruthenium carboxylates. Coordination Chemistry Reviews, 2006, 250, pp. 2194-2211.
4. Aquino, M.A.S. Recent developments in the synthesis and properties of dinuclear tetracarboxylates. Coordination Chemistry Reviews, 2004, 248, pp. 1025-1045.
5. Aquino, M.A.S. Diruthenium and diosmium tetracarboxylates: synthesis, physical properties and applications. Coordination Chemistry Reviews, 1998, 170, pp. 141-202.
6. Stephenson, T.A.; Wilkinson, G. New ruthenium carboxylate complexes. Journal of inorganic and nuclear Chemistry, 1966, 28, pp. 2285-2291.
7. Barral, M.C.; Jiménez-Aparicio, R.; Priego, J.L.; Royer, E.C. Synthesis and structure of a new complex of ruthenium containing the tetra( $\mu$ -tertbutylbenzoate)diruthenium(II,III) unit. Polyhedron, 1992, pp. 2209-2215.
8. Norman, G.J.; Renzoni, G.E.; Case, D.A. Electronic structure of  $\text{Ru}_2(\text{O}_2\text{CR})_4^+$  and  $\text{Rh}_2(\text{O}_2\text{CR})_4^+$  complexes, Journal of the American Chemical Society, 1979, 101, pp. 5256-5267.
9. Telser, J.; Drago, R.S. Reinvestigation of the electronic and magnetic properties of ruthenium butyrate chloride. Inorganic Chemistry, 1984, 23, pp. 3114-3120.
10. Telser, J.; Drago, R.S. Correction: Reinvestigation of the electronic and magnetic properties of ruthenium butyrate chloride. Inorganic Chemistry, 1985, 24(26), p. 4765-4765.

11. Miskowski, V.M.; Loehr, T.M.; Gray, H.B. Electronic and vibrational spectra of  $\text{Ru}_2(\text{carboxylate})_4^+$  complexes. Characterization of a high spin metal-metal groundstate. *Inorganic Chemistry*, 1987, 26, pp. 1098-1108.
12. Miskowski, V.M.; Gray, H.B. Electronic spectra of  $\text{Ru}(\text{carboxylate})^{4+}$  complexes. Higher energy electronic excited states. *Inorganic Chemistry*, 1988, 27, pp. 2501-2506.
13. Ishida, H.; Handa, M.; Mikuriya, M. Synthesis and crystal structure of aqua adduct of dinuclear ruthenium(II,III) 3,4,5-tri(ethoxy-*d*)benzoate tetrafluoroborate. *X-ray Structure Analysis Online*, 2014, 30, pp. 9-10.
14. Hiraoka, Y.; Ikeue, T.; Sakiyama, H.; Guegan, F.; Luneau, D.; Gillon, B.; Hiromitsu, I.; Yoshioka, D.; Mikuriya, M.; Kataoka, Y.; Handa, M. Anunprecedented up-field shifts in the  $^{13}\text{C}$  NMR spectrum of the carboxyl carbons of the lantern-type dinuclear complex  $\text{TBA}[\text{Ru}_2(\text{O}_2\text{CCH}_3)_4\text{Cl}_2]$  ( $\text{TBA}^+ = \text{tetra}(n\text{-butyl})\text{ammonium cation}$ ). *Dalton Transactions*, 2015, 44, pp. 13439-13443.
15. Handa, M.; Ikeue, T.; Iida, M.; Yoshioka, D.; Mikuriya, M. Crystal structure and  $^1\text{H}$  NMR spectral property of a lantern-type diruthenium(II,III) complex with one formamidinato and three acetato bridges. *X-ray Structure Analysis Online*, 2014, 30, pp. 31-32.
16. Ikeue, T.; Karino, K.; Iida, M.; Yamaji, T.; Hiromitsu, I.; Sugimori, T.; Yoshioka, D.; Mikuriya, M.; Handa, M. Structural, magnetic, and  $^1\text{H}$  NMR spectral study on lantern-type *cis*- and *trans*-diruthenium(II,III) complexes with two formamidinato and two acetato bridges. *Inorganic Chemistry Communications*, 2013, 33, pp. 133-137.
17. Sayama, Y.; Handa, M.; Mikuriya, M.; Nukada, R.; Hiromitsu, I.; Kasuga, K. Mixed-valent ruthenium pivalate and its nitroxide adduct. *Coordination Chemistry at the Turn of the Century*. Eds. Ondrejovic, G.; Sirota, A. Slovak Technical University Press: Bratislava, 1999, pp. 447-452.
18. Sayama, S.; Handa, M.; Mikuriya, M.; Hiromitsu, I.; Kasuga, K. Chain compound of mixed-valent ruthenium dimers linked by hydrogen-bonding between the axially coordinated nitronyl nitroxide and water molecules. *Chemistry Letters*, 1999, pp. 453-454.
19. Handa, M.; Yoshioka, D.; Sayama, Y.; Shiomi, K.; Mikuriya, M.; Hiromitsu, I.; Kasuga, K. A new "dimer-of-dimers" complex derived from axial coordination of 7,7,8,8-tetracyanoquinodimethane to  $\text{Ru}(\text{II,III})$  cation dimer. *Chemistry Letters*, 1999, pp. 1033-1034.
20. Yoshioka, D.; Handa, M.; Azuma, H.; Mikuriya, M.; Hiromitsu, I.; Kasuga, K. Synthesis and magnetic property of adducts of ruthenium(II,III) pivalate with 9,10-anthraquinone. *Molecular Crystal and Liquid Crystal*, 2000, 342, pp. 133-138.
21. Sayama, Y.; Handa, M.; Mikuriya, M.; Hiromitsu, I.; Kasuga, K. Structures and magnetic properties of ruthenium(II,III) pivalate cation dimers axially coordinated by pyridyl nitronyl nitroxide radicals through their pyridyl nitrogen atoms. *Bulletin of the Chemical Society of Japan*, 2000, 73, pp. 2499-2504.
22. Sayama, Y.; Handa, M.; Mikuriya, M.; Hiromitsu, I.; Kasuga, K. Synthesis and magnetic properties of ruthenium(II,III) pivalate dimers axially coordinated by nitronyl nitroxide radicals  $[\text{Ru}_2(\text{O}_2\text{CCMe}_3)_4(\text{L})_2]\text{BF}_4$  and  $[\{\text{Ru}_2(\text{O}_2\text{CCMe}_3)_4(\text{L})_2\}\{\text{Ru}_2(\text{O}_2\text{CCMe}_3)_4(\text{H}_2\text{O})_2\}]_n(\text{BF}_4)_{2n}$ ,  $\text{L} = 2,4,4,5,5\text{-pentamethyl-4,5-dihydro-1H-imidazol-1-oxyl-3-}N\text{-oxide}$  and  $2\text{-ethyl-4,4,5,5-tetramethyl-4,5-dihydro-1H-imidazol-1-oxyl-3-}N\text{-oxide}$ . *Bulletin of the Chemical Society of Japan*, 2003, 76, pp. 769-779.
23. Handa, M.; Yoshioka, D.; Mikuriya, M.; Hiromitsu, I.; Kasuga, K. Coordination polymers of ruthenium(II) acetate with pyrazine, 4,4'-bipyridine, and 1,4-diazabicyclo[2.2.2]octane. *Molecular Crystal and Liquid Crystal*, 2002, 376, pp. 257-262.
24. Yoshioka, D.; Mikuriya, M.; Handa, M. Synthesis and characterization of polynuclear chain and tetranuclear complexes of mixed-valent ruthenium(II,III) pivalate with *N,N'*-didentate ligands. *Bulletin of the Chemical Society of Japan*, 2004, 77, pp. 2205-2211.
25. Handa, M.; Ishida, H.; Ito, K.; Adachi, T.; Ikeue, T.; Hiromitsu, I.; Mikuriya, M.; Kasuga, K. Synthesis and magnetic properties of polymeric complexes containing ruthenium(II)-ruthenium(III) tetracarboxylato units linked by cyanato, thiocyanato, and selenocyanato ligands. *Chemical Papers*, 2008, 62, pp. 410-416.
26. Yoshioka, D.; Handa, M.; Mikuriya, M.; Kasuga, K. Coordination polymers of ruthenium pivalate dimer with tetracyanoethylene, 7,7,8,8-tetracyanoquinodimethane, and 2,5-dimethyl-*N,N'*-dicyanobenzoquinonediimine. *Advances in Coordination, Bioinorganic and Inorganic Chemistry*. Eds. Melnik, M.; Sima, J.; Tatarko, M. Slovak Technical University Press: Bratislava, 2005, pp. 218-223.
27. Mikuriya, M.; Tanaka, K.; Handa, M.; Hiromitsu, I.; Yoshioka, D.; Luneau, D. Adduct complexes of ruthenium(II,III) propionate dimer with pyridyl nitroxides. *Polyhedron*, 2005, 24, pp. 2658-2664.
28. Ishida, H.; Handa, M.; Hiromitsu, I.; Ujije, S.; Mikuriya, M. Synthesis and magnetic properties of polymer complexes of ruthenium(II,III) 3,4,5-trioctanoxybenzoate linked by chloro and cyanato ligands with liquid-crystalline behavior. *Achievements in Coordination, Bioinorganic and Applied Inorganic Chemistry*. Eds. Melnik, M.; Sima, J.; Tatarko, M. Slovak Technical University Press: Bratislava, 2007, pp. 121-127.
29. Ishida, H.; Handa, M.; Hiromitsu, I.; Mikuriya, M. Synthesis, magnetic and spectral properties, and crystal structure of mixed-valence ruthenium(II,III) 3,4,5-tributanoxxybenzoate. *Insights into Coordination, Bioinorganic*

- and Applied Inorganic Chemistry. Eds. Melnik, M.; Segl'a, P.; Tatarko, M. Slovak Technical University Press: Bratislava, 2009, pp. 197-203.
30. Ishida, H.; Handa, M.; Hiromitsu, I.; Mikuriya, M. Synthesis, crystal structure, and spectral and magnetic properties of chloro-bridged chain complex of dinuclear ruthenium(II,III) 3,4,5-triethoxybenzoate. *Chemistry Journal of Moldova*, 2009, 4(1), pp. 90-96.
  31. Ishida, H.; Handa, M.; Ikeue, T.; Taguchi, J.; Mikuriya, M. Synthesis, crystal structure, and  $^1\text{H}$  NMR spectra of a chloride-bridged chain complex of dinuclear ruthenium(II,III) 3,4,5-tri(ethoxy- $d_3$ )benzoate. *Chemical Papers*, 2010, 64, pp. 767-775.
  32. Ishida, H.; Handa, M.; Hiromitsu, I.; Mikuriya, M. Fastener effect on magnetic properties of chain compounds of dinuclear ruthenium carboxylates. *Chemical Papers*, 2013, 67, pp. 743-750.
  33. Yoshioka, D.; Mikuriya, M.; Handa, M. Molecular-assembled complexes of mixed-valent ruthenium dimer with hexacyanoferrate(III) and hexacyanocobaltate(III) ions. *Chemistry Letters*, 2002, 31, pp. 1044-1045.
  34. Vos, T.E.; Liao, Y.; Shum, W.W.; Her, J.-H.; Stephens, P.W.; Reiff, W.M.; Miller, J.S. Diruthenium tetraacetate monocation,  $[\text{Ru}^{\text{II/III}}_2(\text{O}_2\text{CMe})_4]^+$ , building blocks for 3-D molecule-based magnets. *Journal of the American Chemical Society*, 2004, 126, pp. 11630-11639.
  35. Vos, T.E.; Miller, J.S. Building blocks for 2D molecule-based magnets: the diruthenium tetrapivalate monocation  $[\text{Ru}^{\text{II/III}}_2(\text{O}_2\text{CtBu})_4]^+$ . *Angewandte Chemie International Edition*, 2005, 44, pp. 2416-2419.
  36. Miller, J.S. Magnetically ordered molecule-based assemblies. *Dalton Transaction*, 2006, pp. 2742-2949.
  37. Kennon, B.S.; Her, J.-H.; Stephens, P.W.; Miller, J.S. Diruthenium tetracarboxylate trianion,  $[\text{Ru}^{\text{II/III}}_2(\text{O}_2\text{CO})_4]^{3-}$ , based molecule-based magnets: three-dimensional network structure and two-dimensional magnetic ordering. *Inorganic Chemistry*, 2009, 48, pp. 6117-6123.
  38. Kennon, B.S.; Miller, J.S. Observation of magnetic ordering for layered (2-D) potassium diruthenium tetracarboxylate,  $\text{K}_3[\text{Ru}^{\text{II/III}}_2(\text{O}_2\text{CO})_4]$ : a rare second row transition. *Inorganic Chemistry*, 2010, 49, pp. 5542-5545.
  39. Matoga, D.; Mikuriya, M.; Handa, M.; Szklarzewicz, J. Self-assembly of mixed-valent ruthenium(II,III) pivalate and octacyanotungstate(V) building blocks. *Chemistry Letters*, 2005, 34, pp. 1550-1551.
  40. Mikuriya, M.; Yoshioka, D.; Borta, A.; Luneau, D.; Matoga, D.; Szklarzewicz, J.; Handa, M. Molecule-based magnetic materials based on dinuclear ruthenium carboxylate and octacyanotungstate. *New Journal of Chemistry*, 2011, 35, pp. 1226-1233.
  41. Mikuriya, M.; Tanaka, Y.; Yoshioka, D.; Handa, M. Mixed-metal complexes of mixed-valent dinuclear ruthenium(II,III) carboxylate and tetracyanonickelate(II). *Chemistry Journal of Moldova*, 2014, 9(1), pp. 93-99.
  42. Mikuriya, M.; Tanaka, Y.; Yoshioka, D.; Handa, M. Molecule-based magnetic compounds made up from dinuclear ruthenium(II,III) carboxylate and dicyanidoargentate(I). *Journal of Superconductivity and Novel Magnetism*, 2015, 28, pp. 1013-1016.
  43. Nakamoto, K. *Infrared and Raman Spectra of Inorganic and Coordination Compounds, Part B: Applications in Coordination, Organometallic, and Bioinorganic Chemistry*. Sixth Ed. John Wiley & Sons, Inc: Hoboken, 2009 pp. 110-117.
  44. Dunbar, K.R.; Heintz, R.A. *Chemistry of Transition Metal Cyanide Compounds: Modern Perspectives*. Progress in Inorganic Chemistry, 1997, 45, pp. 283-391.
  45. Flay, M.-L.; Vahrenkamp, H. Cyanide-bridged oligonuclear complexes containing Ni-CN-Cu and Pt-CN-Cu linkages. *European Journal of Chemistry*, 2003, pp. 1719-1726.
  46. Murakami, Y.; Sakata, K. Chapter 2 Electronic Spectra. In Ueno, K. Ed. *Kireto Kagaku* (Vol. 1). Nankodo: Tokyo, 1976, pp. 228-377 (in Japanese).
  47. O'Connor, C.J. Magnetochemistry-Advances in theory and experimentation. *Progress in Inorganic Chemistry*, 1982, 29, pp. 203-283.

## GC-MS ANALYSIS OF THE FATTY ACIDS METHYL ESTERS IN JAPANESE QUAIL FAT

Ion Dragalin<sup>a\*</sup>, Olga Morarescu<sup>a</sup>, Maria Sedcenco<sup>b</sup>, Radu Marin Rosca<sup>b</sup>

<sup>a</sup>Institute of Chemistry of Academy of Science of Moldova, 3, Academiei str. Chisinau MD-2028, Republic of Moldova

<sup>b</sup>I.I. "Antoni Cristina", 2A, Stefan cel Mare str., Gratiesti MD-2093, Republic of Moldova

\*e-mail: iondragalin@yahoo.com; phone: (+373 22) 73 97 69

**Abstract.** The accumulated waste fat as production from Faraon quail breeds has been investigated for the first time by using GC-MS technique, preventively converting it *via* methanolysis to fatty acid methyl esters. The test results, regarding the content of unsaturated fatty acids having a favorable to human body *cis*-configuration (77.8%), confirm their nutritional value and the possibility of using this fat in cosmetic, pharmaceutical and food industries.

**Keywords:** fatty acid methyl esters, GC-MS analysis, linoleic acid (Z,Z), oleic acid (Z), Japanese quail fat.

Received: June 2015/ Revised final: September 2015/ Accepted: September 2015

### Introduction

The value and chemical composition of quail meat, which contains monounsaturated fatty acids at the amount of about 50%, polyunsaturated acids at the amount of 15%, and *trans*-configured acids at the amount of 3 % is known [1]. The unique composition of quail carcass products determines their nutritional and healing qualities. The antimicrobial activity of fatty acids and their esters against pathogenic microorganisms in the oral cavity is renowned [2]. In Republic of Moldova there are six individual companies that cultivate quails. We have analyzed the accumulated fat at "Antoni Cristina" company, collected from quail carcasses as waste, applying the most efficient method of GC-MS [3], to study whether the quail fat could be used as the raw material for manufacturing solid soap.

This investigation was aimed at pioneering analysis of the fatty acids of the Japanese quail fat accumulated as production waste, for new applications in cosmetics, pharmaceuticals or food industry.

### Experimental

The research materials were collected from the poultry of Faraon breed at the age of 60 days and included the grease surrounding their entrails. The nutritional priorities, chemical composition, and production advantages of Faraon breed are described [4, 5]. For the analysis, the fat was subjected to the catalyzed by potassium hydroxide transesterification by methanolysis, according to the previously described by us methodology [6]. Control of the progress of the methanolysis reaction was performed on Sorbfil silicagel thin-layer plates by eluting the components with an EtOAc-Hexane mixture of solvents (1:5.7).

The analysis of the obtained by methanolysis fatty acids methyl esters was performed by using the GC-MS system Agilent Technologies 7890A with 5975C Mass-Selective Detector(GC-MSD) equipped with split-splitless injector (split, 250 °C, split ratio 1:50, 1 µL) and HP-5ms capillary calibrated column (30m×0.5mm, 0.25µm); Carrier: Helium 1.1 mL/min; Oven: 60 °C - 5 min, 15 °C/min - 300 °C - 10 min; MSD in scan 30-300, 15 min, 30-550 amu, solvent delay 3 min.

For transesterification fat (3.176 g) was placed into a glass flask equipped with a cooler, and a solution of 0.102 g of KOH in 1 mL of MeOH (anh.) was added; the resulting mixture was continuously stirred for 3 hours at 40°C on a magnetic Hotplate Stirrer. After cooling 50 mL of Et<sub>2</sub>O was added and the mixture was neutralized with an aqueous solution of 10 % H<sub>2</sub>SO<sub>4</sub>. The ether extract of fatty acid methyl ethers was rinsed with distilled water to neutral medium and then dried by using anhydrous Na<sub>2</sub>SO<sub>4</sub>.

### Results and discussion

GC-MS analysis of the methyl esters derived from quail fat has demonstrated the presence of 35 organic components in the reaction product (chromatogram, Figure 1), from which the following have been identified by comparison with the mass spectra from the device database (Figures 2 and 3), which constitute 98.97% of total mass (Table 1).

Analysis of the obtained results (Table 2) that are compared with the literary data, regarding the composition and the ratio of fatty acids of meat from 35-days-old Japanese quails [4], demonstrates a higher content of unsaturated acids with *cis*- (Z) configuration representing 77.8 %. The SFA/UFA (saturated fatty acids/unsaturated fatty acids) ratio amounts to 0.27:1 for fat, as compared to 0.52:1 for quail meat. The SFA/PUFA (saturated fatty acids/ polyunsaturated fatty acids) ratio obtained for quail fat is 1.6:1, as compared to 0.73:1 for meat. The absence of Omega-3 acids should be

mentioned: only some traces of alpha-linolenic acid have been detected in quail fat. These results demonstrate nutritive and curative properties of quail fat.

On the basis of the obtained results an inventory patent application has been registered, regarding the preparation of high-quality soap [7].

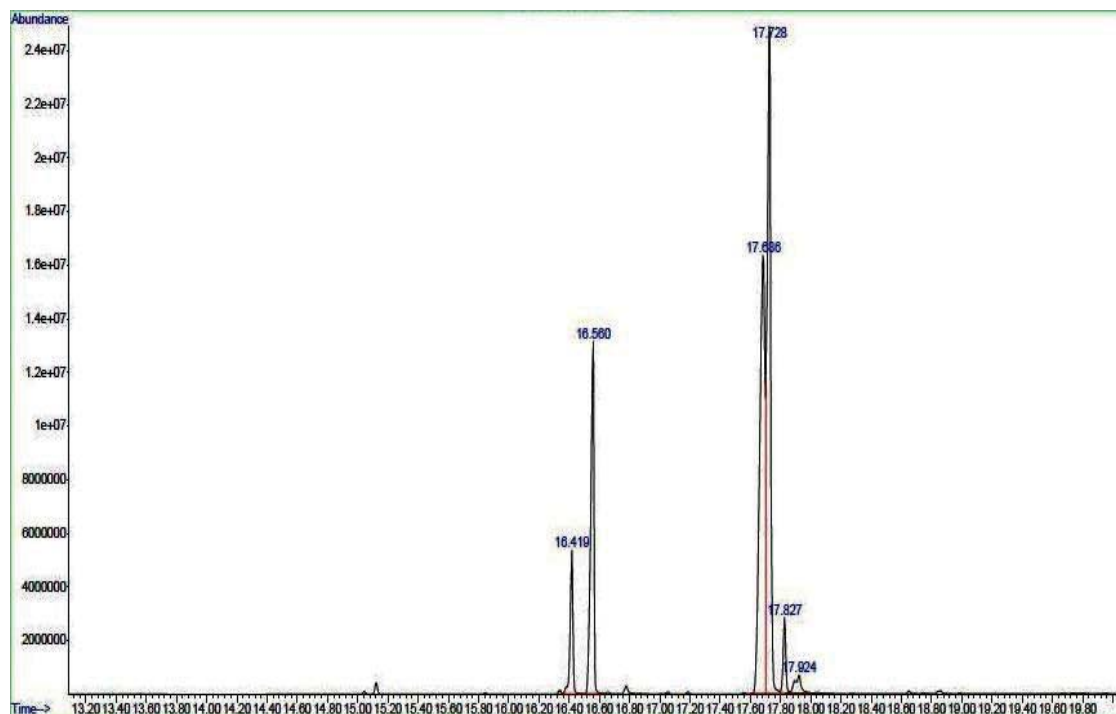


Figure 1. Chromatogram of the reaction product.

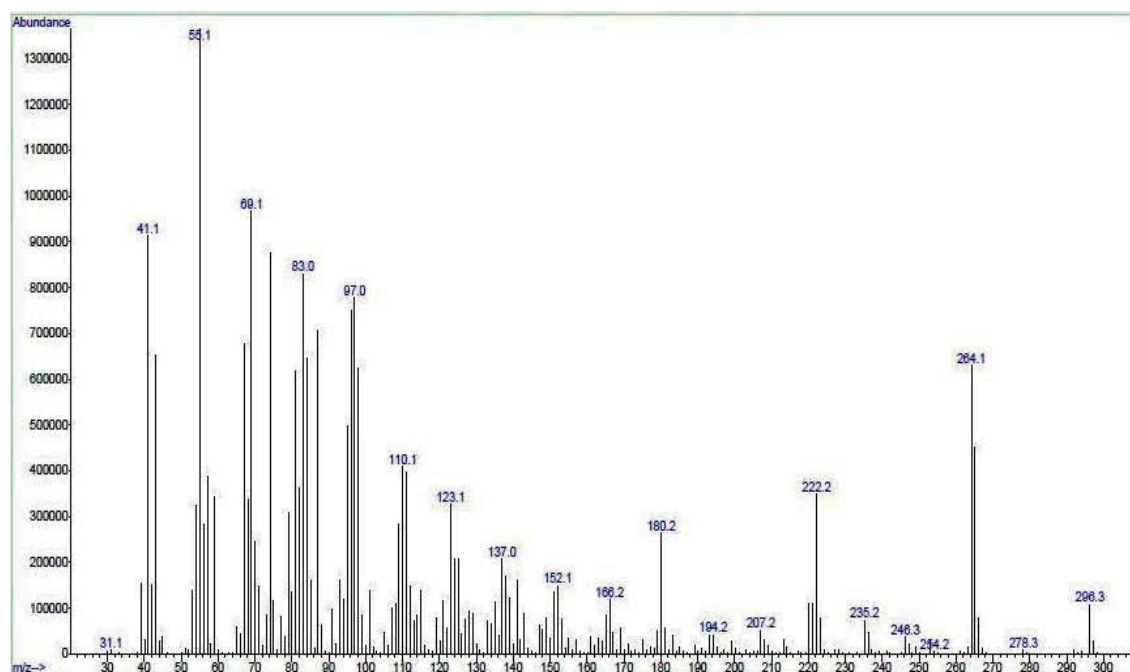


Figure 2. Mass-spectrum of major component of the reaction product, 9-octadecenoic acid, methyl ester, (Z)-.



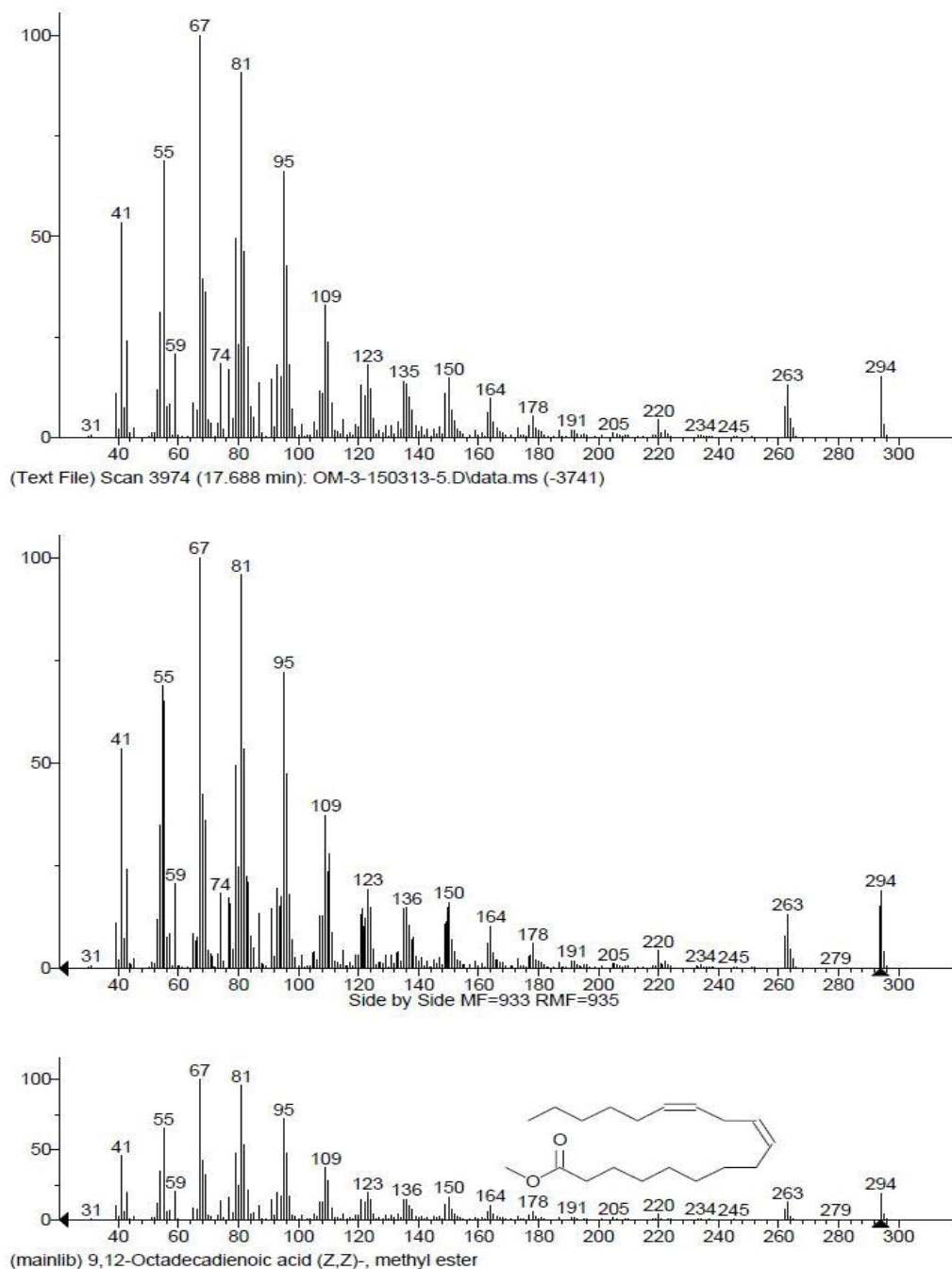


Figure 3. Mass-spectra of linoleic-(Z,Z) acid, methyl ester.

Table 1

The results of GC-MS analysis of the methyl esters of fatty acids  
(% from total mass).

No.	Rt, min	Components of analysis	%
1	15.045	Methyl myristoleate	0.10
2	15.124	Methyl tetradecanoate	0.42
3	15.845	Pentadecanoic acid, methyl ester	0.05
4	16.339	Methyl 7,10-hexadecadienoate	0.15
5	16.419	9-Hexadecenoic acid (Z), methyl ester	5.82
6	16.559	n-Hexadecanoic acid methyl ester	16.85

Continuation of Table 1

	<i>R<sub>t</sub>, min</i>	<i>Components of analysis</i>	<i>%</i>
7	16.779	n-Hexadecanoic acid	0.46
8	17.686	9,12-Octadecadienoic acid(Z,Z) methyl ester	33.05
9	17.727	9- Octadecenoic acid(Z), methyl ester	36.78
10	17.828	Octadecanoic acid, methyl ester	3.00
11	17.923	<i>Cis</i> -13- Octadecenoic acid	1.92
12	18.859	<i>Cis</i> -11- Eicosenoic acid methyl ester	0.23
13	18.652	Arachidonic acid	0.14

Table 2

**Fatty acids content of fat from Faraon breed of Japanese Quails.**

<i>Carbon chain</i>	<i>Fatty acids</i>	<i>% from total lipids</i>
14 : 0	Miristic	0.42
14 : 1	Miristoleic	0.10
15 : 0	Pentadecanoic	0.05
16 : 0	Palmitic	17.31
16 : 1	Palmitoleic	5.82
16 : 2	7,10-Hexadecadienoic	0.15
18 : 0	Stearic	3.00
18 : 1	Oleic(Z)	36.78
18 : 1	<i>Cis</i> -13-Octadecenoic	1.92
18 : 2	Linoleic(Z,Z), Omega-6	33.05
20 : 1	<i>Cis</i> -11- Eicosenoic	0.23
20 : 4	Arachidonic, Omega-6	0.14
	Total Saturated fatty acids (SFA)	20.78
	Total Unsaturated fatty acids (UFA)	78.19
	Total Monounsaturated fatty acids (MUFA)	44.85
	Total Polyunsaturated fatty acids (PUFA)	33.34
	Ratio : SFA / UFA	0.27 : 1
	Ratio : PUFA / SFA	1.60 : 1

**Conclusions**

Analysis of fatty acid methyl esters using a GC-MS high-performance system has demonstrated a high content (77.8%) of Z-configuration acids, in particular, oleic Z (18:1), linoleic-Z,Z (18:2), and palmitoleic-Z (16:1), which confirm the curative and nutritional value of Faraon quail fat and the possibility of its use in cosmetic, pharmaceutical and food industries.

Investigation of the collected Faraon quail fat as production waste has allowed its capitalization by manufacturing high-quality soap that was registered as inventory patent application (Patent MD, No. 932).

**References**

1. Gecgel, U.; Yilmaz, I.; Gurcan, E.K.; Karasu, S.; Dulger, G.C. Comparison of fatty acid composition between female and male japanese quail meats. *Journal of Chemistry*, 2015, Vol. 2015, 8 p., doi:10.1155/2015/569746.
2. El-Dengawy, R.A.; Nassar, A.M. Investigation on the nutritive value and microbiological quality of wild quail carcasses. *Nahrung/Food*, 2001, 45, pp. 50-54.
3. Seppanen-Laakso, T.; Laakso, I.; Hiltunen, R. Analysis of fatty acids by gas chromatography and its relevance to research on health and nutrition. *Analytica Chimica Acta*, 2002, 465, pp. 39-62.
4. Gencev, A.; Mihaylova, G.; Ribarski, S.; Pavlov, A.; Kabakchiev, M. Meat quality and composition in Japanese Quails. *Trakia Journal of Sciences*, 2008, 6, pp. 72-82.
5. Gencev, A.G.; Ribarski, S.S.; Afanasjev, G.D.; Blohin, G.I. Fattening capacities and meat quality of Japanese quails of Faraon and White English breeds. *Journal Central European of Agriculture*, 2005, 6, pp. 495-500.
6. Lupascu, T.; Dragalin, I.; Vlad, P.; Serban, S.; Stepan, E. Process for preparing the mixture of methyl esters of fatty acids from fats, Biodiesel. MD Patent, 2004, No. 2382 (in Romanian).
7. Rosca, R.M.; Rosca, V.; Sadcenco, M. Toilet soap. MD Patent, 2015, No. 932 (in Romanian).



# SYNTHESIS OF NEW NITROGEN-CONTAINING DRIMANE AND HOMODRIMANE SESQUITERPENOIDS FROM SCLAREOLIDE

Lidia Lungu

*Institute of Chemistry of Academy of Sciences of Moldova, 3 Academiei str., Chisinau, MD-2028, Republic of Moldova  
e-mail: lidialungu@ymail.com*

**Abstract.** The synthesis of new nitrogen-containing drimane and homodrimane sesquiterpenoids in cycle B is reported. A comparative study of the microwave (MW) assisted synthesis of drimenone versus classical conditions has been done. The drimanic and homodrimanic oximes were prepared on the base of ketones derived from commercially available sclareolide. The drimanic amine was obtained by reduction of corresponding oxime with  $\text{LiAlH}_4$ . The structure of novel compounds was confirmed using IR,  $^1\text{H}$  and  $^{13}\text{C}$  NMR analyses.

**Keywords:** synthesis, sesquiterpenoids, oxime, reduction, 7-amino-drim-8(9)-ene.

*Received: September 2015/ Revised final: October 2015/ Accepted: October 2015*

## Introduction

Drimane and homodrimane sesquiterpenoids are classes of natural products with a broad spectrum of biological activities, including antifungal, antibacterial, antiviral, cytotoxic, antifeedant, and others [1]. The presence of nitrogen in a molecule is usually accompanied either by the appearance of new activities or by intensification of the original activity characteristic for the native terpenoids.

So far, some drimanic and homodrimanic amines have been synthesized. Urones et al. [2] prepared dihydroxyamine **1** and its derivatives, Barrero et al. [3] – hydroxylamine **2** and products of amino and/or hydroxy group derivatization (Figure 1). Later, 11-aminodrim-7-ene **3** was synthesized from drimenol **4** [4-6]. Recently, 12-amino-11-dihomodrim-8-ol **5** and products **6** and **7** of its dehydration have been synthesized from sclareolide **8** [7] and 13-amino-14,15-dinorlabd-8(9)-ene **9** from sclareol **10** [8] (Figure 1).

In scientific literature there are few examples about syntheses of cycle B functionalized drimanic and homodrimanic amines [2]. Thus, the aim of this research is the synthesis of drimanic and homodrimanic compounds with nitrogen containing functional groups in cycle B.

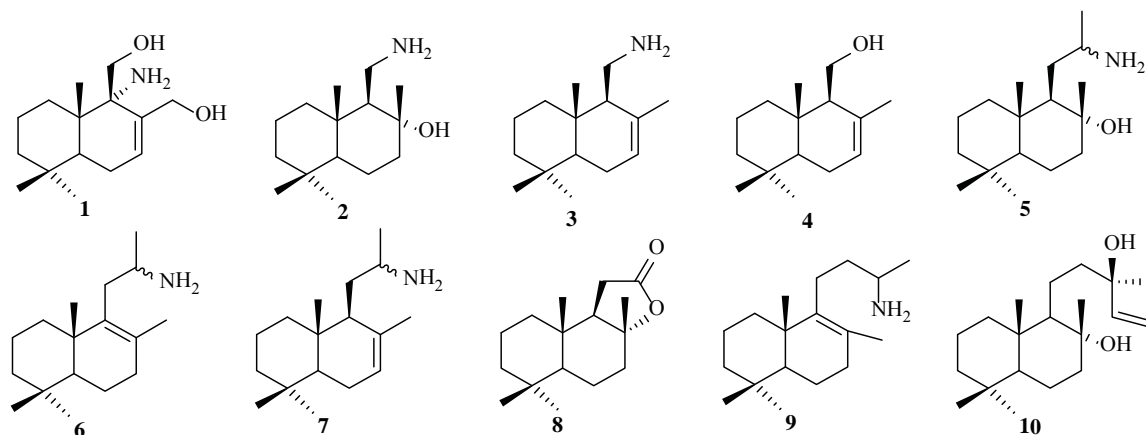


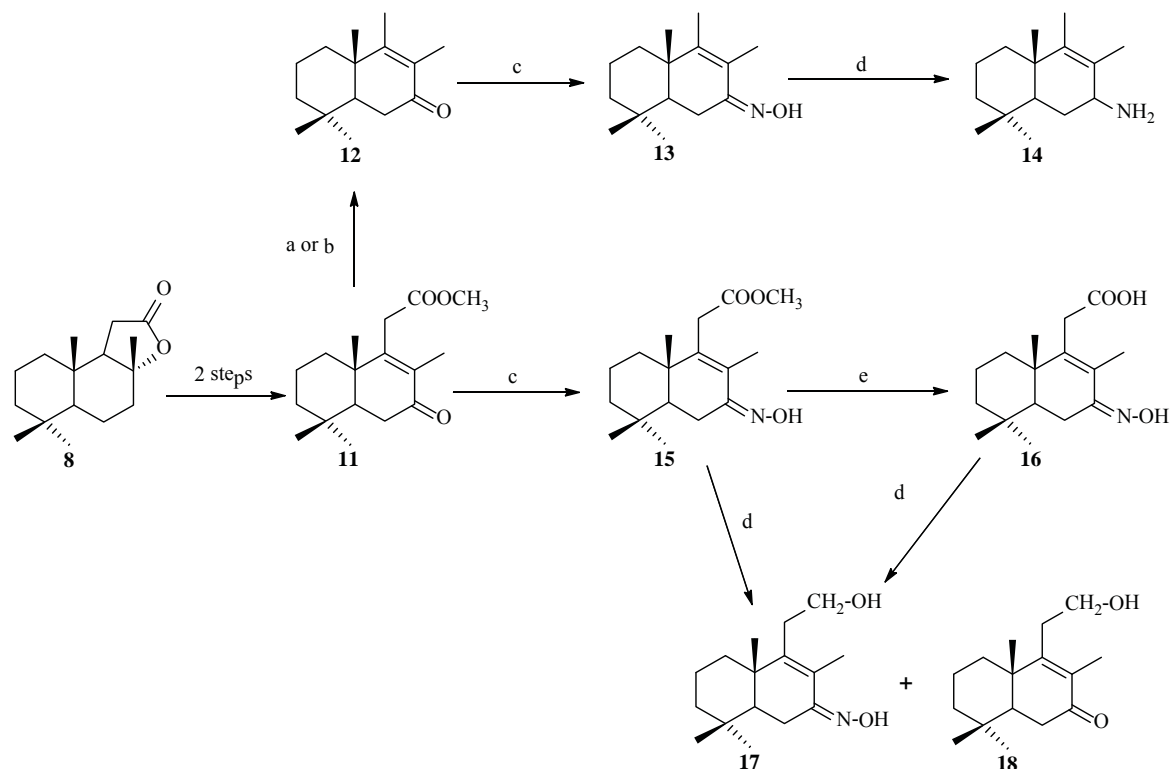
Figure 1. Norlabdanic amines and their precursors.

## Results and discussion

Herein we report the preparation of new nitrogen-containing drimane and homodrimane sesquiterpenoids in cycle B (Scheme 1).

As starting material for the synthesis of the reported compounds methyl 7-oxo-13,14,15,16-tetranorlabd-8-en-12-oate **11** was used, obtained in two steps in 76% overall yield from the commercially available sclareolide **8** [9] (Scheme 1). Drim-8-en-7-one **12** can be obtained from ketoester **11** by known method as depicted in Scheme 1(a) as in [10]. We prepared compound **12** from the same ester **11** using MW irradiation (Scheme 1(b)) in the same 98% yield but two times faster.

Drimene oxime **13** was prepared by the reaction of drim-8-en-7-one **12** with hydroxylamine hydrochloride in a mixture of ethanol:pyridine (1:1) in 98% yield as in [11].



**Scheme 1. Synthesis of nitrogen-containing drimane and homodrimane sesquiterpenoids.**

**Reagents and conditions:** a) KOH, EtOH, reflux, 3h, 98%; b) KOH, EtOH, MW, 1.5h, 98%; c)  $\text{NH}_2\text{OH}\cdot\text{HCl}$ , EtOH, Py, 24h, 96-98%; d)  $\text{LiAlH}_4$ , THF, 5h-24h, 51-60%; e) KOH, MeOH, 95%.

The desired product, 7-amino-drim-8(9)-ene **14**, was obtained in 51% yield by refluxing oxime **13** with  $\text{LiAlH}_4$  in anhydrous THF as in [8]. The structure of compound **14** was confirmed by IR,  $^1\text{H}$ , and  $^{13}\text{C}$  NMR data.

In another case, ketoester **11** was treated with hydroxylamine hydrochloride in a mixture of ethanol:pyridine (1:1), giving ester oxime **15** described in [11], which was subsequently saponified with KOH in methanol into the oxime **16** in 95% yield.

Oximes **15** and **16** were reduced with  $\text{LiAlH}_4$  in anhydrous THF as in [8], giving two compounds: hydroxy oxime **17**, in 55% and 60% yield and hydroxy ketone **18**, in 10% and 12% yield. The structure of compound **17** was confirmed by IR,  $^1\text{H}$ , and  $^{13}\text{C}$  NMR data.

Several attempts to reduce oximic functions from molecules of compounds **15** and **16** were unsuccessful, probably because of steric impediments which appear in the molecules of the mentioned homodrimanic oximes **15** and **16**, but not in the molecules of drimanes.

## Conclusion

Novel nitrogen-containing drimane and homodrimane sesquiterpenoids in cycle B were synthesized. They are of scientific interest as compounds with potential biological activity.

## Experimental

### General experimental procedure

Melting points (m.p.) were taken on a Boetius hot stage apparatus. Optical rotations were determined on a Jasco DIP 370 polarimeter with a 1dm microcell, in  $\text{CHCl}_3$ . IR spectra were obtained on Spectrum-100FT-IR spectrometer (Perkin-Elmer) with ATR technique.

$^1\text{H}$  and  $^{13}\text{C}$  NMR spectra were recorded in  $\text{CDCl}_3$  on Bruker Avance DRX 400 spectrometer. Chemical shifts are given in ppm in  $\delta$  scale and referred to  $\text{CHCl}_3$  ( $\delta_{\text{H}}$  at 7.26 ppm) and to  $\text{CDCl}_3$  ( $\delta_{\text{C}}$  77.00 ppm), respectively. Coupling constants ( $J$ ) are reported in Hertz (Hz). The H, H-COSY, H, C-HSQC and H, C-HMBC experiments were recorded using standard pulse sequences, in the version with  $z$ -gradients, as delivered by Bruker Corporation. Carbon substitution degrees were established by the DEPT pulse sequence.

The microwave assisted (MW) transformations were carried out using a monomode reactor (800W, STAR SYSTEM-2, under a constant irradiation power, but at varying temperature. The best results were obtained when 30% of the full power of the magnetron was used.

For analytical TLC, Merck silica gel plates 60G in 0.25 mm layers were used. The TLC plates were sprayed with conc.  $\text{H}_2\text{SO}_4$  and heated at  $80^\circ\text{C}$ . Column chromatography was carried out on Across silica gel (60–200 mesh) using petroleum ether (PE) (b.p.  $40\text{--}60^\circ\text{C}$ ) and the gradient mixture of PE and EtOAc or the gradient mixture of methanol and  $\text{CHCl}_3$ .

All solvents were purified and dried by standard techniques before use. Solutions in organic solvents were dried over anhydrous  $\text{Na}_2\text{SO}_4$ , then filtered and evaporated under a reduced pressure.

### General procedure of drimenone 12 preparation under microwave irradiation

**Caution!** It is hazardous to rapidly heat reactions under microwave irradiation. Therefore, caution should be exercised when conducting reactions of this type.

A solution of ketoester **11** (1 g, 3.6 mmol) and potassium hydroxide (4.17 g, 74.3 mmol) in ethanol (36 mL) was prepared as described in [10] and placed in the reaction vessel (quartz). The tube was then placed in the microwave cell and irradiated at 240 W for 1.5 h. Once the heating cycle was complete, the tube was cooled to ambient temperature and removed from the reactor. The 2/3 of the solvent volume were removed under a reduced pressure, then the residue was diluted with water (15 mL), extracted with  $\text{Et}_2\text{O}$  (3 x 10 mL), and the organic layer was washed with water (2 x 20 mL) and dried. After the solvent removal, drim-8(9)-en-7-one **12** (0.776 mg, 98 %) was obtained, as white crystals m.p.  $51\text{--}52^\circ\text{C}$ . The spectral data of compound **12** are in accordance with those mentioned in [10].

### General procedure of drimanic and homodrimanic oximes preparation

A solution of **11** (0.57 g, 2.5 mmol), or **12** (0.7 g, 2.5 mmol) in EtOH (5 mL) and Py (5 mL) was treated with  $\text{NH}_2\text{OH}\cdot\text{HCl}$  (0.2 g). The resulted mixture was stirred for 24 h at room temperature, then diluted with water (20 mL) and extracted with  $\text{Et}_2\text{O}$  (3 x 10 mL). The organic layer was washed with 10% HCl (10 mL),  $\text{NaHCO}_3$  solution (10 mL) and water (15 mL), dried over anhydrous  $\text{Na}_2\text{SO}_4$  and filtered. The solvent removal under a reduced pressure as in [11] led to oximes **13** (0.59 g, 98%) or **15** (0.72 g, 98%), as white solids.

**7-Hydroxyimino-drim-8(9)-ene (13)**, 98% yield, as a white solid (EtOH), m.p.  $183\text{--}184^\circ\text{C}$ ,  $[\alpha]_D^{20} = -35.5^\circ$  (c 13.5,  $\text{CHCl}_3$ ). IR (ATR) $\nu$  : 3257, 2930, 1626, 1614, 1439, 950, 928, 772  $\text{cm}^{-1}$ .  $^1\text{H}$  NMR ( $\text{CDCl}_3$ , 400 MHz, ppm):  $\delta$  9.85 (1H, s, N-OH); 1.37 (1H, d,  $J$  14.0 Hz, H-5); 1.86 (3H, s, H-12); 1.81 (3H, s, H-13), 0.98 (9H, s, H-13, H-14, H-15).  $^{13}\text{C}$  NMR ( $\text{CDCl}_3$ , 100 MHz, ppm):  $\delta$  158.44 (C-7), 151.13 (C-9), 122.36 (C-8), 48.26 (C-5), 41.73 (C-3), 39.02 (C-10), 36.60 (C-1), 33.31 (C-4), 32.76 (C-14), 21.25 (C-13), 20.90 (C-6), 18.84 (C-2), 17.78 (C-15), 13.78 (C-11), 13.25 (C-12).

**Methyl-7-hydroxyimino-homodrim-8(9)-en-12-oate (15)**, 98% yield, as a white solid (EtOH), m.p.  $130\text{--}131^\circ\text{C}$ ,  $[\alpha]_D^{20} = +27.9^\circ$  (c 8.5,  $\text{CHCl}_3$ ). IR (ATR) $\nu$  : 3257, 2928, 1739, 1725, 1629, 1435, 1322, 1247, 1161, 955, 762  $\text{cm}^{-1}$ ;  $^1\text{H}$  NMR ( $\text{CDCl}_3$ , 400 MHz, ppm):  $\delta$  9.39 (1H, s, N-OH); 3.29 (1H, d,  $J$  16.8 Hz, H-11); 3.19 (1H, d,  $J$  16.8 Hz, H-11); 1.44 (1H, d,  $J$  14.4 Hz, H-5); 3.69 (3H, s,  $\text{CO}_2\text{Me}$ ); 1.82 (3H, s, H-13), 0.95 (9H, s, H-14, H-15, H-16).  $^{13}\text{C}$  NMR ( $\text{CDCl}_3$ , 100 MHz, ppm):  $\delta$  171.93 (C-12), 158.17 (C-7), 146.57 (C-9), 127.10 (C-8), 51.99 (C-17), 48.12 (C-5), 41.54 (C-3), 39.21 (C-10), 35.18 (C-1), 33.60 (C-11), 33.31 (C-4), 32.66 (C-15), 21.27 (C-14), 20.83 (C-6), 18.71 (C-2), 18.38 (C-16), 13.59 (C-13).

**Synthesis of 7-amino-drim-8(9)-ene (14)**. A solution of oxime **13** (0.5 g, 2.1 mmol) in anhydrous THF (40 mL) was treated with  $\text{LiAlH}_4$  (0.84 g). The resulted mixture was refluxed and stirred for 10 h, then it was diluted with water (20 mL), and treated dropwise with HCl (10%, 20 mL) until the acidic level of pH is reached. The aqueous layer was extracted with  $\text{Et}_2\text{O}$  (2x 20 mL), neutralized with the aqueous saturated  $\text{Na}_2\text{CO}_3$  solution (20 mL) and extracted with EtOAc (3 x 15 mL). The organic layer was washed with water (20 mL) and dried. After the solvent removal, the crude product (0.35 g) was purified by column chromatography on silica gel (10 g, eluent: methanol/ $\text{CHCl}_3$  1:9) to give 7-amino-drim-8(9)-ene (**8**) (0.24 g, 51%), as an oil,  $[\alpha]_D^{20} = +17.6^\circ$  (c 2.7,  $\text{CHCl}_3$ ).

IR (ATR) $\nu$  : 3279, 2924, 1569, 1459, 1442, 1383, 1367  $\text{cm}^{-1}$ .

$^1\text{H}$  NMR ( $\text{CDCl}_3$ , 400 MHz, ppm):  $\delta$  3.16 (1H, s, H-7); 2.07 (2H, s,  $\text{NH}_2$ ); 1.59 (3H, s, H-12); 1.49 (3H, s, H-11), 0.96 (3H, s, H-15), 0.86 (3H, s, H-13), 0.82 (3H, s, H-14).  $^{13}\text{C}$  NMR ( $\text{CDCl}_3$ , 100 MHz, ppm):  $\delta$  139.17 (C-9), 127.97 (C-8), 54.40 (C-7), 50.38 (C-5), 41.53 (C-3), 38.96 (C-10), 36.89 (C-1), 33.05 (C-14), 32.95 (C-4), 30.37 (C-6), 21.50 (C-13), 19.58 (C-15), 18.93 (C-2), 16.11 (C-12), 13.14 (C-11).

**Saponification of methyl 7-hydroxyimino-homodrim-8(9)-en-12-oate (15)**. To a solution of ester oxime **15** (0.3 g, 1.02 mmol) in EtOH (10 mL) solid KOH (1.2 g) was added. The resulted reaction mixture was refluxed for 3 hrs, then 2/3 of alcohol were distilled. The remained mixture was diluted with water (10 mL) and extracted with  $\text{Et}_2\text{O}$  (3x10 mL). The organic layer was washed with water (20 mL), dried on anhydrous sodium sulfate, concentrated, and the title compound **16** (0.27g, 95% yield) was obtained, as a white solid (EtOH), m.p.  $197\text{--}199^\circ\text{C}$ ,  $[\alpha]_D^{20} = +7.4^\circ$  (c 2.3,  $\text{CHCl}_3$ ).

IR (ATR) $\nu$  : 3239, 2931, 1689, 1620, 1422, 1334, 1241, 1216, 973, 723  $\text{cm}^{-1}$ .

$^1\text{H}$  NMR ( $\text{CDCl}_3$ , 400 MHz, ppm):  $\delta$  12.15 (1H, s, OH); 10.78 (1H, s, N-OH); 3.17 (1H, d,  $J$  16.8 Hz, H-11); 3.10 (1H, d,  $J$  16.8 Hz, H-11); 1.30 (1H, d,  $J$  3.6 Hz, H-5); 1.72 (3H, s, H-13), 0.88 (9H, s, H-14, H-15, H-16).  $^{13}\text{C}$  NMR

(CDCl<sub>3</sub>, 100 MHz, ppm):  $\delta$  172.50 (C-12), 155.54 (C-7), 145.03 (C-9), 126.38 (C-8), 48.04 (C-5), 41.18 (C-3), 38.55 (C-10), 35.15 (C-1), 33.48 (C-11), 32.86 (C-4), 32.56 (C-15), 21.03 (C-14), 20.30 (C-6), 18.22 (C-2), 18.07 (C-16), 13.07 (C-13).

**Reduction of methyl 7-hydroxyimino-homodrim-8(9)-en-12-oate (15) and 7-hydroxyimino-homodrim-8(9)-en-12-oic acid (15).** A solution of oximes **15** (0.109 g, 0.37 mmol) or **16** (0.103 g, 0.36 mmol) in anhydrous THF (10 mL) was treated with LiAlH<sub>4</sub> (0.14 g). The resulted mixture was refluxed and stirred for 10 h, then it was diluted with water (10 mL), and treated dropwise with HCl (10%, 5 mL) until the acidic level of pH is reached. The aqueous layer was extracted with Et<sub>2</sub>O (2 x 5 mL), neutralized with saturated aqueous Na<sub>2</sub>CO<sub>3</sub> solution (10 mL), and extracted with EtOAc (3 x 5 mL). The organic layer was washed with water (10 mL) and dried. After the solvent removal, the crude product (305 mg and 325 mg) was purified by column chromatography on silica gel (0.070 g and 0.076 g, eluent: methanol/CHCl<sub>3</sub> 2:9) to give 7-hydroxyimino-homodrim-8(9)-en-12-ol **17** (0.054 g, 55% and 0.058 g, 60%), and 12-hydroxy-homodrim-8(9)-en-7-one **18** (0.009 g, 10% and 0.011 g, 12%), respectively.

7-hydroxyimino-homodrim-8(9)-en-12-ol **17**, as a white solid, m.p. 111-113°C,  $[\alpha]_D^{20} = -15.07^\circ$  (c 0.5, CHCl<sub>3</sub>).

IR (ATR)<sub>v</sub>: 3280, 2927, 1611, 1452, 1442, 1388, 1375, 1028, 955, 757 cm<sup>-1</sup>.

<sup>1</sup>H NMR (CDCl<sub>3</sub>, 400 MHz, ppm):  $\delta$  10.72 (1H, s, N-OH); 4.66 (1H, t, *J* 5.26 Hz OH); 1.77 (3H, s, H-13); 0.88 (6H, s, H-14, H-16), 0.87 (3H, s, H-15). <sup>13</sup>C NMR (CDCl<sub>3</sub>, 100 MHz, ppm):  $\delta$  156.08 (C-7), 148.95 (C-9), 125.34 (C-8), 60.96 (C-12), 48.50 (C-5), 41.73 (C-3), 39.00 (C-10), 36.32 (C-1), 33.45 (C-4), 33.11 (C-15), 32.81 (C-11), 21.64 (C-14), 20.83 (C-6), 18.98 (C-16), 18.85 (C-2), 13.39 (C-13).

12-hydroxy-homodrim-8(9)-en-7-one **18**, as a white solid, m.p. 97-98°C,  $[\alpha]_D^{20} = +58.0^\circ$  (c 0.4, CHCl<sub>3</sub>).

IR (ATR)<sub>v</sub>: 3456, 2979, 1664, 1455, 1392, 1380, 1145, 1074 cm<sup>-1</sup>.

<sup>1</sup>H NMR (CDCl<sub>3</sub>, 400 MHz, ppm):  $\delta$  1.78 (3H, s, H-13); 1.07 (3H, s, H-16); 0.90 (3H, s, H-14). 0.86 (3H, s, H-15), <sup>13</sup>C NMR (CDCl<sub>3</sub>, 100 MHz, ppm):  $\delta$  200.05 (C-7), 163.59 (C-9), 131.56 (C-8), 61.28 (C-12), 50.11 (C-5), 40.61 (C-10), 41.24 (C-3), 36.14 (C-1), 35.23 (C-6), 33.11 (C-4), 32.98 (C-11), 32.45 (C-15), 21.27 (C-14), 18.87 (C-2), 18.10 (C-16), 17.75 (C-13).

## Acknowledgments

I would like to thank my supervisor Professor, Doctor Habilitatus Aculina Aricu for her guidance and kind support.

## References

- Jansen, B.J.M.; De Groot, A. Occurrence, biological activity and synthesis of drimane sesquiterpenoids. *Natural Product Reports*, 2004, 21, pp. 447-449.
- Urones, J.G.; Diez, D.; Gomez, P.M.; Marcos, I.S.; Basabe, P.; Moro, R.F. Drimane homochiral semisynthesis: pereniporinA, 9-epiwarburganal and C-9 nitrogenated drimanes. *Natural Product Letters*, 1998, 11, pp. 145-152.
- Barrero, A.F.; Alvarez-Manzaneda, E.J.; Chahboun, R.; Gonzalez, D.C. New Routes toward drimanes and nor-drimanes from (-)-sclareol, *Synlett*, 2000, 11, pp. 1561-1564.
- Zarraga, M.; Zarraga, A.M.; Rodriguez, B.; Perez, C.; Paz, C.; Paz, P.; Sanhueza C. Synthesis of a new nitrogenated drimane derivative with antifungal activity. *Tetrahedron Letters*, 2008, 49, pp. 4775-4776.
- Kuchkova, K.; Aricu, A.; Vlad, P. Synthesis of 11-aminodrim-7-ene from drimenol. *Chemistry of Natural Compounds*, 2009, 45(3), pp. 367-370.
- Aricu, A. Synthesis of nitrogen-containing compounds from higher terpenoids. *Chemistry Journal of Moldova*, 2011, 6(1), pp. 10-28.
- Kuchkova, K.; Aricu, A.; Barba, A.; Secara, E.; Vlad, P.; Ungur N. Synthesis of 12-amino-11-dihomodrimane sesquiterpenoids from norambreinolide. *Chemistry of Natural Compounds*, 2014, 50, pp. 458-461.
- Kuchkova, K.; Aricu, A.; Secara, E.; Barba, A.; Dragalin, I.; Vlad, P.; Ungur, N. Synthesis of 13-amino-14,15-dinorlabd-8(9)-ene from sclareol. *Russian Chemical Bulletin*, 2014, 63, pp. 2074-2076.
- Vlad, P.; Edu, C.; Koltza, M.; Ciocarlan, A.; Nicolescu, A.; Deleanu, C. Enantioselective synthesis of 11-homodrim-7-en-9 $\alpha$ ,12,13-triol. *Chemistry of Natural Compounds*, 2011, 47(4), pp. 574-578.
- Vlad, P.; Vorob'eva, E. Synthesis of drim-8-en-7-one. *Chemistry of Natural Compounds*, 1983, 19, pp. 139-141 (in Russian).
- Kuchkova, K.; Aricu, A.; Barba, A.; Vlad, P.; Lipkovskii, Ya.; Simonov, Yu.; Kravtsov, V. Synthesis of nitrogen-containing drimane sesquiterpenoids from 11-dihomodrim-8(9)-en-12-one. *Chemistry of Natural Compounds*, 2011, 47(2), pp. 223-228.

## NEW N-GLUCOSYLATED SUBSTITUTED ANILINES

Vsevolod Pogrebnoi

Institute of Chemistry of the Academy of Sciences of Moldova, 3, Academiei str., Chisinau MD-2028, Moldova  
 e-mail: seva.antivirus@gmail.com; phone: (+373 22) 739 754; fax: (+373 22) 739 954

**Abstract.** The reaction of (+)-D-glucose **1** with 4-chloroaniline **6b** or 3,5-dibromoaniline **12** leads almost exclusively to the  $\beta$ -configuration of N-glucosylated anilines **7b** and **13**. Acetylated derivatives **8b**, **14** and **15** were obtained by dissolving/suspending substances **7b** and **13** in Ac<sub>2</sub>O/Py mixture. The acetylation of 2-(3,5-dibromophenylamino)-6-(hydroxymethyl)tetrahydro-2H-pyran-3,4,5-triol **13** is less selective than in the case of the 2-(4-chlorophenylamino)-6-(hydroxymethyl)tetrahydro-2H-pyran-3,4,5-triol **7b** and leads to compounds 2-(acetoxymethyl)-6-(3,5-dibromophenylamino)tetrahydro-2H-pyran-3,4,5-triyl triacetate **14** and 2-(acetoxymethyl)-6-(3,5-dibromophenylamino)-5-hydroxytetrahydro-2H-pyran-3,4-diyl diacetate **15** in a 2:1 ratio. The product **14** is formed with greater selectivity and in a higher yield (up to 80%) when the reaction is catalyzed by DMAP and stored for one week at +4°C.

**Keywords:** N-glucosylated anilines, (+)-D-glucose, 4-chloroaniline, 3,5-dibromoaniline, Convolutamydines A-E.

Received: March 2015/ Revised final: October 2015/ Accepted: November 2015

## Introduction

N-Glycosylated anilines represent an important product scaffold cluster by virtue of their bioactivity and as intermediates for generating further molecular complexity including natural compounds [1], for example some natural alkaloids. The vital roles played by sugars in biological systems continue to be unravelled. It is known that, various drugs, amino acids, sugars and many other chiral natural compounds show different influence on human organism, their biological properties being directly dependent on chirality. That is why the “structure-property” relationship should be studied very well. From the other side, properties are determined by the structure. It means, construction of chemically pure and defined molecule is an interesting and important goal in synthetic chemistry.

Langer *et al.* [1,2] has shortly offered the opinion that the preparation of analogues of N-glycosylated indolinones in high yields remains an important problem of carbohydrate and medicinal chemistry. This challenge also applies to the related problem of synthesis of N-linked alkaloids. For example, Kamano, Y. *et al.* [3], reported the isolation of the alkaloids - Convolutamydines A, B, and C from bryozoan *Amathia convoluta*, see Figure 1. In contrast to the pharmacologically inactive non-glycosylated indigo, N-glycosylated indigo demonstrate a considerable growth inhibitory activity toward various human tumor cell lines [4,5].

Our approaches to N-glucosylated indoline-2,3-dione **4** from (+)-D-glucose **1** and N-glucosylated 3-hydroxy-2-oxindole **5** are presented below. They show benefit from the rapid advances in mainstream carbohydrate chemistry, allowing for convenient integration in glucosylated Convolutamydine A-E and analogues of structure **5** preparation (see Figure 1).

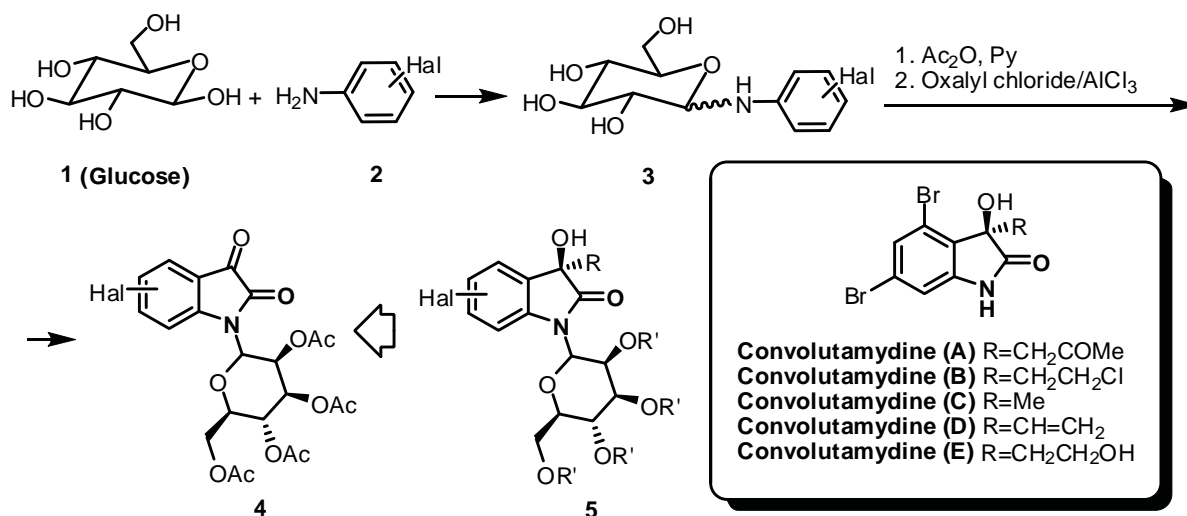


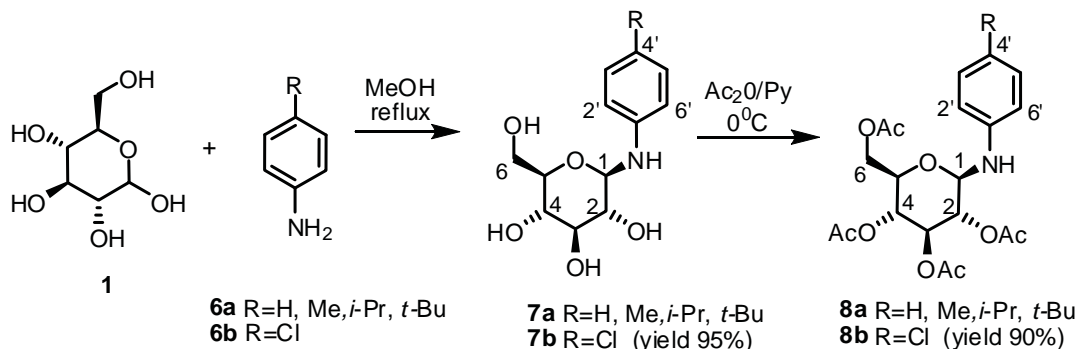
Figure 1. Synthesis of N-glucosylated indoline-2,3-dione (4).



The main purpose of the present research was to test the effectiveness of this approach for the synthesis of halogen phenylamino-6-(hydroxymethyl)tetrahydro-2*H*-pyran-3,4,5-triyl triacetates from the corresponding intermediates **3** (see Figure 1). It has already been demonstrated that such type compounds are suitable building units for the synthesis of a variety of non-halogenated isatin-*N*-glucosides [1,2]. We also report in this paper the preparation of 3,5-dibromoaniline **12**.

## Results and discussion

It was reported [1], that similar aniline-*N*-glucosides **7a** were prepared from corresponding anilines (R=H, Me, *i*-Pr, *t*-Bu) and (+)-*D*-glucose **1**. The formed product **7a** was directly used for the next step (see Scheme 1). However, some of the derivatives of glycosides can be isolated as pure  $\beta$ -anomers **8a**, whereas the others contain a small amount of the corresponding  $\alpha$ -anomer [1,2].



**Scheme 1. Syntheses of N-glucosylated 4-substituted anilines **8a** and **8b** [1].**

In the course of our studies the (2*R*,3*R*,4*S*,5*S*,6*R*)-2-(4-chlorophenylamino)-6-(hydroxymethyl)tetrahydro-2*H*-pyran-3,4,5-triol **7b** was prepared according to the reported method [1] primarily by reason of convenience: medium solubility of (+)-*D*-glucose **1** in MeOH and easy removal from the excess of aniline by filtration and washing with cool MeOH, provides ready access to the solid aminoglycoside, which is slightly soluble in MeOH. A mixture of (+)-*D*-glucose **1** and 4-chloroaniline **6b** was refluxed for 12 hours (see Scheme 1). TLC of the reaction mixture indicated the disappearance of the starting glucose **1** and an increase in the intensity of the neighbouring spot. On keeping the solution overnight in the refrigerator an adduct precipitated that was easily isolated by filtration, being then identified as compound **7b**. It had m.p. 154-156 °C and characteristic IR absorption bands  $\nu_{\text{OH}}$  at 3271 and 3209  $\text{cm}^{-1}$ , the primary (C-6) and secondary (C-2, C-3 and C-4) nature of the alcohol functions being confirmed by the  $^1\text{H}$  NMR spectrum (triplet at  $\delta_{\text{H}}$  4.44-4.47 ppm with a splitting constant  $J=5.8$  Hz and three doublets at  $\delta_{\text{H}}$  4.88-4.90, 4.92-4.9 and 5.00-5.02 ppm with splitting constants  $J=5.4$  Hz,  $J=5.2$  Hz and  $J=4.7$  Hz. NH group shows doublet at  $\delta_{\text{H}}$  6.46-6.48 ppm. Moreover,  $^1\text{H}$  NMR spectrum has resonances at  $\delta_{\text{H}}$  6.67-6.69 ppm (C-2'-H and C-6'-H, doublet,  $J=8.8$  Hz) and  $\delta_{\text{H}}$  7.10-7.12 ppm (C-3'-H and C-5'-H, doublet,  $J=8.8$  Hz), indicating that compound **7b** is an anilide. Additionally, absorption in the low-field region of its  $^{13}\text{C}$  NMR spectrum confirmed the presence of aromatic carbons at  $\delta_{\text{C}}$  115.06 ppm (C-2' and C-6'), 120.7 ppm (C-4'), 128.92 ppm (C-3' and C-5') ppm and 146.7 ppm (C-1').

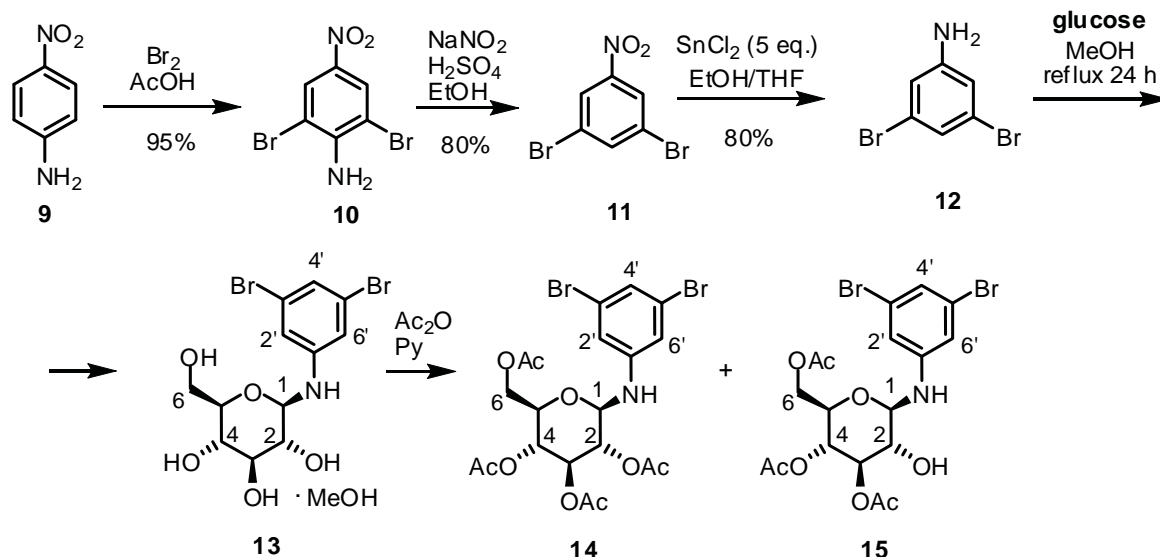
In fact compound **7b** shows in the  $^1\text{H}$  NMR spectrum a clear triplet at  $\delta_{\text{H}}$  4.30-4.34 ppm with the magnitude of a spin-spin coupling constant  $J=8$  Hz and an important peak at 883.8  $\text{cm}^{-1}$  in its IR-spectrum, which is characteristic for a  $\beta$ -anomer.

The reaction of compound **7b** with (+)-*D*-glucose **1** was slow and only after 48 hrs provided a solid compound with m.p. 146-149°C. The substance **8b** was obtained in 97% yield, being identified as (2*R*,3*R*,4*S*,5*S*,6*R*)-2-(4-chlorophenylamino)-6-(hydroxymethyl)tetrahydro-2*H*-pyran-3,4,5-triol **8b** on the basis of its NMR spectroscopic data. Thus, the  $^1\text{H}$  NMR spectrum of it showed in the low-field region two singlets and a doublet at  $\delta_{\text{H}}$  1.95, 1.97, 2.00 ppm characterizing four acetate groups, according to the integral. The  $^1\text{H}$  NMR spectrum of compound **8b** also contains two doublets of aromatic protons, centered at  $\delta_{\text{H}}$  6.75 ppm (2H, C-2'-H and C-6'-H,  $J=8.9$  Hz) and  $\delta_{\text{H}}$  7.14 ppm (2H, C-3'-H and C-5'-H,  $J=8.8$  Hz) and a doublet of NH group at  $\delta_{\text{H}}$  6.71 ppm with the spin-spin coupling constant  $J=9.8$  Hz. The  $^{13}\text{C}$  NMR spectroscopic data totally confirm the structure **8b**, see experimental part. Thus, the preparation of (2*R*,3*R*,4*S*,5*S*,6*R*)-2-(4-chlorophenylamino)-6-(hydroxymethyl)tetrahydro-2*H*-pyran-3,4,5-triol **8b** via aniline-*N*-glucoside **7b** has been successfully reproduced by us.

It was found that the 4,6-dibromohydroxyoxindole nucleus exhibit a potent activity in the differentiation of HL-60 human promyelocytic cells [3,6]. Therefore, as a part of the program aimed at developing new N-glucosylated oxindoles, we supposed, that the 3,5-dibromoaniline **12** scaffold has potential to enhance the selectivity. As obvious precursor for the synthesis of glucosylated Convolutamydines A-E **5**, 3,5-dibromoaniline **12** was prepared by initial bromination of 4-nitroaniline **9**, followed by deamination of aniline **10**, to form 3,5-dibromonitrobenzene **11**.  $\text{SnCl}_2$



reduction of the latter was found to proceed with difficulty, but when 5 equivalents of  $\text{SnCl}_2$  were used, 3,5-dibromoaniline **12** has been produced in good yield (see Scheme 2 and experimental part).



Scheme 2. Synthesis of 3,5-dibromoaniline (**12**) and its N-glucosylated derivatives **13**, **14** and **15**.

As it can be seen from Scheme 2, the reaction of **12** with (+)-*D*-glucose **1** was slow and only after 24 hrs provided a solid compound with m.p. 169-170°C. The substance obtained in 97% yield was identified as (2*R*,3*R*,4*S*,5*S*,6*R*)-2-(3,5-dibromophenylamino)-6-(hydroxymethyl)tetrahydro-2*H*-pyran-3,4,5-triol **13** on the basis of its  $^1\text{H}$  NMR spectrum, which showed in the low-field region signals at  $\delta_{\text{H}}$  6.86 ppm and  $\delta_{\text{H}}$  6.95 ppm (aromatic),  $\delta_{\text{H}}$  6.89 ppm (NH),  $\delta_{\text{H}}$  4.52 ppm,  $\delta_{\text{H}}$  4.96 ppm,  $\delta_{\text{H}}$  4.97 ppm and  $\delta_{\text{H}}$  5.05 ppm (C-6-OH, C-4-OH, C-2-OH and C-3-OH, respectively). Moreover, in its  $^1\text{H}$  spectrum the multiplets at  $\delta_{\text{H}}$  3.10-3.24 ppm (C-2-H, C-3-H, C-4-H, C-5-H, C-6-H) and triplet centred at  $\delta_{\text{H}}$  4.36 ppm (C-1-H) are present. The IR-spectrum showed a low intensity band at 892.4  $\text{cm}^{-1}$  assigned to the C-1-H scissoring of the protons in the  $\beta$ -anomer. Similarly, the  $^1\text{H}$  NMR spectrum indicated the presence of C-1-H (a triplet at  $\delta_{\text{H}}$  4.36 ppm with a splitting constant  $J=8$  Hz). However,  $^1\text{H}$  NMR spectrum shows two additional signals: a doublet attributable to three protons for methanol at  $\delta_{\text{H}}$  3.17 ppm and a quartet of one proton at  $\delta_{\text{H}}$  6.95 ppm (OH), shielded by an additional carbon, which appears in  $^{13}\text{C}$  NMR spectrum at  $\delta_{\text{C}}$  49.10 ppm. Finally, the structure of the product is considered to be **13** on the basis of its elemental analysis, as well. The formation of intermolecular complex **13** has been rationalized by considering the participation of the hydroxyl, as well as NH groups in the addition of **12** with (+)-*D*-glucose in  $\text{MeOH}$  medium.

The acetylation reaction of **13** was performed with acetic anhydride in pyridine and lead to esters **14**. The reaction was very slow (one week) and after work-up two main products in the obtained mixture were then separated by column chromatography over silica gel.

As a result, pure **14** was isolated as the least polar product with m.p. 72-73°C in 35% yield and its structure has been proved by NMR. The  $^1\text{H}$  NMR spectrum of it contains singlets at  $\delta_{\text{H}}$  2.03 ppm,  $\delta_{\text{H}}$  2.06 ppm,  $\delta_{\text{H}}$  2.07 ppm,  $\delta_{\text{H}}$  2.11 ppm (AcO groups), a doublet centered at  $\delta_{\text{H}}$  5.04 ppm ( $J=9.7$  Hz) (NH group), multiplets at  $\delta_{\text{H}}$  3.86, 4.68, 5.00, 5.04, 5.37 ppm (C2-H, C3-H, C4-H, C5-H, C6-H, correspondingly), multiplets at  $\delta_{\text{H}}$  4.14 and 4.23 ppm ( $\text{CH}_2$ ), and doublet of aromatic protons at  $\delta_{\text{H}}$  6.74 ppm (2H,  $J=1.5$ , C-2'-H, C-6'-H) and  $\delta_{\text{H}}$  7.11 ppm (1H, t,  $J=1.5$ , C-4'-H). Moreover, its formulation as an ester has been sustained by peaks in higher field  $^{13}\text{C}$  NMR spectrum at  $\delta_{\text{C}}$  72.7 ppm (C-5), 68.9 (C-4), 72.5 (C-3), 71.0 (C-2), 83.6 (C-1) and 146.7 ppm (C-1') and peaks in lower field at  $\delta_{\text{C}}$  62.3 (C-6), 115.9 (C-2', C-6'), 123.2 (C-3', C-5') and 125.1 ppm (C-4'). This resonance pattern differs markedly from that observed for the initial compound **13**. The comparative examination also suggests that four acetyl group functions should have eight peaks as well. This is consistent with the observation of signals at  $\delta_{\text{C}}$  20.6 ( $\text{CH}_3$ ), 20.65 ( $\text{CH}_3$ ), 20.7 ( $\text{CH}_3$ ), 20.8 ( $\text{CH}_3$ ), 170.7 (C=O), 169.6 (C=O), 169.9 (C=O) and 171.3 (C=O). The IR-spectrum showed bands at 1740  $\text{cm}^{-1}$ , 1588  $\text{cm}^{-1}$ , 3371  $\text{cm}^{-1}$ , 915  $\text{cm}^{-1}$  and 671  $\text{cm}^{-1}$  assigned to the COO, aromatic, NH,  $\beta$ -glucopyranoside and C-Br, respectively.

Additionally, another product was isolated, which presumably corresponded to the structure **15**. According to NMR data, the isolated product is a mixture of compounds **14** and **15** in 2:1 ratio, which has been determined by integration of the signals belonging to the acetate groups. It could be easily identified according to  $^{13}\text{C}$  NMR spectrum by the double set of signals: four C=O groups at  $\delta_{\text{C}}$  169.6, 169.9, 170.7 and 171.3 ppm for compound **14**, and three C=O groups for compound **15** at  $\delta_{\text{C}}$  169.1, 169.5 and 170.4 respectively. Similarly, double set of signals has been noted for pyranic ( $\delta_{\text{C}}$  60-83 ppm) and aromatic ( $\delta_{\text{C}}$  115-147 ppm) parts of molecules of the discussed derivative (see experimental

part). Thus, the  $^1\text{H}$  NMR spectrum shows multiplets at  $\delta_{\text{H}}$  3.85-3.90, 4.01-4.30, 4.99-5.07, 5.16-5.20 and 5.30-5.46 ppm, which are characteristic for pyranic part (CH and OH), two doublets at  $\delta_{\text{H}}$  6.74 and 7.00 ppm and two triplets centered at  $\delta_{\text{H}}$  7.10 and 7.14 ppm (aromatic), four singlets at  $\delta_{\text{H}}$  2.04, 2.05, 2.06 and 2.07 ppm for compound **14**, a singlet at  $\delta_{\text{H}}$  2.03 ppm and a doublet centered at  $\delta_{\text{H}}$  2.08 ppm for compound **15**, respectively.

Catalysis by pyridine is of the nucleophilic type and it is known that 4-(N,N-dimethylamino)pyridine is a better catalyst when pyridine fails. Indeed, compound **13** readily undergoes reaction with acetic anhydride under analogous conditions in presence 4-(N,N-dimethylamino)pyridine to yield up to 90% compound **14**.

## Conclusions

The present work demonstrates that interaction of 4-chloro- and 3,5-dibromo- substituted anilines with (+)-*D*-glucose affords N-glycosylated adducts **7b** and **13** as  $\beta$ -anomers. The position and steric course of further esterification are catalytically dependent. We confirmed that in the case of 4-chloro substituted aniline reaction with  $\text{Ac}_2\text{O}$  in Py occurs mainly to give tetra-acetate **8b**. On the contrary, reaction of 3,5-dibromo substituted aniline gives a mixture of adducts **14** and **15** in a 2:1 ratio with overall yield 65%. In the case when the reaction was catalysed by 4-(N,N-dimethylamino)pyridine only compound **14** was obtained in 80% overall yield. The structures of all new compounds **13**, **14** and **15**, including configurations of anomeric carbon atoms, were characterized through IR and NMR spectroscopic methods.

## Experimental

All used solvents were of reagent quality, and all commercial reagents were used without additional purification. Removal of all solvents was carried out under reduced pressure. Analytical TLC plates Silufol<sup>®</sup> UV-254 (Silpearl on aluminum foil, Czecho-Slovakia) were used and spots were detected under UV-lamp with wavelength 254 nm.

M. p.s (uncorrected) were determined on a Boetius apparatus.

IR spectra were recorded on a Spectrum 100 FT-IR spectrophotometer (Perkin - Elmer) using the universal ATR sampling accessory.  $^1\text{H}$  and  $^{13}\text{C}$  NMR spectra were registered in  $\text{CDCl}_3$  and  $\text{DMSO}-d_6$  2-% solution on a "Bruker-Avance III" (400.13 and 100.61 MHz) spectrometer.

### General procedure for the synthesis of N-glucosylated anilines **7b** and **13**.

To a solution of (+)-*D*-glucose **1** (2g, 0.011 mol) in 25 mL of absolute methanol corresponding aniline (**6b** or **12**) (0.013 mol) was added. The mixture was refluxed for 24 hours. After completion of the reaction (TLC control, solvent system 2% MeOH in  $\text{CH}_2\text{Cl}_2$ ) the mixture was stored in refrigerator at sub-zero temperature so long, as white volume is being precipitated. The precipitate was filtered and washed with methanol and dried at room temperature.

**(2R,3R,4R,5R,6R)-2-(4-chlorophenylamino)-6-(hydroxymethyl)tetrahydro-2H-pyran-3,4,5-triol 7b.** White solid. Yield 95 %. M. p. 154-156°C (MeOH).  $[\alpha]_{\text{D}}^{20}$  -41.0 (c 0.068, DMSO). IR-spectra ( $\text{v}/\text{cm}^{-1}$ ): 3271.5, 3209.1 (OH), 1523.4 (NH), 883.8 (C-1-H), 683.3 (C-Cl).  $^1\text{H}$  NMR (400 MHz,  $\text{DMSO}-d_6$ ,  $\delta$ , ppm,  $J/\text{Hz}$ ): 3.07-3.27 (4H, m, C-2-H, C-3-H, C-4-H, C-5-H), 3.39-3.45 (1H, m, C-6-H), 3.61-3.66 (1H, m, C-6-H), 4.30-4.34 (1H, t, C-1-H,  $J=8$ ), 4.44-4.47 (1H, t, C-6-OH,  $J=5.8$ ), 4.88-4.90 (1H, d, C-4-OH,  $J=5.4$ ), 4.92-4.93 (1H, d, C-2-OH,  $J=5.2$ ), 5.00-5.02 (1H, d, C-3-OH,  $J=4.7$ ), 6.46-6.48 (1H, d, NH,  $J=7.5$ ), 6.67-6.69 (2H, d, C-2'-H, C-6'-H,  $J=8.8$ ), 7.10-7.12 (2H, d, C-3'-H, C-5'-H,  $J=8.8$ ).  $^{13}\text{C}$  NMR (100.6 MHz,  $\text{DMSO}-d_6$ ): 61.4 (C-6), 70.6 (C-4), 73.5 (C-2), 77.8 (C-3), 78.1 (C-5), 85.3 (C-1), 115.0 (C-2', C-6'), 120.7 (C-4'), 128.9 (C-3', C-5'), 146.8 (C-1'). Calculated, %: C 49.75; H 5.57; N 4.83.  $\text{C}_{12}\text{H}_{16}\text{ClNO}_5$ . Found, %: C 49.80; H 5.60; N 4.80.

**(2R,3R,4S,5S,6R)-2-(3,5-dibromophenylamino)-6-(hydroxymethyl)tetrahydro-2H-pyran-3,4,5-triol 13.** White solid. Yield 97 %. M. p. 169-170°C (MeOH).  $[\alpha]_{\text{D}}^{20}$  -62.40 (c 0.05, DMSO). IR-spectra ( $\text{v}/\text{cm}^{-1}$ ): 3367.5, 3210.1, 3073.2 (OH); 1518.0 (NH); 892.4 (C-1-H), 668.2 (C-Br), 1574.5 (aromatics), 3367-3073 (OH).  $^1\text{H}$  NMR (400 MHz,  $\text{DMSO}-d_6$ ,  $\delta$ , ppm,  $J/\text{Hz}$ ): 3.40-3.65 (1H, ddd,  $J=11.8, 5.8, 1.9$ , C-6-H), 3.1 (2H, m, C-4-H, C-2-H), 3.24 (2H, m, C-5-H, C-3-H), 3.17 (3H, d,  $J=5.2$ ,  $\text{CH}_2\text{OH}$ ), 4.18 (1H, q,  $J=5.2$ ,  $\text{CH}_2\text{OH}$ ), 4.36 (1H, t,  $J=8$ , C-1-H), 4.52 (1H, t,  $J=5.8$ , C-6-OH), 4.96, (1H, d,  $J=1.7$ , C-4-OH), 4.97 (1H, d,  $J=1.4$ , C-2-OH), 5.05 (1H, d,  $J=4.8$ , C-3-OH), 6.89 (1H, d,  $J=7.8$ , NH), 6.86 (2H, d,  $J=7.6$ , C-2'-H, C-6'-H), 6.95 (1H, t,  $J=1.6$ , C-4'-H).  $^{13}\text{C}$  NMR (100.6 MHz,  $\text{DMSO}-d_6$ ): 49.1 (MeOH), 61.3 (C-6), 70.7 (C-4), 73.5 (C-2), 77.8 (C-3), 77.9 (C-5), 84.5 (C-1), 115.1 (C-2' and C-6'), 121.5 (C-4'), 123.1 (C-3' and C-5'), 150.7 (C-1'). Calculated, %: C 34.89; H 3.66; N 3.39.  $\text{C}_{12}\text{H}_{15}\text{Br}_2\text{NO}_5$ . Found, %: C 34.94; H 3.64; N 3.41.

### Procedure for the synthesis of compound **8b**.

The anilide **7b** is maximally dissolved in dry pyridine under stirring (for every hydroxyl group 1.8-2.0 eq. of pyridine are used) and cooled in an ice bath to 0°C. Then, freshly distilled acetic anhydride is rapidly added (for every hydroxyl group 1.5-1.6 eq. of acetic anhydride are used). Stirring is continued at the same temperature until a homogeneous solution appeared (about 3 hours). The mixture was hold for 24-48 hours in a refrigerator without stirring. After completion of the

reaction (TLC control, system hexane-ethyl acetate 4:1), the mixture was poured into ice-water (1:2) and extracted with ethyl acetate (4x30 mL). The combined organic phases were washed with sodium hydrogen carbonate solution, water and brine, dried over anhydrous sodium sulfate and the solvent was removed under reduced pressure. The resulting white solid mass was recrystallised from methanol. The bittern was evaporated and recrystallised again. The obtained product is white solid.

**(2R,3R,4S,5R,6R)-2-(acetoxymethyl)-6-(4-chlorophenylamino)tetrahydro-2H-pyran-3,4,5-triyl triacetate 8b.** White solid. Yield 97 %. M. p. 146-149°C (MeOH).  $[\alpha]_D^{20}$  -48.6 (c 0.076, CHCl<sub>3</sub>). IR-spectra (v/cm<sup>-1</sup>): 1059.5, 1180.7 (C-O-C), 1511.7 (NH), 878.9 (C-1-H), 688.4 (C-Cl). <sup>1</sup>H NMR (400 MHz, DMSO-d<sub>6</sub>, δ, ppm, J/Hz): 1.95 (3H, s, CH<sub>3</sub>CO), 1.95 (3H, s, CH<sub>3</sub>CO), 1.97 (3H, s, CH<sub>3</sub>CO), 2.00 (3H, s, CH<sub>3</sub>CO), 4.08-4.18 (2H, m, C-6), 4.88-4.93 (2H, ddd, C-5-H and C-4-H, J=0.9; 1.6; 2.1), 3.93-3.97 (1H, dd, C3-H, J=1.8; 1.8), 5.18-5.22 (1H, t, C-3-H, J=9.4), 5.32-5.36 (1H, t, C-1-H, J=9.5), 6.71 (1H, d, NH, J=9.8), 6.75 (2H, d, C-2'-H and C-6'-H, J=8.9), 7.14 (2H, d, C-3'-H and C-5'-H, J=8.8). <sup>13</sup>C NMR (100.6 MHz, DMSO-d<sub>6</sub>): 20.8 (CH<sub>3</sub>), 20.8 (CH<sub>3</sub>), 20.9 (CH<sub>3</sub>), 20.9 (CH<sub>3</sub>), 62.3 (C-6), 68.7 (C-4), 71.2 (C-3), 71.5 (C-5), 73.7 (C-2), 82 (C-1), 115.8 (C-2' and C-6'), 122.0 (C-4'), 129 (C-3' and C-5'), 145.5 (C-1'), 169.6 (C=O), 169.8 (C=O), 170.1 (C=O), 170.4 (C=O). Calculated, %: C 52.46; H 5.28; N 3.06. C<sub>20</sub>H<sub>24</sub>ClNO<sub>9</sub>. Found, %: C 52.52; H 5.30; N 3.10.

#### General procedure for the synthesis of compounds 14 and 15.

**Method A:** The anilide **13** is maximally dissolved in dry pyridine under stirring (for every hydroxyl group 1.8-2.0 eq. of pyridine are used) and cooled in an ice bath to 0°C. Then, freshly distilled acetic anhydride is rapidly added (for every hydroxyl group 1.5-1.6 eq. of acetic anhydride are used). Stirring is continued at the same temperature until a homogeneous solution appeared (about 3 hours). The mixture was hold for 24-48 hours in a refrigerator without stirring. After completion of the reaction (TLC control, system hexane-ethyl acetate 4:1), the mixture was poured into ice-water (1:2) and extracted with ethyl acetate (4x30 mL). The combined organic phases were washed with sodium hydrogen carbonate solution, water and brine, dried over anhydrous sodium sulfate and the solvent was removed under reduced pressure. The resulting oily mass was purified by column chromatography on silica gel, using as eluent hexane-ethyl acetate (6:1 to 3:1).

**Method B:** The anilide **13** is maximally dissolved in dry pyridine under stirring. For every hydroxyl group is used 1.8-2.0 eq. of pyridine, and cooled in an ice bath to 0°C. Then, freshly distilled acetic anhydride is added rapidly. For every hydroxyl group is used 1.5-1.6 eq., of acetic anhydride. Then 10 mol% of DMAP (catalyst) was added and stirring was continued at the same temperature until a homogeneous solution (about 3 hours). The mixture was hold for one week in a refrigerator without stirring. After completion of the reaction (TLC control, system hexane-ethyl acetate 4:1), the mixture was poured into ice-water (1:2) and extracted with ethyl acetate (4x30 mL). The combined organic phases were washed with sodium hydrogen carbonate solution, water and brine, dried over anhydrous sodium sulfate and the solvent was removed under reduced pressure. The resulting oily was purified by column chromatography on silica gel, using as eluent hexane-ethyl acetate (6:1 to 3:1).

**(2R,3R,4R,5R,6R)-2-(Acetoxymethyl)-6-(3,5-dibromophenylamino)tetrahydro-2H-pyran-3,4,5-triyl triacetate 14.** White solid. Yield 60 %. M. p. 72-73°C (MeOH).  $[\alpha]_D^{16}$  -38.45 (c 0.098, CHCl<sub>3</sub>). IR-spectra (v/cm<sup>-1</sup>): 1083.8, 1059.5 (C-O-C); 1517.3 (NH); 915.3 (C6-H), 671.2 (C-Br). <sup>1</sup>H NMR (400 MHz, CDCl<sub>3</sub>, δ, ppm, J/Hz): 2.03 (3H, s, CH<sub>3</sub>CO), 2.06 (3H, s, CH<sub>3</sub>CO), 2.07 (3H, s, CH<sub>3</sub>CO), 2.11 (3H, s, CH<sub>3</sub>CO), 3.86 (1H, ddd, J=10.1, 6.3, 2.1, C-5-H), 4.14 (1H, dd, J=12.1, 2.1, C-6-H), 4.23 (1H, dd, J=12.1, 6.3, C-6-H), 4.68 (1H, t, J=8.8, C-1-H), 5.00 (1H, t, J=9.1, C-2-H), 5.04 (1H, t, J=9.7, C-4-H), 5.04 (1H, d, J=8.8, NH), 5.37 (1H, t, J=9.1, C-3-H), 6.74 (2H, d, J=1.5, C-2'-H, C-6'-H), 7.11 (1H, t, J=1.5, C-4'-H). <sup>13</sup>C NMR (100.6 MHz, CDCl<sub>3</sub>): 20.6 (CH<sub>3</sub>), 20.6 (CH<sub>3</sub>), 20.7 (CH<sub>3</sub>), 20.8 (CH<sub>3</sub>), 62.3 (C-6), 68.8 (C-4), 71 (C-2), 72.5 (C-3), 72.7 (C-5), 83.6 (C-1), 115.9 (C-2', C-6'), 125.1 (C-4'), 123.2 (C-3', C-5'), 146.7 (C-1'), 169.6 (C=O), 169.9 (C=O), 170.7 (C=O), 171.3 (C=O). Calculated, %: C 41.33; H 3.99; N 2.41. C<sub>20</sub>H<sub>23</sub>Br<sub>2</sub>NO<sub>9</sub>. Found, %: C 41.40; H 4.01; N 2.39.

**Mixture of (2R,3R,4R,5R,6R)-2-(Acetoxymethyl)-6-(3,5-dibromophenylamino)tetrahydro-2H-pyran-3,4,5-triyl triacetate 14 and (2R,3R,4R,5R,6R)-2-(Acetoxymethyl)-6-(3,5-dibromophenylamino)-5-hydroxytetrahydro-2H-pyran-3,4-diyl diacetate 15 in ratio 2:1.**  $[\alpha]_D^{16}$  -29.44 (c 0.119, CHCl<sub>3</sub>). White solid. Yield 32 %.

Minor compound has been identified as **15**. <sup>1</sup>H NMR (400 MHz, CDCl<sub>3</sub>, δ, ppm, J/Hz): 2.03 (s, CH<sub>3</sub>CO), 2.04 (s, CH<sub>3</sub>CO), 2.05 (s, CH<sub>3</sub>CO), 2.06 (s, CH<sub>3</sub>CO), 2.07 (s, CH<sub>3</sub>CO), 2.08 (d, CH<sub>3</sub>CO), 3.85-3.90 (m), 4.04-4.10 (m), 4.11-4.13 (d, J=8), 4.15-4.16 (t, J=4), 4.21-4.30 (m), 5.01-5.02 (d, J=4.5), 5.03-5.04 (d, J=4.7), 5.16-5.20 (kv), 5.30-5.32 (d, J=5.2), 5.37 (t, J=9.4), 6.74 (2H, d, J=1.6). 6.99 (2H, d, J=1.6), 7.10 (2H, d, J=1.6), 7.14 (1H, d, J=1.6). <sup>13</sup>C NMR (100.6 MHz, CDCl<sub>3</sub>): 20.6-20.8 (CH<sub>3</sub>), 61.9, 62.2, 66.4, 68.5, 68.7, 69.5, 70.2, 71.1, 72.6, 72.6, 79.7, 83.5, (C1-C6), 115.9, 116.1 (C-2', C-6'), 123.4, 123.4 (C-4'), 125.1, 125.4 (C-3', C-5'), 146.7 147.2 (C-1'), 169.1, 169.5, 169.6, 169.9, 170.4, 170.7, 171.3 (C=O).

### 2,6-Dibromo-4-nitroaniline 10

To a heated solution (up to 65°C) of 4-nitroaniline **9** (11 g, 0.08 mol) in 100 mL of glacial acetic acid under stirring is added drop wise a solution of bromine (26 g, 0.16 mol) in 60 mL of glacial acetic acid for 2 hours. After dropping of all bromine, the mixture was stirred for another 1.5 hours at the same temperature. The mixture was allowed to cool up to room temperature, next it was poured into a mixture, consisting of 500 mL of water and 250 g of ice and hold for 1.5 hours. The precipitate was filtered and washed 3 times with water to remove residual of acetic acid and dried at 100°C, getting 22 g of product (melting at 199-200°C). Yield 95%. Further recrystallization from ethylene glycol monomethyl gives yellow-green crystals (prisms). Yellow-green prisms. M. p. 201-202°C. IR-spectra (v/cm<sup>-1</sup>): 3417, 1564 (NH<sub>2</sub>), 1525, 1389 (NO<sub>2</sub>), 1599 (aromatics), 695 (C-Br). <sup>1</sup>H NMR (400 MHz, DMSO-d<sub>6</sub>, δ, ppm, J/Hz): 6.69 (2H, s, NH<sub>2</sub>), 8.22 (2H, s, C3-H and C5-H). <sup>13</sup>C NMR (100.6 MHz, CDCl<sub>3</sub>): 105.77 (C-Br), 128.3 (C-3 and C-5), 136.9 (C-4), 149.5 (C-1). Calculated, %: C 24.35; H 1.36; N 9.47. C<sub>6</sub>H<sub>4</sub>Br<sub>2</sub>N<sub>2</sub>O<sub>2</sub>. Found, %: C 24.42; H 1.34; N 9.51.

### 3,5-Dibromonitrobenzene 11

To a heated up to 70°C solution of 2,6-dibromo-4-nitroaniline **10** (20 g, 0.067 mol) in 160 mL of ethanol, concentrated sulfuric acid (11 mL) is slowly added under stirring until the mixture become a homogeneous system. Next, sodium nitrite (10 g, 0.14 mol) is added in small portions, and the mixture is stirred at the same temperature about an hour, until precipitation. After that, the heating was stopped and the mixture was stirred before room temperature. Then 300 mL of water was added, the precipitate was filtered and washed 3 times with water to remove residual sodium nitrite. Further recrystallization from ethanol gives 14 g of product **11**. The product is an orange solid. Yield 80%. M. p. 110°C (EtOH). IR-spectra (v/cm<sup>-1</sup>): 1528, 1336 (NO<sub>2</sub>), 650 (C-Br). <sup>1</sup>H NMR (400 MHz, CDCl<sub>3</sub>, δ, ppm, J/Hz): 7.98-7.99 (1H, t, J=1.6), 8.31 (2H, d, J=1.6). <sup>13</sup>C NMR (100.6 MHz, CDCl<sub>3</sub>): 123.47 (C-2 and C-6), 125.58 (C-Br), 140.05 (C-4), 149 (C-1). Calculated, %: C 25.65; H 1.08; N 4.99. C<sub>6</sub>H<sub>3</sub>Br<sub>2</sub>NO<sub>2</sub>. Found, %: C 25.72; H 1.06; N 5.02.

### 3,5-Dibromoaniline 12

To a solution of 3,5-dibromonitrobenzene **11** (10g, 0.035 mol) in a 1:1 mixture of ethanol and THF (200 mL) tin(II) chloride dihydrate (40g, 0.175 mol) was added portionwise under stirring. The mixture was stirred at room temperature for 20 hours. After reaction solvents were removed *in vacuo*, 250 mL of water was added into remained orange liquid and dry alkali is added under stirring. Stirring was continued for 2 hours in strongly alkaline medium (pH 11-12). Next, the mixture was poured into separatory funnel, extra 150 mL of water was added. The reaction was extracted with diethyl ether (4x40 mL), the combined organic phases were washed with water to remove residues of alkali, dried over anhydrous sodium sulfate and the solvent was removed. The resulting brown mass was purified by column chromatography on silica gel, using as eluent system petroleum ether-ethyl acetate (12:1). As a result, 7.5 g of product **12** have been obtained. Light brown solid. Yield 80 %. M. p. 55-56 °C. IR-spectra (v/cm<sup>-1</sup>): 3417, 1624 (NH<sub>2</sub>), 1581 (aromatics), 670 (C-Br). <sup>1</sup>H NMR (400 MHz, CDCl<sub>3</sub>, δ, ppm, J/Hz): 3.78 (2H, s, NH<sub>2</sub>), 6.75 (2H, d, C2-H, C6-H, J=1.5), 7.02 (1H, t, C4-H, J=1.5). <sup>13</sup>C NMR (100.6 MHz, CDCl<sub>3</sub>): 116.51 (C-2 and C-6), 123.36 (C-Br), 123.70 (C-4), 148.64 (C-1). Calculated, %: C 28.72; H 2.01; N 5.58. C<sub>6</sub>H<sub>3</sub>Br<sub>2</sub>N. Found, %: C 28.77; H 2.00; N 5.60.

### Acknowledgments

Author thanks Prof. Macaev F. and Dr. Barba A. for helpful discussions.

### References

1. Kleeblatt, D.; Siyo, B.; Hein, M.; Iaroshenko, V.O.; Iqbal, J.; Villinger, A.; Langer, P. Synthesis of N,N'-diglycosylated isoindigos. *Organic and Biomolecular Chemistry*, 2013, 11, pp. 886-895.
2. Erben, F.; Kleeblatt, D.; Sonneck, M.; Hein, M.; Feist, H.; Fahrenwaldt, T.; Fischer, C.; Matin, A.; Iqbal, J.; Plötz, M.; Eberlee, J.; Langer, P. Synthesis and antiproliferative activity of selenoindirubins and selenoindirubin-N-glycosides. *Organic and Biomolecular Chemistry*, 2013, 11, pp. 3963-3978.
3. Kamano, Y.; Zhang, H.P.; Ichihara, Y.; Kizu, H.; Komiyama, K.; Pettit, G. R. Convolutamidine A, a novel bioactive hydroxyoxindole alkaloid from marine bryozoans *Amathia convoluta*. *Tetrahedron Letters*, 1995, 36, pp. 2783-2784.
4. Maskey, R.P.; Grün-Wollny, I.; Fiebig, H.H.; Laatsch, H. Akashins A, B, and C: Novel Chlorinated Indigoglycosides from *Streptomyces* sp. GW 48/1497. *Angewandte Chemie International Edition*, 2002, 41, pp. 597-599.
5. Maskey, R.P.; Grün-Wollny, I.; Laatsch, H. Isolation and structure elucidation of diazaquinomycin C from a terrestrial *Streptomyces* sp. and confirmation of the akashin structure. *Natural Product Research*, 2005, 19, pp. 137-142.
6. Zhang, H.P.; Kamano, Y.; Ichihara, Y.; Kizu, H.; Komiyama, K.; Itokawa, H.; Pettit, G.R. Isolation and structure of convolutamidines B -D from marine bryozoans *Amathia convoluta*. *Tetrahedron*, 1995, 51, pp. 5523-5528.



# A SEQUENTIAL DUAL CLEAVAGE OF THE ARYLSULFAMATE LINKER TO PROVIDE BOTH SULFAMATE AND PHENOL DERIVATIVES

Diane Fournier, Liviu Ciobanu, Donald Poirier\*

Laboratory of Medicinal Chemistry, CHU de Québec – Research Center (CHUL, T4), 2705 Laurier Boulevard, Québec (Québec), G1V 4G2, Canada

\*e-mail: donald.poirier@crchul.ulaval.ca; phone: 1(418) 654-2296; fax: 1(418) 654-2298

**Abstract.** Tyramine sulfamate was linked to the trityl chloride resin and this polymeric solid support used to introduce two levels of molecular diversity by formation of peptide bonds. A dual cleavage strategy next generated in a sequential way (without resin split) two different types of compounds (phenol and arylsulfamate derivatives), which are therapeutically attractive types of compounds. Here, we used tyramine as a general scaffold, but other arylsulfamate derivatives could be judiciously used to extend the nature of synthesized compounds.

**Keywords:** solid-phase synthesis, linker, sulfamate, phenol, library.

Received: November 2015/ Revised final: November 2015/ Accepted: November 2015

## Introduction

Sulfamate derivatives have been known for several years as artificial sweeteners (cyclamates) [1], but therapeutic applications are numerous and have significantly broadened in recent years [2,3]. They were first known as anticonvulsants and the drug topimarat, discovered in 1980, is still used in clinical settings for the treatment of refractory epilepsy [4]. Sulfamate derivatives were also found to be potent inhibitors of carbonic anhydrases (CAs) [5,6]. This could explain the high oral availability of these drugs since they were shown to bind reversibly to CA II in red blood cells, which allows them to avoid degradation in the liver. This property could lead to new therapeutic approaches against cancer because CA IX and CA XII are highly expressed in tumours which need them to maintain pH and eliminate CO<sub>2</sub>. Arylsulfamates have shown high potency as inhibitors of steroid sulfatase (STS) [7-10], an important therapeutic target for the treatment of hormone-sensitive diseases such as breast, endometrium and prostate cancers [11,12] in addition to acne and alopecia [13]. STS inhibitors could also have potential in the treatment of Alzheimer's disease through an increase in the level of dehydroepiandrosteronesulfate, a substrate of STS in the brain [14].

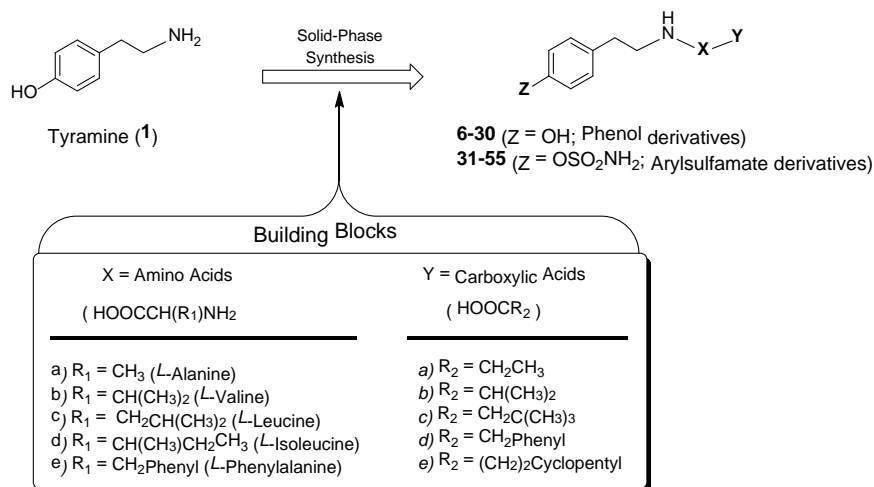


**Figure 1. Building blocks (amino acids and carboxylic acids) used in the elaboration of libraries of diversified phenol derivatives 6-30 and arylsulfamate derivatives 31-55.**

On the other hand, phenol derivatives are present in many biologically active molecules. For example, many natural antioxidants, such as flavonoids and polyphenols, contain the phenol moiety. These compounds are known to exert a protective effect on cardiovascular health through the lowering of low-density lipoproteins. Many similar compounds were synthesized with the hope of optimizing such properties [15]. Phenols are also very abundant in essential oils, contributing to their aroma and antimicrobial properties [16]. Small phenolic molecules have shown potential as analgesics [17] and

some have been tested as non-steroidal anti-inflammatory drugs [18] for their potential anti-rejection properties. Moreover, the phenolic group is essential in selective-estrogen receptor modulator drugs [19], which are used in the treatment of hormone-sensitive breast cancer and osteoporosis. Phenol derivatives are also known as inhibitors of  $17\beta$ -hydroxysteroid dehydrogenases [20-22] and reversible inhibitors of STS [23,24] (although less potent than sulfamate derivatives).

The ability to generate libraries of phenol and arylsulfamate derivatives from the same resins, through rapid parallel synthesis, is thus of high interest for medicinal chemists. Herein, we describe a strategy (Figures 1 and 2) to generate two different kinds of compounds (sulfamate and phenol derivatives) from commercially available building blocks (amino acids and carboxylic acids) and the multidetachable sulfamate linker [25].

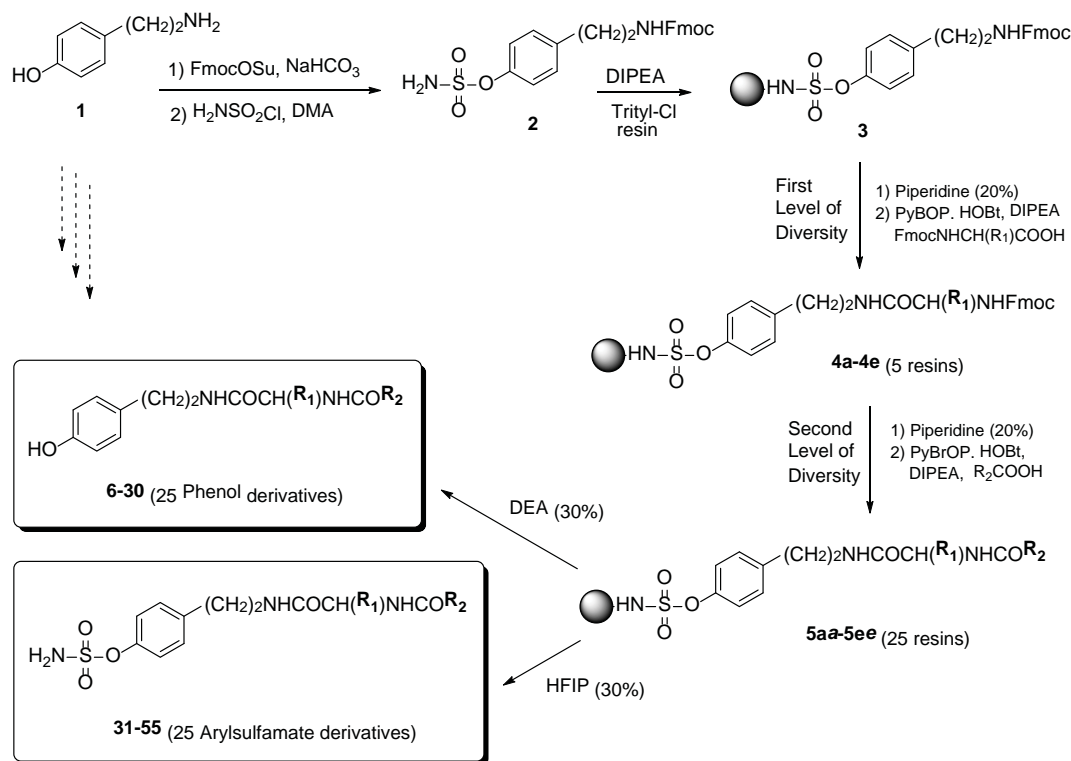


**Figure 2. Solid-phase chemical synthesis of libraries of phenol and arylsulfamate derivatives using the sequential approach of cleavage.** See Figure 1, Table 1 and Table 2 for the building blocks used in the preparation of libraries and the representation of all library members.

## Results and discussion

### Synthesis of libraries

The solid-phase strategy providing two types of diversified molecules, the phenol and sulfamate derivatives, was represented in Figure 2. The primary amine of tyramine (**1**) was first protected as a 9-fluorenylmethoxycarbonyl (Fmoc) derivative, whereas the phenol group was next transformed by the sulfamoyl chloride in *N,N*-dimethylacetamide (DMA) used as base and solvent [26] to provide **2**. This arylsulfamate was linked to a polystyrene solid support by a reaction with trityl chloride resin in presence of diisopropylethylamine (DIPEA), thus providing the resin **3**. The mass increase suggested a quantitative yield for the coupling reaction. The characteristic band of Fmoc (1696 cm<sup>-1</sup>) and sulfamoyl (1350 and 1156 cm<sup>-1</sup>) groups were observed in FTIR spectra. A gel-phase <sup>13</sup>C NMR analysis of resin **3** showed all carbon signals associated with tyramine moiety. Finally, a micro-cleavage under acid conditions released the sulfamate **2**. All these results confirmed the presence of a tyramine residue linked on the trityl resin and consequently the formation of **3**, the precursor of all library members.

The synthesis of libraries started by removing the Fmoc protecting group of **3** to generate the corresponding free primary amine, which was submitted to a coupling reaction using benzotriazol-1-yl-oxy-tris-pyrrolidino-phosphonium hexafluorophosphate (PyBOP), 1-hydroxybenzotriazole (HOBt) and an amino acid. A series of five amino acids (Figure 1) protected as *N*-Fmoc derivative was the key element used to introduce the first level of molecular diversity. The formation of resins **4a-4e** was supported by the presence in FTIR spectra of a new amide (NC=O) band in the range of 1656-1660 cm<sup>-1</sup>. To introduce the second level of diversity, the five resins **4a-4e** were split in 5 groups (25 samples) and submitted to a sequence of two steps, the cleavage of Fmoc group and the coupling of five carboxylic acids using PyBrOP and HOBt, thus producing resins **5a-5ee**.



**Cleavage strategy (recovering the final compounds)**

The sequential dual cleavage consisted in performing, on the same resin sample, first a partial release of a phenol derivative with a nucleophile, and next a cleavage of the remaining linked material with an acid to obtain an arylsulfamate derivative. This approach avoids the step of splitting the resin, which is time-consuming.

The type of cleavage we call «nucleophilic» here is not strictly speaking nucleophilic, but this type of reaction was studied in detail by Spillane *et al.* [27-30]. The mechanism is a two-step base-catalysed E1cb-type mechanism that probably involves a bimolecular complex between a base and the sulfamate NH as intermediate, which is then attacked by a nucleophile to release the phenol. In this case, we carried out an incomplete nucleophilic cleavage at room temperature with 30% of diethylamine (DEA), which released about 50% of the linked material as the phenol derivatives **6-30** (Table 1).

Table 1

**Representation of all library members (phenol derivatives 6-30).**

General structure					
$R_2^{**}$ / $R_1^*$	$\text{CH}_2\text{CH}_3$ (Propionic Acid) <i>a</i>	$\text{CH}(\text{CH}_3)_2$ ( <i>i</i> -Butyric Acid) <i>b</i>	$\text{CH}_2\text{C}(\text{CH}_3)_3$ ( <i>t</i> -Butylacetic Acid) <i>c</i>	$\text{CH}_2$ -Phenyl (Phenylacetic Acid) <i>d</i>	$(\text{CH}_2)_2$ -Cyclopentyl (3-Cyclopentyl-propionic Acid) <i>e</i>
$\text{CH}_3$ (Alanine) <i>a</i>	# 6 $\text{C}_{14}\text{H}_{20}\text{N}_2\text{O}_3$ W: 8.9 mg CY: 59% P: 48%	# 7 $\text{C}_{15}\text{H}_{22}\text{N}_2\text{O}_3$ W: 9.0 mg CY: 56%	# 8 $\text{C}_{17}\text{H}_{26}\text{N}_2\text{O}_3$ W: 16.7 mg CY: 98%	# 9 $\text{C}_{19}\text{H}_{22}\text{N}_2\text{O}_3$ W: 12.2 mg CY: 64%	# 10 $\text{C}_{19}\text{H}_{28}\text{N}_2\text{O}_3$ W: 10.4 mg CY: 55% P: 60%
$\text{CH}(\text{CH}_3)_2$ (Valine) <i>b</i>	# 11 $\text{C}_{16}\text{H}_{24}\text{N}_2\text{O}_3$ W: 10.5 mg CY: 62%	# 12 $\text{C}_{17}\text{H}_{26}\text{N}_2\text{O}_3$ W: 9.7 mg CY: 57% P: 82%	# 13 $\text{C}_{19}\text{H}_{30}\text{N}_2\text{O}_3$ W: 18.4 mg CY: 97%	# 14 $\text{C}_{21}\text{H}_{26}\text{N}_2\text{O}_3$ W: 12.9 mg CY: 64%	# 15 $\text{C}_{21}\text{H}_{32}\text{N}_2\text{O}_3$ W: 10.9 mg CY: 55% P: 81%
$\text{CH}_2\text{CH}(\text{CH}_3)_2$ (Leucine) <i>c</i>	# 16 $\text{C}_{17}\text{H}_{26}\text{N}_2\text{O}_3$ W: 11.9 mg CY: 70% P: 39%	# 17 $\text{C}_{18}\text{H}_{28}\text{N}_2\text{O}_3$ W: 14.8 mg CY: 82%	# 18 $\text{C}_{20}\text{H}_{32}\text{N}_2\text{O}_3$ W: 15.9 mg CY: 80% P: 47%	# 19 $\text{C}_{22}\text{H}_{28}\text{N}_2\text{O}_3$ W: 15.5 mg CY: 74%	# 20 $\text{C}_{22}\text{H}_{34}\text{N}_2\text{O}_3$ W: 13.1 mg CY: 77%
$\text{CH}(\text{CH}_3)\text{CH}_2\text{CH}_3$ (Isoleucine) <i>d</i>	# 21 $\text{C}_{17}\text{H}_{26}\text{N}_2\text{O}_3$ W: 8.7 mg CY: 51%	# 22 $\text{C}_{18}\text{H}_{28}\text{N}_2\text{O}_3$ W: 10.2 mg CY: 57% P: 79%	# 23 $\text{C}_{20}\text{H}_{32}\text{N}_2\text{O}_3$ W: 19.3 mg CY: 96%	# 24 $\text{C}_{22}\text{H}_{28}\text{N}_2\text{O}_3$ W: 17.5 mg CY: 83% P: 48%	# 25 $\text{C}_{22}\text{H}_{34}\text{N}_2\text{O}_3$ W: 10.9 mg CY: 52%
$\text{CH}_2$ -Phenyl (Phenylalanine) <i>e</i>	# 26 $\text{C}_{20}\text{H}_{24}\text{N}_2\text{O}_3$ W: 14.4 mg CY: 76%	# 27 $\text{C}_{21}\text{H}_{26}\text{N}_2\text{O}_3$ W: 16.7 mg CY: 84%	# 28 $\text{C}_{23}\text{H}_{30}\text{N}_2\text{O}_3$ W: 19.7 mg CY: 90% P: 52%	# 29 $\text{C}_{25}\text{H}_{26}\text{N}_2\text{O}_3$ W: 15.9 mg CY: 69% P: 68%	# 30 $\text{C}_{25}\text{H}_{32}\text{N}_2\text{O}_3$ W: 14.4 mg CY: 63%

W: Weight of released compound; CY: crude yield; P: purity determined by quantitative  $^1\text{H}$  NMR.

(\*)  $R_1$ : The residue of amino acids used as building blocks.

(\*\*)  $R_2$ : The residue of carboxylic acids used as building blocks.

The acidic cleavage probably proceeds through protonation of the sulfamate NH and subsequent formation of a trityl anion on the resin (which takes on an intense red color). In the first assays, the acidic cleavage used to produce the arylsulfamate derivative was done using a 5% trifluoroacetic acid (TFA) solution in  $\text{CH}_2\text{Cl}_2$ , which gave better yields with shorter reaction times, but lower purity. Since we intended our solid-phase synthesis products for screening purposes, and thus wanted rapid production with no purification step, milder acid conditions (30% hexafluoroisopropanol (HFIP) in  $\text{CH}_2\text{Cl}_2$ ) were preferred to generate the arylsulfamate derivatives **31-55** (Table 2).

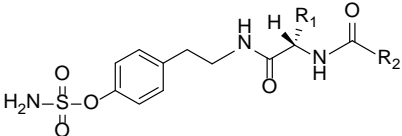
After we generated two libraries of phenol derivatives (Table 1) and arylsulfamate derivatives (Table 2), all the library members were analysed by thin-layer chromatography and showed a good homogeneity (mostly one spot). A sampling of both libraries (10 members by library) was performed and the compounds tested by NMR analysis. We chose quantitative NMR over HPLC for purity assessment because it allows the detection of the real quantity of the

desired product in a given mass even if an impurity is insoluble or invisible to NMR. On the contrary, since purity assessment with HPLC depends on what is visible to the detector, insoluble or detector-invisible material is not taken into account, and thus artificially high purity values are read.

It should be noted that no purification steps whatsoever are used in the procedure described above. Nonetheless, we think the average purity of the products (phenol derivatives: 39 to 82%, average 60%; arylsulfamate derivatives: 38 to 66%, average 53%) could be increased by optimizing the coupling steps. Moreover, we noticed that some resins developed a red-brownish color after an amino-acid coupling cycle, and this color could not be washed away. After cleavage, the products showed low purity. Impurities were sometimes visible on  $^1\text{H}$  NMR spectra as direct capping (resulting from incomplete amino-acid coupling) or phosphorus derivatives (from PyBOP and PyBrOP coupling agents). These results do not seem to be systematic since different amino acids are affected in different trials. They were not observed in two compounds previously generated as models, as in those cases average purity of the crude product was 80% and excellent purity and yields were obtained after chromatography. The lower purities could have many causes. For example, it is known that PyBOP and PyBrOP produce deleterious esters when left in solution in DMF for long periods (more than one hour). These esters probably form a large part of the impurities and could be avoided by shortening coupling cycles (one hour each), by choosing other coupling reagents, or by using DMA instead of DMF (PyBOP and PyBrOP are stable for several days in DMA). The low purity could also result from cross-contamination when using the synthesizer, which was not used in the preparation of the two model compounds. However, products with higher purity could be obtained by performing a silica gel filtration or a flash chromatography [31]. Libraries of steroidal sulfamates have also been successfully generated in high yields and purities [31-33].

Table 2

## Representation of all library members (arylsulfamate derivatives 31-55).

General structure					
$R_2^{**}$ $R_1^*$	$\text{CH}_2\text{CH}_3$ (Propionic Acid) <i>a</i>	$\text{CH}(\text{CH}_3)_2$ ( <i>i</i> -Butyric Acid) <i>b</i>	$\text{CH}_2\text{C}(\text{CH}_3)_3$ ( <i>t</i> -Butylacetic Acid) <i>c</i>	$\text{CH}_2$ -Phenyl (Phenylacetic Acid) <i>d</i>	$(\text{CH}_2)_2$ - Cyclopentyl (3-Cyclopentyl-propionic Acid) <i>e</i>
$\text{CH}_3$ (Alanine) <i>a</i>	# 31 $\text{C}_{14}\text{H}_{21}\text{N}_3\text{O}_5\text{S}$ W: 15.5 mg CY: 78% P: 52%	# 32 $\text{C}_{15}\text{H}_{23}\text{N}_3\text{O}_5\text{S}$ W: 10.5 mg CY: 52%	# 33 $\text{C}_{17}\text{H}_{27}\text{N}_3\text{O}_5\text{S}$ W: 15.2 mg CY: 69%	# 34 $\text{C}_{19}\text{H}_{23}\text{N}_3\text{O}_5\text{S}$ W: 16.1 mg CY: 70%	# 35 $\text{C}_{19}\text{H}_{29}\text{N}_3\text{O}_5\text{S}$ W: 13.5 mg CY: 59% P: 48%
$\text{CH}(\text{CH}_3)_2$ (Valine) <i>b</i>	# 36 $\text{C}_{16}\text{H}_{25}\text{N}_3\text{O}_5\text{S}$ W: 10.3 mg CY: 49%	# 37 $\text{C}_{17}\text{H}_{27}\text{N}_3\text{O}_5\text{S}$ W: 13.0 mg CY: 59% P: 46%	# 38 $\text{C}_{19}\text{H}_{31}\text{N}_3\text{O}_5\text{S}$ W: 13.7 mg CY: 57%	# 39 $\text{C}_{21}\text{H}_{27}\text{N}_3\text{O}_5\text{S}$ W: 15.7 mg CY: 63%	# 40 $\text{C}_{21}\text{H}_{33}\text{N}_3\text{O}_5\text{S}$ W: 12.2 mg CY: 49% P: 38%
$\text{CH}_2\text{CH}(\text{CH}_3)_2$ (Leucine) <i>c</i>	# 41 $\text{C}_{17}\text{H}_{27}\text{N}_3\text{O}_5\text{S}$ W: 16.2 mg CY: 74% P: 66%	# 42 $\text{C}_{18}\text{H}_{29}\text{N}_3\text{O}_5\text{S}$ W: 16.6 mg CY: 72%	# 43 $\text{C}_{20}\text{H}_{33}\text{N}_3\text{O}_5\text{S}$ W: 16.1 mg CY: 67% P: 53%	# 44 $\text{C}_{22}\text{H}_{29}\text{N}_3\text{O}_5\text{S}$ W: 16.9 mg CY: 65%	# 45 $\text{C}_{22}\text{H}_{35}\text{N}_3\text{O}_5\text{S}$ W: 14.8 mg CY: 57%
$\text{CH}(\text{CH}_3)\text{CH}_2\text{CH}_3$ (Isoleucine) <i>d</i>	# 46 $\text{C}_{17}\text{H}_{27}\text{N}_3\text{O}_5\text{S}$ W: 11.1 mg CY: 50%	# 47 $\text{C}_{18}\text{H}_{29}\text{N}_3\text{O}_5\text{S}$ W: 11.7 mg CY: 51% P: 65%	# 48 $\text{C}_{20}\text{H}_{33}\text{N}_3\text{O}_5\text{S}$ W: 14.1 mg CY: 59%	# 49 $\text{C}_{22}\text{H}_{29}\text{N}_3\text{O}_5\text{S}$ W: 13.8 mg CY: 53% P: 54%	# 50 $\text{C}_{22}\text{H}_{35}\text{N}_3\text{O}_5\text{S}$ W: 12.2 mg CY: 47%
$\text{CH}_2$ -Phenyl (Phenylalanine) <i>e</i>	# 51 $\text{C}_{20}\text{H}_{25}\text{N}_3\text{O}_5\text{S}$ W: 14.5 mg CY: 60%	# 52 $\text{C}_{21}\text{H}_{27}\text{N}_3\text{O}_5\text{S}$ W: 15.8 mg CY: 63%	# 53 $\text{C}_{23}\text{H}_{31}\text{N}_3\text{O}_5\text{S}$ W: 14.8 mg CY: 57% P: 50%	# 54 $\text{C}_{25}\text{H}_{27}\text{N}_3\text{O}_5\text{S}$ W: 16.2 mg CY: 60% P: 57%	# 55 $\text{C}_{25}\text{H}_{33}\text{N}_3\text{O}_5\text{S}$ W: 13.7 mg CY: 49%

W: Weight of released compound; CY: crude yield; P: purity determined by quantitative  $^1\text{H}$  NMR.

(\*)  $R_1$ : The residue of amino acids used as building blocks.

(\*\*)  $R_2$ : The residue of carboxylic acids used as building blocks.

## Conclusions

The multidetachable sulfamate linker used herein allowed the preparation of both phenol and arylsulfamate derivatives, which are therapeutically attractive types of compounds. The loading step on trityl chloride resin is quantitative and the peptide coupling reactions are compatible with this linker. The dual cleavage strategy allowed us to generate two different types of compounds in a sequential way (without resin split). Here, we used the Fmoc-tyramine sulfamate (**2**) as a general scaffold to introduce two levels of diversification, but other arylsulfamates could be judiciously used to extend the nature of the synthesized compounds. The sulfamate linker thus represents a valuable addition to the chemical tools available to the medicinal and organic chemists.

## Experimental

### General remarks

9-Fluorenylmethyl succinimidyl carbonate (FmocOSu) and Fmoc-protected amino-acids were purchased from Advanced ChemTech, (Louisville, KY, USA). PyBOP, PyBrOP, anhydrous DMF and trityl resin were purchased from Novabiochem (EMD Biosciences, San Diego, CA, USA). Other reagents were purchased from Aldrich (Milwaukee, WI, USA). The sulfamoyl chloride (moisture sensitive) was prepared from chlorosulfonyl isocyanate and concentrated HCl according to a known procedure [34]. All reagents were used as provided. A Jouan RC1010 SpeedVac apparatus (Winchester, VA, USA) was used for the solvent evaporation of the final library compounds. FTIR spectra were obtained on a Perkin-Elmer 1600 spectrophotometer (Norwalk, CT, USA).  $^{13}\text{C}$  NMR spectra were recorded at 75.5 MHz on a Bruker AC/F 300 spectrometer (Billerica, MA, USA).  $^1\text{H}$  NMR spectra with and without internal reference were recorded at 400 MHz on a Bruker Avance 400 Spectrometer (Billerica, MA, USA). The NMR purity of the cleaved products was determined using the external reference method. The reference compound (1,2,4-triazole) was dissolved in DMSO- $d_6$  and placed in a WGS-5BL coaxial insert (WILMAD, Buena, NJ, USA).

### Synthesis of sulfamate derivative **2**

To a stirred solution of tyramine (**1**) (1.80 g, 13.12 mmol) in THF/ $\text{H}_2\text{O}$  (3:1, v/v) (225 mL) were added, successively, aqueous 1.0 N  $\text{NaHCO}_3$  (27 mL) and FmocOSu (4.47 g, 13.25 mmol). After 2 h at room temperature, water (200 mL) was added and the crude product extracted with EtOAc (200 mL) and  $\text{CH}_2\text{Cl}_2$  (2 x 200 mL). The combined organic layer was dried over  $\text{MgSO}_4$ , filtered, the solvent evaporated under reduced pressure and the product dried under a vacuum overnight. The crude Fmoc derivative was dissolved in DMA (22 mL) and the solution cooled to  $0^\circ\text{C}$  in an ice bath. A first portion of sulfamoyl chloride (3.71 g, 32.11 mmol) was gradually added over 15 min and the mixture was allowed to react at room temperature. After 1 h, the same amount of sulfamoyl chloride was added as described above, and the mixture stirred at room temperature for 3 additional hours. The mixture was then poured in a cool solution of brine and extracted with EtOAc (3 x 200 mL). The combined organic layer was washed with brine (1 x 500 mL), dried over  $\text{MgSO}_4$ , and evaporated to dryness. Purification by flash chromatography with hexanes/acetone (7:3 to 6:4) yielded 4.05 g (72%) of **2**.  $^1\text{H}$  NMR (acetone- $d_6$ )  $\delta$ , ppm: 2.04 – 2.07 (m, 2H), 3.35 – 3.38 (m, 2H), 4.21 (t,  $J = 6.9$  Hz, 1H), 4.35 (d,  $J = 6.9$  Hz, 2H), 6.62 (bt, 1H, NH), 7.14 – 7.45 (m, 8H), 7.68 (d,  $J = 7.4$  Hz, 2H), 7.87 (d,  $J = 7.6$  Hz, 2H).  $^{13}\text{C}$  NMR (acetone- $d_6$ )  $\delta$ , ppm: 148.1, 141.0, 136.1, 133.1, 130.0, 121.8, 119.5, 118.9, 117.0, 114.0, 111.8, 57.7, 39.1, 34.0, 27.0.

### Synthesis of resin **3** (loading of sulfamate **2** on trityl resin)

Trityl chloride resin (2.51 g) (1.10 mmol/g loading) and sulfamate **2** (1.45 g) were added in a 50 mL peptide flask equipped with a three-way stopcock and swollen under argon in dry  $\text{CH}_2\text{Cl}_2$  (24 mL). Diisopropylethylamine (DIPEA) (4.81 mL) was then added and the mixture was stirred overnight at room temperature. The resin was filtered and washed with  $\text{CH}_2\text{Cl}_2$  (3 x 25 mL), MeOH (3 x 25 mL), THF (3 x 25 mL) and again with  $\text{CH}_2\text{Cl}_2$  (3 x 25 mL), then dried overnight under a vacuum to afford 3.84 g of resin **3**. The coupling yield calculated by means of the mass increase was quantitative. Resin **3**: FTIR (KBr matrix)  $\nu$ ,  $\text{cm}^{-1}$ : 1696 (C=O, Fmoc group), 1350 and 1156 (sulfonamide). Gel-Phase  $^{13}\text{C}$  NMR (150 mg resin swelled in  $\text{CD}_2\text{Cl}_2$ /benzene- $d_6$  with the following conditions:  $d_1 = 1.0$  s,  $p_1 = 30^\circ$  (3.0  $\mu\text{s}$ ),  $a_q = 430$  ms, RG 800 SI = 32 K)  $\delta$ , ppm: 156.1, 144.0, 141.3, 137.7, 132.1, 125.0, 122.0, 119.9, 73.5, 66.2, 47.2, 40.8, 35.9.

### Library synthesis: Introducing the first level of molecular diversity

A 96-well Teflon reaction vessel from Advanced ChemTechLabtech Manual Organic Synthesizer-Platform IV was used for the solid-phase synthesis. Small-volume peptide flasks or PD-10 columns (Amersham Biosciences, Uppsala, Sweden) fitted with a three-way stopcock (Bio-Rad, Hercules, CA, USA) could alternatively be used. In 25 wells of a 96-well reaction block loaded with resin **3** (25 x 120 mg) was added a solution of 20% piperidine in  $\text{CH}_2\text{Cl}_2$  (1.5 mL) and the mixture was stirred at room temperature to hydrolyze the Fmoc. After 1 h, the resins were filtered to remove the solvent, washed with  $\text{CH}_2\text{Cl}_2$  (5 x 2 mL) and dried under a vacuum for 2 h. Five stock solutions, each containing PyBOP (450 mg, 0.870 mmol) and HOBt (120 mg, 0.870 mmol), as well as one of the Fmoc-protected amino acids from the *L* series (alanine, valine, leucine, isoleucine or phenylalanine) (0.870 mmol), were prepared in DMF (7.5 mL) and reacted 2 min with DIPEA (0.3 mL, 1.74 mmol). Next, one of the stock solutions was added (in equal proportions of 1.5 mL) in

each of the 25 reaction vessels (five wells for each amino acid) containing the resin with the tyramine. The resins were stirred under argon for 3 h, then filtered, washed with DMF (3 x 2 mL) and CH<sub>2</sub>Cl<sub>2</sub> (5 x 2 mL), and dried overnight under a vacuum to afford five groups (5 x 5) of resins **4a-4e**. FTIR (KBr matrix)  $\nu$ , cm<sup>-1</sup>: 1708-1709 (C=O, Fmoc group), 1656-1662 (C=O, amide) and 1350 and 1156 (sulfonamide).

#### Library synthesis: Introducing the second level of molecular diversity

To the five groups of resins **4a-4e** (25 wells) obtained above was added a solution of 20% piperidine in CH<sub>2</sub>Cl<sub>2</sub> (1.5 mL) and the block was stirred at room temperature. After 1 h, the resins were filtered, washed with CH<sub>2</sub>Cl<sub>2</sub> (5 x 3 mL) and dried under vacuum (2 h). Each of the five resins with distinct amino acid diversity was reacted with a solution (1.5 mL) of carboxylic acid (propionic, isobutyric, *t*-butyl acetic, phenyl acetic or 3-cyclopentyl propionic) (0.870 mmol) activated with PyBrOP (405 mg, 0.870 mmol), HOBT (120 mg, 0.870 mmol) and DIPEA (0.85 mL, 0.30 mmol) in DMF (7.5 mL). The 25 resins (5 x 5) were stirred for 3 h at room temperature, then filtered and washed with DMF (3 x 2 mL), CH<sub>2</sub>Cl<sub>2</sub> (5 x 2 mL), THF (3 x 2 mL), THF/H<sub>2</sub>O (3 x 2 mL), H<sub>2</sub>O (3 x 2 mL), H<sub>2</sub>O/MeOH (3 x 2 mL) and MeOH, and were dried overnight under vacuum to afford 25 different resins **5aa-5ee**. FTIR (KBr matrix)  $\nu$ , cm<sup>-1</sup>: 1640-1658 (C=O, amides).

#### Cleavage strategy providing phenol derivatives (Nucleophilic cleavage)

To each of the 25 resins **5aa-5ee** in their reaction vessels was added a solution of 30% diethylamine (DEA) in THF (1 mL) and the resins were stirred under argon. After 24 h at room temperature, 1 mL of 30% DEA/THF solution was added and the resins were stirred for 24 additional hours. The resins were then filtered under vacuum, washed with 30% DEA in THF (2 x 1.5 mL), and the filtrates were collected in pre-weighed glass tubes. The solvent was evaporated in a SpeedVac apparatus, THF (3 mL) was then added to each tube and the solutions were evaporated again (2x). The procedure was repeated with Et<sub>2</sub>O. The crude products were dried for 48 h under vacuum pump to afford phenol derivatives **6-30**. A sampling of 10 compounds from the 25 library members was characterized by <sup>1</sup>H NMR and MS. Purity was also assessed by quantitative <sup>1</sup>H NMR (Table 1).

N-[2-(4-hydroxyphenyl)-ethyl]-2-propionylamino-propionamide (**6**): <sup>1</sup>H NMR (DMSO-d<sub>6</sub>)  $\delta$ , ppm: 9.20 (s, 1H, OH), 7.90 - 7.86 (m, 2H, NH), 6.98 (d, 2H, J = 8.4 Hz), 6.66 (d, 2H, J = 8.5 Hz), 4.23 - 4.16 (m, 1H), 3.24 - 3.13 (m, 2H), 2.57 (t, 2H, 7.4 Hz), 2.11 (q, 2H, J = 7.6 Hz), 1.15 - 1.12 (m, 1H), 0.97 (t, 3H, 7.6 Hz). MS/EI (C<sub>14</sub>H<sub>20</sub>N<sub>2</sub>O<sub>3</sub>) calculated: 264.1; observed: 265.1 (M+H)<sup>+</sup>.

3-Cyclopentyl-N-{1-[2-(4-hydroxyphenyl)-ethyl]carbamoyl}-ethyl}-propionamide (**10**): <sup>1</sup>H NMR (DMSO-d<sub>6</sub>)  $\delta$ , ppm: 9.20 (s, 1H, OH), 7.92 (bd, 1H, NH, J = 7.6 Hz), 7.85 (bt, 1H, NH, J = 5.6 Hz), 6.97 (d, 2H, J = 8.4 Hz), 6.66 (d, 2H, J = 8.4 Hz), 4.23 - 4.16 (m, 1H), 3.26 - 3.11 (m, 2H), 2.56 (t, 2H, J = 7.3 Hz), 2.11 (t, 2H, J = 7.6 Hz), 1.74 - 1.42 (m, 9H), 1.12 (d, 3H, J = 7.1 Hz), 1.10 - 1.00 (m, 2H). MS/EI (C<sub>19</sub>H<sub>28</sub>N<sub>2</sub>O<sub>3</sub>) calculated: 332.2; observed: 333.1 (M+H)<sup>+</sup>.

N-[2-(4-hydroxyphenyl)-ethyl]-2-isobutyrylamino-3-methyl-butyramide (**12**): <sup>1</sup>H NMR (DMSO-d<sub>6</sub>)  $\delta$ , ppm: 9.21 (s, 1H, OH), 7.99 (bt, 1H, NH, J = 5.5 Hz), 7.72 (bd, 1H, NH, J = 9.1 Hz), 6.98 (d, 2H, J = 8.4 Hz), 6.65 (d, 2H, J = 8.4 Hz), 4.07 (dd, 1H, J = 7.4 Hz and J = 9.0 Hz), 3.31 - 3.14 (dm, 2H), 2.60 - 2.55 (m, 2H), 1.93 - 1.83 (m, 1H), 1.24 - 1.22 (m, 1H), 0.98 (q, 6H, J = 6.8 Hz), 0.78 (d, 6H, J = 6.8 Hz). MS/EI (C<sub>17</sub>H<sub>26</sub>N<sub>2</sub>O<sub>3</sub>) calculated: 306.2; observed: 307.1 (M+H)<sup>+</sup>.

2-(Cyclopentylpropionylamino)-N-[2-(4-hydroxyphenyl)-ethyl]-3-methyl-butyramide (**15**): <sup>1</sup>H NMR (DMSO-d<sub>6</sub>)  $\delta$ , ppm: 9.19 (s, 1H, OH), 7.97 (bt, 1H, NH, J = 5.5 Hz), 7.79 (bd, 1H, NH, J = 9.0 Hz), 6.98 (d, 2H, J = 8.4 Hz), 6.66 (d, 2H, J = 8.4 Hz), 4.08 (dd, 1H, J = 7.3 Hz and J = 8.9 Hz), 3.26 - 3.15 (m, 2H), 2.57 (t, 2H, J = 6.5 Hz), 2.23 - 2.09 (m, 2H), 1.73 - 1.43 (m, 9H), 1.24 - 1.22 (m, 1H), 1.10 - 1.01 (m, 2H), 0.78 (d, 6H, J = 6.7 Hz). MS/EI (C<sub>21</sub>H<sub>32</sub>N<sub>2</sub>O<sub>3</sub>) calculated: 360.2; observed: 361.2 (M+H)<sup>+</sup>.

4-Methyl-2-propionylaminopentanoic acid [2-(4-hydroxyphenyl)-ethyl]-amide (**16**): <sup>1</sup>H NMR (DMSO-d<sub>6</sub>)  $\delta$ , ppm: 9.20 (s, 1H, OH), 7.93 (bt, 1H, NH, J = 5.6 Hz), 7.85 (bd, 1H, NH, J = 8.4 Hz), 6.97 (d, 2H, J = 8.4 Hz), 6.66 (d, 2H, J = 8.4 Hz), 4.25 - 4.19 (m, 1H), 3.25 - 3.14 (m, 2H), 2.56 (t, 2H, J = 7.3 Hz), 2.11 (qd, 2H, J = 2.0 Hz and J = 7.5 Hz), 1.53 - 1.46 (m, 1H), 1.25 - 1.21 (m, 2H), 0.97, (t, 3H, J = 7.6 Hz), 0.83 (dd, 6H, J = 6.6 Hz and J = 18.2 Hz). MS/EI (C<sub>17</sub>H<sub>26</sub>N<sub>2</sub>O<sub>3</sub>) calculated: 306.2; observed: 307.1 (M+H)<sup>+</sup>.

2-(3,3-Dimethylbutyrylamino)-4-methylpentanoic acid [2-(4-hydroxyphenyl)-ethyl]-amide (**18**): <sup>1</sup>H NMR (DMSO-d<sub>6</sub>)  $\delta$ , ppm: 9.20 (s, 1H, OH), 7.90 (bt, 1H, NH, J = 5.4 Hz), 7.80 (bd, 1H, NH, J = 8.3 Hz), 6.97 (d, 2H, J = 8.4 Hz), 6.66 (d, 2H, J = 8.5 Hz), 4.26 - 4.20 (m, 1H), 3.26 - 3.14 (m, 2H), 2.58 - 2.54 (m, 2H), 2.04 - 1.91 (m, 2H), 1.55 - 1.51 (m, 1H), 1.26 - 1.21 (m, 2H), 0.94 (s, 9H), 0.83 (dd, 6H, J = 6.6 Hz and J = 19.0 Hz). MS/EI (C<sub>20</sub>H<sub>32</sub>N<sub>2</sub>O<sub>3</sub>) calculated: 348.5; observed: 349.3 (M+H)<sup>+</sup>.



2-Isobutyrylamino-3-methylpentanoic acid [2-(4-hydroxyphenyl)-ethyl]-amide (**22**):  $^1\text{H}$  NMR (DMSO- $d_6$ )  $\delta$ , ppm: 9.18 (s, 1H, OH), 8.00 (bd, 1H, NH,  $J = 9.1$  Hz), 7.72 (bt, 1H, NH,  $J = 5.5$  Hz), 6.98 (d, 2H,  $J = 8.5$  Hz), 6.65 (d, 2H,  $J = 8.5$  Hz), 4.10 (t, 1H, 8.8 Hz), 3.24 – 3.16 (m, 2H), 2.59 – 2.55 (m, 2H), 1.70 – 1.60 (m, 1H), 1.38 – 1.32 (m, 1H), 1.07 – 1.00 (m, 2H), 0.97 (dd, 6H,  $J = 6.8$  Hz and  $J = 11.0$  Hz), 0.78 (t, 3H,  $J = 7.3$  Hz), 0.75 (d, 3H,  $J = 6.8$  Hz). MS/EI ( $\text{C}_{18}\text{H}_{28}\text{N}_2\text{O}_3$ ) calculated: 320.2; observed: 321.1 (M+H) $^+$ .

3-Methyl-2-phenylacetylaminopentanoic acid [2-(4-hydroxyphenyl)-ethyl]-amide (**24**):  $^1\text{H}$  NMR (DMSO- $d_6$ )  $\delta$ , ppm: 9.19 (s, 1H, OH), 7.99 (bd, 1H, NH,  $J = 9.0$  Hz), 7.81 (bt, 1H, NH,  $J = 5.5$  Hz), 7.31 – 7.17 (m, 5H), 6.98 (d, 2H,  $J = 8.2$  Hz), 6.65 (d, 2H,  $J = 8.4$  Hz), 4.10 (m, 1H), 3.25 – 3.17 (m, 2H), 2.57 (bt, 2H), 2.20 – 2.08 (m, 2H), 1.37 – 1.30 (m, 1H), 1.09 – 0.99 (m, 2H), 0.79 (d, 3H,  $J = 7.1$  Hz), 0.74 (t, 3H,  $J = 6.5$  Hz). MS/EI ( $\text{C}_{22}\text{H}_{28}\text{N}_2\text{O}_3$ ) calculated: 368.2; observed: 369.3 (M+H) $^+$ .

N-{1-[2-(4-hydroxyphenyl)-ethylcarbamoyl]-2-phenylethyl}-3,3-dimethylbutyramide (**28**):  $^1\text{H}$  NMR (DMSO- $d_6$ )  $\delta$ , ppm: 9.22 (s, 1H, OH), 7.98 (bt, 1H, NH,  $J = 5.4$  Hz), 7.92 (bd, 1H, NH,  $J = 8.5$  Hz), 7.26 – 7.14 (m, 5H), 6.97 (d, 2H,  $J = 8.5$  Hz), 6.66 (d, 2H,  $J = 8.4$  Hz), 4.50 – 4.44 (m, 1H), 3.26 – 3.15 (m, 2H), 2.73 – 2.67 (m, 2H), 2.57 – 2.50 (m, 2H), 1.92 (s, 2H), 0.80 (s, 9H). MS/EI ( $\text{C}_{23}\text{H}_{30}\text{N}_2\text{O}_3$ ) calculated: 382.2; observed: 383.2 (M+H) $^+$ .

N-[2-(4-hydroxyphenyl)-ethyl]-3-phenyl-2-phenylacetylaminopropionamide (**29**):  $^1\text{H}$  NMR (DMSO- $d_6$ )  $\delta$ , ppm: 9.19 (s, 1H, OH), 8.33 (bd, 1H, NH), 8.08 (bt, 1H, NH), 7.26 – 7.06 (m, 10H), 6.97 (d, 2H,  $J = 8.4$  Hz), 6.66 (d, 2H,  $J = 8.3$  Hz), 4.45 – 4.42 (m, 1H), 3.26 – 3.14 (m, 2H), 2.75 – 2.66 (m, 2H), 2.56 – 2.50 (m, 2H), 2.04 – 1.99 (m, 2H). MS/EI ( $\text{C}_{25}\text{H}_{26}\text{N}_2\text{O}_3$ ) calculated: 402.2; observed: 403.3 (M+H) $^+$ .

#### *Cleavage strategy providing sulfamate derivatives (Acidic cleavage)*

To each of the 25 resins **5aa-5ee** previously submitted to nucleophilic cleavage was added a solution of 30% hexafluoroisopropanol (HFIP) in  $\text{CH}_2\text{Cl}_2$  (1.5 mL) and the resins were stirred under argon. After 6 h at room temperature, the resins were filtered under vacuum, washed with 30% HFIP in  $\text{CH}_2\text{Cl}_2$  (2 x 1 mL) and THF (2 x 1 mL), and the filtrate was collected in pre-weighed tubes. The solvent was evaporated in a SpeedVac apparatus, THF (2 x 3 mL) was then added to each tube and the solutions were evaporated again. The procedure was repeated with  $\text{Et}_2\text{O}$ . The crude products were dried 48 h under vacuum pump to afford sulfamate derivatives **31-55**. A sampling of 10 compounds from the 25 library members was characterized by  $^1\text{H}$  NMR and MS. Purity was also assessed by quantitative  $^1\text{H}$  NMR (Table 2).

Sulfamic acid 4-[2-(2-propionylamino-propionylamino)-ethyl]-phenyl ester (**31**):  $^1\text{H}$  NMR (DMSO- $d_6$ )  $\delta$ , ppm: 7.98 – 7.86 (m, 3H, NH and  $\text{NH}_2$ ), 7.31 – 7.17 (m, 4H), 4.23 – 4.17 (m, 1H), 3.33 – 3.21 (m, 2H), 2.72 (t, 2H,  $J = 7.3$  Hz), 2.11 (q, 2H,  $J = 7.6$  Hz), 1.15 – 1.12 (m, 3H), 0.97 (t, 3H,  $J = 7.6$  Hz). MS/EI ( $\text{C}_{14}\text{H}_{21}\text{N}_3\text{O}_5\text{S}$ ) calculated: 343.2; observed: 344.1 (M+H) $^+$ .

Sulfamic acid 4-{2-[2-(3-cyclopentylpropionylamino)-propionylamino]-ethyl}-phenyl ester (**35**):  $^1\text{H}$  NMR (DMSO- $d_6$ )  $\delta$ , ppm: 7.98 – 7.92 (m, 3H, NH and  $\text{NH}_2$ ), 7.31 – 7.17 (m, 4H), 4.23 – 4.16 (m, 1H), 3.30 – 3.22 (m, 2H), 2.71 (t, 2H,  $J = 7.3$  Hz), 2.10 (t, 2H,  $J = 7.2$  Hz), 1.79 – 1.42 (m, 9H), 1.13 (d, 3H,  $J = 7.1$  Hz), 1.09 – 0.99 (m, 2H). MS/EI ( $\text{C}_{19}\text{H}_{29}\text{N}_3\text{O}_5\text{S}$ ) calculated: 411.2; observed: 412.1 (M+H) $^+$ .

Sulfamic acid 4[2-(2-isobutyrylamino-3-methylbutyrylamino)-ethyl]-phenyl ester (**37**):  $^1\text{H}$  NMR (DMSO- $d_6$ )  $\delta$ , ppm: 8.08 (bt, 1H, NH,  $J = 5.4$  Hz), 7.97 (bs, 1H,  $\text{NH}_2$ ), 7.74 (bd, 1H, NH,  $J = 8.9$  Hz), 7.31 – 7.16 (m, 4H), 4.07 (dd, 1H,  $J = 7.6$  Hz and  $J = 9.1$  Hz), 3.33 – 3.19 (m, 2H), 2.73 (t, 2H,  $J = 5.9$  Hz), 1.93 – 1.83 (m, 1H), 1.25 – 1.22 (m, 1H), 0.98 (q, 6H,  $J = 6.8$  Hz), 0.79 (d, 6H,  $J = 6.6$  Hz). MS/EI ( $\text{C}_{17}\text{H}_{27}\text{N}_3\text{O}_5\text{S}$ ) calculated: 385.2; observed: 386.1 (M+H) $^+$ .

Sulfamic acid 4-{2-[2-(3-cyclopentylpropionylamino)-3-methylbutyrylamino]-ethyl}-phenyl ester (**40**):  $^1\text{H}$  NMR (DMSO- $d_6$ )  $\delta$ , ppm: 8.06 (bt, 1H, NH,  $J = 4.9$  Hz), 7.96 (bs, 1H,  $\text{NH}_2$ ), 7.81 (bd, 1H, NH,  $J = 8.9$  Hz), 7.33 – 7.16 (m, 4H), 4.08 – 4.02 (m, 1H), 3.32 – 3.19 (m, 2H), 2.72 (t, 2H,  $J = 7.2$  Hz), 2.23 – 2.08 (m, 2H), 1.76 – 1.41 (m, 9H), 1.26 – 1.21 (m, 1H), 1.11 – 1.01 (m, 2H), 0.78 (dd, 6H,  $J = 2.1$  Hz and  $J = 6.6$  Hz). MS/EI ( $\text{C}_{21}\text{H}_{33}\text{N}_3\text{O}_5\text{S}$ ) calculated: 439.2; observed: 440.2 (M+H) $^+$ .

Sulfamic acid 4-[2-(4-methyl-2-propionylaminopentanoylamino)-ethyl]-phenyl ester (**41**):  $^1\text{H}$  NMR (DMSO- $d_6$ )  $\delta$ , ppm: 8.02 (bt, 1H, NH,  $J = 5.8$  Hz), 7.96 (bs, 1H,  $\text{NH}_2$ ), 7.86 (bt, 1H, NH,  $J = 8.2$  Hz), 7.30 – 7.16 (m, 4H), 4.29 – 4.19 (m, 1H), 3.31 – 3.20 (m, 2H), 2.71 (t, 2H,  $J = 7.4$  Hz), 2.14 – 2.07 (m, 2H), 1.54 – 1.44 (m, 1H), 1.25 – 1.13 (m, 2H), 0.97 (t, 3H,  $J = 7.6$  Hz), 0.83 (dd, 6H,  $J = 6.5$  Hz and  $J = 17.6$  Hz). MS/EI ( $\text{C}_{17}\text{H}_{27}\text{N}_3\text{O}_5\text{S}$ ) calculated: 385.2; observed: 386.1 (M+H) $^+$ .

Sulfamic acid 4-{2-[2-(3,3-dimethylbutyrylamino)-4-methylpentanoylamino]-ethyl}-phenyl ester (**43**):  $^1\text{H}$  NMR (DMSO- $d_6$ )  $\delta$ , ppm: 8.01 (bt, 1H, NH), 7.97 (bs, 1H,  $\text{NH}_2$ ), 7.83 (bd, 1H, NH,  $J = 8.0$  Hz), 7.31 – 7.16 (m, 4H), 4.29 – 4.20 (m, 1H), 3.32 – 3.21 (m, 2H), 2.71 (t, 2H,  $J = 7.0$  Hz), 2.05 – 1.95 (m, 2H), 1.58 – 1.47 (m, 1H), 1.25 – 1.14 (m, 2H), 0.94 (s, 9H), 0.84 (q, 6H,  $J = 6.4$  Hz). MS/EI ( $\text{C}_{20}\text{H}_{33}\text{N}_3\text{O}_5\text{S}$ ) calculated: 427.2; observed: 428.1 ( $\text{M}+\text{H}$ ) $^+$ .

Sulfamic acid 4-[2-(2-isobutyrylamino-3-methylpentanoylamino)-ethyl]-phenyl ester (**47**):  $^1\text{H}$  NMR (DMSO- $d_6$ )  $\delta$ , ppm: 8.09 (bt, 1H, NH,  $J = 5.3$  Hz), 7.97 (bs, 1H,  $\text{NH}_2$ ), 7.75 (bd, 1H, NH,  $J = 9.1$  Hz), 7.31 – 7.16 (m, 4H), 4.10 (t, 1H,  $J = 8.5$  Hz), 3.33 – 3.19 (m, 2H), 2.72 (td, 2H,  $J = 2.9$  Hz and  $J = 7.3$  Hz), 1.71 – 1.61 (m, 1H), 1.39 – 1.32 (m, 1H), 1.08 – 1.01 (m, 2H), 0.98 (q, 6H,  $J = 6.8$  Hz), 0.78 (t, 3H,  $J = 7.3$  Hz), 0.75 (d, 3H,  $J = 6.8$  Hz). MS/EI ( $\text{C}_{18}\text{H}_{29}\text{N}_3\text{O}_5\text{S}$ ) calculated: 399.2; observed: 400.1 ( $\text{M}+\text{H}$ ) $^+$ .

Sulfamic acid 4-[2-(3-methyl-2-phenylacetylaminopropionylamino)-ethyl]-phenyl ester (**49**):  $^1\text{H}$  NMR (DMSO- $d_6$ )  $\delta$ , ppm: 8.08 (bt, 1H, NH,  $J = 4.9$  Hz), 7.97 (bs, 1H,  $\text{NH}_2$ ), 7.83 (bd, 1H, NH,  $J = 8.9$  Hz), 7.31 – 7.16 (m, 9H), 4.10 (m, 1H), 3.32 – 3.19 (m, 2H), 2.71 (t, 2H,  $J = 7.0$  Hz), 2.20 – 2.07 (m, 2H), 1.38 – 1.31 (m, 1H), 1.09 – 0.99 (m, 2H), 0.78 (t, 3H,  $J = 7.4$  Hz), 0.73 (d, 3H,  $J = 5.5$  Hz). MS/EI ( $\text{C}_{22}\text{H}_{29}\text{N}_3\text{O}_5\text{S}$ ) calculated: 447.2; observed: 448.2 ( $\text{M}+\text{H}$ ) $^+$ .

Sulfamic acid 4-{2-[2-(3,3-dimethylbutyrylamino)-3-phenylpropionylamino]-ethyl}-phenyl ester (**53**):  $^1\text{H}$  NMR (DMSO- $d_6$ )  $\delta$ , ppm: 8.06 (bt, 1H, NH,  $J = 6.4$  Hz), 7.96 (bs, 1H,  $\text{NH}_2$ ), 7.94 (bd, 1H, NH,  $J = 8.5$  Hz), 7.29 – 7.15 (m, 9H), 4.52 – 4.44 (m, 1H), 3.29 – 3.21 (m, 2H), 2.97 – 2.86 (m, 2H), 2.72 – 2.69 (m, 2H), 2.00 (s, 2H), 0.80 (s, 9H). MS/EI ( $\text{C}_{23}\text{H}_{21}\text{N}_3\text{O}_5\text{S}$ ) calculated: 461.2; observed: 462.1 ( $\text{M}+\text{H}$ ) $^+$ .

Sulfamic acid 4[2-(3-phenyl-2-phenylacetylaminopropionylamino)-ethyl]-phenyl ester (**54**):  $^1\text{H}$  NMR (DMSO- $d_6$ )  $\delta$ , ppm: 8.37-7.94 (m, 3H, NH and  $\text{NH}_2$ ), 7.30 – 7.05 (m, 14H), 4.45 (td, 1H,  $J = 4.7$  Hz and  $J = 9.1$  Hz), 3.31 – 3.19 (m, 2H), 2.96 – 2.71 (m, 2H), 2.71 – 2.64 (m, 2H), 2.05 – 1.99 (m, 2H). MS/EI ( $\text{C}_{25}\text{H}_{27}\text{N}_3\text{O}_5\text{S}$ ) calculated: 481.2; observed: 482.1 ( $\text{M}+\text{H}$ ) $^+$ .

## Acknowledgments

We are grateful to the Canadian Institutes of Health Research for their financial support, to Mrs. Marie-Claude Trottier for NMR analyses and to Mrs. Micheline Harvey for careful reading of the manuscript.

## References

1. Spillane, W.J.; Ryder, C.A.; Walsh, R.M.; Curran, P.J.; Concagh, D.G.; Wall, S.N. Sulfamate sweeteners. *Food Chemistry*, 1996, 56, pp. 255-261.
2. Spillane, W.; Malaubier, J.F. Sulfamic acid and its N- and O-substituted derivatives. *Chemical Reviews*, 2014, 114, pp. 2507-2586.
3. Winum, J.-Y.; Scozzafava, A.; Montero, J.-L.; Supuran, C.T. Therapeutic applications of sulfamate. *Expert Opinion on Therapeutic Patents*, 2004, 14, pp. 1273-1308.
4. Maryanoff, B.E.; Costanzo, M.J.; Nortey, S.O.; Greco, M.N.; Shank, R.P.; Schupsky, J.J.; Ortegon, M.P.; Vaught, J.L. Structure-activity studies on anticonvulsant sugar sulfamates related to topiramate. Enhanced potency with cyclic sulfate derivatives. *Journal of Medicinal Chemistry*, 1998, 41, pp. 1315-1343.
5. Pastorekova, S.; Parkkila, S.; Pastorek, J.; Supuran, C.T. Carbonic anhydrase: Current state of the art, therapeutic applications and future prospects. *Journal of Enzyme Inhibition and Medicinal Chemistry*, 2004, 19, pp. 199-229.
6. Winum, J.Y.; Scozzafava, A.; Montero, J.L.; Supuran C.T. Sulfamates and their therapeutic potential. *Medicinal Research Reviews*, 2005, 25, pp. 186-228.
7. Mostafa, Y.A.; Taylor, S.D. Steroid derivatives as inhibitors of steroid sulfatase. *The Journal of Steroid Biochemistry and Molecular Biology*, 2013, 137, pp. 183-198.
8. Purohit, A.; Foster, P.A. Steroid sulfatase inhibitors for estrogen-and androgen-dependent cancers. *Journal of Endocrinology*, 2012, 212, pp. 99-110.
9. Maltais, R.; Poirier, D. Steroid sulfates inhibitors: A review covering the promising 2000-2010 decade. *Steroids*, 2011, 76, pp. 929-948.
10. Nussbaumer, P.; Billich, A. Steroid sulfatase inhibitors. *Medicinal Research Reviews*, 2004, 24, pp. 529-576.
11. Purohit, A.; Woo, L.W.L.; Chander, S.K.; Newman, S.P.; Ireson, C.; Ho, Y.; Grasso, A.; Leese, M.P.; Potter, B.V.L.; Reed, M.J. Steroid sulphatase inhibitors for breast cancer therapy. *The Journal of Steroid Biochemistry and Molecular Biology*, 2003, 86, pp. 423-432.
12. Selcer, K.W.; Kabler, H.; Sarap, J.; Xiao, Z.; Li, P.-K. Inhibition of steryl sulfatase activity in LNCaP human prostate cancer cells. *Steroids*, 2002, 67, pp. 821-826.
13. Hoffmann, R.; Rot, A.; Niyama, S.; Billich, A. Steroid Sulfatase in the Human Hair Follicle Concentrates in the Dermal Papilla. *Journal of Investigative Dermatology*, 2001, 117, pp. 1342-1348.



14. Johnson, D.A.; Wu, T.-H.; Li, P.-K.; Maher, T.J. The effect of steroid sulfatase inhibition on learning and spatial memory. *Brain Research*, 2000, 865, pp. 286-290.
15. Parker, R.A.; Barnhart, R.L.; Chen, K.S.; Edwards, M.L.; Matt, J.E.; Rhinehart, B.L.; Robinson, K.M.; Vaal, M.J.; Yates, M.T. Antioxidant and cholesterol lowering properties of 2,6-di-*t*-butyl-4-[(dimethylphenylsilyl)methoxy]phenol and derivatives: a new class of anti-atherogenic compounds. *Bioorganic & Medicinal Chemistry Letters*, 1996, 6, pp. 1559-1562.
16. Davidson, P.M.; Naidu, A.S. Phyto-phenol. In: *Natural Food Antimicrobial Systems*. Naidu, A.S. Eds. CRC Press: Boca Raton, FL, 2000, pp. 265-294.
17. Wrigglesworth, R.; Walpole, C.S.J.; Bevan, S.; Campbell, E.A.; Dray, A.; Hugues, G.A.; James, I.; Masdin, K.J.; Winter, J. Analogues of capsaicin with agonist activity as novel analgesic agents: structure-activity studies. 4. Potent, orally active analgesics. *Journal of Medicinal Chemistry*, 1996, 39, pp. 4942-4951.
18. Murata, S.; Sundell, C.L.; Lijkwan, M.A.; Balsam, L.B.; Hammainen, P.; Coleman, C.; York, C.; Luchoomun, J.; Suen, K.-L.; Howard, R.; Somers, P.K.; Morris, R.E.; Robbins, R.C. Effects of AGI-1096, a novel antioxidant compound with anti-inflammatory and antiproliferative properties, on rodent allograft arteriosclerosis. *Transplantation*, 2004, 77, pp. 1494-1500.
19. Jordan, V.C. Antiestrogens and selective estrogen receptor modulators as multifunctional medicines. 2. Clinical considerations and new agents. *Journal of Medicinal Chemistry*, 2003, 46, pp. 1081-1111.
20. Poirier, D. 17 $\beta$ -Hydroxysteroid dehydrogenase inhibitors: a patent review. *Expert Opinion on Therapeutic Patents*, 2010, 20, pp. 1123-1145.
21. Poirier, D. Inhibitors of 17 $\beta$ -hydroxysteroid dehydrogenases. *Current Medicinal Chemistry*, 2003, 10, pp. 453-477.
22. Marchais-Oberwinkler, S.; Henn, C.; Moller, G.; Klein, T.; Negri, M.; Oster, A.; Spadaro, A.; Werth, R.; Wetzel, M.; Xu, K.; Frotscher, M.; Hartmann, R.W.; Adamski, J. 17 $\beta$ -Hydroxysteroid dehydrogenases (17 $\beta$ -HSDs) as therapeutic targets: protein structures, functions, and recent progress in inhibitor development. *The Journal of Steroid Biochemistry and Molecular Biology*, 2011, 125, pp. 66-82.
23. Fournier, D.; Poirier, D. Chemical synthesis and evaluation of 17 $\alpha$ -alkylated derivatives of estradiol as inhibitors of steroid sulfatase. *European Journal of Medicinal Chemistry*, 2011, 46, pp. 4227-4237.
24. Boivin, R.P.; Luu-The, V.; Lachance, R.; Labrie, F.; Poirier, D. Structure-activity relationships of 17 $\alpha$ -derivatives of estradiol as inhibitors of steroid sulfatase. *Journal of Medicinal Chemistry*, 2000, 43, pp. 4465-4478.
25. Ciobanu, L.C.; Maltais, R.; Poirier, D. The sulfamate functional group as a new anchor for solid-phase organic synthesis. *Organic Letters*, 2000, 2, pp. 445-448.
26. Okada, M.; Iwashita, S.; Koizumi, N. Efficient general method for sulfamoylation of a hydroxyl group. *Tetrahedron Letters*, 2000, 41, pp. 7047-7051.
27. Spillane, W.J.; Hogan, G.; McGrath, P.; King, J.; Brack, C.J. Aminolysis of sulfamate esters in non-aqueous solvents. Evidence consistent with a concerted E2-type mechanism. *Journal of the Chemical Society, Perkin Transactions 2*, 1996, 10, pp. 2099-2104.
28. Spillane, W.J.; McHugh, F.A.; Burke, P.O. Aminolysis of sulfamate esters in chloroform – nonlinear kinetics. *Journal of the Chemical Society, Perkin Transactions 2*, 1998, 2, pp. 309-313.
29. Spillane, W.J. Novel change in rate-determining step within an E1cB mechanism during aminolysis of a sulfamate ester in acetonitrile. *Chemical Communications*, 1998, 9, pp. 1017-1018.
30. Spillane, W.J.; McGrath, P.; Brack, O.; O'Byrne, A.B. Change in rate-determining step in an E1cB mechanism during aminolysis of sulfamate esters in acetonitrile. *Journal of Organic Chemistry*, 2001, 66, pp. 6313-6316.
31. Ciobanu, L.C.; Poirier, D. Solid-phase parallel synthesis of 17 $\alpha$ -substituted estradiol sulfamate and phenol libraries using the multidetachable sulfamate linker. *Journal of Combinatorial Chemistry*, 2003, 5, pp. 429-440.
32. Ciobanu, L.C.; Poirier, D. Synthesis of libraries of 16 $\beta$ -aminopropyl estradiol derivatives for targeting two key steroidogenic enzymes. *ChemMedChem*, 2006, 1, pp. 1249-1259.
33. Bérubé, M.; Delagoutte, F.; Poirier, D. Preparation of libraries of 16 $\beta$ -estradiol derivatives as bisubstrate inhibitors of type 1 17 $\beta$ -hydroxysteroid dehydrogenase using the multidetachable sulfamate linker. *Molecules*, 2010, 15, pp. 1590-1631.
34. Peterson, E.M.; Brownell, J.; Vince, R. Synthesis and biological evaluation of 5'-sulfamoylated purinyl carbocyclic nucleosides. *Journal of Medicinal Chemistry*, 1992, 35, pp. 3991-4000.

# OXAZIRIDINE ( $C-CH_3NO$ ), $C-CH_2NO$ RADICALS AND $Cl$ , $NH_2$ AND METHYL DERIVATIVES OF OXAZIRIDINE; STRUCTURES AND QUANTUM CHEMICAL PARAMETERS

Mohammad Taghi Taghizadeh\*, Morteza Vatanparast, Saeed Nasirianfar

University of Tabriz, Faculty of Chemistry, 29, Bahman Blvd., Tabriz 51666-14766, Iran

\*e-mail: mttaghizadeh1947@gmail.com, mttaghizadeh@tabrizu.ac.ir; phone: (+98) 41 33 393 137; fax: (+98) 41 33 340 191

**Abstract.** Oxaziridine [ $c-CH_3NO$  ( $X^1A$ )],  $c-CH_2NO$  ( $X^2A$ ) radicals and  $Cl$ ,  $NH_2$  and methyl derivatives of oxaziridine structures have been optimized via DFTB3LYP level of theory using 6-311++G (d, p) basis set. Population analysis had been carried out. Vertical ionization energy ( $VIE$ ) and adiabatic ionization energy ( $AIE$ ), Fukui indices and some quantum chemical parameters were calculated. N-O bond was determined as weakest bond in oxaziridine triangle. The effect of electron withdrawing and electron donating groups on stability of weakest bond were assessed.

**Keywords:** oxaziridine, DFT, Fukui function, vertical ionization energy, adiabatic ionization energy.

Received: August 2015/ Revised final: October 2015/ Accepted: October 2015

## Introduction

Oxaziridine [ $c-CH_3NO$  ( $X^1A$ )] (structure 1 in Figure 1) has a triangular heterocycle containing oxygen, nitrogen, and carbon.

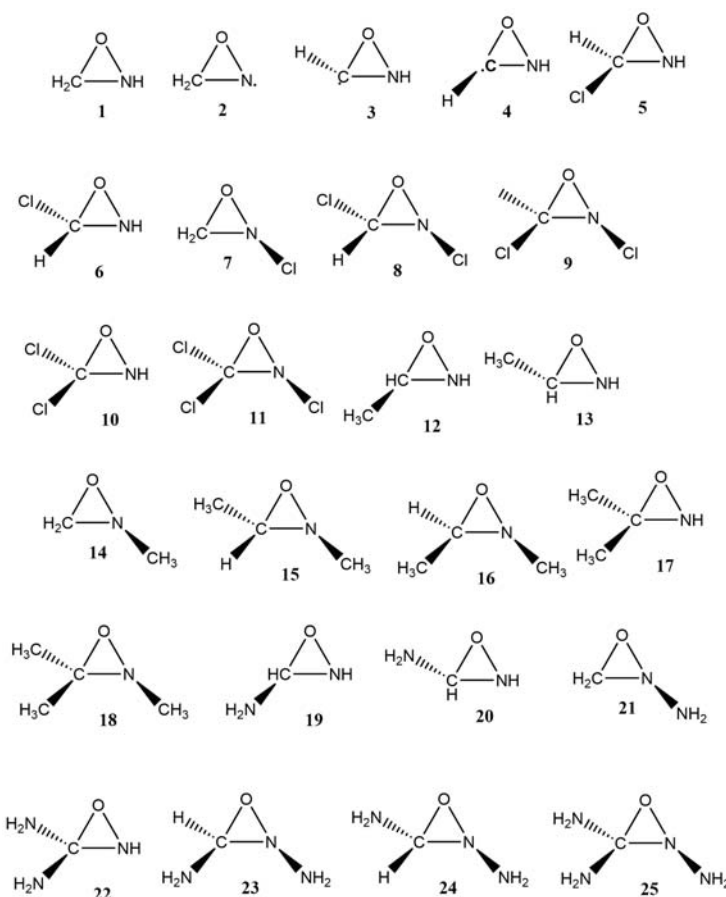


Figure 1. Structures have been investigated in this study:

(1) oxaziridine [ $CH_3NO$  ( $^1A$ )] (2) radical 1 [ $CH_2NO$  ( $^2A$ )] (3) radical 2 [ $CH_2NO$  ( $^2A$ )] (4) radical 3 [ $CH_2NO$  ( $^2A$ )] (5)  $CH_2NOCI$  ( $^1A$ ) (6)  $CH_2NOCI$  ( $^1A$ ) (7)  $CH_2NOCI$  ( $^1A$ ) (8)  $CHNOCI_2$  ( $^1A$ ) (9)  $CHNOCI_2$  ( $^1A$ ) (10)  $CHNOCI_2$  ( $^1A$ ) (11)  $CNOCI_3$  ( $^1A$ ) (12)  $C_2H_5NO$  ( $^1A$ ) (13)  $C_2H_5NO$  ( $^1A$ ) (14)  $C_2H_5NO$  ( $^1A$ ) (15)  $C_3H_7NO$  ( $^1A$ ) (16)  $C_3H_7NO$  ( $^1A$ ) (17)  $C_3H_7NO$  ( $^1A$ ) (18)  $C_4H_9NO$  ( $^1A$ ) (19)  $CH_4N_2O$  ( $^1A$ ) (20)  $CH_4N_2O$  ( $^1A$ ) (21)  $CH_4N_2O$  ( $^1A$ ) (22)  $CH_5N_3O$  ( $^1A$ ) (23)  $CH_5N_3O$  ( $^1A$ ) (24)  $CH_5N_3O$  ( $^1A$ ) (25)  $CH_6N_4O$  ( $^1A$ ).

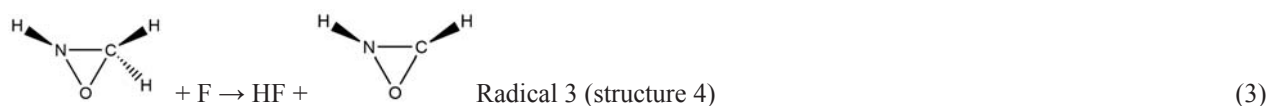
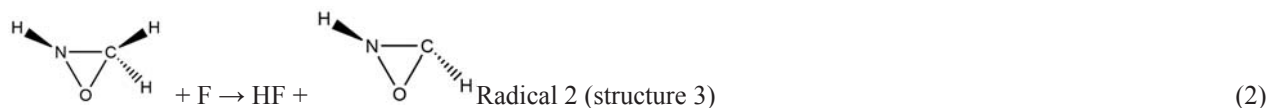
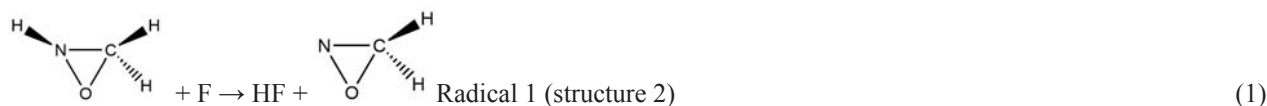
Oxaziridine derivatives were first discovered by Emmons [1]. A series of N-protected oxaziridines as electrophilic amination reagents were studied by Vidal et al. [2, 3] and Armstrong and Cooke [4]. Armstrong and Draffan researched on intramolecular epoxidation in oxaziridines [5]. Oxyfunctionalization of nonactivated sites were studied by Arnone et al. [6]. Research on synthesis and properties of 3, 3-disubstituted N-sulfonyloxaziridine [7] have been worked by Davis and et al. Also they investigated the kinetics and mechanism of the oxidation of oxaziridines [8] and their applications in organic synthesis [9].

Transition states of epoxidation and stereo selectivity in oxaziridines were investigated by Houk and et al. [10]. Oxaziridines have been studied as intermediate and their activation has been investigated [11, 12]. Oxygen and nitrogen typically act as nucleophiles due to their high electronegativity that lead to weak N-O bond. Unusual reactivity of oxaziridine is due to the highly strained three-membered ring and the relatively weak N-O bond.

Because of unstable nature of oxaziridine structure, most of studies have been implemented on oxaziridine derivatives [13] and oxaziridine as intermediate [14]. Some theoretical studies have been carried out on oxaziridine [ $c\text{-CH}_3\text{NO}$  ( $X^1\text{A}$ )] [15, 16]. All structures have been showed in Figure 1. Optimized structures with B3LYP/6-311++G(d,p) have been represented in Figure S1 (*Supplementary material*).

### Computational details

In this study oxaziridine [ $c\text{-CH}_3\text{NO}$  ( $X^1\text{A}$ )] (structure 1) reaction with fluorine atom (F) has been presumed that produce HF and a radical [ $c\text{-CH}_2\text{NO}$  ( $X^2\text{A}$ )], and possible reactions are presented in Eq.(1), Eq.(2) and Eq.(3). One of the oxaziridine hydrogen atoms has been removed by F atom. Three probable cyclic radical have been produced.



All geometries have been optimized by Density Functional B3LYP method with 6-311++G (d, p) basis set. Use of this basis set is ordinary for C, H, N, and O and obtained results are in good agreement with experimental ones [17].

Vertical Ionization Energy (*VIE*), Adiabatic Ionization Energy (*AIE*), global hardness ( $\eta$ ), global softness (*S*), chemical potential ( $\mu$ ), electronegativity ( $\chi$ ) and electrophilicity ( $\omega$ ) have been calculated. Natural bond orbital (*NBO*) analysis has been used for study of oxaziridine and its radicals and derivatives. Changes in free energy and chemical potential for reactions (1)–(3) were calculated. It can be noted that results of calculations belong to the gas phase. Before this, MP2 and B3LYP have been used for ring opening study [18]; B3LYP has been used for study of interaction between chemical species [19] and for study of complex compounds [20]. The effect of substituted groups on bond strength in ring and vertical ionization energy has been studied. For finding weak bond in molecule and radicals, *NBO* charges, and population analysis have been used. Geometry and structure parameters have been used by Arnold and Carpenter [18] for study of ring opening in cyclopropyl radical and cyclopropyl cation.

In this study Cl has been used as electron withdrawing group, and  $\text{NH}_2$  and  $\text{CH}_3$  groups have been used as electron donor groups. All calculations were performed with the GAMESS program suite [21].

### Results and discussion

#### Structures

#### Oxaziridine ( $c\text{-CH}_3\text{NO}$ ) Molecule and $c\text{-CH}_2\text{NO}$ radicals

Geometry of oxaziridine (structure 1) and three radicals were optimized. Optimized geometries are presented in Table S1 (*Supplementary material*) and Figure S1. Important structural parameters have been presented in Table 1. Results are in good agreement with the results of Turecek et al. [16]. Vibrational frequencies have been computed for all optimized structures to ensure that the local minima had no imaginary frequencies and the excited species had one.

C-O bond in radical 1 (structure 2) is longer than this bond in oxaziridine, but in radicals 2 (structure 3) and 3 (structure 4) this bond is smaller than molecule C-O. C-N-O angle is against C-O bond. This angle increased in radical 1 but decreased in radicals 2 and 3. This evidence shows that C-O bond is weak in radical 1 in comparison with oxaziridine molecule and radicals 2 and 3. C-N bond decreased some deal in all radicals. N-O-C angle increased a little in radical 1 and decreased a little in radicals 2 and 3. N-O bond length decreased in radical 1 and increased in radicals 2 and 3.

O-C-N angle that against N-O bond decreased in radical 1 and increased in radicals 2 and 3. In radical 1 N-O bond length is near to double bond and this bond can be viewed as N=O.

Table 1

Comparison of ring structure in compounds, calculated by B3LYP/6-311++G (d,p).

Structure	Bond lengths (Å)			Bond angles (°)		
	C-O	C-N	O-N	OCN	CNO	CON
1	1.398	1.436	1.496	63.7	56.9	59.4
2	1.426	1.429	1.383	58.0	60.9	61.1
3	1.347	1.414	1.544	68.0	54.0	58.1
4	1.348	1.409	1.541	67.9	54.1	57.9
5	1.365	1.421	1.522	66.2	55.2	58.7
6	1.369	1.424	1.513	65.6	55.5	59.0
7	1.408	1.445	1.436	60.4	58.5	61.0
8	1.377	1.439	1.468	62.8	56.5	60.7
9	1.378	1.448	1.481	63.2	56.1	60.7
10	1.350	1.419	1.530	67.0	54.3	58.6
11	1.359	1.450	1.498	64.4	54.9	60.8
12	1.403	1.438	1.499	63.7	57.0	59.3
13	1.404	1.440	1.497	63.5	57.0	59.4
14	1.405	1.425	1.499	64.0	57.4	58.7
15	1.410	1.429	1.501	63.8	57.5	58.7
16	1.409	1.433	1.502	63.8	57.3	58.9
17	1.410	1.443	1.499	63.4	57.2	59.4
18	1.417	1.439	1.501	63.4	57.6	59.0
19	1.409	1.427	1.516	64.6	57.1	58.3
20	1.386	1.450	1.516	64.6	55.7	59.8
21	1.391	1.421	1.648	71.7	53.3	55.0
22	1.402	1.442	1.522	64.7	56.4	59.0
23	1.314	1.529	2.022	90.3	40.5	49.1
24	1.369	1.437	1.768	78.1	49.3	52.7
25	1.310	1.530	2.038	91.4	40.0	48.6

H3-C-H4 angle in radicals are some larger than this angle in oxaziridine. Order of ring angles in oxaziridine is: OCN > CON > CNO. That depict O-N bond is weak.

Order of ring angles in radical 1 is: CON > CNO > OCN. The decreasing of N-O bond length in radical 1 and comparison of radical 1 ring angles with oxaziridine angles show that N-O bond in radical 1 strengthen.

Orders of ring angles in radicals 2 and 3 are: OCN > CON > CNO. Study on bond length and angles in these radicals and compare them with correspondent bonds and angles in oxaziridine show that N-O bond weaken and indeed this bond is broken and ring is opened. This result is in good agreement with other results [2-4, 15, 16, 18].

### Cations structure

For calculation of adiabatic ionization energy (AIE) the geometry optimization has been carried out for cations. Optimized geometries of cations are presented in Table S1 (*Supplementary material*). Results are in good agreement with the Tureceket et al. work [16].

#### Oxaziridine in comparison with its positive ion:

H3-C-H4 angle in ion is larger than this angle in molecule. C-O bond and C-N-O angle increase in cation. In comparison with oxaziridine, C-N bond and C-O-N angle in ion have not important change. N-O bond in cation is shorter than this bond in oxaziridine and O-C-N angle is smaller than this angle in molecule. This evidence presents that N-O bond strengthen in cation in comparison with this bond in oxaziridine. This leads to decreasing of N-O bond cleavage probability, but C-O bond weaken.

#### Radical 1 in comparison with its positive ion:

H3-C-H4 in ion is larger than this angle in radical. C-O bond length and C-N-O angle in cation increase. C-N bond and C-N-O angle do not show important change in comparison with radical 1. N-O bond and N-C-O angle in cation decrease. This evidence shows that N-O bond in cation strengthen but C-O bond weaken.

#### Radical 2 in comparison with its positive ion:

C-O bond length and C-N-O angle in cation decrease. C-N bond length and C-N-O angle in cation decrease too. But N-O bond length and N-C-O angle in cation increase. In cation C-O and C-N bonds shortened, but N-O bond weaken and most probable bond breaking happen for N-O bond that leads to ring opening.

*Radical 3 in comparison with its positive ion:*

C-O bond length and C-N-O angle decrease in cation. C-N bond and C-N-O angle in cation decrease too. But N-O bond length and N-C-O angle in cation increase. C-O and C-N bonds strengthen and N-O bond weaken and breaking in cation, that leads to ring opening. In comparison with  $C_3H_7^+$  with C-C bond length 1.4 Å and 1.8 Å [22]; ring bonds in oxaziridine radical cations are small.

*Cl, NH<sub>2</sub> and methyl derivatives structures*

For comparison, ring structure, C-O, C-N and N-O bond lengths and corresponding angles in oxaziridine ring were presented in Table 1. Cl acts as electron withdrawing group and NH<sub>2</sub> and CH<sub>3</sub> act as electron donating groups. In c-CH<sub>2</sub>NOCl (structures 5, 6 and 7) Cl acts as electronegative atom. In these compounds C-N bond do not show important change in comparison with oxaziridine (structure 1). C-O bond strengthen in structures 5 and 6 but do not has important change in structure 7. N-O bond length in structures 5 and 6 are longer than bond length in structure 1, but decrease of this bond in structure 7 shows that N-O bond strengthen in this structure. Because of Cl electronegativity, negative charge on N atom decrease and repulsion between N and O decrease. No important changes have been seen in c-CHNOC<sub>l</sub><sub>2</sub> (structures 8, 9 and 10) and c-CNOC<sub>l</sub><sub>3</sub> (structure 11) bond lengths and bond angles.

Also, c-CH<sub>2</sub>NOCH<sub>3</sub> (structures 12, 13 and 14), c-CHNOC<sub>2</sub>H<sub>6</sub> (structures 15, 16 and 17) and c-CNOC<sub>3</sub>H<sub>9</sub> (structure 18) do not show important changes in bond lengths and bond angles.

In c-CH<sub>2</sub>NONH<sub>2</sub> (structures 19, 20 and 21) C-O bond do not have important change, C-N bond shortened and strengthen, but N-O bond can be larger than structure 1. This means that N-O bond are weak in structures 19, 20 and 21 in comparison with structure 1. In c-CHNON<sub>2</sub>H<sub>4</sub> (structures 22, 23 and 24) C-O bond length in 22 is near to C-O bond length in 1 but in 23 and 24 this bond length decrease and bond strengthen. C-N bond in 23 in comparison with 1 is large and weak. This bond length in 22 and 24 is near to 1 amount. N-O bond length in 22, 24 and special in 23 is longer than 1. Bond lengths and angles in structure 25 are similar to 23. In both of them NN linkage are double bond and do not exist N-O bond. This means that structures 23 and 25 do not exist. Optimum geometry of them was presented in Figure 2.

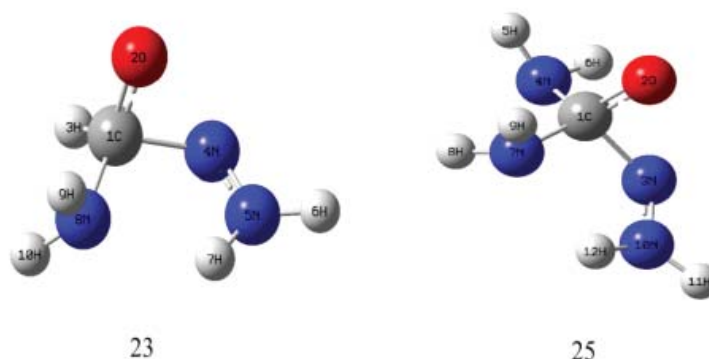


**Figure 2. Optimum geometry of (23) CH<sub>5</sub>N<sub>3</sub>O and (25) CH<sub>6</sub>N<sub>4</sub>O with double bond and cleavage ring.**

It should be noted that bond lengths 1.492 Å for N-O, 1.420 Å for C-O and 1.460 Å for C-N have been seen in almost stable structure (CHPhNCOOCH<sub>3</sub>O) [2]. But 2.02 Å and 1.035 Å for N-O, 1.47 Å and 1.801 Å for C-O and 1.39 Å and 1.357 Å for C-N have been reported for transition states [10, 23]. In a work on photochemical and thermal rearrangement of oxaziridines bond lengths of N-O, C-O and C-N is 1.535 Å, 1.428 Å and 1.456 Å respectively [24]. Furthermore in theoretical study of the mechanisms of iron-catalyzed amino hydroxylation reactions, 1.48 Å, 1.41 Å and 1.46 Å have been reported for N-O, C-O and C-N bond length respectively in N-sulfonyloxaziridine [12].

*Atomic charge*

It is possible to note that the values of Mulliken charges on atoms are substantially different from those obtained in the NBO analysis. Along with this, it should be noted that it is difficult to judge about the orders of the corresponding bonds by the overlap population values [25].

Atomic charges are presented in Table S2 (*Supplementary material*). N, O and C atoms make ring. N and O atoms have negative charge but carbon atom has positive charge. Negative charge on O atom in three radical deal some decreases in comparison with oxaziridine. Positive charge on C atom decreases in radical 1 but increase in radicals 2 and 3. Considering charges on N atom in oxaziridine molecule and radicals depict that nitrogen charge in radical 1 decreases, but in radicals 2 and 3 increases a little.

Severe decrease of negative charge on nitrogen atom in radical 1 shows that most of this charge share with neighboring atoms and strengthen C-N and O-N bonds. Dipole moment shows the molecular charge distribution and



is given as a vector in three dimensions. It can depict the charge movement across the chemical species depends on the center of charges [26]. In oxaziridine dipole moment vector is oriented to C-H bond, in radical 1 is oriented to C atom, in radicals 2 and 3 is oriented to C-N bond. In radical 1 negative charge contributed with neighbouring atoms and dipole moment oriented to carbon. But in radicals 2 and 3, dipole moment is oriented to C-N bond. Decreasing of negative charge on O and N atoms in radical 1 (structure 2) cause the N-O bond strengthen.

Molecular electrostatic potential (*MEP*) gives many data about the electrostatic effect produced by total charge distribution of the chemical space [27]. It also depicts the relative polarity of the molecule [28]. An electronic density isosurface mapped with electrostatic potential surface show the size, shape, charge density and reactive sites of the molecules [27]. *MEP* and the electronic density are related together; it is a useful descriptor to indicate sites for electrophilic and nucleophilic reactions [29-31].

To study on reactive sites for electrophilic and nucleophilic attack the molecular electrostatic potential (*MEP*) were calculated using DFTB3LYP method and 6-311++G(d,p) basis set for optimum geometry of compounds. The negative part of *MEP* was related to electrophilic reactivity (presented by red and yellow), the positive part to nucleophilic reactivity (shown by blue) and green represents regions of zero potential [27] (Figure 3). In oxaziridine (structure 1) the negative regions are on oxygen and nitrogen atoms, at the same time the hydrogen atoms are positive. In structures 2, 3 and 4, the negative charge on O and N atoms is weaker than in structure 1, but they are obedient of structure 1 charge order. In Cl derivatives of oxaziridine (structures 5-11) the chlorine atom contribute to decreasing of negative charge on O and N in molecules and the most of negative regions are presented in green (zero potential), but hydrogen remain positive. In structure 11 chlorine atoms give some positive charge.

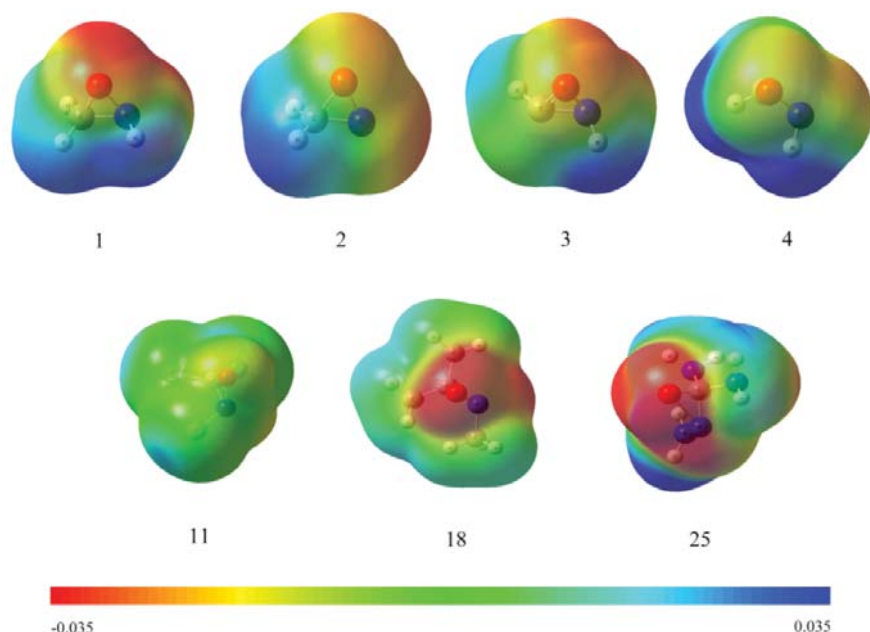


**Figure 3. Molecular electrostatic potential map calculated by B3LYP/6-311++G(d,p) method. Only structures 1, 2, 3, 4, 11, 18 and 25 have been shown.**

In the methyl derivatives of oxaziridine (structures 12-18), the methyl group have been amplified negative charge on O and N atoms, in comparison with Cl derivatives. In the  $\text{NH}_2$  derivatives of oxaziridine (structures 19-25) the negative charge mostly are on oxygen atom and nitrogen atom in ring, but when the number of  $\text{NH}_2$  groups is increasing the negative charge on the nitrogen ring is decreasing. In all cases the positive charge are on hydrogen atoms (when exist).

### HOMO-LUMO

*HOMO* is defined as the outer occupied orbital, containing electrons that can donate electrons and *LUMO* is defined as the inner unoccupied orbital, containing free places to accept electrons. Considering *HOMO* coefficients in oxaziridine molecule and radicals depict that O and N atomic orbitals have important contribution in *HOMO*. Also in radical 1 O and N atoms are important, but in radicals 2 and 3 C and O atoms have important contribution in *HOMO*. This evidence shows that N atomic orbitals contribution decreases in radicals 2 and 3, and N-O bonds weaken.

In oxaziridine cation the most important orbitals for produce *HOMO* are O and N atomic orbitals; that show N-O bond strengthen in ion in comparison with this bond in oxaziridine. This leads to decrease probability of N-O bond cleavage, but C-O bond weaken.



In radical 1 the atomic orbitals of O and N atoms have important contribution in *HOMO*, but in its cation furthermore O and N atoms, atomic orbitals of carbon have important role in *HOMO* producing. With considering foregoing cases, N-O bond in cation strengthen but C-O bond weaken in cation. In radical 2 and its cation in optimum geometry, the most important atomic orbitals in radical 2 that make *HOMO* are C and O atomic orbitals. But in cation, O and N atomic orbitals are important. In this case C-O and C-N bonds in ion are shortened, but N-O bond is weaken and most probability for ring opening is produced by break of N-O bond. In radical 3 the atomic orbitals of O and C are important in *HOMO*, but in its cation atomic orbitals of O and N are important in *HOMO*. In this case C-O and C-N bonds strengthen and N-O bond weaken in ion and ring opening probably happen because of N-O bond breaking.

The energy gap of *HOMO* and *LUMO* shows the chemical activity of the molecule. A chemical species with a larger *HOMO*–*LUMO* gap have less reactivity than one having a smaller gap [32]. Large *HOMO*–*LUMO* energy gap means high excitation energies for many of excited states [29]. The value of the *HOMO*–*LUMO* energy separation are 7.14 eV, 7.02 eV, 5.44 eV and 5.42 eV for oxaziridine, radicals 1, 2 and 3, respectively, for  $\alpha$  spin orbitals radicals and 6.63 eV, 5.63 eV and 5.76 eV for  $\beta$  spin orbitals in radicals 1, 2 and 3, respectively, (values from B3LYP/6-311++G (d, p)). Oxaziridine and radical 1 have large *HOMO*–*LUMO* energy gap in comparison with radicals 2 and 3. Oxaziridine and radical 1 are relatively stabler than radicals 2 and 3. Difference between *HOMO*–*LUMO* energies are presented in Table 2. More data can be finding in Table S3 (*Supplementary material*).

Isodensity plots of the frontier molecular orbitals and energy levels of the *HOMO* and *LUMO* orbitals computed by B3LYP/6-311++G (d,p) method for Oxaziridine and for radicals 1, 2 and 3 are presented in Figure 4 and Figures S2, S3 and S4 (*Supplementary material*), respectively. Energy gap for chlorinated oxaziridines in structures 5, 6 and 10 is higher than oxaziridine (structure 1) and in structures 7, 8, 9 and 11 is smaller than of structure 1.

Table 2

Difference between *HOMO* and *LUMO* energy (eV) calculated using B3LYP/6-311++G(d,p).

Structure	Spin	$ \varepsilon_{HOMO} - \varepsilon_{LUMO} $	Structure	$ \varepsilon_{HOMO} - \varepsilon_{LUMO} $
1		7.14	12	7.01
2	$\alpha$	7.02	13	7.05
	$\beta$	6.63	14	6.93
3	$\alpha$	5.44	15	6.81
	$\beta$	5.63	16	6.54
4	$\alpha$	5.42	17	6.82
	$\beta$	5.76	18	6.40
5		7.34	19	6.53
6		7.54	20	6.42
7		5.90	21	6.58
8		6.07	22	6.54
9		5.91	23	4.12
10		7.20	24	5.49
11		5.98	25	4.04

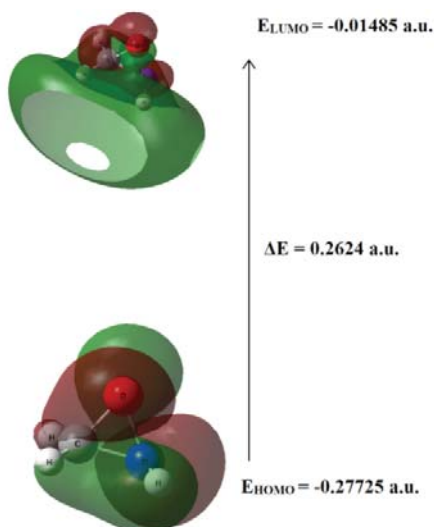


Figure 4. Isodensity plots of the frontier molecular orbitals of oxaziridine.

For methyl derivatives of oxaziridine, *HOMO-LUMO* energy gap are near and some deal smaller than structure 1 energy gap. Energy gap in  $\text{NH}_2$  derivatives decreases in comparison with structure 1. Specially 23 and 25 structures energy gap are smaller than energy gaps in radicals 1, 2 and 3. Structures 23 and 25 have not ring and  $\text{N}=\text{N}$  is a double bond (Figure 2).

### NBO analysis

The *NBO* analysis have been carried out using B3LYP level of theory with 6-311++G (d,p) basis set. Selected natural bond orbital occupancies of oxaziridine and related radicals are presented in Table S4 (*Supplementary material*). Also these results for other compounds have been presented in Table S5 (*Supplementary material*). *NBO* results have been reported for both  $\alpha$  and  $\beta$  spin for radicals [33, 34]. *NBO* occupancies have been used for identified  $\pi$  character of bonds. *NBO* occupancies show that in radical 1 N-O bond have  $\pi$  character and this bond strengthen in comparison with oxaziridine N-O bond, but C-O bond in radical 1 weaken, and similar to oxaziridinyl methyl radical ring opening of radical 1 by C-O bond cleavage favoured over other bonds in ring [35]. In radicals 2 and 3 C-O bond has  $\pi$  character and strengthened, but N-O bond weaken. This highlights the ring cleavage in radical 1 due to C-O bond breaking, but in radicals 2 and 3 because of N-O bond breaking ring opened. In other structures the bonds that make ring have single bond, except structures 23 and 25. In these structures N-O bond is broken and NN connection is double bond. Table S6 (*Supplementary material*) shows selected second order perturbation theory analysis of Fock Matrix in *NBO* Basis for structures 1-25 that calculated by B3LYP/6-311++G (d, p) method. Interaction between different parts has been studied by them.

According to this data, O2-N5 has been weaken by C1-O2 as in structures. Interactions between them in structure 2 have been weakened and leads to N-O bond strengthen. In structures 5-11 lone pair on Cl atom interacts with bonds that chlorine connect to one of the bond composer atom in ring. When methyl group connects to nitrogen on of C-H bond as donor *NBO* can affect the bonds in ring while the carbon of methyl connect to composer atom and weaken it some deal. For example in structures 14, 15, 16 and 18 C-H bond as donor impress on N-O bond in ring. Look like above,  $\text{NH}_2$  impress on neighbouring bonds. In 23 and 25 lone pair of nitrogen atom in  $\text{NH}_2$ -C as donor in *cis* position of  $\text{N}=\text{N}$  has been weaken N-H bond in  $\text{N}=\text{N}$ . Furthermore, interaction between  $\text{BD}^*(2) \text{N}=\text{N}$  and  $\text{BD}^*(1) \text{N}=\text{N}$  cause the  $\text{N}=\text{N}$  bond strengthen.

### Quantum chemical parameters

Vertical ionization energy (*VIE*) and adiabatic ionization energy (*AIE*) were calculated for oxaziridine and three radicals. The vertical ionization energy is defined as the energy difference between the molecule in its ground state and the ion in a particular electronic state, but with the nuclei in the same positions as they had in the neutral molecule.

According to Franck-Condon principle, a vibronic transition happen so fast that nuclear positions don't change. The most intense vibrational component is said to be due to a vertical ionization, because it most closely corresponds to the vertical transition in a classical picture of the Franck-Condon principle [36]. It is to be noted that not in all cases the Franck-Condon transition is the most intensive one. The Jahn-Teller effect can bring some essential complications so that the Franck-Condon transition manifests itself as a deep well in the band shape, for example in the singlet-doublet transition [37].

Adiabatic transitions are often seen in photoelectron spectra as the first vibrational lines in the different bands [38]. *AIE* is the energy of the thermal transition between the neutral molecule in its electronic, vibrational and rotational ground state and the ion in the lowest vibrational and rotational level of a particular electronic state.

*VIE* has been calculated as the difference between the total energies of the neutral molecule or radical and the cation at same structure with parent molecule or radical (cation without geometry optimization). *AIE* has been computed as the total energy differences between the neutral molecule or radical and the cation at the optimum geometry.

$$VIE = E_{\text{total}}(\text{Ion in radical Z-matrix}) - E_{\text{total}}(\text{molecule or radical in optimum Z-matrix}) \quad (4)$$

$$AIE = E_{\text{total}}(\text{Ion in optimum Z-matrix}) - E_{\text{total}}(\text{molecule or radical in optimum Z-matrix}) \quad (5)$$

*VIE* and *AIE* of the oxaziridine and three radicals are presented in Table S7 (*Supplementary material*). Turecek et al. [16] results are in good agreement with the DFT results in this work. The difference between *VIE* and *AIE* is a crude measure of the degree of distortion of the molecule caused by ionization. The stabilization energy is equivalent to the difference between the vertical and adiabatic ionization energy for a normal band [38].

The difference between *VIE* and *AIE* is 0.92 eV, 0.64 eV, 1.45 eV and 1.50 eV for oxaziridine and radicals 1, 2 and 3, respectively. This result reveals that radical 1 cation has most likeness with parent radical (radical 1) among four structures and don't have many distortions by ionization. After radical 1 cation, cations from oxaziridine and radicals 2 and 3 have less different between cation and parent chemical species. *VIEs* have been calculated and presented in Table S8 (*Supplementary material*). In radicals 2 and 3 (structures 3 and 4) *VIE* decreases in comparison with oxaziridine and radical 1 (structures 1 and 2), because of less electronegativity in carbon atom.

In Cl substituted oxaziridines, chlorine acts as electron-withdrawing group and increases the *VIE*, but NH<sub>2</sub> and CH<sub>3</sub> act as electron donor groups that decrease the *VIE*. NH<sub>2</sub> is more powerful electron donor than methyl and the decreasing of *VIE* in NH<sub>2</sub> derivatives is more severe than of methyl derivatives (Figure 5).

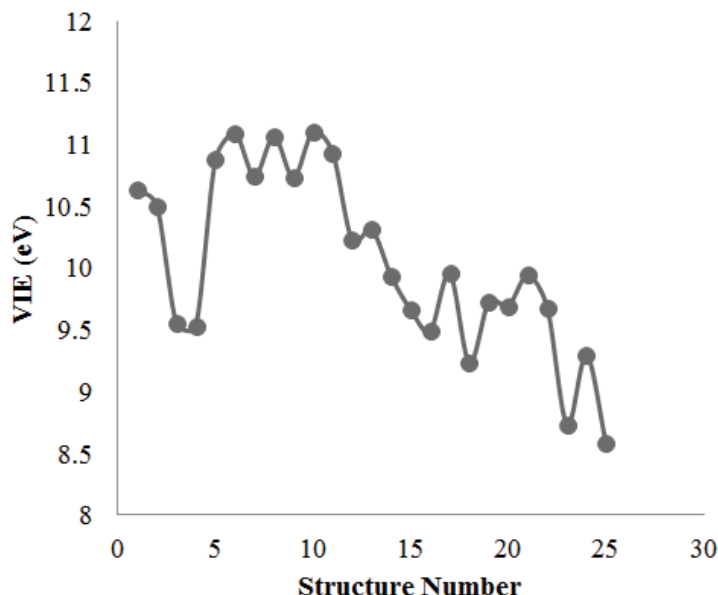


Figure 5. Effects of substituted groups (Cl, CH<sub>3</sub> and NH<sub>2</sub>) on *VIE* (eV).

Furthermore, some quantum chemical parameters are calculated: ionization potential (Eq.(6)), electron affinity ((Eq.(7)), absolute electronegativity (Eq.(8)), global hardness (Eq.(9)) and global softness, *S* or  $\sigma$ , (Eq.(10)) [39].

$$IP = VIE \quad (6)$$

$$EA = VAE \quad (7)$$

$$\chi = \frac{IP+EA}{2} \quad (8)$$

$$\eta = \frac{IP-EA}{2} \quad (9)$$

$$S = \frac{1}{\eta} \quad (10)$$

*VIE* (vertical ionization energy) and *VAE* (vertical electron affinity) have been used for ionization potential and electron affinity, respectively. *VAE* was calculated as the difference between the total energies of the neutral molecule or radical and the anion at same structure with parent molecule or radical (anion without optimization geometry).

Chemical potential (Eq.(11)) is defined as the negative of the electronegativity [40]. The propensity of an electrophile to accept electrons is measured in terms of the electrophilicity within a relative scale, which is generally considered to be a kinetic quantity. Global electrophilicity index (Eq.(12)) was introduced by Parret et al. [38].

$$\mu = -\chi \text{ Or } \mu = \frac{-(IP+EA)}{2} \quad (11)$$

$$\omega = \frac{\mu^2}{2\eta} \quad (12)$$

The electrophilicity index encompasses both, the propensity of the electrophile to acquire an additional electronic charge driven and the resistance of the system to exchange electronic charge with the environment [41]. Jaque et al. [42] related the electrophilicity to electron population. The electrophilicity values follow the hardness trend.

The quantum chemical parameters of the oxaziridine and of three radicals are presented in Table S9 (*Supplementary material*).

The values of softness and hardness show that radicals 2 and 3 are softer than oxaziridine and radical 1. The changes in free energies were calculated through difference between reactants and products [43] for oxaziridine reaction with F atom (reactions 1-3). Results are presented in Table 3. Free energies were obtained from vibrational frequency calculations. These results show that reaction 1 is thermodynamically most probable than reactions 2 and 3.

Table 3

**Free energy change (kJ mol<sup>-1</sup>) of the reactions (1), (2) and (3), B3LYP method and 6-311++G (d, p) basis set have been used, (1Hartree = 627.5095 kcal/mol = 2625.499748 kJ/mol).**

	Free energy changes
Reaction 1	-232/16
Reaction 2	-138/68
Reaction 3	-133/30

### Fukui functions

Fukui functions are one of the local reactivity descriptors that explain the chemical reactivity at a particular site of chemical species [44]. Fukui indices are reactivity indices and give information about which atoms in a chemical system have a larger tendency to either lose or accept an electron that means nucleophilic or electrophilic attack, respectively. The Fukui function is defined as (Eq.(13)):

$$f(r) = \frac{\delta \rho(r)}{\delta N} r \quad (13)$$

where  $\rho(r)$  is the electronic density,  $N$  is the number of electrons,  $r$  is the external potential that rooted from the nucleus.

The Fukui function indicates the preferred regions where a chemical species will change its density when the number of electrons is modified [45]. Therefore, it indicates the desire of the electronic density to deform at a certain position upon accepting or denoting electrons [46, 47]. Atomic Fukui functions on the  $k^{\text{th}}$  atom site is defined as [45]:

$$f_k^+ = q_k(N + 1) - q_k(N) \quad \text{for nucleophilic attack} \quad (14)$$

$$f_k^- = q_k(N) - q_k(N - 1) \quad \text{for electrophilic attack} \quad (15)$$

$$f_k^0 = \frac{1}{2} [q_k(N + 1) - q_k(N - 1)] \quad \text{for radical attack} \quad (16)$$

Where +, - and 0 represent nucleophilic, electrophilic and radical attack, respectively. Also  $q_k$  is the atomic charge (calculated from Mulliken population analysis) at the  $k^{\text{th}}$  atomic site is the neutral ( $N$ ), anionic ( $N + 1$ ) or cationic ( $N - 1$ ) chemical species. To calculate the Fukui function, the atomic charges have been calculated by Mulliken population analysis (*MP4*). Molecular geometry has been optimized by DFTB3LYP/6-311++G(d,p) method for molecule and used for *MP4* in molecule, cation and anion; with respect of charge and multiplicity. Fukui functions have been represented in Table 4 for oxaziridine (structure 1). This table shows negative values of the Fukui function.

Table 4

**Values of the Fukui function calculated by B3LYP/6-311++G(d,p) according to Eq.(14-16).**

Atom	$f_k(+)$	$f_k(-)$	$f_k(0)$
C 1	2.7895	0.0472	1.4183
O 2	-0.0852	-0.4051	-0.2451
H 3	-1.6041	-0.1270	-0.8656
H 4	-0.9829	-0.1209	-0.5519
N 5	-0.3508	-0.2786	-0.3147
H 6	-0.7664	-0.1157	-0.4411

Negative Fukui function value means that when adding an electron to the molecule, in some spots, the electron density is reduced. Alternatively, when removing an electron from the molecule, in some spots, the electron density is increased [48]. In order to solve the negative value of Fukui functions some attempts have been made by different researchers [49-51].

Kolandaivel et al. [52] introduced the atomic descriptor to characterize the local reactive sites of the chemical system. In the present study, the optimized molecular geometry has been used in single-point energy calculations, which have been performed for the anions and cations of oxaziridine (structure 1) using the ground state with doublet multiplicity. Table 4 shows the  $f_k$  values for the oxaziridine. It shows that C1 has higher  $f_k^-$  value in comparison with other atoms that indicates C1 is the possible site for electrophilic attack. The calculated  $f_k^+$  value predicts that the possible site for nucleophilic attack is C1 and the radical attack was predicted at C1 site, too. By comparison of the three kinds of attacks, it has been observed that nucleophilic attack has bigger reactivity related to the radical and electrophilic attack.

## Conclusions

Ab initio and DFT calculations have been performed for oxaziridine [ $c\text{-CH}_3\text{NO}$  ( $X^1\text{A}$ )], three cyclic radicals [ $c\text{-CH}_2\text{NO}$  ( $X^2\text{A}$ )] and Cl,  $\text{NH}_2$  and methyl derivatives of oxaziridine. Geometries have been optimized. Bonds length and angles show that in radical 1 C-O bond weaken and in radicals 2 and 3 N-O bonds weaken, that lead to bond breaking and ring opening. Population analysis had been carried out and results confirm geometry optimization results. Some quantum chemical parameters were calculated. Radicals 2 and 3 are softer than radical 1. Free energy and chemical potential changes have been calculated for three reactions that show reaction 1 is thermodynamically most probable. All foregoing cases depict that ring opening happened because of C-O, N-O and N-O bonds cleavage in radicals 1, 2 and 3, respectively; and make cyclic radical 1 more probable than cyclic radicals 2 and 3 in oxaziridine reaction with F atom. These radicals are short life time species, among them radical 1 is more stable than radicals 2 and 3, because radicals 2 and 3 have large global softness in comparison with radical 1.

Cl atom acts as electron withdrawing group. When Cl atom conjuncts to N atom in oxaziridine ring, it forms the stable ring structure with strengthen weak bond N-O.  $\text{NH}_2$  acts as electron donating group. Specifically, when two  $\text{NH}_2$  groups bonded to N and C atoms in ring in *cis* position the ring structure has been destroyed, because of N-O cleavage and N=N double bond has been made. Electron withdrawing group (Cl) on N strengthen N-O bond, but Cl on C weaken N-O bond. 2 and 3 Chlorine atoms substituted on triangle don't make important change on N-O strength (in some cases weaken N-O bond a little). Electron donating groups ( $\text{NH}_2$  and  $\text{CH}_3$ ) weaken N-O bond in triangle.

In oxaziridine derivatives electron-withdrawing group (Cl) vertical ionization energy (*VIE*) increases but in electron donor groups *VIE* decreases. Calculation for Fukui functions shows that nucleophilic attack has bigger reactivity related to the radical and electrophilic attack on C1 atom.

## References

- Emmons, W.D. The Preparation and properties of oxaziranes. *Journal of the American Chemical Society*, 1957, 79, pp. 5739-5754.
- Vidal, J.; Damestoy, S.; Guy, L.; Hannachi, J.C.; Aubry, A.; Collet, A. N-Alkyloxycarbonyl-3-aryloxaziridines: their preparation, structure, and utilization as electrophilic amination reagents. *Chemistry - A European Journal*, 1997, 3, pp.1691-1709.
- Vidal, J.; Hannachi, J.C.; Hourdin, G.; Mulatier, J.C.; Collet, A. N-Boc-3-trichloromethyloxaziridine: a new, powerful reagent for electrophilic amination. *Tetrahedron Letters*, 1998, 39, pp. 8845-8848.
- Armstrong, A.; Cooke, R.S. Efficient amination of sulfides with aketomalonate-derived oxaziridine: application to [2, 3]-sigmatropic rearrangements of allylic sulfimides. *Chemical Communications*, 2002, pp. 904-905.
- Armstrong, A.; Draffan, A.G. Intramolecular epoxidation in unsaturated ketones and oxaziridines. *Journal of the Chemical Society, Perkin Transactions*, 2001, 1, pp. 2861-2873.
- Arnone, A.; Foletto, S.; Metrangolo, P.; Pregnotato, M.; Resnati, G. Highly Enantiospecific Oxyfunctionalization of Nonactivated Hydrocarbon Sites by Perfluoro-*cis*-2-*n*-butyl-3-*n*-propyloxaziridine. *Organic Letters*, 1999, 1, pp. 281-284.
- Davis, F.A.; Towson, J.C.; Vashi, D.B.; Reddy, T.; McCauley, J.P.; Harakal, M.E.; Gosciniak, D.J. Chemistry of Oxaziridines. 13. ' Synthesis, Reactions and Properties of 3-Substituted 1, 2-Benzisothiazole 1, 1-Dioxide Oxides. *The Journal of Organic Chemistry*, 1990, 55, pp. 1254-1261.
- Davis, F.A.; Chattopadhyay, S.; Towson, J.C.; Lal, S.; Reddy, T. Chemistry of Oxaziridines. 9. ' Synthesis of 2-Sulfonyl- and 2-Sulfamoyloxaziridines Using Potassium Peroxymonosulfate (Oxone). *The Journal of Organic Chemistry*, 1988, 53, pp. 2087-2089.
- Davis, F.A.; Sheppard, A.C. Applications of oxaziridines in organic synthesis. *Tetrahedron*, 1989, 45, pp. 5703-5742.
- Houk, K.N.; Liu, J.; DeMello, N.C.; Condroski, K.R. Transition states of epoxidation: diradical character, spiro geometries, transition state flexibility, and the origins of stereoselectivity. *Journal of the American Chemical Society*, 1997, 119, pp. 10147-10152.



11. Srivastava, R.M.; Pereira, M.C.; Faustino, W.W. M.; Coutinho, K.; dos Anjos, J. V.; de Melo, S. J. Synthesis, mechanism of formation, and molecular orbital calculations of arylamidoximes. *Monatshefte fur Chemie*, 2009, 140, pp. 1319-1324.
12. Ren, Q.; Guan, S.; Shen, X.; Fang, J. Density Functional Theory Study of the Mechanisms of Iron Catalyzed Aminohydroxylation Reactions. *Organometallics*, 2014, 33, pp. 1423-1430.
13. Couche, E.; Fkyerat, A.; Tabacchi, R. Asymmetric Synthesis of the cis- and trans-3, 4-Dihydro-2, 4, 8-trihydroxynaphthalen-1(2H)-ones. *Helvetica Chimica Acta*, 2003, 86, pp. 210-221.
14. Seebach, D.; Yoshinari, T.; Beck, A.K.; Ebert, M.O.; Castro-Alvarez, A.; Vilarrasa, J.; Reiher, M. How small amounts of impurities are sufficient to catalyze the interconversion of carbonyl compounds and iminium ions, or is there a metathesis through 1, 3-oxazetidinium ions experiments, speculations and calculations. *Helvetica Chimica Acta*, 2014, 97, pp. 1177-1203.
15. Oliveros, E.; Riviere, M.; Malrieu, J.P.; Teichtel, C. Theoretical exploration of the photochemical rearrangement of oxaziridines. *Journal of the American Chemical Society*, 1979, 101, pp.318-322.
16. Turecek, F.; Polasek, M.; Sadilek, M. High-energy [C, H3, N, O] cation radicals and molecules. *International Journal of Mass Spectrometry*, 2000, 195-196, pp. 101-114.
17. Jankovic, N.; Bugarcic, Z.; Markovic, S. Double catalytic effect of  $(\text{PhNH}_3)_2\text{CuCl}_4$  in a novel, highly efficient synthesis of 2-oxo and thioxo-1, 2, 3, 4-tetrahydropyrimidines. *Journal of the Serbian Chemical Society*, 2015, 80, pp. 595-604.
18. Arnold, P.A.; Carpenter, B.K. Computational studies on the ring openings of cyclopropyl radical and cyclopropyl cation. *Chemical Physics Letters*, 2000, 328, pp. 90-96.
19. Spataru, T.; Fernandez, F. Hydrogen molecule interaction with  $\text{CpCr}(\text{Co})_3$  Catalyst. *Chemistry Journal of Moldova*, 2012, 7, pp. 21-26.
20. Gorinchoy, N.N.; Dobrova, B.; Gorbachev, M.Yu.; Munteanu, G.; Ogurtsov, I.Ya. Activation of Acetylene by Coordination to Bis-Triphenylphosphine Complex of Pt (0): DFT Study. *Chemistry Journal of Moldova*, 2009, 4, pp. 123-128.
21. Hasanzadeh, N.; Nori-Shargh, D. Correlations between hardness, electronegativity, anomeric effect associated with electron delocalizations and electrostatic interactions in 1, 4, 5, 8-tetraoxadecalin and its analogs containing S and Se atoms. *Computational and Theoretical Chemistry*, 2015, 1051, pp. 1-9.
22. Tulub, A.V.; Simon, K.V. Molecular fragmentation on collision with protons for Freon and propane molecules. *Journal of Structural Chemistry*, 2007, 48, pp. S79-S93.
23. Davis, F.A.; Chen, B.C. Asymmetric hydroxylation of enolates with N-suifonyloxaziridines. *Chemical Reviews*, 1992, 92, pp. 919-934.
24. Lattes, A.; Oliveros, E.; RiviBre, M.; Belzecki, C.; Mostowicz, D.; Abramskj, W.; Piccinni-Leopardi, C.; Germain, G.; Van Meerssche, M. Photochemical and Thermal Rearrangement of Oxaziridines: Experimental Evidence in Support of the Stereo electronic Control Theory. *Journal of the American Chemical Society*, 1982, 104, pp. 3929-3934.
25. Sliznev, V.V.; Belova, N.V.; Girichev, G.V. An *ab initio* study of the electronic and geometric structure of bis-of dipivaloylmethane with manganese, iron, and cobalt. *Journal of Structural Chemistry*, 2010, 51, pp. 622-634.
26. Balachandran, V.; Lalitha, S.; Rajewari, S. Rotational isomers, density functional theory, vibrational spectroscopic studies, thermodynamic functions, NBO and HOMO-LUMO analyses of 2, 6-Bis (chloromethyl) pyridine. *Spectrochimica Acta, Part A*, 2012, 97, pp. 1023-1032.
27. Thul, P.; Gupta, V.P.; Ram, V.J.; Tandon, P. Structural and spectroscopic studies on 2-pyranones. *Spectrochimica Acta, Part A*, 2010, 75, pp. 251-260.
28. Balachandran, V.; Rajeswari, S.; Lalitha, S. Vibrational spectral analysis, computation of thermodynamic functions for various temperatures and NBO analysis of 2, 3, 4, 5-tetrachlorophenol using *ab initio* HF and DFT calculations. *Spectrochimica Acta, Part A*, 2013, 101, pp. 356-369.
29. Tanak, H. Quantum chemical computational studies on 2-methyl-6-[2-(trifluoromethyl) phenyliminomethyl] phenol. *THEOCHEM*, 2010, 950, pp. 5-12.
30. Luque, F.J.; Lopez, J.M.; Orozco, M. Perspective on "Electrostatic interactions of a solute with a continuum. A direct utilization of *ab initio* molecular potentials for the prevision of solvent effects". *Theoretical Chemistry Accounts*, 2000, 103, pp. 343-345.
31. Okulik, N.; Jubert, A.H. Theoretical analysis of the reactive sites of non-steroidal anti-inflammatory drugs. *Internet Electronic Journal of Molecular Design*, 2005, 4, pp. 17-30.
32. Padmaja, L.; Ravi Kumar, C.; Sajan, D.; Hubert Joe, I.; Jaya Kumar, V.S.; Pettit, G.R.; Nielsen, O.F. Density functional study on the structural conformations and intramolecular charge transfer from the vibrational spectra of the anticancer drug combretastatin-A2. *Journal of Raman Spectroscopy*, 2009, 40, pp. 419-428.
33. Sizova, O.V.; Skripnikov, L.V.; Sokolov, A.Y.; Lyubimova, O.O. Features of the electronic structure of ruthe-



- nium tetracarboxylates with axially coordinated nitric oxide (II). *Journal of Structural Chemistry*, 2007, 48, pp. 28-36.
34. de Aguiar, I.; Lima, F.C.A.; Ellena, J.; Malta, V.R.S.; Carlos, R.M. Study of the phenanthroline-Mn-imidazole bonding in Mn (I) triscarbonyl complex: A X-ray and DFT computational analysis. *Computational and Theoretical Chemistry*, 2011, 965, pp. 7-14.
  35. Pasto, D. J. Ab initio theoretical studies on the ring-opening modes of the oxiranyl-, aziridinyl-, oxaziridinyl-, and thiaranylmethyl radical systems. *Journal of Organic Chemistry*, 1996, 61, pp. 252-256.
  36. Ellis, A.M.; Feher, M.; Wright, T.G. *Electronic and Photoelectron Spectroscopy: Fundamentals and Case Studies*. Cambridge University Press: Cambridge, 2005, 286 p.
  37. Perlin, Yu. E.; Tsukerblat, B. S. Optical Bands and Polarization Dichroism of Jahn-Teller Centers, in: *Dynamical Jahn-Teller Effect in Localized Systems*. Elsevier Publications: Amsterdam, 1984, pp. 251-346.
  38. Eland, J.H.D. *Photoelectron spectroscopy: an introduction to ultraviolet photoelectron spectroscopy in the gas phase*, Butterworths, 1984, pp. 105-122.
  39. Muthu, S.; Renuga, S. Molecular orbital studies (hardness, chemical potential, electronegativity and electrophilicity), vibrational spectroscopic investigation and normal coordinate analysis of 5-{1-hydroxy-2-[(propan-2-yl)amino]ethyl}benzene-1,3-diol. *Spectrochimica Acta, Part A*, 2014, 118, pp. 683-694.
  40. Iczkowski, R.P.; Margrave, J. V. Electronegativity. *Journal of the American Chemical Society*, 1961, 83, pp. 3547-3551.
  41. Campodonico, P.R.; Aizman, A.; Contreras, R. Group electrophilicity as a model of nucleofugality in nucleophilic substitution reactions. *Chemical Physics Letters*, 2006, 422, pp. 340-344.
  42. Correa, J.V.; Jaque, P.; Olah, J.; Toro-Labbe, A.; Geerlings, P. Nucleophilicity and electrophilicity of silylenes from a molecular electrostatic potential and dual descriptor perspectives. *Chemical Physics Letters*, 2009, 470, pp. 180-186.
  43. Arsene, I. The theoretical study of some reactions with the participation of O & H and HO & 2 radicals. *Chemistry Journal of Moldova*, 2008, 3, pp. 109-113.
  44. Yang, W.; Parr, R.G. Hardness, softness, and the Fukui function in the electronic theory of metals and catalysis. *Proceedings of the National Academy of Sciences of the United States of America*, 1985, 82, pp. 6723-6726.
  45. Sheela, N.R.; Sampathkrishnan, S.; Thirumalai Kumar, M.; Muthu, S. Quantum mechanical study of the structure and spectroscopic, first order hyperpolarizability, Fukui function, NBO, normal coordinate analysis of Phenyl-N-(4-Methyl Phenyl) Nitro. *Spectrochimica Acta, Part A*, 2013, 112, pp. 62-77.
  46. Ayers, P.W.; Parr, R.G.J. Variational Principles for Describing Chemical Reactions: The Fukui Function and Chemical Hardness Revisited. *Journal of the American Chemical Society*, 2000, 122, pp. 2010-2018.
  47. Parr, R.G.; Yang, W.J. Density functional approach to the frontier-electron theory of chemical reactivity. *Journal of the American Chemical Society*, 1984, 106, pp. 4049-4050.
  48. Demircioglu, Z.; Albayrak Kastas, C.; Buyukgungor, O. The spectroscopic (FTIR, UV-vis), Fukui function, NLO, NBO, NPA and tautomerism effect analysis of (E)-2-[(2-hydroxy-6-methoxybenzylidene) amino] benzonitrile. *Spectrochimica Acta, Part A*, 2015, 139, pp.539-548.
  49. Roy, R. K.; Hirao, H.; Krishnamurthy, S.; Pal, S. Mulliken population analysis based evaluation of condensed Fukui function indices using fractional molecular charge. *Journal of Chemical Physics*, 2001, 115, pp. 2901-2907.
  50. Bultinck, P.; Carbo-Dorca, R.; Langenaekar, W. Negative Fukui functions: New insights based on electronegativity equalization. *Journal of Chemical Physics*, 2003, 118, pp. 4349-4356.
  51. Bultinck, P.; Carbo-Dorca, R.; Negative and Infinite Fukui Functions: The Role of Diagonal Dominance in the Hardness Matrix. *Journal of Mathematical Chemistry*, 2003, 34, pp. 67-74.
  52. Kolandaivel, P.; Praveen, G.; Selvarengan, P. Study of atomic and condensed atomic indices for reactive sites of molecules. *Journal of Chemical Sciences*, 2005, 117, pp. 591-598.

# THE SURFACE PHOTOCHEMISTRY OF PROCYMIDONE IN PRESENCE OF AMMONIUM FERRIC CITRATE

Ivan Osipov

*Institute of Chemistry of Academy of Sciences of Moldova, 3, Academiei str., Chisinau MD-2028, Republic of Moldova  
e-mail: osipov\_i@yahoo.com; phone: (+373) 692 45 899*

**Abstract.** The knowledge of the behaviour and fate of pesticides after their application is very important from the environmental, human health and economical points of view. The problem of pesticide residues on fruits is of major concern. Procymidone was chosen as the model compound and its phototransformation was followed under sunlight irradiation. The main photodegradation products on silica are: 3,5-dichloroaniline and 3,5-dichlorophenyl isocyanate.

The use of ammonium ferric citrate can enhance the degradation of procymidone.

**Keywords:** procymidone, ammonium ferric citrate, silica, phototransformation.

*Received: September 2015/ Revised final: October 2015/ Accepted: October 2015*

## Introduction

Natural solid-gas interfaces, such as soil and vegetation, can accumulate some globally relevant pollutants, such as Persistent Organic Pollutants (POPs) and chemicals coming from chemical spills or resulting from applications with a specific purpose. Surfaces are, in most cases, the first contaminated environmental compartment and from which the generalized spread of organic pollutants takes place. A particular case is that of pesticide applications. They are needed to actuate on the surfaces during a certain period of time, but after this they become unwanted compounds and their residues should be removed. Photodegradation is recognized to be one of the major dissipation pathways of pesticides on solid surfaces under natural conditions [1]. Due to high agriculture impact and necessity of treatment in harvest close period, especially for wine production area, we have chosen procymidone as a model fungicide. The diffuse reflectance ground state absorption spectra of procymidone on silica showed the expected absorption band between 250 and 290 nm (see Figure 1). Under natural conditions, only the solar radiation above 290 nm arrives to the earth surface. Low overlap with the absorption of procymidone on silica occurs and therefore low direct photodegradation rates are expected under solar irradiation. Presence of additives, like ammonium ferric citrate, allows us to increase the photodegradation pathway by absorption of sunlight irradiation above 300 nm. From the ground state absorbance of impregnated on silica procymidone with addition of ammonium ferric citrate as photosensitizer under sunlight irradiation (Figure 1), one can conclude, that the indirect phototransformation represents the main photodegradation pathway.

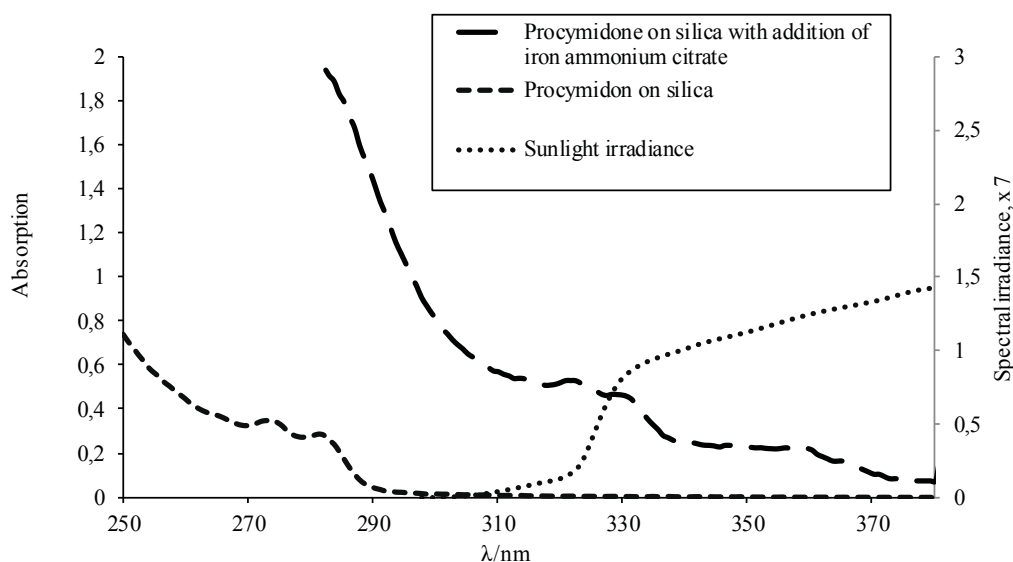


**Figure 1.** Normalized ground-state absorption spectra registered for impregnated on silica procymidon.

In this field, advanced oxidation processes (AOPs) represent an important potential [3]. Iron aqua complexes are involved in formation of hydroxyl radical species *via* electron processes from excitation into ligand to metal charge transfer band [4]. Ammonium ferric citrate was used due to good iron solubilisation in the Fenton and photo-Fenton processes. Ammonium ferric citrate can be used at pH values up to 9.0 [5], therefore field experiments in neutral pH can also be performed. In order to gain more insights into the process of procymidone phototransformation in the presence of ammonium ferric citrate, it is important to compare photoproducts of the impregnated on silica procymidone with its photodegradation products obtained after addition of ammonium ferric citrate. The acceleration of phototransformation of procymidone in the presence of ammonium ferric citrate is expected to take place.

## Materials and methods

### Materials

Ammonium ferric citrate (Aldrich); Procymidon (Fluka); cellulose DSO (Fluka); silica (60 Å) (Merck); methanol, ethanol, acetonitrile (Merck Lichrosolv) were used without further treatment. Water was distilled and deionized.

### Sample preparation

Samples of impregnated on silica procymidone were initially prepared by using the solvent evaporation method. The final concentration of procymidone was determined by extracting the samples with methanol (a known weight of sample in a known volume of solvent), followed by centrifugation and HPLC analysis. All samples (10, 20, 50, 100 and 400 mg/100 g silica) were prepared by mechanical mixture. To the correspondent amount of solid support the prepared samples were added, followed by magnetic stirring during 3 days. The final concentration of procymidone was determined by using HPLC.

### Irradiation conditions

Photolysis studies were conducted in a system previously used to study pesticides and 4-chlorophenol [6]. The 254 nm radiation was obtained using a 16 W low-pressure mercury lamp (Applied Photophysics) without filters and without refrigeration. The photodegradation kinetics and product formation studies, under lamp and sunlight irradiation, were made by using samples prepared by spreading the solid powder on glass microscope slides (~50 mg spread on ~10cm<sup>2</sup>) covered with quartz slides. The edges of the slides were then sealed with parafilm to prevent the losses by volatilization. The samples used for the volatilization studies were prepared in the same way, but were kept opened (without the cover slide) in the dark. All the experiments were repeated three times.

The sunlight irradiation studies were performed in Algarve (South Portugal, latitude: 37° N, longitude: 8° W) in July and August. After irradiation procymidone residue and its photoproducts were extracted with methanol. The solar radiation was monitored using an International Light IL 700 A Research Radiometer, equipped with a SEE240 #3358 detector, a W # 6237 diffuser and a UVB #12813 filter.

### Diffuse reflectance ground state absorption spectra

Ground state absorption spectra of the solid powdered samples were recorded using a Cintra 40 GCB Scientific Equipment spectrophotometer, with a diffuse reflectance attachment. The measured reflectance was used to calculate the remission function using the Kubelka-Munk equation.

## Results and discussion

In order to determine concentration of procymidone all samples were first analyzed by HPLC. Figure 2 presents the GS-MS traces of the impregnated on silica procymidone after 5 hrs of sunlight irradiation with addition of ammonium ferric citrate and without additive. Samples were extracted with ethanol (ammonium ferric citrate is insoluble in ethanol).

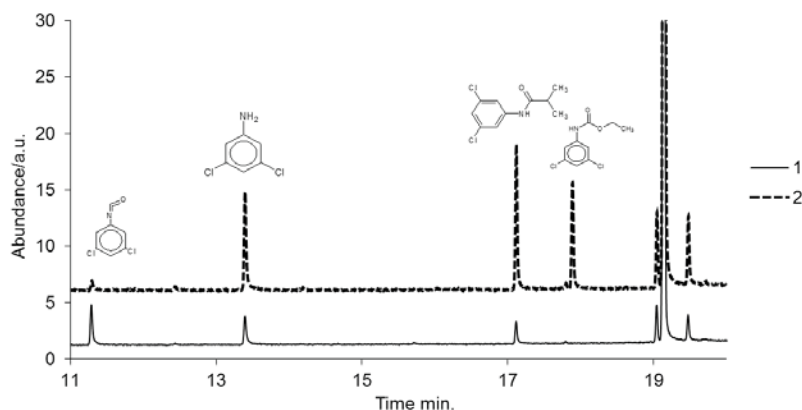


Figure 2. Normalized GS-MS traces of procymidone after 5 hrs of sunlight irradiation without additive (1) and with addition of ammonium ferric citrate (2).

The main photoproducts of indirect phototransformation of procymidone in the presence of ammonium ferric citrate as photosensitizer on silica are: 3,5-dichlorophenyl isocyanate, 3,5-dichloroaniline and N-(3,5-dichlorophenyl)-2-methylpropanamide. The degradation photoproducts of procymidone in the presence of ammonium ferric citrate are identical to the products of its phototransformation without additives. A product with retention time of 18 min is formed in reaction of 3,5-dichlorophenyl isocyanate with ethanol, which was used for extraction. We have established that in the samples with addition of ammonium ferric citrate, after 5 hours of sunlight irradiation 75 % of procymidone remained unchanged, in comparison with the samples, which were placed in the same conditions, but without photosensitizer.

## Conclusions

In the course of our investigations it was shown, that by using ammonium ferric citrate as photosensitizer the indirect phototransformation of impregnated on silica procymidone under sunlight irradiation at neutral pH increased up to 25% decay in 5 hours. The obtained in these conditions phototransformation products are identical to those formed *via* natural pathway.

## Acknowledgments

I would like to acknowledge and express my sincere gratitude to my scientific adviser Acad. Gheorghe Duca for continuous guidance and encouragement throughout every process of my research. Also I would like to thank Dr. José Paulo Da Silva, for his valuable and constructive suggestions during planning and development of this research work.

## References

1. Leifer, A. The Kinetics of Environmental Aquatic Photochemistry. ACS Professional Reference Book: Washington, 1988, 336 p.
2. Da Silva, J.P.; Vieira Ferreira, L.F.; Oliveira, A.S. Photochemistry of 4-chlorophenol on cellulose and silica. *Environmental Science & Technology*, 2003, 37, pp. 4798-4803.
3. Legrini, O.; Oliveros, E.; Braun, A. M. Photochemical processes for water treatment. *Chemical Reviews*, 1993, 49, pp. 671-698.
4. Brand, N.; Mailhot, G.; Bolte, M. Degradation photoinduced by Fe(III): method of alkylphenoethoxylates removal in water. *Environmental Science & Technology*, 1998, 32, pp. 2715-2720.
5. Zepp R.G.; Faust, B.C.; Hoigne, J. Hydroxyl radical formation in aqueous reactions (pH 3-8) of iron(II) with hydrogen peroxide: the photo-Fenton reaction. *Environmental Science & Technology*, 1992, 26, pp. 313-319.
6. Da Silva, J.P.; Vieira Ferreira, L.F.; Osipov, I.; Machado, I.F. Surface photochemistry of pesticides containing 4-chlorophenoxy chromophore. *Journal of Hazardous Materials*, 2010, 179, pp. 187-191.

## MODIFICATION OF CARBONACEOUS ADSORBENTS WITH MANGANESE COMPOUNDS

Irina Ginsari<sup>a</sup>, Larisa Postolachi<sup>a</sup>, Vasile Rusu<sup>a</sup>, Oleg Petuhov<sup>a</sup>, Tatiana Goreacioc<sup>a,b</sup>,  
Tudor Lupascu<sup>a</sup>, Raisa Nastas<sup>a\*</sup>

<sup>a</sup>Institute of Chemistry of Academy of Sciences of Moldova, 3, Academiei str., Chisinau MD-2028, Republic of Moldova

<sup>b</sup>Institute of Ecology and Geography of Academy of Sciences of Moldova, 1, Academiei str.,

Chisinau MD-2028, Republic of Moldova

\*e-mail: nastasraisa@yahoo.com

**Abstract.** Four series of samples containing manganese supported carbonaceous adsorbents were prepared. Samples of series AC-B, synthesised from the carbonaceous support with basic surface, were obtained with a yield of 50-60%, while manganese was loaded in amount of 1.44-1.65 % depending on applied method. The samples of series AC-A, synthesised from the carbonaceous support with acidic surface, were obtained with a higher yield (92-98%), but with small quantities of loaded manganese. Obtained results reveal the importance of surface chemistry of carbonaceous adsorbents on the manganese loading.

**Keywords:** active carbon, modification, manganese, surface chemistry, thermal treatment.

*Received: October 2015/ Revised final: October 2015/ Accepted: November 2015*

### Introduction

It is well known that modification of carbonaceous adsorbents with metal oxides improves their physico-chemical characteristics, influencing the catalytic activity in redox reactions. A number of catalysts consisted of various transition metal oxides (Co, Ni, Mn, Fe, Cu etc.) on active carbons have been studied for removal/oxidation of hydrogen sulphide, ammonium ions, dyes etc. [1-5]. Among these catalysts, manganese oxides supported on active carbons have attracted much interest due to their high catalytic activities.

Various active manganese state and dispersion of particles can be obtained using different precursors and preparation methods [2,6,7]. Different quantities of loaded manganese on active carbon have been obtained depending on initial concentration of the precursor solution [7]. Thermal treatment (autoclave or furnace, under oxic or anoxic conditions) also are important parameters exploited by researchers [2,6]. However, any reports about the dependence between the surface chemistry of carbonaceous adsorbents and amount of loaded manganese are not presented in the literature.

The aim of this work was to highlight the influence of surface chemistry of carbonaceous adsorbents on the manganese oxides loading.

### Experimental

#### Materials

In this study a commercially available activated carbon with basic surface (Norit®), designated as AC-B, and a sample of active carbon with acidic surface obtained by chemical activation method [8], designated as AC-A, have been used. All the chemical reagents used in this study were of analytical grade.

#### Samples

Four series of samples containing manganese were prepared, supported on carbonaceous adsorbents (particle size 0.8-1.3 mm). The carbonaceous adsorbents were impregnated with an aqueous solution of manganese salt (at a solid/liquid ratio equal to 10) for ca. 24 h, followed by treatment with an alkaline solution to generate manganese hydroxide within carbon pores. Dried samples (110°C) were subjected to thermal treatment at different temperatures (300, 450, 600°C) to obtain manganese oxides. Obtained samples were washed several times with distilled water to remove soluble species and dried at 110°C.

#### Characterization methods

Prior characterization measurements the active carbon samples were dried at 110°C for 3 h.

**Elemental analysis (C, H, N, Cl, S)** was carried out by the Elemental Analysis group of the Institute of Chemistry of Academy of Sciences of Moldova.

The **content of metals** was determined by atomic absorption spectroscopy (AAS-1N, Laboratory of Atomic Spectroscopy of the Institute of Chemistry of A.S.M.).

The **ash content** of the samples was determined by burning off the carbon at 700°C for 2 h.

The **pH of the samples** has been evaluated by determination of pH value of active carbon suspension (10 g of dried sample/100 mL of distilled water) equilibrated for 24 h [9].



**Thermal analysis measurements** were performed using a Derivatograph Q-1000 analyzer. The samples were heated from room temperature up to 1000 °C in a flowing air atmosphere (100 mL/min) at a heating rate of 10 °C/min.

## Results and discussion

Active carbons used for impregnation with manganese ions are very different concerning surface chemistry and ash content. Sample AC-B has higher content of ash due to compounds of calcium, magnesium and iron, and has a basic surface pH (9.5) (Table 1). Sample AC-A has only traces of ash (0.29%, Table 1) and an acidic surface (pH 4.0).

Table 1

Humidity, ash content and analyses of mineral matters of initial active carbon samples.

Sample	Humidity, wt%	Ash, wt%	Constituents in mineral matter (wt%)							
			CaO	MgO	Fe <sub>2</sub> O <sub>3</sub>	MnO <sub>2</sub>	CuO	Cr <sub>2</sub> O <sub>3</sub>	NiO	ZnO
AC-B	4.09	7.24	3.34	0.85	0.490	0.016	0.002	0.001	0.001	0.001
AC-A	10.72	0.29	-	-	0.004	0.001	0.001	0.001	0.001	-

The initial samples, as well as the modified by impregnation with manganese salts were subjected to thermal analysis in order to choose the treatment temperatures. Initial sample AC-B is quite stable till around 450 °C and then the sample buns out (Figure 1). TGA curves of the modified samples (AC-B-0, AC-B-A) show an initial weight loss of about 10-14% around 100 °C, which is related to thermo-desorption of physically adsorbed water. For series of AC-B samples, impregnation with manganese salts leads to the decomposition of the carbonaceous support. Above 325 °C TGA curves show a drastic decrease in weight of these samples (Figure 1).

Thermo-gravimetric curves (TGA) of AC-A series samples are presented in Figure 2. All samples show generally similar thermal behaviour: weight losses of ca. 7-15 % around 100 °C, most probably due to thermo-desorption of physically adsorbed water; above ca. 450 °C the burning of the carbon skeleton occurs.

Summarizing, the temperatures of 300, 450 and 600 °C have been chosen for thermal treatment of impregnated samples. After thermal treatment obtained samples were washed. Thermal treated samples of series AC-B were obtained with a yield of 50-60% and manganese was loaded in amount of 1.44-1.65 % depending on applied method (Table 2). The samples of series AC-A were obtained with a higher yield (92-98 %), but with small quantities of loaded manganese, and don not contain chloride ions (Table 3).

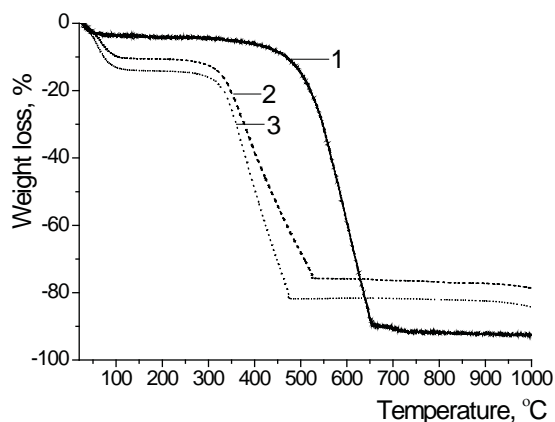


Figure 1. TGA curves measured in air for unmodified AC-B (1) and modified AC-B-0 (2), AC-B-A (3) samples.

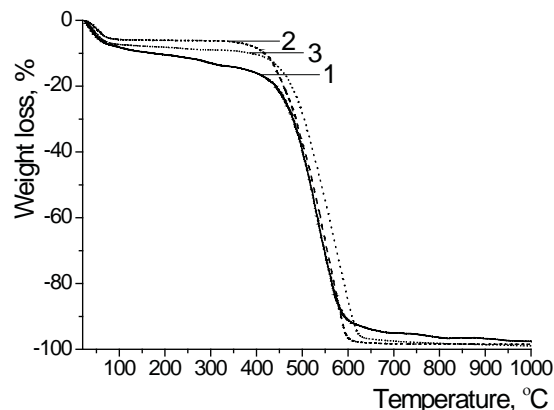


Figure 2. TGA curves measured in air for unmodified AC-A (1) and modified AC-A-A (2), AC-A-Ac (3) samples.

Table 2

Physical-chemical characteristics of manganese modified samples.

Sample	Description	$\eta$ , %	Humidity, %	Ash, %	Mn, %
AC-B-0	Obtained by impregnation with manganese (ii) chloride solution, followed by treatment at 300 °C.	56.33	8.65	7.08	1.65
AC-B-A	Obtained by impregnation with acidulated manganese (ii) chloride solution, followed by treatment at 300 °C.	56.00	7.00	4.57	1.44
AC-A-A	Obtained by impregnation with acidulated manganese (ii) chloride solution, followed by treatment at 300 °C.	96.40	5.86	0.81	0.51
AC-A-Ac	Obtained by impregnation with manganese (ii) acetate solution, followed by treatment at 300 °C.	97.20	5.65	0.54	0.22

Table 3

**Elemental analyses of active carbon samples (wt%, determined on dry and ash free basis).**

<i>Sample</i>	<i>C</i>	<i>H</i>	<i>N</i>	<i>S</i>	<i>Cl</i>
<b>AC-B</b>	91.34	1.90	-	2.57	traces
<b>AC-B-0</b>	90.56	1.83	-	-	-
<b>AC-B-A</b>	85.62	1.49	-	-	-
<b>AC-A</b>	89.60	3.06	-	-	-
<b>AC-A-A</b>	88.28	2.28	-	-	-
<b>AC-A-Ac</b>	88.63	2.51	-	-	-

Present work highlights the influence of surface chemistry of carbonaceous adsorbents on the manganese oxides loading. Following researches will be focused on the determination of the oxidation state of the supported manganese phases  $Mn_xO_y$ , dispersion of the manganese oxide particles, and evaluation of physical-chemical characteristics of modified adsorbents.

### Conclusions

Obtained results reveal the importance of surface chemistry of carbonaceous adsorbents on the manganese loading. Samples of series AC-B, synthesised from the carbonaceous support with basic surface, were obtained with a yield of 50-60% while manganese was loaded in amount of 1.44-1.65% depending on applied method. The samples of series AC-A, synthesised from the carbonaceous support with acidic surface, were obtained with a higher yield (92-98%), but with small quantities of loaded manganese.

### Acknowledgements

The present work was performed within Joint Moldova-Belarus Project "Supported catalysts for underground water treatment: synthesis, properties and using" (No. 15.820.18.02.04/B, 2015-2016).

### References

1. Tseng, H.-H.; Wey, M.-Y.; Fu, Ch.-H. Carbon materials as catalyst supports for  $SO_2$  oxidation: catalytic activity of CuO-AC. *Carbon*, 2003, 41, pp. 139-149.
2. Andreev, A.; Prahov, L.; Gabrovska, M.; Eliyas, A.; Ivanova, V. Catalytic oxidation of sulphide ions to elementary sulphur in aqueous solutions over transition metal oxides. *Applied Catalysis B: Environmental*, 1994, 8, pp. 365-373.
3. Lupascu, T.; Nastas, R.; Rusu, V. Treatment of sulfurous waters using activated carbons. In: Duca, Gh. Ed. *Management of Water Quality in Moldova*. Springer International Publishing: Switzerland, 2014, pp. 209-224.
4. Lupascu, T.; Ciobanu, M.; Botan, V.; Gromovoy, T.; Cibotaru, S.; Petuhov, O.; Mitina T. Study of hydrogen sulfide removal from groundwater. *Chemistry Journal of Moldova*, 2013, 8(1), pp. 37-42.
5. Lupascu, T.; Ciobanu, M. Adsorption of ammonia ions and ammonium from aqueous solutions on modified activated carbons. *Chemistry Journal of Moldova*, 2008, 3(2), pp. 55-57.
6. Wang, J.; Qiu, B.; Han, L.; Feng, G.; Hu, Y.; Chang, L.; Bao, W. Effect of precursor and preparation method on manganese based activated carbon sorbents for removing  $H_2S$  from hot coal gas. *Journal of Hazardous Materials*, 2012, 213–214, pp. 184–192.
7. Safieh, K.A.; Al-Degs, Y.S.; Sunjuk, M.S.; Saleh, A.I.; Al-Ghouti, M.A. Selective removal of dibenzothiophene from commercial diesel using manganese dioxide-modified activated carbon: a kinetic study. *Environmental Technology*, 2015, 36(1), pp. 98-105.
8. Lupascu, T.; Nastas, R. Procedure for obtaining of active carbons from vegetal raw materials and phosphates as supplement. MD Patent, 2004, No. 2496 (in Romanian).
9. Goreacioc, T. Oxidation and characterization of active carbon AG-5. *Chemistry Journal of Moldova*, 2015, 10(1), pp. 76-83.

# COORDINATION COMPOUNDS OF OXOVANADIUM(IV) BASED ON S-METHYLISOTHIOSEMICARBAZIDE AS DYES FOR THERMOPLASTIC POLYMERS

Maria Cocu\*, Stefan Manole

Institute of Chemistry of Academy of Sciences of Moldova, 3, Academiei str., Chisinau MD-2028, Republic of Moldova

\*e-mail: mariacocu@gmail.com

**Abstract.** The colouring properties of two coordination compounds previously synthesized by us: 8-(1',2'-naphthyl)-1-R-3-methyl-6-thiomethyl-4,5,7-triazanona-1,3,5,7-tetraenato-1,1'-diolato(-)-O<sup>1</sup>, O<sup>1'</sup>, N<sup>4</sup>, N<sup>7</sup>-vanadyl, where R=CH<sub>3</sub> (**1**), C<sub>6</sub>H<sub>5</sub> (**2**) have been investigated. These compounds meet the requirements to be used as dyes for thermoplastic polymers. Colouring complexes have a high photostability (7 points), thermostability (>250 °C) and an intensity of colour, which give a low consumption (0.006 to 0.015 g medium tone, 0.020-0.100 g to 100 g polystyrene intense tone and 0.005 to 0.010 g medium tone and 0.015-0.035 g intense tone for 100 g polyethylene). The investigated compounds stained polystyrene and polyethylene in claret-brick. Compound **2** has a higher thermostability (365 °C) than compound **1** (285 °C).

**Keywords:** coordination compounds, oxovanadium(IV), dyes, thermoplastic polymer.

Received: March 2015/ Revised final: October 2015/ Accepted: October 2015

## Introduction

Colour is an integral part of the plastic material and it should not be considered as an afterthought. The colorants that are used in the plastics industries can be both dyes and pigments. Dyes must be very strong, transparent and show good heat stability. In the plastics industry dyes are limited in use; therefore they can only be used for a selected number of resins.

Aromatic azo compounds have found a broad spectrum of applications, such as dyes, pigments, food additives, indicators, radical reaction initiators and therapeutic agents [1]. These compounds are mainly used as dyes for textile fibers, wood, wool, leather, metal foil and plastic, also exhibiting a variety of useful properties for biomedical applications [2].

Recently, considerable effort has been dedicated to the synthesis of azo coordination compounds based on Schiff-base ligands, due to their mixed soft-hard donor character (O, N and S donor sites), versatile coordination behaviour [3] and diverse pharmacological properties [4], optical and thermal properties [5], biological properties [6] and their possibility of being used as dyes [7].

The most widely used metal-complex dyes are derived from azo compounds. Although they deliver a multitude of shades, only a few basic components are necessary to produce metal-complex azo dyes.

The template method, where the central ion guides the assembly of polydentate ligands, has an important role in the synthesis of coordination compounds [8]. A number of complex compounds, primarily of transition metals, involving thiosemicarbazones of different denticity, have been prepared and investigated [9]. The condensation of salicylaldehyde thiosemicarbazone with salicylaldehyde in the presence of 3d- elements has changed the thiosemicarbazide functionalized synthetic possibilities (with a coordinating node MN<sub>2</sub>O<sub>2</sub>). Previously, 3d - element compounds containing thiosemicarbazide (selenosemicarbazidic) block and anthranilic aldehyde [8, 9], acetylacetone S-alchilzotiosemicarbazone and anthranilic aldehyde [10], acetyl(benzoyl) acetone S-alchilzotiosemicarbazones and 1-hydroxy-2- naphthaldehyde were studied [11]. The use of these blocks lead to the diverse sets of coordinated atoms: N<sub>4</sub> [8], N<sub>5</sub> [12], N<sub>4</sub>O [9], N<sub>2</sub>O<sub>4</sub> [13], N<sub>2</sub>O<sub>2</sub> [14] and N<sub>3</sub>O [15]. The coordination mode of thiosemicarbazidic fragment depends on the geometry of the assembling species and is governed by stereochemical preferences of central ion.

In view of the foregoing discussion and continuing interest in coordination chemistry, our present work describes the colouring properties of two mononuclear open-chain complexes, containing N<sub>2</sub>O<sub>2</sub> set of donor atoms, previously obtained by us *via* condensation of acetyl(benzoyl)acetone S-methylisotiosemicarbazone with 1-hydroxy-2-naphthaldehyde on the matrix of oxovanadium (VOSO<sub>4</sub>•3H<sub>2</sub>O): 8-(1',2'-naphthyl)-1-R-3-methyl-6-thiomethyl-4,5,7-triazaocta-1,3,5,7-tetraenato-1,1'-diolato(-)-O<sup>1</sup>, O<sup>1'</sup>, N<sup>4</sup>, N<sup>7</sup>-vanadyl(II) [16], where R=CH<sub>3</sub> **1**, C<sub>6</sub>H<sub>5</sub> **2** (Figure 1).

Structures of complexes **1** and **2** were characterized by elemental analyses, IR, UV-Vis, <sup>1</sup>H and <sup>13</sup>C NMR spectroscopies and mass spectrometry. Complexes were obtained as fine dark-brown crystalline powder, insoluble in water, methanol, slightly soluble in chloroform, soluble in dimethylsulfoxide and dimethylformamide [11].

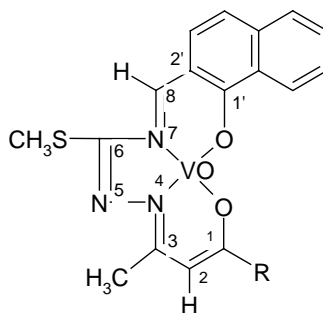
Study of some practical properties of these compounds showed, that they can be used in various fields. The influence of compounds **1** and **2** on the biosynthesis of pectolytic enzymes by *Penicillium viride* fungus has been studied, through the variation of their concentration in the nutrient medium. The obtained results indicated that the presence of tested compounds induces the biomass accumulation and increases the enzymatic activity. It was established, that by

adding the compounds at a concentration of 5 mg/L to the culture medium, the pectolytic activity increases with *cca* 14 %, in comparison with the control solution [11].

## Results and discussion

A series of compounds with the above-mentioned formula, which differ only by the metal nature, have been studied as dying agents for plastics [13]. It was established, that the colour tone is greatly influenced by the metal atom and is insignificantly influenced by the nature of radical R: nickel(II) compounds colour polystyrene and polyethylene in claret, cobalt(II) compounds - in green with yellow tint, copper(II) compounds - in deep red with yellow tint [17].

The produced compounds have a high thermostability (>250°C), photostability (7 points), migration luminescence, stability and physical-mechanical processing. Given the mentioned properties and both the diversity and intensity of colour [18], they can be used as plastics dyes.



where R=CH<sub>3</sub> (1), R=C<sub>6</sub>H<sub>5</sub> (2)

**Figure 1. Structure of compounds 1 and 2.**

Current article presents the results of our investigations regarding the colouring properties of compounds **1** and **2**. These compounds were tested as dyes for colouring polystyrene block, suspension, emulsion and both high and low density polyethylene. The carried out under laboratory conditions experiments are promising for the use of these compounds as dyes for colouring polystyrene and polyethylene.

Coordination compounds **1** and **2** colour polystyrene and polyethylene in claret-brick. The influence of the radical R on the colour change of plastic parts is not visually observed, but analysis of the absorption spectra in the visible region suggests an insignificant influence (for complex **1**:  $\lambda(\text{nm}) = 334; 281; 242$ , respectively  $\lg \epsilon = 4.37; 4.50; 4.26$ , for complex **2**:  $\lambda(\text{nm}) = 335; 282; 244$ , respectively  $\lg \epsilon = 4.29; 4.53; 4.33$ ).

It should be noted, that one of the advantages of the investigated dyes is their very low consumption for colouring polystyrene (block, emulsion or suspension) and low or high density polyethylene (0.006 to 0.015 g medium tone, 0.020 to 0.100 g intense tone to 100 g polystyrene and 0.005 - 0.010 g medium tone, 0.015 - 0.035 g intense tone to 100g polyethylene), as shown in Table 1.

Table 1

**Characteristics of dyes 1 and 2.**

Dye		Thermostability, °C	Photostability, points	Color of polystyrene	Color of polyethylene	Uniformity of color	Consumption dyes, g/100 g polymer							
No	R						Polystyrene				Polyethylene			
							Block type		Emulsion, suspension		High density		Low density	
							Middle tone	Intense tone	Middle tone	Intense tone	Middle tone	Intense tone	Middle tone	Intense tone
1	CH <sub>3</sub>	285	7	Claret - brick		Uniformly	0.006 - 0.010	0.050 - 0.100	0.010 - 0.015	0.020 - 0.080	0.005 - 0.010	0.015 - 0.035	0.008 - 0.010	0.015 - 0.035
2	C <sub>6</sub> H <sub>5</sub>	365	7											

It should be noted, that changing the concentration of dye, transparent plastic parts with different shades or uniformly coloured non-transparent ones were obtained. Thus, on the basis of their high photostability, the stability towards physico-mechanical processing, the reported complexes may potentially be good choices as dyes for thermoplastic masses. Due to the adhesion of compounds **1** and **2** to polystyrene, their use as dyes for thermoplastic masses does not require additional agents for grain processing. In this case the dye consumption is reduced significantly.

## Conclusion

Due to their colouring capacities, along with the other useful properties, such as high thermo- and photo stability and very simple and inexpensive methods of synthesis, the proposed complexes can be used as dyes for colouring thermoplastic polymers.

## Experimental

Polystyrene in block, emulsion or granulated suspension is mixed with the dye in a reactor supplied with a thermometer, a stirrer and a tap to release the obtained content from the reactor into the form. The mixture in the reactor is stirred and heated up until components melt; afterwards they are fused in the required form. When colouring polyethylene, a more intense stirring is required, since the adherence of the dye to polyethylene is lower than to polystyrene.

## References

1. You, W.; Zhu, H-Y.; Huang, W.; Hu, B.; Fan, Y.; You, X-Z. The first observation of azohydrazone and cis-trans tautomerisms for disperse yellow dyes and their nickel(II) and copper(II) complexes. *Dalton Transaction*, 2010, 39, pp. 7876-7880.
2. Kowol, C.R.; Heffeter, P.; Miklos, W.; Gille, L.; Trondl, R.; Cappellacci, L.; Berger, W.; Keppler, B. K. Mechanisms underlying reductant-induced reactive oxygen species formation by anticancer copper(II) compounds. *Journal of Biological Inorganic Chemistry*, 2012, 17, pp. 409-423.
3. Roy, S; Mandal, T.; Barik, A.; Pal, S; Gupta, S.; Hazra, A.; Ray, J.; Butcher, A.; Hunter, M.; Zeller, S.; Kumar, K. Metal complexes of pyrimidine derived ligands - syntheses, characterization and X-ray crystal structures of Ni(II), Co(III) and Fe(III) complexes of Schiff base ligands derived from S-methyl/S-benzyl dithiocarbamate and 2-S-methylmercapto-6-methylpyrimidine-4-carbaldehyde. *Polyhedron*, 2007, 26, pp. 2603-2614.
4. Pahontu, E.; Fala, V.; Gulea, A.; Poirier, D.; Tapcov, V.; Rosu, T. Synthesis and characterization of some new Cu(II), Ni(II) and Zn(II) complexes with salicylidene thiosemicarbazones: antibacterial, antifungal and *in vitro* antileukemia activity. *Molecules*, 2013, 18, pp. 8812-8836.
5. Hamid, K.; Maryam, D. Copper (II) Complexes of pyridazine-based azo-azomethine ligands: synthesis, characterization thermal and absorption properties. *Journal of Inorganic and Organometallic Polymers*, 2011, 21, pp. 541-546.
6. Serda, M.; Mrozek-Wilczkiewicz, A.; Jampilek, J.; Pesko, M.; Kralova, K.; Vejsova, M.; Musiol, R.; Ratuszna, A.; Polanski, J. Investigation of the biological properties of (hetero)aromatic thiosemicarbazones. *Molecules*, 2012, 17, pp. 13483-13502.
7. Hamid, K.; Khatereh, R.; Mostafa M. A.; Seik, W. N. Azo-azomethine dyes with N, O, S donor set of atoms and their Ni(II) complexes: Synthesis, characterization and spectral properties. *Dyes and Pigments*, 2013, 98, pp. 557-564.
8. Garbalau, N.; Arion, V. Template synthesis of macrocyclic compound. *Stiinta: Chisinau*, 1990, 374 p. (in Russian).
9. Gerbeleu, N.; Arion, V.; Burges, J. Template synthesis of macrocyclic compound. *Wiley-VCH: Weinheim*, 1999, 565 p.
10. Gradinaru, J.; Forni A.; Druta, V. Ni(II) complexes with [N<sub>3</sub>O] Schiff base ligands bearing S-methylisothiosemicarbazide unit: design, synthesis and structure. *Inorganica Chimica Acta*, 2002, 338, pp. 169-181.
11. Cocu, M.; Gradinaru, J.; Revenco, M.; Rybak-Akimova, E.; Garbalau, N. Template synthesis and investigation of some 3d-elements coordination compounds with tetradentate ligands derived from alkylated thiosemicarbazide. *Chemistry Journal of Moldova*, 2008, 3(2), pp. 38-47.
12. Leovac, V.; Bogdanovic, G.; Ceslijevic, V. and Divjakovic, V. Transition metal complexes with thiosemicarbazide-based ligands. XV. A square-pyramidal Ni<sup>II</sup> complex with an asymmetric coordination of 2,6-diacetylpyridine bis(S-methylisothiosemicarbazone). *Acta Crystallographica. Section C*, 2000, 56, pp. 936-938.
13. Garbalau, N.; Joymir, T. Template synthesis and properties of nickel coordination compounds with binuclear ligands based on thiosemicarbazide and 3-formylsalicylic acid. *Journal of Inorganic Chemistry*, 1984, 29(9), pp. 2304-2308 (in Russian).
14. Gradinaru, J.; Forni, A.; Simonov, Yu.; Popovici, M.; Zecchin, S.; Gdaniec, M.; Fenton, D. Mononuclear nickel(II) and copper(II) complexes with Schiff base ligands derived from 2,6-diformyl-4-methylphenol and S-methylisothiosemicarbazones. *Inorganica Chimica Acta*, 2004, 357, pp. 2728-2736.



15. Forni, A.; Gradinaru, J.; Druta, V.; Zecchin, S.; Quici, S.; Gerbelevu N. Cu(II) complexes with asymmetrical [N<sub>3</sub>O] Schiff-base ligands derived from *S*-methylisothiosemicarbazide. *Inorganica Chimica Acta*, 2003, 353, p. 336-343.
16. Cocu, M. Template synthesis and investigation of some 3d-elements coordination compounds with tetradentate ligands derived from alkylated thiosemicarbazide. Ph.D. Thesis, Institute of Chemistry of ASM. Chisinau, Republic of Moldova, 2007 (in Romanian).
17. Manole, S.; Cocu, M. Coordination compounds of nickel(II), copper(II) and cobalt(II) based on *s*-methylisothiosemicarbazide as dyes for thermoplastic polymers. *Chemistry Journal of Moldova*, 2011, 6(2), pp. 70-72.
18. Bastian, M. Coloration of plastics. Profession: St. Petersburg, 2011, 107 p. (in Russian).

# OXAZIRIDINE (C-CH<sub>3</sub>NO), C-CH<sub>2</sub>NO RADICALS AND CL, NH<sub>2</sub> AND METHYL DERIVATIVES OF OXAZIRIDINE; STRUCTURES AND QUANTUM CHEMICAL PARAMETERS (Supplementary material)

Mohammad Taghi Taghizadeh\*, Morteza Vatanparast, Saeed Nasirianfar

University of Tabriz, Faculty of Chemistry, 29, Bahman Bolvd., Tabriz, 51666-14766, Iran

\*e-mail: mttaghizadeh1947@gmail.com, mttaghizadeh@tabrizu.ac.ir, phone: (+98) 41 33 393 137; fax: (+98) 41 33 340 191

Supplementary material contains Tables S1 to S9 and Figures S1 to S4.

Received: August 2015/ Revised final: October 2015/ Accepted: October 2015

Table S1

Structure of oxaziridine, radicals and their corresponding cations calculated using B3LYP/6-311++G (d, p) method [16].

Oxaziridine			Radical 1		Radical 2		Radical 3	
B3lyp	Ref [16]		B3lyp		B3lyp		B3lyp	
Bond lengths (Å)			Bond lengths (Å)		Bond lengths (Å)		Bond lengths (Å)	
C1-O2	1.398	1.403	C1-O2	1.426	C1-O2	1.347	C1-O2	1.348
C1-H3	1.090	1.089	C1-H3	1.087	C1-H3	1.091	C1-H3	1.092
C1-H4	1.088	1.091	C1-H4	1.087	C1-N4	1.414	C1-N4	1.409
C1-N5	1.436	1.439	C1-N5	1.429	N4- H5	1.025	N4- H5	1.028
N5-H6	1.025	1.026	O2-N5	1.383	O2-N4	1.544	O2-N4	1.541
O2-N5	1.496	1.500						
Bond angles(°)			Bond angles(°)		Bond angles(°)		Bond angles(°)	
H3-C1-O2	115.8		O2-C1-H3	115.6	H3-C1-O2	122.9	H3-C1-O2	123.0
O2-C1-H4	116.3	115.8	O2-C1-H4	115.7	O2-C1-N4	68.0	O2-C1-N4	67.9
N5-C1-H3	119.7	116.2	H3-C1-H4	117.3	C1-N4-H5	107.7	C1-N4-H5	109.5
C1-N5-H6	107.7	107.6	N5-C1-H3	118.3	O2-N4-H5	102.6	O2-N4-H5	103.1
O2-N5-H6	103.1		N5-C1-H4	118.3	N4-O2-C1	58.1	N4-O2-C1	57.9
H3-C1-H4	115.8		O2-C1-N5	58.0	C1-N4-O2	54.0	C1-N4-O2	54.1
N5-O2-C1	59.4		N5-O2-C1	61.1				
O2-C1-N5	63.7		C1-N5-O2	60.9				
C1-N5-O2	56.9							
Torsion angles(°)			Torsion angles(°)		Torsion angles(°)		Torsion angles(°)	
H4-C1-N5-H6	-157.5		N5-O2-C1-H3	108.7	H3-C1-N4-H5	-151.5	H3-C1-N4-H5	-23.2
H3-C1-N5-H6	-11.67		N5-O2-C1-H4	-108.7				
Oxaziridine Cation			Rad.1 Cation		Rad.2 Cation		Rad.3 Cation	
B3lyp	Ref [16]		B3lyp		B3lyp		B3lyp	
Bond lengths (Å)			Bond lengths (Å)		Bond lengths (Å)		Bond lengths (Å)	
C1-O2	1.502	1.507	C1-O2	1.529	C1-O2	1.239	C1-O2	1.239
C1-H3	1.085	1.086	C1-H3	1.086	C1-H3	1.092	C1-H3	1.092
C1-H4	1.084	1.088	C1-H4	1.086	C1-N4	1.338	C1-N4	1.338
C1-N5	1.416	1.439	C1-N5	1.442	N4- H5	1.037	N4- H5	1.037
N5-H6	1.032	1.032	O2-N5	1.223	O2-N4	1.677	O2-N4	1.677
O2-N5	1.311	1.317						
Bond angles(°)			Bond angles(°)		Bond angles(°)		Bond angles(°)	
H3-C1-O2	113.3		O2-C1-H3	112.8	H3-C1-O2	136.0	H3-C1-O2	136.0
O2-C1-H4	114.0	113.3	O2-C1-H4	112.8	O2-C1-N4	81.1	O2-C1-N4	81.1
N5-C1-H3	119.0	113.9	H3-C1-H4	124.7	C1-N4-H5	115.8	C1-N4-H5	115.8
C1-N5-H6	140.3	140.3	N5-C1-H3	116.6	O2-N4-H5	106.4	O2-N4-H5	106.4
O2-N5-H6	122.1		N5-C1-H4	116.6	N4-O2-C1	52.0	N4-O2-C1	52.0
H3-C1-H4	121.9		O2-C1-N5	48.5	C1-N4-O2	46.9	C1-N4-O2	46.9
N5-O2-C1	56.0		N5-O2-C1	62.0				
O2-C1-N5	53.3		C1-N5-O2	69.5				
C1-N5-O2	66.7							
Torsion angles(°)			Torsion angles(°)		Torsion angles(°)		Torsion angles(°)	
H4-C1-N5-H6	-145.5		N5-O2-C1-H3	106.1	H3-C1-N4-H5	-96.2	H3-C1-N4-H5	-96.2
H3-C1-N5-H6	14.1		N5-O2-C1-H4	-106.0				

Table S2

Atomic charges on C, N and O atoms from NBO calculation calculated using B3LYP level of theory and 6-311++G (d, p) basis set.

Structure	C	O	N
1	0.104	-0.419	-0.334
2	0.031	-0.344	-0.030
3	0.247	-0.382	-0.355
4	0.264	-0.384	-0.352
5	0.229	-0.394	-0.320
6	0.219	-0.395	-0.318
7	0.098	-0.358	-0.152
8	0.212	-0.347	-0.164
9	0.215	-0.360	-0.189
10	0.289	-0.391	-0.312
11	0.273	-0.362	-0.190
12	0.256	-0.429	-0.334
13	0.256	-0.429	-0.345
14	0.115	-0.424	-0.221
15	0.268	-0.436	-0.229
16	0.273	-0.437	-0.223
17	0.382	-0.439	-0.341
18	0.401	-0.453	-0.229
19	0.400	-0.446	-0.338
20	0.405	-0.428	-0.352
21	0.120	-0.507	-0.078
22	0.681	-0.450	-0.362
23	0.423	-0.660	-0.081
24	0.409	-0.567	-0.090
25	0.695	-0.687	-0.082

Table S3

HOMO and LUMO energy calculated using B3LYP/6-311++G(d,p).

Structure		HOMO	LUMO	$ \epsilon_{\text{HOMO}} - \epsilon_{\text{LUMO}} /(a.u)$	$ \epsilon_{\text{HOMO}} - \epsilon_{\text{LUMO}} /(eV)$
1		-0.27725	-0.01485	0.26240	7.14
2	$\alpha$	-0.26441	-0.00640	0.25801	7.02
	$\beta$	-0.34121	-0.09747	0.24374	6.63
3	$\alpha$	-0.23618	-0.03616	0.20002	5.44
	$\beta$	-0.29604	-0.08922	0.20682	5.63
4	$\alpha$	-0.23490	-0.03582	0.19908	5.42
	$\beta$	-0.29651	-0.08498	0.21153	5.76
5		-0.30005	-0.03029	0.26976	7.34
6		-0.30595	-0.02904	0.27691	7.54
7		-0.29704	-0.08020	0.21684	5.90
8		-0.31679	-0.09387	0.22292	6.07
9		-0.30450	-0.08717	0.21733	5.91
10		-0.31627	-0.05155	0.26472	7.20
11		-0.31728	-0.09750	0.21978	5.98
12		-0.27033	-0.01281	0.25752	7.01
13		-0.27300	-0.01402	0.25898	7.05
14		-0.26317	-0.00845	0.25472	6.93
15		-0.25903	-0.00860	0.25043	6.81
16		-0.25189	-0.01155	0.24034	6.54
17		-0.26570	-0.01498	0.25072	6.82
18		-0.24766	-0.01233	0.23533	6.40
19		-0.25804	-0.01804	0.24000	6.53
20		-0.25814	-0.02235	0.23579	6.42
21		-0.27093	-0.02900	0.24193	6.58
22		-0.26037	-0.02011	0.24026	6.54
23		-0.23782	-0.08651	0.15131	4.12
24		-0.25659	-0.05476	0.20183	5.49
25		-0.23626	-0.08794	0.14832	4.04

Table S4

**Selected natural bond orbital occupancies of oxaziridine and related radicals (a.u.) calculated using B3LYP/6-311++G (d, p) basis set. Only ring bonds (C-O, N-O and C-N) have been presented.**

<i>Oxaziridine (structure 1)</i>			<i>Radical 1 (structure 2)</i>		
			<i>Spin</i>	$\alpha$	$\beta$
BD (1) C - O	1.98513		BD (1) C - O	0.99319	0.99300
BD (1) O - N	1.97718		BD (1) O - N	0.99144	0.99134
BD (1) C - N	1.98439		BD (2) O - N		0.97258
BD*(1) C - O	0.01374		BD (1) C - N	0.99452	0.99424
BD*(1) O - N	0.02295		BD*(1) C - O	0.00894	0.01014
BD*(1) C - N	0.00802		BD*(1) O - N	0.00683	0.00624
			BD*(2) O - N		0.00730
			BD*(1) C - N	0.00345	0.00361
<i>Radical 2 (structure 3)</i>			<i>Radical 3 (structure 4)</i>		
<i>Spin</i>	$\alpha$	$\beta$	<i>Spin</i>	$\alpha$	$\beta$
BD (1) C - O	0.99240	0.99507	BD (1) C - O	0.99233	0.98646
BD (2) C - O		0.98108	BD (2) C - O		0.98261
BD (1) O - N	0.98739	0.98321	BD (1) O - N	0.98745	0.98255
BD (1) C - N	0.99088	0.98911	BD (1) C - N	0.99123	0.99145
BD*(1) C - O	0.00579	0.00562	BD*(1) C - O	0.00559	0.00861
BD*(2) C - O		0.04363	BD*(2) C - O		0.04443
BD*(1) O - N	0.01445	0.02413	BD*(1) O - N	0.01429	0.02355
BD*(1) C - N	0.00364	0.00424	BD*(1) C - N	0.00392	0.00354

Table S5

**Selected natural bond orbital occupancies (a.u.) of compounds (structures 5-25) calculated using B3LYP/6-311++G (d, p) basis set. Only ring bonds (C-O, N-O and C-N) have been presented.**

	<i>Structure 5</i>	<i>Structure 6</i>	<i>Structure 7</i>	<i>Structure 8</i>	<i>Structure 9</i>
BD (1) C - O	1.98624	1.98613	1.98420	1.98506	1.98530
BD (1) O - N	1.96892	1.96922	1.98121	1.97272	1.97513
BD (1) C - N	1.98344	1.98368	1.98628	1.98508	1.98529
BD*(1) C - O	0.04670	0.05145	0.01402	0.05537	0.05370
BD*(1) O - N	0.02277	0.02240	0.04655	0.05493	0.06143
BD*(1) C - N	0.03697	0.03714	0.01387	0.04906	0.06139
	<i>Structure 10</i>	<i>Structure 11</i>	<i>Structure 12</i>	<i>Structure 13</i>	<i>Structure 14</i>
BD (1) C - O	1.98781	1.98622	1.98185	1.98230	1.98166
BD (1) O - N	1.95967	1.96585	1.97570	1.97616	1.97175
BD (1) C - N	1.98324	1.98409	1.98038	1.98005	1.98017
BD*(1) C - O	0.08643	0.09434	0.03075	0.03229	0.01496
BD*(1) O - N	0.02071	0.06635	0.02365	0.02372	0.04600
BD*(1) C - N	0.06978	0.09901	0.02258	0.02260	0.01378
	<i>Structure 15</i>	<i>Structure 16</i>	<i>Structure 17</i>	<i>Structure 18</i>	<i>Structure 19</i>
BD (1) C - O	1.97894	1.97817	1.97905	1.97580	1.98453
BD (1) O - N	1.97063	1.97024	1.97441	1.97053	1.97379
BD (1) C - N	1.97629	1.97812	1.97625	1.97386	1.98273
BD*(1) C - O	0.03383	0.03198	0.04968	0.05103	0.07579
BD*(1) O - N	0.04681	0.04703	0.02372	0.04661	0.02329
BD*(1) C - N	0.02760	0.03011	0.03723	0.04394	0.04123
	<i>Structure 20</i>	<i>Structure 21</i>	<i>Structure 22</i>		
BD (1) C - O	1.98405	1.98364	1.98277		
BD (1) O - N	1.97361	1.96576	1.96992		
BD (1) C - N	1.98332	1.97633	1.98002		
BD*(1) C - O	0.04616	0.01478	0.10272		
BD*(1) O - N	0.02411	0.21708	0.02338		
BD*(1) C - N	0.06810	0.01355	0.08428		
	<i>Structure 23</i>	<i>Structure 24</i>		<i>Structure 25</i>	
BD (1) C1 - O2	1.99510	BD (1) C1 - O2	1.98593	BD (1) C1 - O2	1.95925
BD (1) N4 - N5	1.98808	BD (1) O2 - N4	1.95523	BD (1) N3 - N10	1.98582
BD (2) N4 - N5	1.98367	BD (1) N4 - N5	1.99294	BD (2) N3 - N10	1.98158
BD (1) C1 - N4	1.96699	BD (1) C1 - N4	1.96393	BD (1) C1 - N3	1.96159
BD*(1) C1 - O2	0.05408	BD*(1) C1 - O2	0.06452	BD*(1) C1 - O2	0.06288
BD*(1) N4 - N5	0.07885	BD*(1) O2 - N4	0.31694	BD*(1) N3 - N10	0.10405
BD*(2) N4 - N5	0.31404	BD*(1) N4 - N5	0.00963	BD*(2) N3 - N10	0.27438
BD*(1) C1 - N4	0.13001	BD*(1) C1 - N4	0.04954	BD*(1) C1 - N3	0.15597



Table S6  
Selected second order perturbation theory analysis of Fock Matrix in NBO Basis for structures calculated by B3LYP/6-311++G (d, p) method.  
E (2) (kcal/mol) were reported.

Donor NBO (i)	Acceptor NBO (j)	E(2)	Donor NBO (i)	Acceptor NBO (j)	E(2)	Donor NBO (i)	Acceptor NBO (j)	E(2)
<b>1</b>								
BD (1) C1 - O2	BD*(1) O2 - N5	4.02	<b>2 a</b>		<b>2 b</b>			
BD (1) O2 - N5	BD*(1) C1 - O2	5.27	BD (1) C1 - O2	BD*(1) O2 - N5	2.10	BD (1) C1 - O2	BD*(1) O2 - N5	2.17
BD (1) O2 - N5	BD*(1) C1 - N5	3.87	BD (1) O2 - N5	BD*(1) C1 - O2	2.58	BD (1) O2 - N5	BD*(1) C1 - O2	2.55
<b>3 a</b>								
BD (1) C1 - O2	BD*(1) O2 - N5	2.09	<b>3 b</b>		<b>4 a</b>			
BD (1) O2 - N4	BD*(1) C1 - O2	3.01	BD (2) C1 - O2	BD*(1) O2 - N4	3.59	BD (1) C1 - O2	BD*(1) O2 - N5	2.22
<b>4 b</b>								
BD (2) C1 - O2	BD*(1) O2 - N4	2.64	LP (1) N4	BD*(2) C1 - O2	4.43	BD (1) O2 - N4	BD*(1) C1 - O2	2.98
BD (1) O2 - N4	BD*(1) C1 - O2	3.20	<b>5</b>		<b>6</b>			
LP (1) N4	BD*(2) C1 - O2	3.24	BD (1) C1 - O2	BD*(1) O2 - N6	3.54	BD (1) C1 - O2	BD*(1) O2 - N5	3.39
<b>7</b>								
BD (1) C1 - O2	BD*(1) O2 - N5	3.36	BD (1) C1 - O2	BD*(1) C1 - O2	5.22	BD (1) O2 - N5	BD*(1) C1 - O2	5.15
BD (1) O2 - N5	BD*(1) C1 - O2	4.27	BD (1) O2 - N4	BD*(1) C1 - O2	4.07	BD (1) O2 - N5	BD*(1) C1 - N5	4.04
LP (3) Cl6	BD*(1) O2 - N5	6.12	LP (3) Cl5	BD*(1) C1 - O2	6.62	LP (3) Cl6	BD*(1) C1 - O2	7.38
<b>8</b>								
BD (1) C1 - O2	BD*(1) O2 - N5	3.36	BD (1) C1 - O2	BD*(1) O2 - N4	2.73	BD (1) C1 - O2	BD*(1) O2 - N4	2.88
BD (1) O2 - N5	BD*(1) C1 - O2	4.27	BD (1) O2 - N4	BD*(1) C1 - O2	4.24	BD (1) O2 - N4	BD*(1) C1 - O2	4.17
LP (3) Cl6	BD*(1) O2 - N5	6.12	LP (3) Cl5	BD*(1) C1 - O2	6.22	LP (3) Cl6	BD*(1) O2 - N4	8.61
<b>9</b>								
LP (3) Cl5	BD*(1) C1 - N4	5.30	LP (3) Cl5	BD*(1) C1 - N4	5.30			
<b>10</b>								
BD (1) C1 - O2	BD*(1) O2 - N4	2.88	BD (1) C1 - O2	BD*(1) O2 - N4	7.35			
BD (1) O2 - N4	BD*(1) C1 - O2	4.61	LP (3) Cl4	BD*(1) O2 - N3	2.14	BD (1) C1 - O2	BD*(1) O2 - N5	4.11
LP (3) Cl5	BD*(1) C1 - O2	7.94	LP (2) Cl5	BD*(1) C1 - O2	9.40	BD (1) O2 - N5	BD*(1) C1 - O2	5.47
LP (3) Cl5	BD*(1) C1 - O2	6.95	LP (3) Cl5	BD*(1) C1 - N3	5.35			
<b>11</b>								
LP (3) Cl6	BD*(1) C1 - O2	5.24	LP (3) Cl6	BD*(1) C1 - O2	8.08			
<b>12</b>								
LP (3) Cl6	BD*(1) C1 - N3	6.29	LP (3) Cl6	BD*(1) C1 - N3	5.24			
<b>13</b>								
BD (1) C1 - O2	BD*(1) O2 - N5	4.03	BD (1) C1 - O2	BD*(1) O2 - N5	4.83	BD (1) C1 - O2	BD*(1) O2 - N4	4.85
BD (1) O2 - N5	BD*(1) C1 - O2	5.38	BD (1) O2 - N5	BD*(1) C1 - O2	5.40	BD (1) O2 - N4	BD*(1) C1 - O2	5.60
<b>14</b>								
BD (1) C6 - H7	BD*(1) O2 - N5	5.53	BD (1) C6 - H7	BD*(1) O2 - N5	5.53	BD (1) C5 - H6	BD*(1) O2 - N4	5.56

Continuation of Table S6					
Donor NBO (i)	Acceptor NBO (j)	E(2)	Donor NBO (i)	Acceptor NBO (j)	E(2)
<b>16</b>					
<b>17</b>					
BD (1) C1 - O2	BD*(1) O2 - N4	4.93	BD (1) C1 - O2	BD*(1) O2 - N4	4.03
BD (1) O2 - N4	BD*(1) C1 - O2	5.60	BD (1) O2 - N4	BD*(1) C1 - O2	5.36
BD (1) C5 - H6	BD*(1) O2 - N4	5.82	BD (1) C5 - H6	BD*(1) C1 - O2	5.09
				BD (1) C8 - H9	5.09
				BD (1) C12 - H13	5.41
				BD (1) C12 - H14	5.37
<b>19</b>					
<b>20</b>					
BD (1) C1 - O2	BD*(1) O2 - N5	4.35	BD (1) O2 - N5	BD*(1) C1 - O2	5.13
BD (1) O2 - N5	BD*(1) C1 - O2	5.53	BD (1) O2 - N4	BD*(1) C1 - O2	5.13
LP (1) N6	BD*(1) C1 - O2	15.00	LP (2) O2	BD*(1) C1 - H3	7.91
			LP (2) O2	BD*(1) C1 - N6	7.54
			LP (1) N4	BD*(1) C1 - N6	4.75
			LP (1) N6	BD*(1) C1 - O2	4.06
			LP (1) N6	BD*(1) C1 - N4	15.14
<b>22</b>					
<b>23</b>					
BD (1) C1 - O2	BD*(1) O2 - N4	3.69	BD (1) C1 - O2	LP (3) O2	7.77
BD (1) O2 - N4	BD*(1) C1 - O2	5.11	BD (1) C1 - N4	LP (3) O2	8.53
LP (1) N5	BD*(1) C1 - O2	17.23	BD (1) C1 - N4	BD*(1) N5 - H6	5.49
LP (1) N8	BD*(1) C1 - N4	14.67	LP (3) O2	BD*(1) C1 - O2	15.76
BD*(1) C1 - O2	BD*(1) C1 - N4	34.83	LP (3) O2	BD*(1) C1 - N4	19.75
			LP (3) O2	BD*(2) N4 - N5	19.56
			LP (1) N4	BD*(1) N5 - H7	8.18
			LP (1) N8	BD*(1) C1 - N4	10.13
			LP (1) N8	BD*(1) N5 - H7	6.61
			BD*(2) N4 - N5	BD*(1) N4 - N5	23.69
<b>25</b>					
LP (3) O2	BD*(1) C1 - O2	5.90			
LP (3) O2	BD*(1) C1 - N3	15.52			
LP (3) O2	BD*(1) N3 - N10	10.34			
LP (1) N4	BD*(1) C1 - O2	12.98			
LP (1) N7	BD*(1) C1 - N3	10.37			
LP (1) N7	BD*(1) N10 - H12	7.63			
BD*(2) N3 - N10	BD*(1) N3 - N10	41.17			

Table S7

**VIE and AIE (eV) for oxaziridine and three radicals calculated using B3LYP/6-311++G (d, p) method (1Hartree=27.2114 eV) [16].**

		<i>This work</i>			<i>Reference [16]</i>			
<i>IE</i> <i>B3LYP</i>		<i> VIE-AIE </i>		<i>IE</i>		<i> VIE-AIE </i>		
			<i>B3LYP</i>	<i>QCISD(T)</i>	<i>G2(MP2)</i>	<i>B3LYP</i>	<i>QCISD(T)</i>	<i>G2(MP2)</i>
Oxaziridine	AIE	9.71	0.92	9.67	9.69	9.82	0.94	0.96
	VIE	10.63		10.61	10.65	10.76		0.94
Radical 1	AIE	9.86	0.64					
	VIE	10.50						
Radical 2	AIE	8.10	1.45					
	VIE	9.55						
Radical 3	AIE	8.03	1.50					
	VIE	9.53						

Table S8

**Vertical Ionization Energies (eV) calculated using B3LYP/6-311++G (d, p).**

<i>Structure</i>	<i>VIE</i>	<i>Structure</i>	<i>VIE</i>
1	10.63	14	9.93
2	10.50	15	9.66
3	9.55	16	9.49
4	9.53	17	9.95
5	10.87	18	9.23
6	11.09	19	9.72
7	10.74	20	9.69
8	11.06	21	9.94
9	10.73	22	9.67
10	11.10	23	8.73
11	10.93	24	9.29
12	10.22	25	8.58
13	10.31		

Table S9

**The value of the HOMO-LUMO energy (a.u.), Quantum chemical parameters: Ionization potential (*I*), Electron Affinity (*A*), Electronegativity ( $\chi$ ), Chemical Potential ( $\mu$ ), Global Hardness ( $\eta$ ), Global Softness (*S*,  $\sigma$ ) and Electrophilicity ( $\omega$ ); for oxaziridine and three radicals calculated using B3LYP method and 6-311++G (d, p) basis set.**

<i>Parameter</i>	<i>Oxaziridine</i>	<i>Radical 1</i>	<i>Radical 2</i>	<i>Radical 3</i>
<i>I</i> =VIE (a.u.)	0.39 66	0.38587	0.35096	0.35016
<i>A</i> =VEA (a.u.)	0.02241	0.00114	0.00209	0.00399
$\chi$ (a.u.)	0.20653	0.19351	0.17652	0.17708
$\mu$ (a.u.)	-0.20653	-0.19351	-0.17652	-0.17708
$\eta$ (a.u.)	0.18413	0.19237	0.17446	0.17309
<i>S</i> or $\sigma$ (a.u.) <sup>-1</sup>	5.43103	5.19835	5.73277	5.77749
$\omega$ (a..)	0.11583	0.09732	0.08932	0.09058

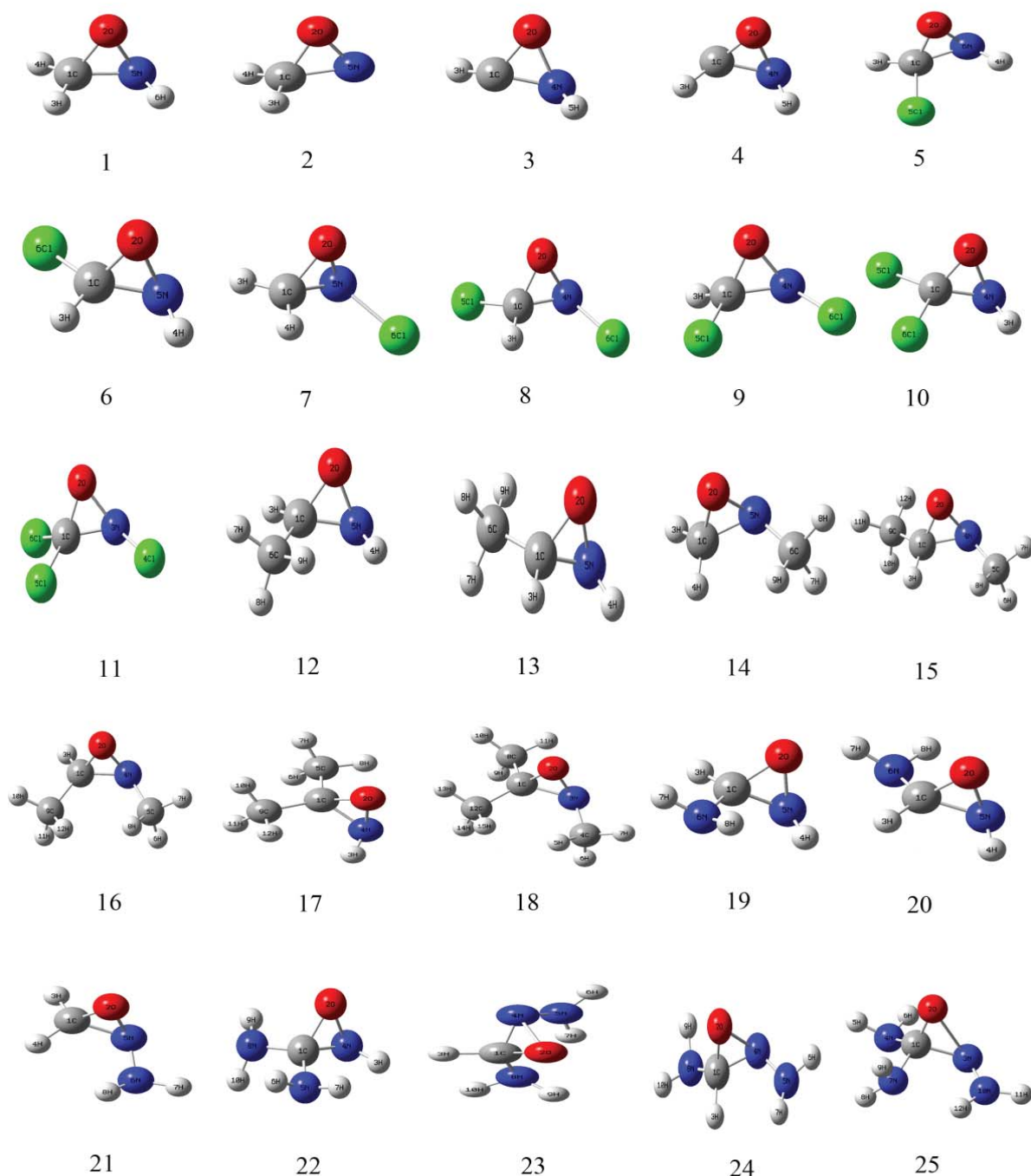


**Figure S1.** Optimum geometry of (1) oxaziridine [ $\text{CH}_3\text{NO}$  ( $^1\text{A}$ )] (2) radical 1 [ $\text{CH}_2\text{NO}$  ( $^2\text{A}$ )] (3) radical 2 [ $\text{CH}_2\text{NO}$  ( $^2\text{A}$ )] (4) radical 3 [ $\text{CH}_2\text{NO}$  ( $^2\text{A}$ )] (5)  $\text{CH}_2\text{NOCl}$  ( $^1\text{A}$ ) (6)  $\text{CH}_2\text{NOCl}$  ( $^1\text{A}$ ) (7)  $\text{CH}_2\text{NOCl}$  ( $^1\text{A}$ ) (8)  $\text{CHNOCl}_2$  ( $^1\text{A}$ ) (9)  $\text{CHNOCl}_2$  ( $^1\text{A}$ ) (10)  $\text{CHNOCl}_2$  ( $^1\text{A}$ ) (11)  $\text{CNOC}_2\text{H}_5$  ( $^1\text{A}$ ) (12)  $\text{C}_2\text{H}_5\text{NO}$  ( $^1\text{A}$ ) (13)  $\text{C}_2\text{H}_5\text{NO}$  ( $^1\text{A}$ ) (14)  $\text{C}_2\text{H}_5\text{NO}$  ( $^1\text{A}$ ) (15)  $\text{C}_3\text{H}_7\text{NO}$  ( $^1\text{A}$ ) (16)  $\text{C}_3\text{H}_7\text{NO}$  ( $^1\text{A}$ ) (17)  $\text{C}_3\text{H}_7\text{NO}$  ( $^1\text{A}$ ) (18)  $\text{C}_4\text{H}_9\text{NO}$  ( $^1\text{A}$ ) (19)  $\text{CH}_4\text{N}_2\text{O}$  ( $^1\text{A}$ ) (20)  $\text{CH}_4\text{N}_2\text{O}$  ( $^1\text{A}$ ) (21)  $\text{CH}_4\text{N}_2\text{O}$  ( $^1\text{A}$ ) (22)  $\text{CH}_5\text{N}_3\text{O}$  ( $^1\text{A}$ ) (23)  $\text{CH}_5\text{N}_3\text{O}$  ( $^1\text{A}$ ) (24)  $\text{CH}_5\text{N}_3\text{O}$  ( $^1\text{A}$ ) (25)  $\text{CH}_6\text{N}_4\text{O}$  ( $^1\text{A}$ ).

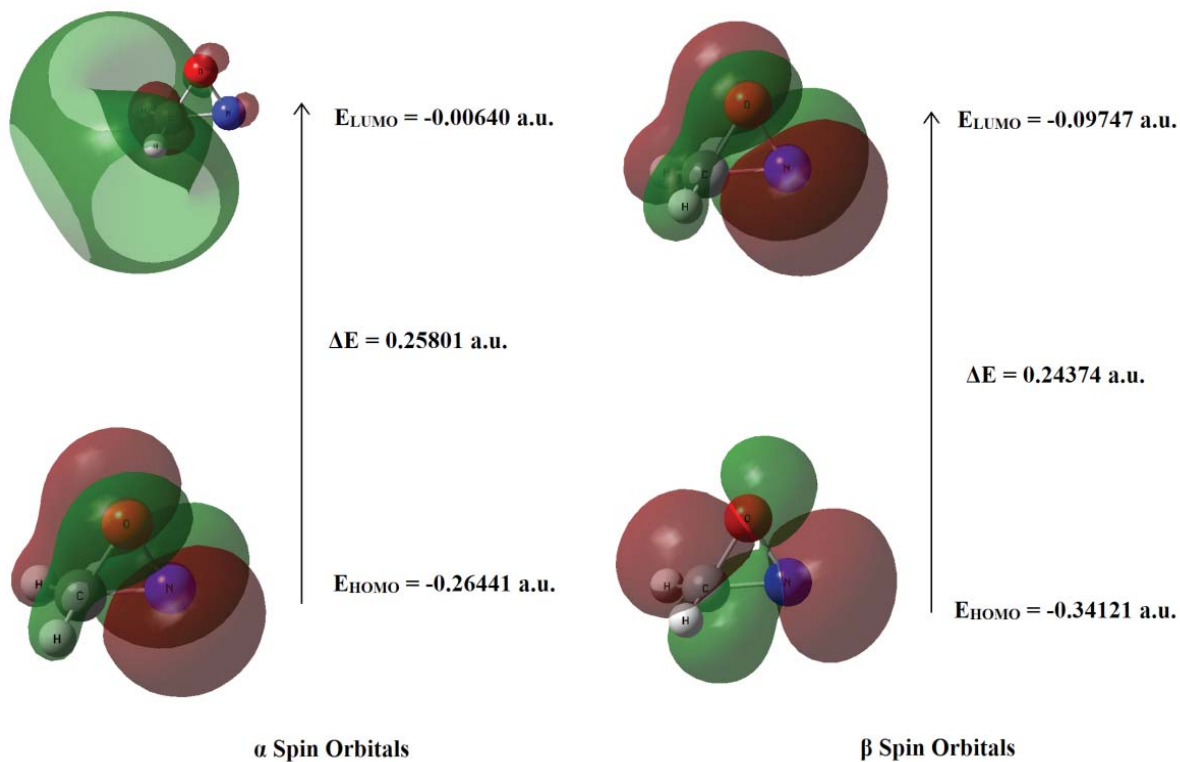


Figure S2. Isodensity plots of the frontier molecular orbitals of radical 1.

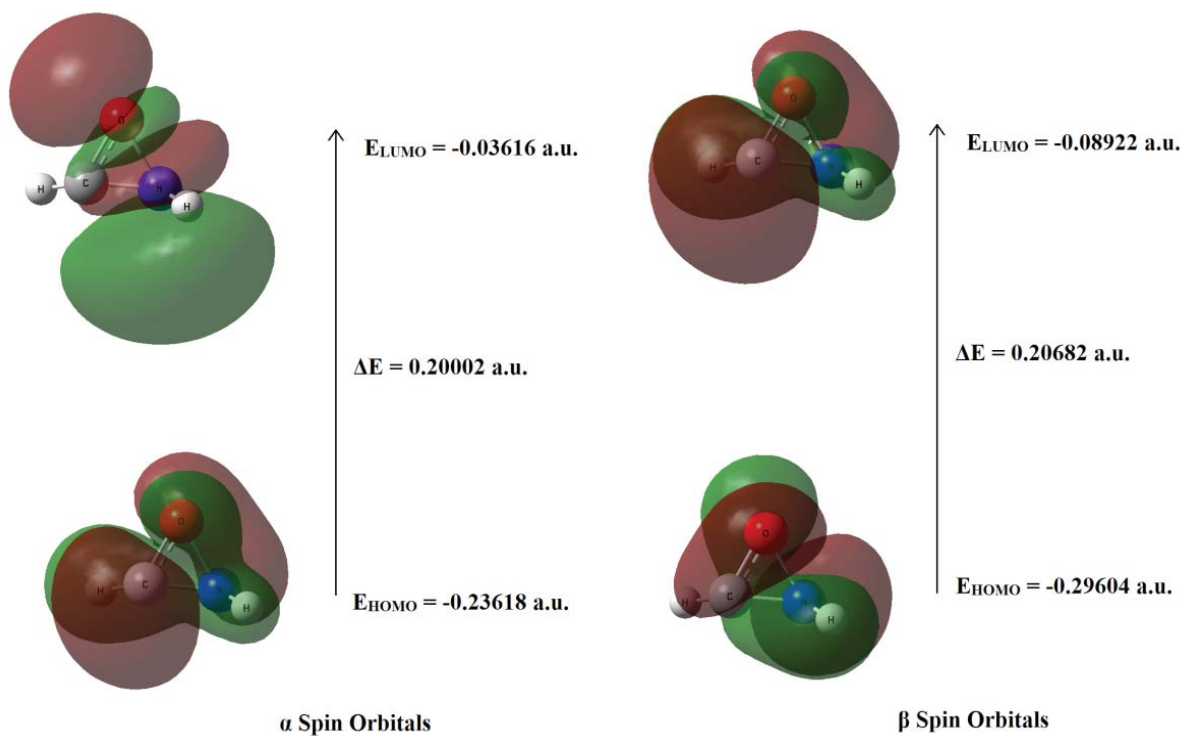


Figure S3. Isodensity plots of the frontier molecular orbitals of radical 2.



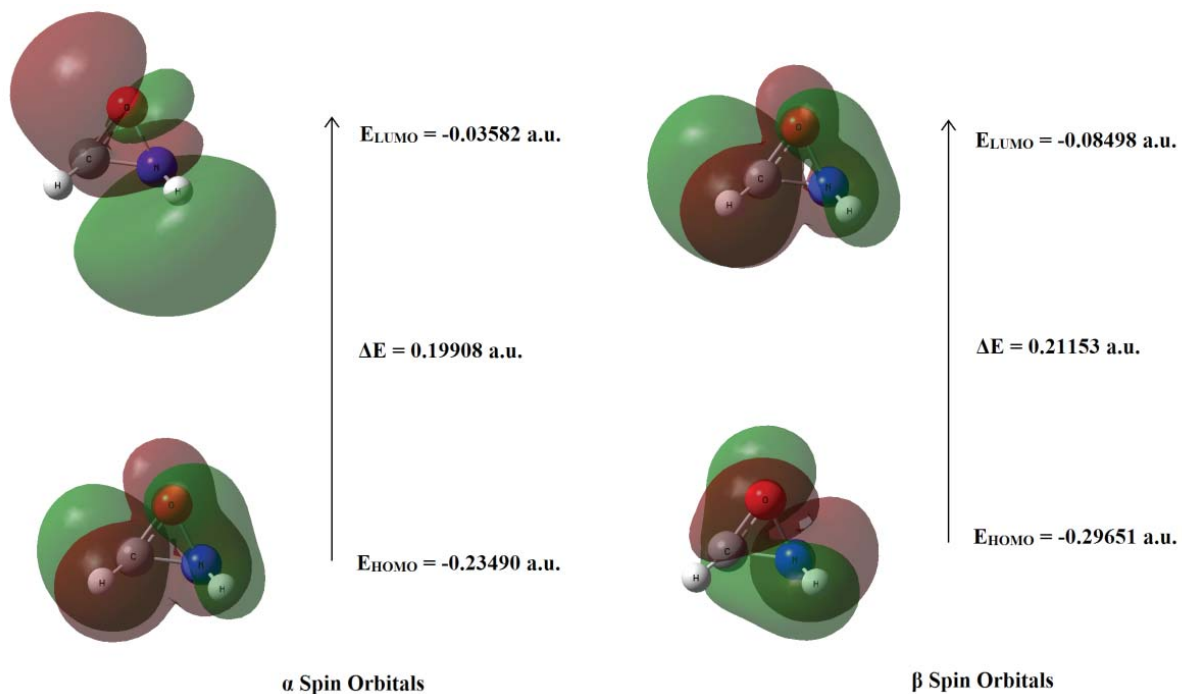


Figure S4. Isodensity plots of the frontier molecular orbitals of radical 3.

## Instructions for authors

Please follow these instructions carefully to ensure that the review and publication of your paper are as quick and efficient as possible. These notes may be copied freely. The electronic version of these notes is freely available for download on the web page of Chemistry Journal of Moldova (consult the section of the site **Instructions for authors** [www.cjm.asm.md/author\\_instructions](http://www.cjm.asm.md/author_instructions)). Instruction notes and an example of manuscript formatting are available in the MS Word template file that can be found on the web page of Chemistry Journal of Moldova ([www.cjm.asm.md](http://www.cjm.asm.md)).

### Journal policy

“Chemistry Journal of Moldova. General, Industrial and Ecological Chemistry” seeks to publish experimental or theoretical research results of outstanding significance and timeliness in all fields of Chemistry, including Industrial and Ecological Chemistry. The main goal of this edition is strengthening the Chemical Society of Moldova, following development of research in Moldovan chemical institutions and promotion of their collaboration with international chemical community.

#### Fields of research:

- |                         |  |  |
|-------------------------|--|--|
| 1. Analytical chemistry | 4. Industrial chemistry                    | 7. Organic chemistry                       |
| 2. Ecological chemistry | 5. Inorganic and coordination chemistry    | 8. Physical chemistry and chemical physics |
| 3. Food chemistry       | 6. Natural product chemistry and synthesis | 9. Supramolecular chemistry                |

Publications may be in the form of *Short Communications*, *Full Papers* and *Review Papers*.

*Short Communications* should describe preliminary results of an investigation and for their significance are due to rapid communication. For this kind of publications, experimental confirmation is required only for the final conclusion of the communication. Maximum allowed length – 2 pages.

*Full Papers* should describe original research in chemistry of high quality and timeliness. Experimental work should be accompanied by full experimental details. Priority will be given to those contributions describing scientific work having as broad appeal as possible to the diverse readership. Maximum allowed length – 10 pages.

*Review Papers* are specially commissioned reviews of research results of topical importance. Maximum allowed length – 20 pages.

The language of submission is English, articles in other languages will not be considered. Papers are submitted on the understanding that the subject matter has not been previously published and is not being submitted elsewhere.

Authors must accept full responsibility for the factual accuracy of the data presented and should obtain any authorization necessary for publication.

The contents of papers are the sole responsibility of the authors, and publication shall not imply the concurrence of the Editors or Publisher.

All papers are sent to referees who advise the Editor on the matter of acceptance in accordance with the high standards required.

Referees' names are not disclosed, but their views are forwarded by the Editor to the authors for consideration.

Authors are strongly encouraged to suggest the names and addresses of suitable referees.

### Journal conventions

#### Nomenclature

Authors will find the following reference books and websites useful for recommended nomenclature:

- IUPAC Nomenclature of Organic Chemistry; Rigaudy, J.; Klesney, S. P., Eds; Pergamon: Oxford, 1979.
- A Guide to IUPAC Nomenclature of Organic Compounds (Recommendations 1993); Panico, R.; Powell, W. H.; Richer, J. C., Eds; Blackwell Publishing: Oxford, 1993.
- <http://www.acdlabs.com/iupac/nomenclature>
- <http://www.chem.qmul.ac.uk/iupac/>

It is the responsibility of the author to provide correct chemical nomenclature.

#### X-ray crystallographic data

Prior to submission of the manuscript, the author should deposit crystallographic data for organic and metal-organic structures with the Cambridge Crystallographic Data Centre (CCDC). The data, without structure factors, should be sent by e-mail to: [deposit@ccdc.cam.ac.uk](mailto:deposit@ccdc.cam.ac.uk), as an ASCII file, in CIF format. CCDC deposition numbers (one per structure deposited) should be included with the following standard text in the manuscript: “CCDC-\*\*\*\*\*” - contains

the supplementary crystallographic data for this paper. These data can be obtained free of charge via <http://www.ccdc.cam.ac.uk/conts/retrieving.html>. Deposited data may be accessed by the journal and checked as part of the refereeing process. If data are revised prior to publication, a replacement file should be sent to CCDC.

### *Experimental*

Authors should be as concise as possible in experimental descriptions. The experimental section must contain all the information necessary to guarantee reproducibility. An introductory paragraph containing information concerning solvents, sources of less common starting materials, special equipment, etc. should be provided. The procedures should be written in the past tense and include the weight, mmol, volume, etc. in brackets after the names of the substances or solvents. General reaction conditions should be given only once. The title of an experiment should include the chemical name and compound number of the product prepared: subsequently, these compounds should be identified by their number. Details of the work up procedure must be included. An experimental procedure is not normally required for known compounds prepared by a literature procedure; in such cases, the reference will suffice. For known compounds prepared by a novel procedure, comparative data together with the literature reference are required (e.g. m.p. and published m.p. with a reference to the latter).

### *Characterization of new compounds*

All new compounds should be fully characterized with relevant physical and spectroscopic data, normally including compound description, m.p./b.p. if appropriate, IR, NMR, MS and  $[\alpha]_D$  values for enantiopure compounds. In addition, microanalyses should be included whenever possible. Under appropriate circumstances, and at the Editor's discretion, high resolution mass data may serve in lieu of microanalyses; in this case a statement must be included regarding the purity of the products and how this was determined [e.g. all new compounds were determined to be >95% pure by HPLC (or GLC or  $^1\text{H}$  NMR spectroscopy)]. For compound libraries prepared by combinatorial methods, a significant number of diverse examples must be fully characterized (normally half of the members for libraries up to 40 compounds, 20 representative examples for bigger libraries). Resin-bound intermediates do not have to be fully characterized if acceptable characterization of released products is provided. No supplementary data are accepted in addition to the basic material.

## **Manuscript preparation**

Please follow these guidelines for manuscript preparation. Please ensure that the required formats for text and figure submission are followed strictly.

### *General requirements*

Manuscripts will be accepted only in electronic form in A4 format, orientation *Portrait*, one column layout, single-spaced, margins 2.15 cm on all sides. Ensure that each new paragraph is clearly indicated, using TAB at 1.25 pts. Manuscript must be edited in Times New Roman font. Contributions should comprise an even number of pages. Authors are also kindly requested to adhere to the formatting instructions for font size and layout. Use the automatic page numbering function.

**Please ensure that the required formats for text and figure submission are followed strictly. MS Word template can be found on the web page of Chemistry Journal of Moldova ([www.cjm.asm.md](http://www.cjm.asm.md)). Use of this template is mandatory.**

The manuscript should be compiled in the order depending on the paper type.

A theoretical or physicochemical paper normally contains the *Title*, *Authors*, *Affiliations*, *Abstract*, *Keywords*, a brief *Introduction* and formulation of the problem, an *Experimental* (or methodological part), *Results and discussion*, *Conclusions*, followed by *Acknowledgments* and *References*.

A paper devoted to synthesis contains the *Title*, *Authors*, *Affiliations*, *Abstract*, *Keywords*, *Introduction*, *Results and discussion*, *Conclusions*, *Experimental*, *Acknowledgments* and *References*.

### **Title**

The title should be brief, specific and rich in informative words. Avoid the abbreviations where is possible. The title is in size 14 pt Bold (all capital letters).

### **Authors and affiliations**

Include all authors in a single list. The style for the names is: first name, last name (full names, without initials). The names of the authors must be written in size 12 pt and separated by a comma.

Affiliations should be as detailed as possible and must include the country name and must be written in size 9 pt *Italic*. The corresponding author should be indicated with an asterisk, and contact details (e-mail, phone, fax) should be placed after nomination of affiliations. There should be only one corresponding author.

An example of formatting for authors and affiliations is available in the MS Word template that can be found on the web page of Chemistry Journal of Moldova ([www.cjm.asm.md](http://www.cjm.asm.md)).

### **Abstract**

Authors must include a short abstract of approximately four to six lines that states briefly the purpose of the research, the principal results and major conclusions. Compound numbers should not be mentioned in the abstract. The abstract body is 9 pt in size with the heading in Bold.

### **Keywords**

Authors are expected to provide a maximum of 5 keywords, separated by a comma (10 pt, Normal). These keywords will facilitate database searching. Avoid general, plural terms and multiple concepts (avoid, for example, “and”, “of”).

### **Text**

Text should be subdivided in the simplest possible way consistent with clarity. Headings should reflect the relative importance of the sections. The text body is 10 pt in size Times New Roman font with the heading in Bold. Ensure that all tables, figures and schemes are cited in the text in numerical order. The graphics and artworks should be integrated in the paper.

Trade names should have an initial capital letter, and trademark protection should be acknowledged in the standard fashion, using the superscripted characters TM and ® for trademarks and registered trademarks respectively (although not for words which have entered common usage, e.g. pyrex).

Authors are requested to draw attention to hazardous materials or procedures by adding the word CAUTION followed by a brief descriptive phrase and literature references if appropriate.

*Abbreviations* must be defined at the first mention in the text and used consistently thereafter.

SI units must be used throughout.

In order to avoid possible confusion between the numeral 1 (one) and the lower-case letter l (el), please use the capital letter L to express liter units.

Decimal numbers should be expressed using the point (do not use comma).

*Experimental* information should be as concise as possible, but it should contain all the information necessary to guarantee reproducibility.

*Tables* should be edited considering the requirements indicated below.

Tables should be centered and should occupy the full width of the page.

Table must fit in a size of a page A4, Portrait. Vertical lines should not be used.

If table transfers partially to the next page it should be mentioned on the next page that this is a continuation of the table and the headings must be indicated again.

All table columns should have a brief explanatory heading typed in *Italic* and where appropriate, units of measurement. The punctuation at the end of the table title must be used.

All tables should be cited in the text, and numbered in order of appearance with Arabic numerals. Tables should be numbered sequentially—“Table 1”, “Table 2”, and should be cited in the text as “Table 1”, “Table 2”.

An example of Tables formatting is available in the MS Word template that can be found on the web page of Chemistry Journal of Moldova ([www.cjm.asm.md](http://www.cjm.asm.md)).

*Figures, schemes and equations* must be cited in the text and numbered in order of appearance with Arabic numerals; other graphics should be placed at a particular position in the text but not specifically referenced.

*Figures and schemes* should normally be centered.

It is also more convenient for referees of the article if figures are placed as close as possible, and ideally after, the point where they are first mentioned in the text. Figures should be numbered sequentially—“Figure 1”, “Figure 2”, and should be cited in the text as “Figure 1”, “Figure 2”.

Each figure should have a concise caption describing accurately what figure depicts. Figure captions begin with the term Figure, followed by figure number, punctuation and figure title, all in Bold type. Also, use the punctuation at the end of the caption. We recommend placing figures and their captions in a table with no margins.

An example of Figures formatting is available in the MS Word template that can be found on the web page of Chemistry Journal of Moldova ([www.cjm.asm.md](http://www.cjm.asm.md)).

Chemical structures must be edited using the following settings: font 7 pt Arial, chain angle 120°, bond spacing 20% of length, fixed length 0.43 cm, Bold width 0.056 cm, line width 0.016 cm, margin width 0.044 cm and hash spacing 0.062 cm. Compound numbers should be in Bold face.

**Figures must be submitted in a very good resolution (but do not submit graphics that are disproportionately large for the content).**

Figures will be printed in black and white. Color artwork will be available only in the electronic form of the published articles on the web page of Chemistry Journal of Moldova (www.cjm.asm.md). The quality of the figures must be such that they can be reproduced directly after size reduction and the numbers, letters, and symbols must be large enough to still be legible. Figures should be sent with the highest resolution possible (at least 300 dpi).

**Figure and table titles must be typed in Bold and should appear below the figures and above the tables. If you are using previously published material please include the source in the form of reference citation at the end of the figure caption and/or table title.**

*Equations and formulas* will be edited using Equation Editor or MathType (version 1999-2003). Quote them on the right side, between brackets. Equation must be cited in text as “Eq.(1)”, “Eq.(2)”.

$$\lambda = 2d \sin\left(\frac{\Theta}{2}\right) \quad (2)$$

Please use size 10 pt and *Italic* for symbols, Bold face for vectors and normal fonts for standard functions (i.e. log, ln, exp) and subscripts (i.e. //<sub>app</sub> i).

Large and complex chemical formulas should be presented in text as figures.

Please follow the IUPAC nomenclature for your chemical compound.

### Conclusions

Concluding section will provide a summary of the main obtained results, formulated in a concise form. The author must not indicate the literature references in this section.

### Acknowledgments

This is an optional section. The authors have to decide acknowledgement of certain collaborators, funds or programs who contributed in a way to the research described in the paper.

### References

In the text, references should be indicated by Arabic numerals taken in square brackets, which run consecutively through the paper and appear before any punctuation; ensure that all references are cited in the text and vice versa.

References should be numbered in the text in the order they are cited [1]. Multiple consecutive references may be abbreviated as [2-5].

Do not cite references in the abstract and conclusions.

**References should be written in English only. If it's in a different language then the reference must be translated with an appropriate title in English. The original language must be indicated in round brackets.**

Complete bibliographic information for all cited references is required. If abbreviated names of the journals are used then authors are expected to consult American Chemical Society guidelines (The ACS Style Guide; Dodd, J. S.; Solla, L.; Berard, P.M. Ed.: American Chemical Society: Washington, DC, 2006) or the policy of the cited journal.

All references must be edited in the same style.

**Each reference should contain only one literature citation.**

The following style must be used for all contributions:

#### Books:

1. Katritzky, A.R. Handbook of Organic Chemistry. Pergamon: Oxford, 1985, 200 p.
2. Wipke, W.T.; Heller, S.R.; Feldmann, R.J.; Hyde, E. Eds. Computer representation and manipulation of chemical information. John Wiley: New York, 1974, pp. 287–298.

#### Symposia volumes:

3. Bravo-Suárez, J.; Kidder, M.K.; Schwartz, V. Novel Materials for Catalysis and Fuels Processing. ACS Symposium Series; American Chemical Society: Washington, DC, 2013, vol. 1132, 400 p.

#### Translated journal papers:

4. Garaba, V. Problems of water supply in rural localities. Environment, 2005, 19, pp. 19-22 (in Romanian).
5. Magerramov, A.M.; Ramazanov, M.A.; Gadzhiev, F.V. Investigation of the structure and dielectric properties

of nanocomposites based on polypropylene and zirconia nanoparticles. Surface Engineering and Applied Electrochemistry, 2013, 49(5), pp. 1-5 (in Russian).

#### **Journal papers:**

6. Shin, S.; Yoon, H.; Jang, J. Polymer-encapsulated iron oxide nanoparticles as highly efficient Fenton catalysts. Catalysis Communications, 2008, 10, pp. 178–182.

#### **Patents:**

7. Grant, P. Device for Elementary Analyses. USA Patent, 1989, No. 123456.

#### **Theses:**

8. Cato, S.J. Thermodynamic study of polymer solutions. Ph.D. Thesis, University of Florida, Florida, USA, 1987.

#### **Legal regulations and laws, organizations:**

9. EC Directive, Directive 2000/76/EC of the European Parliament and of the Council of 4 December 2000, on the incineration of waste, Annex V, Official Journal of the European Communities, L 332/91, 28.12.2000, Brussels.

#### **Web references:**

The full URL should be given in text as a citation, if no other data are known. It should be accompanied by a sentence indicating the explanation of the content. When you are indicating the URL you should remove the Hiperlink, this can be achieved by selecting the URL then click the right button of the mouse and chose from the menu *Remove Hyperlink*.

10. Spectral Database for Organic Compounds, SDBS. [http://sdb.sdb.aist.go.jp/sdb/cgi-bin/cre\\_index.cgi](http://sdb.sdb.aist.go.jp/sdb/cgi-bin/cre_index.cgi).

#### **Graphical Abstract**

Authors must supply a graphical abstract at the time the paper is first submitted.

Graphical abstract will include *Title*, *Authors* and *Abstract body*.

The abstract body will summarize the contents of the paper in a concise form and it should not exceed 50 words. Carefully drawn chemical structures or figures are desired to be included, these will serve to illustrate the theme of the paper. Authors must supply the graphical abstract in a separate document. The graphics which are a part of the graphical abstract should be sent separately in its original format.

An MS Word template for the Graphical Abstract can be found on the web page of Chemistry Journal of Moldova ([www.cjm.asm.md](http://www.cjm.asm.md)). Use of this template is mandatory.

#### **Copyright guidelines**

Upon acceptance of an article the copyright transfer will be automatic. This transfer will ensure the widest possible dissemination of information. If excerpts from other copyrighted works are included, the Author(s) must obtain written permission from the copyright owners and credit the source(s) in the article.

#### **Submission of manuscripts**

Please send your contribution as an e-mail attachment to:

Journal Editor, Academician Gheorghe DUCA  
e-mail: [chemjm@asm.md](mailto:chemjm@asm.md) / [chemjm@gmail.com](mailto:chemjm@gmail.com)

using Microsoft Word (Office 97 or higher for PCs) word processing soft.

Please prepare a file (allowed formats: \*.doc or \*.rtf) containing a short cover letter to the Editor, justifying why your article should appear in "Chemistry Journal of Moldova. General, Industrial and Ecological Chemistry".

The manuscript with all schemes, figures, tables integrated in the text should be submitted in a separated document file.

Graphical abstract must be provided in a separated document file.

**Authors should indicate the research field of their paper as well as the nature of contribution (Short Communication, Full Paper or Review Article) in their accompanying letters, along with their mailing address, daytime phone number and fax if available. Names and addresses of three potential referees are welcomed.**

Authors will be notified by email if their contribution is received and accepted.

Proofs will be dispatched via e-mail and should be returned to the publisher with corrections as quickly as possible, normally within 48 hours of receipt.